Annals of the ICRP

ICRP PUBLICATION 130

Occupational Intakes of Radionuclides: Part 1

Editor-in-Chief
C.H. CLEMENT

Associate Editor
N. HAMADA

Authors on behalf of ICRP
F. Paquet, G. Etherington, M.R. Bailey, R.W. Leggett, J. Lipsztein, W. Bolch, K.F. Eckerman, J.D. Harrison

PUBLISHED FOR

The International Commission on Radiological Protection

by

SAGE

Please cite this issue as 'ICRP, 2015. Occupational Intakes of Radionuclides: Part 1. ICRP Publication 130. Ann. ICRP 44(2).'

CONTENTS

GUEST EDITORIAL 00

ABSTRACT 00

PREFACE 00

GLOSSARY 00

1. INTRODUCTION 00

1.1. Scope of this series of reports 00
1.2. Protection quantities and dose coefficients in this series of reports 00
1.3. Previous reports on occupational intakes of radionuclides 00
1.4. Changes in *Publication 103* (ICRP, 2007) that affect the calculation of equivalent and effective dose 00
1.5. Biokinetic models implemented in this series of reports 00
1.6. Dosimetry implemented in this series of reports 00
1.7. Interpretation of bioassay data 00
1.8. Structure of the report 00

2. MONITORING AND ASSESSMENT OF INTERNAL OCCUPATIONAL EXPOSURES TO RADIONUCLIDES 00

2.1. Assessment of worker doses 00
2.2. Objectives of monitoring 00
2.3. Categories of individual monitoring programme 00
2.4. Needs for individual monitoring 00
2.5. Pregnancy and breast feeding 00

3. BIOKINETIC AND DOSIMETRIC MODELS 00

3.1. Introduction 00
3.2. Human Respiratory Tract Model 00
3.3. Human Alimentary Tract Model 00
3.4. Intact skin and wounds 00
3.5. Biokinetic models for systemic radionuclides 00
3.6. Medical intervention 00
3.7. Methodology for dose calculations: the ICRP dosimetry system 00

4. METHODS OF INDIVIDUAL AND WORKPLACE MONITORING ... 00

4.1. Introduction 00

4.2. Body activity measurements (in-vivo measurements) 00
4.3. Analysis of excreta and other biological materials 00
4.4. Exposure monitoring of the workplace 00

5. MONITORING PROGRAMMES 00

5.1. Introduction 00
5.2. General principles for the design of individual monitoring programmes 00
5.3. Categories of monitoring programmes 00
5.4. Derived investigation levels 00
5.5. Record keeping and reporting 00
5.6. Quality management system 00

6. GENERAL ASPECTS OF RETROSPECTIVE DOSE ASSESSMENT AND RETROSPECTIVE DOSE VERIFICATION 00

6.1. Introduction 00
6.2. Types of analysis 00
6.3. Understanding exposure situations 00
6.4. Data collection, processing, and dose assessments 00
6.5. Uncertainties in internal dose assessment based on bioassay 00

7. DATA PROVIDED FOR ELEMENTS AND RADIOISOTOPES 00

7.1. Dose coefficients and bioassay functions 00
7.2. Data provided in the printed reports and electronic annex 00
7.3. Quality assurance of data presented 00

REFERENCES 00

ANNEX A. REVISION OF THE HUMAN RESPIRATORY TRACT MODEL 00

ANNEX B. EVOLUTION OF ICRP'S SYSTEMIC BIOKINETIC MODELS 00

SAGE

ICRP Publication 130

ICRP
Annals of the ICRP

Guest Editorial

DOSES FROM RADIATION EXPOSURE

A frequently asked question is why the radiological protection community is having to wait so long for revised dose coefficients relating to the 2007 Recommendations of the International Commission on Radiological Protection (ICRP, 2007). As in previous recommendations, revised radiation and tissue weighting factors were introduced, necessitating the recalculation of all equivalent and effective dose coefficients. If weighting factors had been the only change, it would have been a relatively simple task to provide revised dose coefficients. However, substantial additional complexity was introduced in the 2007 Recommendations by the requirement for use of reference anatomical models based on medical imaging data. This change from using stylised mathematical representations of body organs and their positions to the use of Reference Male and Female models has required a large programme of work to construct models and undertake radiation transport calculations for all radiation types. The adult models were published in *Publication 110* (ICRP, 2009) and, at the time of writing, completion of final radiation transport calculations is anticipated. Models for children at specified ages and the fetus and pregnant woman are under development.

Committee 2 and its task groups have added considerably to this workload by seeking to make a large number of additional improvements. The first of these was the updating of nuclear decay data, issued in *Publication 107* (ICRP, 2008). Second, all biokinetic models used in the calculation of dose coefficients for inhaled and ingested radionuclides have been reviewed, and updated in many cases. This report describes changes made to the Human Respiratory Tract Model, use of the Human Alimentary Tract Model, and approaches to specification of systemic models for radionuclides absorbed into blood. Third, it was decided to provide dose coefficients and bioassay data for measurement interpretation together for this series of reports on occupational intakes of radionuclides, rather than separately, as has been done in the past.

The work of Committee 2 in this area is scientifically and technically innovative and demanding. There is a small number of experts worldwide who contribute to this ICRP work, and the community benefits from their willingness to do so without specific additional funding. However, it is important for national authorities to recognise the need to provide and, preferably, coordinate financial support and training

to ensure that adequate capacity is maintained. Careful planning will be required to ensure that the most effective use is made of limited resources.

Arguably, the level of sophistication of the biokinetic and dosimetric models used to calculate ICRP dose coefficients is greater than required for radiological protection purposes, given the simplifications and approximations inherent in the calculation of equivalent and effective dose using weighting factors and involving sex-averaging. While simpler models may be adequate for radiological protection purposes, ICRP models are used to calculate organ and tissue absorbed doses for scientific purposes, in addition to their use to calculate equivalent and effective dose. The biokinetic models produced can be used in many other areas, including toxicology, pharmacology, and medicine. It is also important to ensure that models are sufficiently reliable to ensure adequate protection.

The United Nations Scientific Committee on the Effects of Atomic Radiation (UNSCEAR) is currently reviewing the biological effects of selected internal emitters; a topic that it has not addressed previously in detail. Reviews of data on tritium and uranium isotopes are in progress, and others may follow. In each case, considerations will include whether ICRP models take appropriate account of available scientific data. The report will also address the overall question of whether risks from internal emitters can be assessed adequately using modelled organ and tissue doses, and stochastic risk estimates derived for external exposures. This UNSCEAR initiative is welcomed by ICRP as complementary to the current work of Committees 1 and 2.

As Part 1 of the Occupational Intakes of Radionuclides series, this report provides a description of biokinetic and dosimetric methodology, and the use of bioassay data. Subsequent Parts 2–5 will consist of element sections describing element-specific biokinetic models, and provide dose coefficients and bioassay data. Planned publications are as follows:

- Part 2 – hydrogen (H), carbon (C), phosphorus (P), sulphur (S), calcium (Ca), iron (Fe), cobalt (Co), zinc (Zn), strontium (Sr), yttrium (Y), zirconium (Zr), niobium (Nb), molybdenum (Mo), and technetium (Tc);
- Part 3 – ruthenium (Ru), antimony (Sb), tellurium (Te), iodine (I), caesium (Cs), barium (Ba), iridium (Ir), lead (Pb), bismuth (Bi), polonium (Po), radon (Rn), radium (Ra), thorium (Th), and uranium (U);
- Part 4 – lanthanides and remaining actinides; and
- Part 5 – remaining elements.

The schedule of work for Committee 2 and its task groups also includes replacement of all currently available dose coefficients for ingestion and inhalation of radionuclides by members of the public. It is hoped that much of this work will be

completed during the current term of the Commission (i.e. by 2017). The expertise and hard work of those involved deserve full recognition.

JOHN D. HARRISON
CHAIR, ICRP COMMITTEE 2

FRANCOIS PAQUET
VICE-CHAIR, ICRP COMMITTEE 2

SAGE

ICRP Publication 130

ICRP
Annals of the ICRP

Occupational Intakes of Radionuclides: Part 1

ICRP PUBLICATION 130

Approved by the Commission in November 2012

Abstract–This report is the first in a series of reports replacing *Publications 30* and *68* to provide revised dose coefficients for occupational intakes of radionuclides by inhalation and ingestion. The revised dose coefficients have been calculated using the Human Alimentary Tract Model (*Publication 100*) and a revision of the Human Respiratory Tract Model (*Publication 66*) that takes account of more recent data. In addition, information is provided on absorption into blood following inhalation and ingestion of different chemical forms of elements and their radioisotopes. In selected cases, it is judged that the data are sufficient to make material-specific recommendations. Revisions have been made to many of the models that describe the systemic biokinetics of radionuclides absorbed into blood, making them more physiologically realistic representations of uptake and retention in organs and tissues, and excretion.

The reports in this series provide data for the interpretation of bioassay measurements as well as dose coefficients, replacing *Publications 54* and *78*. In assessing bioassay data such as measurements of whole-body or organ content, or urinary excretion, assumptions have to be made about the exposure scenario, including the pattern and mode of radionuclide intake, physical and chemical characteristics of the material involved, and the elapsed time between the exposure(s) and measurement. This report provides some guidance on monitoring programmes and data interpretation.

Keywords: Occupational exposure; Internal dose assessment; Biokinetic and dosimetric models; Bioassay interpretation

AUTHORS ON BEHALF OF ICRP
F. PAQUET, G. ETHERINGTON, M.R. BAILEY, R.W. LEGGETT,
J. LIPSZTEIN, W. BOLCH, K.F. ECKERMAN, J.D. HARRISON

PREFACE

The system of radiological protection recommended by the International Commission on Radiological Protection (ICRP) is the basis for standards and working practices throughout the world (ICRP, 1991, 2007; IAEA, 1996). Fundamental to the application of ICRP recommendations are the protection quantities defined by ICRP: equivalent dose and effective dose. While the definition of these quantities remains unchanged in the most recent 2007 Recommendations (ICRP, 2007), there have been important changes that affect the values calculated per radiation exposure. Committee 2 of ICRP is responsible for the provision of these reference dose coefficients for the assessment of internal and external radiation exposure, calculated using reference biokinetic and dosimetric models, and reference data for workers and members of the public. Since *Publication 103* (ICRP, 2007), Committee 2 and its task groups have been engaged in a substantial programme of work to provide new dose coefficients for various circumstances of radiation exposure.

Publication 103 (ICRP, 2007) introduced changes to the radiation weighting factors used in the calculation of equivalent dose to organs and tissues, and also changes to the tissue weighting factors used in the calculation of effective dose. In addition, an important development was the adoption of reference anatomical computational phantoms (i.e. models of the human body based on medical imaging data) in place of the composite mathematical models that have been used for all previous calculations of organ doses. This process commenced with the adoption of Reference Adult Male and Female models (ICRP, 2009), and will be continued with the adoption of paediatric phantoms. *Publication 103* (ICRP, 2007) also clarified the need for separate calculation of equivalent dose to males and females, and sex-averaging in the calculation of effective dose. In the revision of dose coefficients, the opportunity has also been taken to improve calculations by updating radionuclide decay data (ICRP, 2008), and implementing more sophisticated treatments of radiation transport (ICRP, 2010) using the ICRP reference anatomical phantoms of the human body (ICRP, 2009). These improvements impact on dose calculations for external exposures as well as for internal emitters.

This report is the first in a series of reports replacing the *Publication 30* series (ICRP, 1979, 1980, 1981, 1988b) and *Publication 68* (ICRP, 1994b) to provide revised dose coefficients for occupational intakes of radionuclides by inhalation and ingestion. The revised dose coefficients have been calculated using the Human Alimentary Tract Model (ICRP, 2006) and a revision of the Human Respiratory Tract Model (ICRP, 1994a) that takes account of more recent data. In addition, information is provided on absorption into blood following inhalation and ingestion of different chemical forms of elements and their radioisotopes. In selected cases, it is judged that the data are sufficient to make material-specific recommendations. Revisions have been made to many of the models that describe the systemic biokinetics of

radionuclides absorbed into blood, making them more physiologically realistic representations of uptake and retention in organs and tissues, and excretion.

The reports in this series provide data for the interpretation of bioassay measurements as well as dose coefficients, replacing *Publications 54* and *78* (ICRP, 1988a, 1997b). In assessing bioassay data such as measurements of whole-body or organ content, or urinary excretion, assumptions have to be made about the exposure scenario, including the pattern and mode of radionuclide intake, physical and chemical characteristics of the material involved, and the elapsed time between the exposure(s) and measurement. This report provides some guidance on monitoring programmes and data interpretation.

This first report in the series provides an introduction to the series of reports, and includes sections on control of occupational exposures, biokinetic and dosimetric models, monitoring methods, monitoring programmes, and retrospective dose assessment. Subsequent reports provide data on individual elements and their radioisotopes, including biokinetic data and models, dose coefficients, and data for bioassay interpretation. An electronic annex accompanying this series of reports gives extensive additional information.

The membership of the Task Group on Internal Dosimetry (INDOS) at the time of completion of this report was as follows:

F. Paquet (Chair)	G. Etherington	J. Lipsztein
E. Ansoborlo	A. Giussani	D. Melo
M.R. Bailey	R.A. Guilmette	
E. Blanchardon	J.D. Harrison	
H. Doerfel	R.W. Leggett	

The corresponding members were:

A. Bouville	A. Luciani	D. Whillans
C-M. Castellani	D. Newton	
R. Cruz-Suarez	D. Nosske	
C. Hurtgen	D.M. Taylor	

The membership of the Task Group on Dose Calculations (DOCAL) at the time of completion of this report was as follows:

W.E. Bolch (Chair)	T.P. Fell	M. Pelliccioni
V. Berkovski	N.E. Hertel	N. Petoussi-Henss

L. Bertelli	J.G.S. Hunt	M. Zankl
K.F. Eckerman	N. Ishigure	
A. Endo	D. Noßke	

The corresponding members were:

A. Birchall	C. Lee	R. Tanner
G. Gualdrini	H. Schlattl	X.G. Xu
D. Jokisch	M. Stabin	

Main Commission critical reviewers were:

J.K. Lee	H-G. Menzel

The authors were aided by significant contributions from V. Berkovski, D. Nosske, D. Gregoratto, J.R.H. Smith, T. Smith, and all the INDOS and DOCAL members.

The membership of Committee 2 during the period of preparation of this report was:

(*2009–2013*)

H-G. Menzel (Chair)	R. Cox	R. Leggett
M.R. Bailey	G. Dietze	J.L. Lipsztein
M. Balonov	K.F. Eckerman	J. Ma
D. Bartlett	A. Endo	F. Paquet
V. Berkovski	J.D. Harrison	N. Petoussi-Henss
W.E. Bolch	N. Ishigure	A.S. Pradhan

(*2013–2017*)

J.D. Harrison (Chair)	M. Degteva	D. Noßke
M.R. Bailey	A. Endo	F. Paquet
V. Berkovski	J.G. Hunt	N. Petoussi-Henss
L. Bertelli	C. Hyeong Kim	F. Wissmann
W.E. Bolch	R. Leggett	
D. Chambers	J. Ma	

The report was adopted by the Main Commission at its meeting in Fukushima, Japan on 2 November 2012.

GLOSSARY

For convenience, this glossary has been structured under the subheadings of terms for general dosimetry and radiological protection, biokinetic models, and bioassay interpretation.

Terms for general dosimetry and radiological protection

Absorbed dose (D)

The absorbed dose is given by:

$$D = \frac{\mathrm{d}\bar{\varepsilon}}{\mathrm{d}m}$$

where $\mathrm{d}\bar{\varepsilon}$ is the mean energy imparted by ionising radiation to matter of mass $\mathrm{d}m$. The SI unit of absorbed dose is joule per kilogram (J kg^{-1}), and its special name is gray (Gy).

Absorbed fraction (AF), $\phi(r_T \leftarrow r_S, E_{R,i})$

Fraction of energy $E_{R,i}$ of the i^{th} radiation of type R emitted within the source region r_S that is absorbed in the target region r_T. These target regions may be tissues (e.g. liver) or cell layers within organs (e.g. stem cells of the stomach wall) (see definitions for 'Target region' and 'Target tissue').

Active (bone) marrow

Active marrow is haematopoietically active and gets its red colour from the large numbers of erythrocytes (red blood cells) being produced. Active bone marrow serves as a target region for radiogenic risk of leukaemia.

Activity

The number of nuclear transformations of a radioactive material during an infinitesimal time interval, divided by its duration (s). The SI unit of activity is the becquerel (Bq; 1 Bq = 1 s^{-1}).

Annual limit on intake (ALI). See also 'Derived air concentration'

ALI was defined in *Publication 60* (ICRP, 1991, Para. S30) as an intake (in Bq) of a radionuclide in 1 year that would lead to a committed effective dose of 20 mSv. The average ALI for workers is thus:

$$\mathrm{ALI_j} = \frac{0.02}{e_j\,(50)}$$

The Commission does not recommend the use of ALI because it considers that, for compliance with dose limits, it is the total dose from external radiation as well as from intakes of radionuclides that must be taken into account.

Becquerel (Bq)

The special name for the SI unit of activity ($1\ \mathrm{Bq} = 1\ \mathrm{s}^{-1}$).

Biological half-time

The time required for a compartment of a biological system to eliminate (in the absence of additional input and radioactive decay) half of its radionuclide content.

Bone marrow. See also 'Active (bone) marrow' and 'Inactive (bone) marrow'

Bone marrow is a soft, highly cellular tissue that occupies the cylindrical cavities of long bones and the cavities defined by the bone trabeculae of the axial and appendicular skeleton. Total bone marrow consists of a sponge-like, reticular, connective tissue framework called 'stroma', myeloid (blood-cell-forming) tissue, fat cells (adipocytes), small accumulations of lymphatic tissue, and numerous blood vessels and sinusoids. There are two types of bone marrow, active (red) and inactive (yellow), where these adjectives refer to the marrow's potential for production of blood cell elements (haematopoiesis).

Committed effective dose [$E(\tau)$]. See also 'Effective dose'

In this series of reports, the integration time τ following the intake is taken to be 50 years. The committed effective dose $E(50)$ is calculated with the use of male and female committed equivalent doses to individual target organs or tissues T according to the expression:

$$E(50) = \sum_T w_T \cdot \left[\frac{H_T^M(50) + H_T^F(50)}{2}\right]$$

The SI unit for committed effective dose is the same as for absorbed dose, $J\,kg^{-1}$, and its special name is sievert (Sv).

Committed equivalent dose [H_T (50)]. See also 'Equivalent dose'

In this series of reports, the equivalent dose to an organ or tissue region is calculated using a 50-year commitment period. It is taken as the time integral of the equivalent dose rate in a target organ or tissue T of the Reference Adult Male or the Reference Adult Female. These, in turn, are predicted by reference biokinetic and dosimetric models following the intake of radioactive material into the body of the Reference Worker. The integration period is thus 50 years following the intake:

$$H_T(50) = \int_0^{50} \dot{H}(r_T, t)\mathrm{d}t$$

For both sexes, the equivalent dose rate $\dot{H}(r_T, t)$ in target region r_T at time t after an acute intake is expressed as:

$$\dot{H}(r_T, t) = \sum_{r_S} A(r_S, t) \cdot S_w(r_T \leftarrow r_S)$$

where:

$A(r_S, t)$ is the activity of the radionuclide in source region r_S at time t after intake, in Bq, as predicted by the reference biokinetic models for the Reference Worker.

$S_w(r_S \leftarrow r_T)$ is the radiation weighted S coefficient (i.e. the equivalent dose to target region r_T per nuclear transformation in source region r_S), in Sv $(Bq\ s)^{-1}$, for the Reference Adult Male and Female.

The SI unit for committed equivalent dose is the same as for absorbed dose, $J\,kg^{-1}$, and its special name is sievert (Sv).

Derived air concentration (DAC). See also 'Annual limit on intake'

The DAC is the activity concentration in air, in Bq m^{-3}, of the radionuclide considered that would lead to intake of an annual limit on intake (ALI) assuming a sex-averaged breathing rate of 1.1 $m^3\ h^{-1}$ and an annual working time of 2000 h. DAC is given by:

$$\mathrm{DAC_j} = \frac{\mathrm{ALI_j}}{2200}$$

The Commission does not recommend the use of DAC because it considers that, for compliance with dose limits, it is the total dose from external radiation as well as from intakes of radionuclides that must be taken into account.

Dose coefficient

For adult workers, a dose coefficient is defined as either the committed equivalent dose in organ or tissue T per intake, $h_T(50)$, or the committed effective dose per intake, $e(50)$, where 50 is the dose-commitment period in years over which the dose is calculated. Note that elsewhere, the term 'dose per intake coefficient' is sometimes used for dose coefficient.

Dose constraint

A prospective and source-related restriction on the individual equivalent dose to an organ or tissue or effective dose from a source that provides a basic level of protection for the most highly exposed individuals from a source, and serves as an upper bound on the equivalent dose or effective dose in optimisation of protection for that source. For occupational exposures, the dose constraint is a value of individual equivalent dose to an organ or tissue or effective dose used to limit the range of options considered in the process of optimisation.

Dose limit

Value of the effective dose or the organ- or tissue-specific equivalent dose to an individual that shall not be exceeded in planned exposure situations.

Dose of record (E)

In this series of reports, the dose of record refers to the effective dose, assessed by summing the measured personal dose equivalent $H_p(10)$ and the committed effective dose retrospectively determined for the Reference Worker using results of individual monitoring of the worker and ICRP reference biokinetic and dosimetric computational models. Dose of record may be assessed using site-specific parameters of exposure such as the absorption type of the material and the activity median aerodynamic diameter/activity median thermodynamic diameter of the inhaled aerosol, but the parameters of the Reference Worker shall be fixed as defined by ICRP in this series of reports. Dose of record is assigned to the worker and required to be kept for purposes of reporting and retrospective demonstration of compliance with regulatory requirements.

Dose per content function

In this series of reports, a set of tabulated values $z(t) = e(50)/m(t)$ or $z(t) = h_T(50)/m(t)$, where $e(50)$ is the effective dose coefficient, $h_T(50)$ is the equivalent dose coefficient for a tissue or organ, and $m(t)$ is the reference bioassay (retention or excretion) function. Values of $z(t)$ represent the committed effective dose or committed equivalent dose to an organ r_T per predicted activity content in the body or in a given organ (Sv Bq^{-1}), or per daily excretion.

Dose per intake coefficient. See also 'Dose coefficient'

In this series of reports, the committed effective dose per radionuclide intake, $e(50)$, or committed equivalent dose to the tissue or organ r_T per radionuclide intake, $h_T(r_T,50)$, where the dose-commitment period over which the dose is calculated is 50 years.

Effective dose (E)

In accordance with the generic definition of effective dose in ICRP (2007), the effective dose is calculated as:

$$E = \sum_T w_T \left[\frac{H_T^M + H_T^F}{2} \right]$$

where H_T^M and H_T^F are the equivalent doses to the tissues or organs r_T of the Reference Adult Male and Female, respectively, and w_T is the tissue weighting factor for target tissue T, with $\sum_T w_T = 1$. The sum is performed over all organs and tissues of the human body considered to be sensitive to the induction of stochastic effects. As w_R and w_T are dimensionless, the SI unit for effective dose is the same as for absorbed dose, J kg^{-1}, and its special name is sievert (Sv).

Endosteum (or endosteal layer)

A 50-μm-thick layer covering the surfaces of the bone trabeculae in regions of trabecular spongiosa and those of the cortical surfaces of the medullary cavities within the shafts of all long bones. It is assumed to be the target region for radiogenic bone cancer. This target region replaces that previously introduced in *Publications 26* and *30* (ICRP, 1977) – the bone surfaces – which had been defined as a single-cell layer, 10 μm in thickness, covering the surfaces of both the bone trabeculae and the Haversian canals of cortical bone.

Equivalent dose (H_T)

The equivalent dose to a tissue or organ is defined as:

$$H_T = \sum_R w_R D_{R,T}$$

where w_R is the radiation weighting factor for radiation type R, and $D_{R,T}$ is the organ absorbed dose from radiation type R in a tissue or organ r_T of the Reference Adult Male or Female. As w_R is dimensionless, the SI unit for the equivalent dose is the same as for absorbed dose, J kg^{-1}, and its special name is sievert (Sv).

Exposure

The state or condition of being subject to irradiation. External exposure is exposure to radiation from a source outside the body, and internal exposure is exposure to radiation from a source within the body.

Gray (Gy)

The special name for the SI unit of absorbed dose (1 Gy = 1 J kg^{-1}).

Inactive (bone) marrow

In contrast to active marrow, inactive marrow is haematopoietically inactive (i.e. does not support haematopoiesis directly). It gets its yellow colour from fat cells (adipocytes) that occupy most of the space of the bone marrow framework.

Marrow cellularity

The fraction of bone marrow volume in a given bone that is haematopoietically active. Age- and bone-site-dependent reference values for marrow cellularity are given in Table 41 of *Publication 70* (ICRP,1995a). As a first approximation, marrow cellularity may be thought of as 1 minus the fat fraction of bone marrow.

Mean absorbed dose ($D_{R,T}$)

The mean absorbed dose in a specified organ or tissue region r_T is given by:

$D_T = 1/m_T \int D \, dm$, where m_T is the mass of the organ or tissue, and D is the absorbed dose in the mass element dm. The SI unit of mean absorbed dose is joule per kilogram (J kg^{-1}), and its special name is gray (Gy).

Occupational exposure

The radiation exposure of workers incurred as a result of their work. ICRP limits its use of 'occupational exposures' to radiation exposures incurred at work as a result of situations that can reasonably be regarded as being the responsibility of the operating management.

Personal dose equivalent [$H_p(d)$]

The dose equivalent in soft tissue at an appropriate depth d below a specified point on the human body. The unit of personal dose equivalent is joule per kilogram (J kg^{-1}), and its special name is sievert (Sv). The specified point is usually given by the position where the individual dosimeter is worn. For the assessment of effective dose, a depth of 10 mm is recommended, and for the assessment of equivalent dose to the skin and for the lens of the eye, depths of 0.07 mm and 3 mm, respectively, are recommended.

Protection quantities

Quantities that ICRP has developed for radiological protection that allow quantification of the extent of exposure to ionising radiation from both whole- and partial-body external irradiation, and from intakes of radionuclides.

Radiation weighting factor (w_R)

A dimensionless factor by which the organ or tissue absorbed dose component of a radiation type R is multiplied to reflect the relative biological effectiveness of that radiation type. It is used to derive the organ equivalent dose from the mean absorbed dose in an organ or tissue.

Red (bone) marrow

See 'Active (bone) marrow'

Reference level

In emergency or existing controllable exposure situations, this represents the level of dose or risk above which it is judged to be inappropriate to plan to allow exposures to occur, and below which optimisation of protection should be implemented. The chosen value for a reference level will depend upon the prevailing circumstances of the exposure under consideration.

Reference Male and Reference Female (Reference Individual)

An idealised male or female with anatomical and physiological characteristics defined by ICRP for the purpose of radiological protection.

Reference parameter value

The value of a parameter, factor, or quantity that is regarded as valid for use in dosimetric calculations and recommended by ICRP. These values are fixed and are not subject to uncertainties.

Reference Person

An idealised person, for whom the equivalent doses to organs and tissues are calculated by averaging the corresponding doses of the Reference Male and the Reference Female. The equivalent doses of the Reference Person are used for calculation of effective dose.

Reference phantom

The computational phantom of the human body (male or female voxel phantom based on medical imaging data), defined in *Publication 110* (ICRP, 2009) with anatomical characteristics reasonably similar to those of the Reference Male and the Reference Female defined in *Publication 89* (ICRP, 2002a).

Reference Worker

The adult Reference Person combined with the reference biokinetic and dosimetric models and their parameter values, as defined in this series of reports for the Reference Worker (systemic biokinetic models, Human Respiratory Tract Model, Human Alimentary Tract Model, and dosimetric models). The structure and parameter values of biokinetic models of the Reference Worker are invariant on the sex, age, race, and other individual-specific characteristics, but based on the Reference Male parameter values where sex-specific models are available.

Sievert (Sv)

The special name for the SI unit (J kg^{-1}) of equivalent dose and effective dose.

Source region (r_s)

Region of the body containing the radionuclide. The region may be an organ, a tissue, the contents of the alimentary tract or urinary bladder, or the surfaces of tissues as in the skeleton and the respiratory tract.

Specific absorbed fraction [$\Phi(r_T \leftarrow r_S, E_{R,i})$]

Fraction of radiation R of energy $E_{R,i}$ emitted within the source region r_S that is absorbed per mass in the target region r_T.

Spongiosa

Term referring to the combined tissues of the bone trabeculae and marrow tissues (both active and inactive) located beneath cortical bone cortices across regions of the axial and appendicular skeleton. Spongiosa is one of three bone regions defined in the *Publication 110* (ICRP, 2009) reference phantoms, the other two being cortical bone and medullary marrow of the long bone shafts. As the relative proportions of trabecular bone, active marrow, and inactive marrow vary with skeletal site, the homogeneous elemental composition and mass density of spongiosa are not constant but vary with skeletal site [see Annex B of *Publication 110* (ICRP, 2009)].

S coefficient (radiation weighted) [$S_w(r_T \leftarrow r_S)$]

The equivalent dose to target region r_T per nuclear transformation of a given radionuclide in source region r_S, Sv (Bq s)$^{-1}$, for the Reference Male and the Reference Female.

$$S_w(r_T \leftarrow r_S) = \sum_R w_R \sum_i E_{R,i}\, Y_{R,i}\, \Phi\left(r_T \leftarrow r_S, E_{R,i}\right)$$

where:

$E_{R,i}$ is the energy, in joules, of the i^{th} radiation of type R emitted in nuclear transformations of the radionuclide;

$Y_{R,i}$ is the yield of the i^{th} radiation of type R per nuclear transformation (Bq s)$^{-1}$;

w_R is the radiation weighting factor for radiation type R (Table 1.1); and

$\Phi\left(r_T \leftarrow r_S, E_{R,i}\right)$ is the specific absorbed fraction, defined as the fraction of energy $E_{R,i}$ of radiation type R emitted within the source region r_S that is absorbed per mass in the target region r_T, kg^{-1}.

Note that no change in anatomical parameters with time (age) are considered for adults; in this case, therefore, S_w is invariant with respect to time, and its value represents either the equivalent dose rate (Sv s^{-1}) per activity (Bq), or the equivalent dose (Sv) per nuclear transformation (Bq-s) in the target region.

Target region (r_T)

Organ or tissue region of the body in which a radiation absorbed dose is received.

Target tissue (T)

Organs or tissues in the body for which tissue weighting factors are assigned in the effective dose (see definition in Glossary and Table 1.2). In many cases, each target tissue T corresponds to a single target region r_T. In the case of the extrathoracic airways, thoracic airways, colon, and lymphatic nodes, however, a fractional weighting of more than one target region r_T defines the target tissue T (see Table 3.5 and Section 3.7).

Tissue weighting factor (w_T). See also 'Effective dose'

The factor by which the equivalent dose to an organ or tissue r_T is weighted to represent the relative contribution of that organ or tissue to overall radiation detriment from stochastic effects. It is defined such that:

$$\sum_T w_T = 1$$

Worker

In this series of reports, any person who works, whether full time, part time, or temporarily, for an employer and those who have recognised rights and duties in relation to occupational radiation protection.

Terms for the biokinetic models

Absorption

Transfer of material into blood regardless of mechanism. Generally applies to dissociation of particles and the uptake into blood of soluble substances and material dissociated from particles.

Aerodynamic diameter (d_{ae})

Diameter (μm) of a unit density (1 g cm^{-3}) sphere that has the same terminal settling velocity in air as the particle of interest.

Alimentary tract

The tube from mouth to anus in which food is digested.

Alimentary tract transfer factor (f_A)

The fraction of activity entering the alimentary tract that is absorbed into blood, taking no account of losses due to radioactive decay or endogenous input of activity into the tract.

Alveolar–interstitial (AI) region

Part of the respiratory tract, consisting of the respiratory bronchioles, alveolar ducts and sacs with their alveoli, and the interstitial connective tissue (airway generations 16 and beyond).

Activity median aerodynamic diameter (AMAD) (see also 'Count median diameter')

Fifty percent of the activity in the aerosol is associated with particles of aerodynamic diameter (d_{ae}) greater than the AMAD. Used when deposition depends principally on inertial impaction and sedimentation, typically when the AMAD is more than approximately 0.3 μm.

Activity median thermodynamic diameter (AMTD)

Fifty percent of the activity in the aerosol is associated with particles of thermodynamic diameter (d_{th}) greater than the AMTD. Used when deposition depends principally on diffusion, typically when the activity median aerodynamic diameter is less than approximately 0.3 μm.

Basal cells

Cuboidal epithelial cells attached to the basement membrane of extrathoracic and bronchial epithelium, and not extending to the surface.

Blood

Corresponds to the transfer compartment in the biokinetic models. Also called 'transfer compartment' or 'body fluids' in previous ICRP publications.

Bronchial region (BB)

Part of the respiratory tract, consisting of the trachea (airway generation 0) and bronchi (airway generations 1–8).

Bronchiolar region (bb)

Part of the respiratory tract, consisting of the bronchioles and terminal bronchioles (airway generations 9–15).

Bone surfaces

See 'Endosteum'

Clearance

The removal of material from the respiratory tract by particle transport and absorption into blood.

Count median diameter (CMD) (see also 'Mass median diameter')

Fifty percent (by number) of the particles in the sample measured (e.g. by microscopy) have diameters greater than the CMD.

Compartment

In this series of reports, defined as a mathematical pool of radioactive materials in the body which can be characterised by first-order kinetics. A compartment can be associated with an organ (e.g. the liver), a part of an organ (e.g. the bronchial region of the lungs), a tissue (e.g. the bone), a part of a tissue (e.g. the bone surface), or another substance of the body (e.g. the blood). Activity is considered to be distributed uniformly in a compartment.

Deposition

Refers to the initial processes determining how much of the material in the inspired air remains behind in the respiratory tract after exhalation. Deposition of material occurs during both inspiration and exhalation.

Endogenous excretion

Term used to specify the excretion of materials from blood to the alimentary tract, applying to biliary excretion and passage of materials through the alimentary tract wall.

Endosteum (or endosteal layer)

A 50-μm-thick layer covering the surfaces of the bone trabeculae in regions of trabecular spongiosa and those of the cortical surfaces of the medullary

cavities within the shafts of all long bones. It is assumed to be the target region for radiogenic bone cancer. This target region replaces that previously introduced in *Publications 26* and *30* (ICRP, 1977, 1979) – the bone surfaces – which had been defined as a single-cell layer, 10 μm in thickness, covering the surfaces of both the bone trabeculae and the Haversian canals of cortical bone.

Exogenous excretion

Term used to specify the (faecal) excretion of material that passes through the alimentary tract without absorption.

Extrathoracic (ET) airways

Part of the respiratory tract, consisting of the anterior nasal passage (the ET_1 region) and the posterior nasal passage, pharynx, and larynx (the ET_2 region). Note that the oral part of the pharynx is no longer part of the ET_2 region because it is included in the Human Alimentary Tract Model.

Exposure (in the context of inhalation)

The product of the air concentration of a radionuclide to which a person is exposed (Bq m^{-3}) and the time of exposure. More generally, when the air concentration varies with time, the time integral of the air concentration of a radionuclide to which a person is exposed, integrated over the time of exposure.

Fractional absorption in the gastrointestinal tract (f_1) (see also 'Alimentary tract transfer factor')

The fraction of an element directly absorbed from the gut into blood, used in the *Publication 30* (ICRP, 1979) gastrointestinal tract model.

Human Alimentary Tract Model (HATM)

Biokinetic model for describing the movement of ingested materials through the human alimentary tract; published in *Publication 100* (ICRP, 2006).

Human Respiratory Tract Model (HRTM)

Biokinetic model for describing the deposition, translocation, and absorption of inhaled materials in the human respiratory tract; published in *Publication 66* (ICRP, 1994a) and updated in this report.

Inhalability

Fraction of particles that enter the nose and mouth of those present in the volume of ambient air before inspiration.

Intake (see also 'Uptake')

Radionuclide that enters the respiratory tract or gastrointestinal tract from the environment. Acute intake is defined as a single intake by inhalation or ingestion, taken to occur instantaneously; and chronic intake is defined as a protracted intake over a specified period of time.

Mass median diameter (MMD) (see also 'Activity median aerodynamic diameter' and 'Count median diameter')

Fifty percent of the mass of material in the aerosol is associated with particles of diameter greater than the MMD. For a log-normal distribution with geometric standard deviation σ_g, the MMD can be calculated from the count median diameter (CMD):

$$\mathrm{MMD} = \mathrm{CMD} + 3\exp\left(\left(\ln\sigma_g\right)^2\right)$$

If the material is of uniform specific activity, the MMD will be equal to the activity median diameter (AMD). Fifty percent of the activity in the aerosol is associated with particles of diameter greater than the AMD. The relationship of particle diameter to particle aerodynamic diameter, and hence of the AMD and CMD to the activity median aerodynamic diameter of an aerosol formed from the particles, depends on the density and shape of the particles, and on how the diameters were measured (see Section A.3.3 for further information).

Nasal augmenter

A person who breathes entirely through the nose at the exercise levels of 'sleep', 'sitting', and 'light exercise', but oronasally (partly through the nose and partly through the mouth) during 'heavy exercise'. Also known as a 'normal nose breather', because most people breathe according to this pattern. All reference subjects, including the Reference Worker, are assumed to be nasal augmenters.

Normal nose breather

See 'Nasal augmenter'

Particle transport

Processes that clear material from the respiratory tract to the alimentary tract and to the lymph nodes, and move material from one part of the respiratory tract to another.

Reference biokinetic model

A biokinetic model adopted in this series of reports for the Reference Worker. A reference biokinetic model describes the intake, uptake, distribution, and retention of a radionuclide in various organs or tissues of the body, and the subsequent excretion from the body by various pathways.

Secretory cells

Non-ciliated epithelial cells that have mucous or serous secretions.

Subcutaneous tissue

Loose fibrous tissue situated directly below the skin. It includes blood vessels, connective tissue, muscle, fat, and glands. In the context of intake through wounds, it represents tissue at the wound site in which radionuclides could be retained prior to removal of soluble or dissolved material into blood or insoluble material via lymphatic vessels.

Target region in the bronchial region of the Human Respiratory Tract Model

See Table 3.3. For each of the other regions, only one target is specified and hence no special symbol is required. BB_{bas} is defined as tissue in the bronchial region through which basal cell are distributed, and BB_{sec} is defined as tissue in the bronchial region through which secretory cell are distributed.

Thermodynamic diameter (d_{th})

Diameter (μm) of a spherical particle that has the same diffusion coefficient in air as the particle of interest.

Thoracic (TH) airways

Combined bronchial, bronchiolar, and alveolar–interstitial regions.

Transfer compartment

The compartment introduced for mathematical convenience into many of the biokinetic models previously used by ICRP to account for the translocation of radioactive material through the blood from where it is deposited in tissues.

Types of materials, classified according to their rates of absorption from the respiratory tract into blood

Type F is defined as deposited materials that are readily absorbed into blood from the respiratory tract (fast absorption). Type M is defined as deposited materials that have intermediate rates of absorption into blood from the respiratory tract (moderate absorption). Type S is defined as deposited materials that are relatively insoluble in the respiratory tract (slow absorption). Type V is defined as deposited materials that, for dosimetric purposes, are assumed to be instantaneously absorbed into blood from the respiratory tract (only certain gases and vapours; very fast absorption).

Uptake (see also 'Intake')

Activity that enters blood from the respiratory or alimentary tract or through the skin.

Terms for bioassay interpretation

Action level

A preset level above which some remedial action should be considered.

Bioassay

Any procedure used to determine the nature, activity, location, or retention of radionuclides in the body by direct (in-vivo) measurement or by indirect (in-vitro) analysis of material excreted or otherwise removed from the body.

Bioassay function

See 'Reference bioassay function'

Content

The activity of radioactive material in a specific organ, tissue, or the body.

Decision threshold

Fixed value of a measured quantity that, when exceeded by the result of an actual measurement quantifying a physical effect (e.g. the presence of a radionuclide in a sample), may be taken to indicate that the physical effect is present (ISO, 2010a,b). The decision threshold is the critical value of a statistical test for the decision between the hypothesis that the physical effect is not present and the alternative hypothesis that it is present. When the critical value is exceeded by the result of an actual measurement, this is taken to indicate that the hypothesis should be rejected. The statistical test is designed in such a way that the probability of wrongly rejecting the hypothesis (Type I error) is, at most, equal to a given value, α. The decision threshold is an a-posteriori quantity, evaluated after a particular measurement in order to decide whether the result of the measurement is significant. The decision threshold is also referred to as the 'critical level' or the 'minimum significant activity'.

Derived investigation level (DIL) (see also 'Investigation level')

A preset level of a measurable quantity, derived from the investigation level or another primary level. A DIL can be set for any operational parameter related to the individual or to the working environment. For individual monitoring of exposure to intakes of radionuclides, a DIL is most likely to relate to a measured body or organ/tissue content, an activity level in excreta, or an air concentration measured by a personal air sampler.

Detection limit

The smallest true value of a measured quantity that ensures a specified probability of being detectable by the measurement procedure (ISO, 2010a,b). The detection limit is the smallest true value that is associated with the statistical test and hypothesis in accordance with the decision threshold, as follows: if in reality the true value is equal to or exceeds the detection limit, the probability of wrongly not rejecting the hypothesis (Type II error) is, at most, equal to a given value, β. The detection limit is an a-priori quantity, evaluated for a particular measurement method in advance of the performance of a measurement.

Direct measurement

Generic term for any type of in-vivo measurement of incorporated radionuclides (i.e. whole-body counting, lung counting, thyroid counting, etc.).

Excretion function.

See 'Reference bioassay function'

Excretion rate (instantaneous)

The instantaneous rate at which a radionuclide is removed in excreta (Bq s^{-1}).

Investigation level (IL) (see also 'Derived investigation level')

A preset level, expressed in protection quantities, above which the cause or the implications of an intake should be examined (ICRP, 1997b). ILs can be set for any operational parameter related to the individual or to the working environment. For individual monitoring of exposure to intakes of radionuclides, they are most likely to relate to a measured body or organ/tissue content, an activity level in excreta, or an air concentration measured by a personal air sampler.

Measured quantity (M)

Primary result of incorporation monitoring; the measured quantity represents, in the case of in-vivo measurements, the activity of a radionuclide (Bq) in the whole body, an organ, or a tissue; and in the case of in-vitro measurements, the activity of a radionuclide in excreta samples. In many cases, 24-h samples are used.

Recording level

A preset level above which a result should be recorded, lower values being ignored.

Reference bioassay function

In this series of reports, defined as a set of tabulated values $m(t)$ predicted by a reference biokinetic model describing the time course of the activity in the body ('retention function') or the activity excreted in urine or faeces ('excretion function') following an acute intake at time $t = 0$. A retention function $m(t)$ represents the predicted activity of a radionuclide in the body, organ, or tissue at a time t after the intake, whereas an excretion function $m(t)$ represents the predicted activity of a radionuclide in a 24-h excreta sample at a time t after the intake. In the case of an excretion function, in this series of reports, t is the number of days up to the end of the 24-h sample collection period; the radioactive decay in the sample during the sample collection period is taken into account.

Retention function

See ‘Reference bioassay function’

Threshold levels

Values of measured quantities above which some specified action or decision should be taken. They include recording levels, above which a result should be recorded, lower values being ignored; investigation levels, above which the cause or the implication of the result should be examined; and action levels, above which some remedial action should be considered.

1. INTRODUCTION

1.1. Scope of this series of reports

(1) Occupational intakes of radionuclides (OIR) may occur during routine operations in a range of industrial, medical, educational, and research facilities. They may also occur after an incident involving radioactive material.

(2) An adequate assessment of occupational internal exposure resulting from intakes of radionuclides is essential for the design, planning, and authorisation of a facility or activity; for the optimisation of radiation protection of workers; for operational radiation protection; and for the retrospective demonstration of compliance with regulatory requirements.

(3) After intake of radionuclides, doses received by organs and tissues are protracted over time, so equivalent and effective doses are accumulated over time. The resulting quantities are referred to as 'committed doses'.

(4) Internal exposure of workers should be assessed in terms of the protection quantity 'committed effective dose'.

(5) This series of reports provides a comprehensive set of dose coefficients (i.e. committed effective dose and committed equivalent doses to organs or tissues per intake), and also provides values for dose per content function. A dose per content function is the committed effective dose, or committed equivalent dose to an organ or tissue, resulting from an intake that would give rise to unit activity content in the body or in a given organ, or unit activity in a daily excretion sample, at a specified time.

(6) These data may be used for both prospective and retrospective assessments. Prospective assessments provide estimates of intakes and resulting doses for workers engaged in specific activities, using information on projected exposures to radionuclides obtained at the design and planning stage of a facility or practice. These assessments generally make use of default assumptions about exposure conditions and default values for parameters describing material-specific properties, such as the particle size distribution of an inhaled aerosol or the absorption characteristics of a material after inhalation or ingestion. Retrospective assessments use the results of individual monitoring and workplace monitoring to assess doses in order to maintain individual dose records and demonstrate compliance with regulatory requirements. These assessments may, in some circumstances, make use of specific information relating to the exposure, as discussed in Section 6.

(7) The individual exposure of a worker resulting from operations at a facility should be assessed retrospectively, and recorded and reported in terms of dose of record. In general, the dose of record is the sum of two components: (a) the committed effective dose determined retrospectively for the Reference Worker using results of individual monitoring of the worker; and (b) for external exposure, the measured personal dose equivalent, $H_p(10)$. Each of the two components may be referred to individually as components of the dose of record. The use of the term 'dose of record' is intended to emphasise the fact that components of this quantity

are formally assessed, recorded, and reported in accordance with the definition of the term given in the Glossary.

(8) This series of reports contains detailed information on the ICRP reference models used for the derivation of dose coefficients. The information provided in this first report of the series includes a description of revisions made to the ICRP reference Human Respiratory Tract Model (HRTM) (ICRP, 1994a) and an overview of the ICRP reference Human Alimentary Tract Model (HATM) (ICRP, 2006). Subsequent reports in the series present descriptions of the structures and parameter values of the reference systemic biokinetic models.

(9) This report also presents an overview of monitoring methods and programmes, and generic guidance on the interpretation of bioassay data. Subsequent reports in the series present radionuclide-specific information for the design and planning of monitoring programmes, and retrospective assessment of occupational internal doses.

(10) The material presented in this series of reports is not intended for applications beyond the scope of occupational radiation protection. An example of such an application is the assessment of a case of substantial radionuclide intake, where organ doses can approach or exceed the thresholds for tissue reactions, and where medical treatment may require an individual-specific reconstruction of the magnitude of absorbed doses and associated parameters characterising the exposure. In such a case, the formally assessed dose of record should be complemented by individual-related estimates of absorbed doses in organs or tissues. Such individual-related assessments are beyond the scope of this series of reports.

(11) In some exceptional circumstances, when public exposure has occurred and absorbed doses in organs or tissues are below the thresholds for tissue reactions, the material presented in this series of reports could be used for planning of bioassay monitoring programmes (usually based on the use of whole-body and/or thyroid monitors) and interpretation of bioassay monitoring data obtained for adult members of the public.

1.2. Protection quantities and dose coefficients in this series of reports

(12) The protection quantities defined by ICRP – equivalent dose and effective dose – are fundamental to the application of ICRP recommendations. The concept of effective dose provides a single quantity that may be used to characterise both internal and external individual exposures in a manner that is independent of the individual's body-related parameters, such as sex, age (for adults), anatomy, physiology, and race. In order to achieve wide applicability, effective dose and equivalent dose are defined using computational models with broad averaging of physiological parameter values. Specifically, *Publication 89* (ICRP, 2002a) defines the key parameters of the Reference Individuals (the mass, geometry, and composition of human organs and tissues), while this series of reports provides relevant parameters for the Reference Worker (ICRP, 1994b) including an associated set of ICRP reference biokinetic models.

(13) Effective dose is not an individual-specific dose quantity, but rather the dose to the Reference Person under specified exposure conditions. In the general case, the

Reference Person can be either the Reference Worker (see Glossary) or the Reference Member of the Public of a specified age.

(14) In internal dosimetry, no operational dose quantities have been defined that provide a direct assessment of equivalent dose or effective dose. Different methods are applied to assess the equivalent or effective dose due to radionuclides in the human body. They are mainly based on various activity measurements and the application of biokinetic models (computational models).

(15) In this series of reports, dose coefficients and dose per content functions are presented for the Reference Worker. These data are provided for a range of physicochemical forms for each radionuclide and for a range of aerosol particle size distributions. Data for ingestion and injection (i.e. direct entry to the blood) are provided to allow the interpretation of bioassay data for cases of inadvertent ingestion (e.g. of material on contaminated skin) or rapid absorption through intact or damaged skin (injection).

(16) While the generic definition of protection quantities remains unchanged in the most recent recommendations (ICRP, 2007), there have been changes that affect calculated values of dose per radiation exposure, including changes to radiation and tissue weighting factors, adoption of reference computational phantoms (ICRP, 2009), and the development of the new generation of reference biokinetic models.

(17) This series of reports provides revised dose coefficients for OIR replacing the *Publication 30* series (ICRP, 1979, 1980, 1981, 1988b) and *Publication 68* (ICRP, 1994b). Data for the interpretation of bioassay measurements are also provided, replacing *Publications 54* and *78* (ICRP, 1988a, 1997b), and consolidating all of the information needed to interpret the results of bioassay measurements for a particular radionuclide in a single ICRP publication.

(18) The full data set of the series of reports is provided as an electronic annex. The printed reports contain a selected set of data and materials. Data are presented in a standard format for each element and its radioisotopes. Tabulated dose coefficients may be used to determine committed effective dose and committed equivalent doses to an organ or tissue from a known intake of a radionuclide. Tabulated values for dose per content function may be used to assess committed doses directly from measurements of appropriate bioassay quantities (e.g. radionuclide activity in whole body or lungs, or daily excretion of a radionuclide in urine or faeces). Similarly, values of radionuclide activities per intake in the body or in daily excreta samples, presented in tabular and graphical formats, may be used to assess the intake corresponding to a single bioassay measurement. Committed doses may then be assessed from the intake using the tabulated dose coefficients. A full description of the information provided for each element and radioisotope is given in Section 7.

(19) The revised dose coefficients, dose per content functions, and reference bioassay functions have been calculated using the *Publication 100* (ICRP, 2006) HATM and a revision of the *Publication 66* (ICRP, 1994a) HRTM which takes account of more recent data. The revisions made to the HRTM are described in Section 3.2 and Annex A of this report. In addition, information is provided in this series of reports

on absorption into blood following inhalation and ingestion of different chemical forms of elements and their radioisotopes. In selected cases, it is judged that the data are sufficient to make material-specific recommendations. Revisions have been made to many models for the systemic biokinetics of radionuclides, making them more physiologically realistic representations of uptake and retention in organs and tissues, and of excretion.

(20) Biokinetic models, reference physiological data, computational phantoms, and radiation transport calculation codes are used for the calculation of dose coefficients (ICRP, 2007). ICRP publishes dose coefficients for the inhalation or ingestion of individual radionuclides by workers, giving both equivalent doses to organs and tissues, and effective dose (ICRP, 1991, 2007). The steps in the calculation (Fig. 1.1) can be summarised as follows:

- By use of the reference biokinetic models, the distribution and retention of radionuclides in body organs and tissues of the Reference Worker are determined as a function of time after intake by inhalation or ingestion. For radiation protection purposes, it is assumed that all biokinetic parameters of the Reference Worker are invariant on sex, anatomy, physiology, race, and other individual-related factors, but based on the Reference Male parameter values where sex-specific models are available. The total number of nuclear transformations (radioactive decays) occurring within a 50-year period in each source region is calculated.
- The dosimetric models based on male and female reference computational phantoms and Monte Carlo radiation transport codes are used to calculate the sex-specific absorbed dose in each target organ or tissue resulting from a nuclear disintegration in each source region.

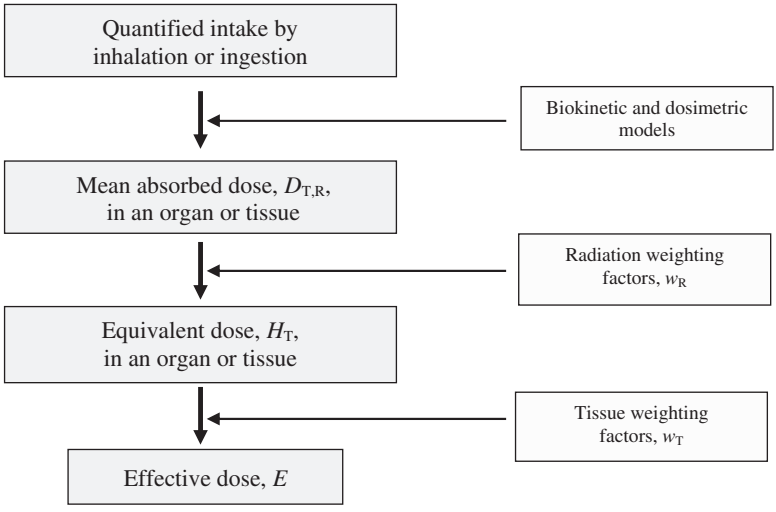

Fig. 1.1. Calculation of absorbed dose and the protection quantities – equivalent and effective dose – for intakes of radionuclides.

- The radiation weighting factors are applied to determine sex-specific committed equivalent doses to an organ or tissue.
- The sex-specific committed equivalent doses are sex-averaged.
- The tissue weighting factors are applied to determine the sex-averaged committed effective dose.

(21) The details of the computational procedure used in this series of reports are described in Section 3.7.

1.3. Previous reports on occupational intakes of radionuclides

(22) *Publication 30* (ICRP, 1979, 1980, 1981, 1988b) and its supplements gave dose coefficients and values of the annual limit on intake (ALI) for workers, for intakes of radionuclides by inhalation and ingestion, referencing the recommendations issued in *Publication 26* (ICRP, 1977) and the anatomical and physiological data in *Publication 23* (ICRP, 1975). *Publication 68* (ICRP, 1994b) provided updated dose coefficients for workers following the 1990 Recommendations in *Publication 60* (ICRP, 1991). It applied the *Publication 66* HRTM (ICRP, 1994a) for inhaled radionuclides, the updated basic anatomical and physiological data for the skeleton in *Publication 70* (ICRP, 1995a), and revised systemic biokinetic models for selected isotopes of 31 elements given in *Publications 56*, *67*, *69*, and *71* (ICRP, 1989, 1993b, 1995b,c). Biokinetic models for other elements were taken from *Publication 30* (ICRP, 1979, 1980, 1981, 1988b) and modified by addition of explicit excretion pathways to improve dose estimates for the urinary bladder and colon walls. *Publication 68* (ICRP, 1994b) did not give ALIs, because ICRP wished to emphasise the need to take account of all exposures to ionising radiation in the workplace from external radiation and intakes of all radionuclides.

(23) *Publications 54* and *78* gave guidance on the design of monitoring programmes and the interpretation of results to estimate doses to workers following radionuclide inhalation or ingestion (ICRP, 1988a, 1997b). The guidance was supported by numerical data to enable the assessment of intakes and doses from bioassay data (i.e. measurements of body and organ content, and daily urinary and faecal excretion). These data were provided for a number of radionuclides selected as those most likely to be encountered in the workplace. Predicted values of the measured quantities for various times after a single intake or for routine monitoring were given in terms of the activity of the intake per activity measured. Standard dose coefficients would then be used to calculate effective dose from the assessed intake.

1.4. Changes in *Publication 103* (ICRP, 2007) that affect the calculation of equivalent and effective dose

(24) In the 2007 Recommendations issued in *Publication 103* (ICRP, 2007), the concept and use of equivalent and effective dose remain unchanged, but a number of

Table 1.1. International Commission on Radiological Protection radiation weighting factors.

	Radiation weighting factor, w_R	
Radiation type	*Publication 103* (ICRP, 2007)	*Publication 60* (ICRP, 1991)
Photons	1	1
Electrons and muons	1	1
Protons and charged pions	2	5*
Alpha particles, fission fragments, heavy ions	20	20
Neutrons	Revised continuous function of neutron energy	Step and continuous functions of neutron energy

*Pions were not considered.

Table 1.2. *Publication 103* (ICRP, 2007) tissue weighting factors.

Tissue	w_T	$\Sigma\ w_T$
Bone marrow, breast, colon, lung, stomach, remainder tissues (13*)	0.12	0.72
Gonads	0.08	0.08
Urinary bladder, oesophagus, liver, thyroid	0.04	0.16
Bone surface, brain, salivary glands, skin	0.01	0.04

*Remainder tissues: adrenals, extrathoracic regions of the respiratory tract, gall bladder, heart, kidneys, lymphatic nodes, muscle, oral mucosa, pancreas, prostate (male), small intestine, spleen, thymus, and uterus/cervix (female).

revisions were made to the methods used in their calculation. Changes were introduced in the radiation and tissue weighting factors from the values previously recommended in *Publication 60* (ICRP, 1991). As radiation weighting factors (w_R) for photons, electrons, and alpha particles are unchanged, the only difference of potential importance to internally deposited radionuclides is for neutrons (Table 1.1). The changes made do not reflect the availability of additional data, but rather a reconsideration of the appropriate treatment of radiation weighting for protection purposes. The abandonment of a step function for neutron w_R as a function of energy is a reflection of the fact that, in practice, only a continuous function has been used. The major change in the continuous function is a lower w_R value at low energies that more properly reflects the low linear energy transfer contribution from secondary photons. In addition, there are good theoretical reasons for assuming that w_R values at high energies will converge with that for protons.

(25) The values of tissue weighting factors (w_T) recommended in *Publication 103* (ICRP, 2007) are shown in Table 1.2. Changes from values given in *Publication 60* (ICRP, 1991) reflect improved knowledge of radiation risks. The main sources of

data on cancer risks are the follow-up studies of the Japanese atomic bomb survivors, used to derive risk coefficients averaged over seven Western and Asian populations with different background cancer rates (ICRP, 2007). The new w_T values are based on cancer incidence rather than mortality data, adjusted for lethality, loss of quality of life, and years of life lost. Weighting for hereditary effects is now based on estimates of disease in the first two generations rather than at theoretical equilibrium. The main changes in w_T values in the 2007 Recommendations (ICRP, 2007) are an increase for breast (from 0.05 to 0.12), a decrease for gonads (from 0.2 to 0.08), and inclusion of more organs and tissues in a larger 'remainder' (from 0.05 to 0.12). The remainder dose is now calculated as the arithmetic mean of the doses to the 13 organs and tissues for each sex (Table 1.2). Tissue weighting factors continue to represent averages across the sexes and across all ages.

(26) A further important change introduced in the 2007 Recommendations (ICRP, 2007) is that doses from external and internal sources are calculated using reference computational phantoms of the human body (ICRP, 2009). In the past, the Commission did not specify a particular phantom, and various mathematical phantoms such as hermaphrodite Medical Internal Radiation Dose (MIRD)-type phantoms (Snyder et al., 1969), the sex-specific models of Kramer et al. (1982), or the age-specific phantoms of Cristy and Eckerman (1987) have been used. Voxel models, constructed from medical imaging data of real people, give a more realistic description of the human body than afforded in mathematical (or stylised) phantoms. Thus, ICRP decided to use voxel models to define the reference phantoms to be used in the calculations of dose distribution in the body for both internal and external exposures. These models (or computational phantoms), described in *Publication 110* (ICRP, 2009), represent the Reference Adult Male and Female. They are designed specifically for calculation of the radiological protection quantities corresponding to the effective dose concept of the 2007 Recommendations (ICRP, 2007). Equivalent doses to organs and tissues, H_T, are calculated separately for the Reference Adult Male and Female and then averaged in the calculation of effective dose, E:

$$
\begin{aligned}
&E = \sum_T w_T \left[\frac{H_T^M + H_T^F}{2} \right] \\
&\text{where :} \\
&H_T^M = \sum_T w_R D_{T,R} \quad \text{(male)} \\
&H_T^F = \sum_T w_R D_{T,R} \quad \text{(female)}
\end{aligned}
\tag{1.1}
$$

(27) It is made clear in *Publication 103* (ICRP, 2007) that effective dose is intended for use as a protection quantity on the basis of reference values, and relates to reference persons rather than specific individuals. The main uses of effective dose are in prospective dose assessment for planning and optimisation in radiological protection, and retrospective demonstration of compliance for regulatory purposes.

Sex-averaging in the calculation of equivalent and effective doses, implicit in the past use of hermaphrodite mathematical phantoms, is now explicit in the averaging of equivalent doses to adult male and female phantoms. Sex- and age-averaging in the derivation of tissue weighting factors can be seen to obscure differences in estimates of absolute radiation detriment between men and women, and between adults and children. However, practical protection would not be improved by calculating effective dose separately for males and females or different age groups, and to do so might give a misleading impression of the precision of these quantities.

1.5. Biokinetic models implemented in this series of reports

(28) Biokinetic models for individual elements and their radioisotopes are used to calculate the total number of transformations occurring within specific tissues, organs, or body regions (source regions) during a given period of time (usually 50 years for adults, or to age 70 years for children) by determining the time-integrated activity in each source region. Dosimetric models are used to calculate the deposition of energy in all important organs/tissues (targets) for transformations occurring in each source region, taking account of the energies and yields of all emissions (ICRP, 2008). Committed absorbed dose in target regions (in grays) can then be calculated, knowing the number of decays occurring in source regions and energy deposition in target regions.

(29) Biokinetic models of the alimentary and respiratory tracts are used to define the movement of radionuclides within these systems, resulting in absorption into blood and/or loss from the body. The behaviour of radionuclides absorbed into blood is described by element-specific systemic models that range in complexity. These models are intended both for the derivation of dose coefficients and the interpretation of bioassay data. The models used in this series of reports are as given below, with more information provided in Section 3.

1.5.1. Human Respiratory Tract Model

(30) The HRTM described in *Publication 66* (ICRP, 1994a) has been updated in this report to take account of data accumulated since its publication, although the basic features of the model remain unchanged. Inhaled particles containing radionuclides deposit in the extrathoracic (ET) airways (nose, larynx, etc.), the bronchial (BB) and bronchiolar (bb) airways of the lung, and the alveolar–interstitial (AI) region, with deposition in the different regions being mainly dependent on particle size (ICRP, 1994a, 2002b). Removal from the respiratory tract occurs mainly by dissolution and absorption into blood, and the competing process of transport of particles to the throat followed by their entry into the alimentary tract. The proportions absorbed into blood or cleared by particle transport depend on the speciation and the solubility of the material, and on the radioactive half-life of the radionuclide.

The ICRP model for the respiratory tract is also applied here to gases and vapours, and to inhalation of radon and its radioactive progeny.

(31) For absorption into blood, the main changes introduced in this report are as follows.

- Redefinition of the Type F, M, and S absorption defaults: larger rapid dissolution fraction (f_r) values for Types M and S of 0.2 and 0.01, rather than 0.1 and 0.001, respectively, with lower rapid dissolution rate (s_r) values of 3 d^{-1} for Types M and S, and 30 d^{-1} for Type F, rather than 100 d^{-1}.
- Material-specific parameter values for f_r, s_r, and the slow dissolution rate (s_s) in selected cases where sufficient information is available (e.g. forms of uranium).
- Element-specific values of s_r and the bound state parameters, f_b and s_b, where sufficient information is available.
- Revised treatment of gases and vapours in which solubility and reactivity are defined in terms of the proportion deposited in the respiratory tract. The default assumption is 100% deposition (20% ET_2, 10% BB, 20% bb and 50% AI) and Type F absorption. The SR-0, -1, -2 classification described in *Publication 66* (ICRP, 1994a) has not been found to be helpful and is no longer used.

(32) For clearance by particle transport, the main changes are as follows.

- More realistic clearance from the nasal passage, including transfer from the anterior to the posterior region, based on recent human experimental studies.
- Revised characteristics of slow particle clearance from the bronchial tree based on recent human experimental studies. It is now assumed that it occurs only in the bronchioles rather than as a particle-size-dependent phenomenon throughout the bronchial tree.
- Longer retention in the AI region of the lung, with a revised model structure, based on recent data including long-term follow-up of workers exposed to insoluble ^{60}Co particles and plutonium dioxide.

1.5.2. Human Alimentary Tract Model

(33) The *Publication 30* (ICRP, 1979) model of the gastrointestinal tract has been replaced by the HATM described in *Publication 100* (ICRP, 2006). The main features of the HATM can be summarised as follows.

- Inclusion of all alimentary tract regions: oral cavity, oesophagus, stomach, small intestine, right colon, left colon, and rectosigmoid (sigmoid colon and rectum).
- A default assumption that absorption of an element and its radioisotopes into blood occurs exclusively in the small intestine (i.e. the total fractional absorption, f_A, equals the fractional absorption from the small intestine, f_{SI}). A model structure that allows for absorption in other regions, where information is available.

- A model structure that allows for retention in the mucosal tissues of the walls of alimentary tract regions, and on teeth, where information is available.
- Explicit specification of the location of target regions for cancer induction within each region of the alimentary tract.

(34) *Publication 100* (ICRP, 2006) gave preliminary values of electron and alpha particle absorbed fractions to stem cell layers of sections of the alimentary tract. As part of this report, new calculations have been performed for both particle types, and for both content and wall sources. For regions within the small intestine, new models of segment folding have been implemented. Additional details will be given in a forthcoming publication (ICRP, 2016c).

1.5.3. Systemic models

(35) A systemic model describes the time-dependent distribution and retention of a radionuclide in the body after it reaches the systemic circulation, and its excretion from the body. In contrast to ICRP's current and past biokinetic models describing the behaviour of radionuclides in the respiratory and alimentary tracts, ICRP's systemic models have generally been element-specific with regard to model structure as well as parameter values. A single generic model structure that depicts all potentially important systemic repositories and paths of transfer of all elements of interest in radiation protection would be too complex to be of much practical use. However, generic model structures have been used in previous ICRP reports to address the systemic biokinetics of groups of elements, typically chemical families, known (or expected) to have qualitatively similar behaviour in the body. For example, *Publication 20* (ICRP, 1973) introduced a generic model formulation for the alkaline earth elements calcium, strontium, barium, and radium, but provided element-specific values for most model parameters. In Parts 1–3 of *Publication 30* (ICRP, 1979, 1980, 1981), a model developed for plutonium, including parameter values as well as model structure, was applied to most actinide elements. The use of generic systemic model structures was increased in ICRP reports on doses to members of the public from intake of radionuclides (ICRP, 1993, 1995b,c), and is further expanded in this report because it facilitates the development, description, and application of systemic biokinetic models. An important development is that, as the availability of data allows, models have been made to be more physiologically realistic with regard to the dynamics of organ retention and excretion, so that they are applicable to the interpretation of bioassay data as well as the calculation of dose coefficients.

1.5.4. Rules for treatment of radioactive progeny

(36) A dose coefficient for a radionuclide that gives rise to a chain of radionuclides through radioactive decay (called a 'parent' radionuclide) includes doses from radioactive progeny produced in vivo following intake of the parent. The dose coefficient

may depend strongly on assumptions concerning the biokinetics of the progeny. The following assumptions are made in this series of reports concerning the fate of progeny radionuclides produced in the body by radioactive decay.

(37) For all radionuclides with the exception of noble gases:

- The parameter values describing absorption of the inhaled parent from the respiratory tract into blood are applied to all members of the decay chain formed in the respiratory tract.
- The systemic biokinetics of a progeny radionuclide produced by decay in a systemic compartment, or absorbed into blood following production by decay in the respiratory tract or alimentary tract, are defined in the element section for the parent, given in a later part of this series of reports. As a rule with some exceptions, the systemic biokinetics of the progeny are assumed to be independent of the systemic biokinetics of the parent. For decay chains whose members are all isotopes of the same element, the progeny are assigned the same kinetics as the parent throughout the body.
- The default absorption fraction, f_A, for a progeny radionuclide produced by decay in the contents of the alimentary tract (in the small intestine or a higher compartment) following ingestion of a parent radionuclide, or produced in a systemic compartment and subsequently transferred into the alimentary tract content, is the reference value of f_A for the progeny radionuclide when ingested as a parent. If the radionuclide has multiple reference values corresponding to different chemical or physical forms, the default value of f_A is the highest reference value provided.
- The default absorption fraction, f_A, for a progeny radionuclide produced in the respiratory tract following inhalation of a parent, or produced in the alimentary tract following transfer of activity from the respiratory tract to the alimentary tract, is the product of the fraction of inhaled material with rapid dissolution (f_r) for the assigned absorption type, and the reference value of f_A for the progeny radionuclide when ingested as a parent radionuclide. If the progeny radionuclide has multiple reference values of f_A when ingested as a parent, corresponding to different chemical or physical forms, the default value of f_A is the product of f_r for the absorption type and the highest reference value provided.

(38) Noble gases produced in compartments of the respiratory tract and in the alimentary tract models by radioactive decay are assumed to escape from these compartments directly to the environment at a rate of 100 d^{-1}, without transfer to the blood compartment and without transfer between compartments of respiratory tract and alimentary tract models. It is assumed that progeny of such noble gases formed within the body follow the rules stated in Para. 37.

1.6. Dosimetry implemented in this series of reports

(39) Dose calculations involve the use of nuclear decay data, anthropomorphic phantoms that describe the human anatomy, and codes that simulate radiation

transport and energy deposition in the body. The data provided in this series of reports are calculated using revised decay data (ICRP, 2008), the ICRP reference computational phantoms of the adult male and female based on medical imaging data (ICRP, 2009), and well-established Monte Carlo codes (Pelowitz, 2008; Kawrakow et al., 2009; Niita et al., 2010).

(40) For all dose calculations, radionuclides are assumed to be uniformly distributed throughout source regions, although these can be whole organs (e.g. liver) or a thin layer within a tissue (e.g. bone surfaces). Similarly, target cells are assumed to be distributed uniformly throughout target regions that vary in size from whole organs to layers of cells. Doses from 'cross-fire' radiation between source and target regions are important for penetrating photon radiation. For 'non-penetrating' alpha and beta particle radiations, energy will, in most cases, be largely deposited in the tissue in which the radionuclide is deposited. Photon and electron transport are followed for most source and target combinations. Additionally, special considerations are taken into account for alpha and beta emissions in a number of important cases. These include:

- doses to target cells in the walls of the respiratory tract airways from radionuclides in the airways (ICRP, 1994a);
- doses to target cells in the alimentary tract from radionuclides in the lumen (ICRP, 2006); and
- doses to cells adjacent to inner bone surfaces (50-μm layer; see below) and all red marrow from radionuclides on bone surfaces and within mineral bone.

1.6.1. Nuclear decay data, *Publication 107* (ICRP, 2008)

(41) A fundamental requirement for dose calculations is reliable information on half-life, modes of decay, and the energies and yields of the various radiations emitted by radionuclides and their progeny (Eckerman et al., 1994; Endo et al., 2003, 2005). The calculations in this report use the nuclear decay data provided in *Publication 107* (ICRP, 2008). This publication replaces *Publication 38* (ICRP, 1983) and consists of an explanatory text, with an accompanying CD-ROM providing data on the radiation emissions of 1252 radioisotopes of 97 elements. Radioisotopes of elements with an atomic number below 101 were included in *Publication 107* (ICRP, 2008) if their half-lives exceed 1 min or if they are the progeny of a selected radionuclide and if the basic nuclear structure data enabled a meaningful analysis of their emissions. CD-ROM use has enabled the complete listing of emitted radiations, and more details of Auger cascades and spontaneous fission data. The data given include: energies and intensities of emitted radiations; beta, neutron, and Auger and Coster-Kronig (CK) electrons spectra; spontaneous fission radiations and alpha recoil; half-lives, branching decay, and chains; and no cut-off on the number of emissions.

(42) In this series of reports, dose coefficients and bioassay functions are presented for almost all radionuclides included in *Publication 107* (ICRP, 2008) that have half-lives equal to or greater than 10 min, and for other selected radionuclides. For

radionuclides with decay chains, all parent radionuclides with half-lives equal to or greater than 10 min are included, but no constraint is placed on the half-lives of daughter radionuclides.

1.6.2. Adult reference computational phantoms, *Publication 110* (ICRP, 2009)

(43) Traditionally, stylised computational phantoms of human anatomy have been used in the calculation of dose coefficients for both external and internal radiation protection. These phantoms are constructed using mathematical surface equations to describe internal organ anatomy and exterior body surfaces of reference individuals (Cristy, 1980; Cristy and Eckerman, 1987), and, as such, are limited in their ability to capture anatomical realism. As an alternative format for radiation transport simulation, voxel phantoms are based on segmented tomographic data of real individuals obtained from computed tomography (CT) or magnetic resonance imaging (Zankl et al., 2002, 2003, 2007). As outlined above, the 2007 Recommendations (ICRP, 2007) adopted the use of realistic anatomical models for the revision of dose coefficients for both internal and external radiation sources. *Publication 110* (ICRP, 2009) describes the development and intended use of the computational phantoms of the Reference Adult Male and Female. The reference phantoms were constructed after modifying the voxel models of two individuals whose body height and mass closely matched reference values. The report describes the methods used for this process and the anatomical and computational characteristics of the resulting phantoms.

(44) The computational phantoms of the Reference Adult Male and Female may be used, together with codes that simulate radiation transport and energy deposition, for assessment of the mean absorbed dose, D_T, in an organ or tissue T, from which equivalent doses and the effective dose may be calculated successively.

1.6.3. Advances in skeletal dosimetry

(45) In this report, the skeletal dosimetry models of *Publication 30* (ICRP, 1979) have been updated substantially for all radiations emitted from internalised radionuclides – alpha particles, electrons, beta particles, photons, and neutrons (e.g. from spontaneous fission). Improvements over the *Publication 30* models include more refined treatment of the dependence of the absorbed fraction on particle energy, marrow cellularity, and bone-specific spongiosa micro-architecture. Two reference sets of skeletal images were established for radiation transport simulation. The first included 1-mm ex-vivo CT images of some 38 skeletal sites harvested from a 40-year-old male cadaver (Hough et al., 2011). These images were used to establish fractional volumes of cortical bone, trabecular spongiosa, and medullary cavities by skeletal site, and to serve as the macroscopic geometric model for particle transport. The second included 30-μm micro-CT images of cored samples of trabecular spongiosa to

establish fractional volumes of trabecular bone and marrow tissues, and to serve as the microscopic geometric model for particle transport. Both image sets were combined during paired-image radiation transport of internally emitted electrons (Shah et al., 2005). Source tissues were: bone marrow (active and inactive), mineral bone surfaces (trabecular and cortical), and mineral bone volumes (trabecular and cortical). Target regions considered were: active marrow (surrogate tissue for the haematopoietic stem and progenitor cells), and a revised 50-μm model of the skeletal endosteum (surrogate tissue for the osteoprogenitor cells) (see 'endosteum' in the Glossary). Absorbed fractions for internalised alpha particles and neutron-generated recoil protons were established based on path-length-based transport algorithms given in Jokisch et al. (2011a,b). Values of absorbed fractions to active marrow and endosteum for internally-emitted photons and neutrons were obtained by first tallying energy-dependent particle fluences within the spongiosa and medullary cavity regions of the *Publication 110* Reference Adult Male and Female voxel phantoms (ICRP, 2009), and then applying fluence-to-absorbed dose response functions (DRFs). Further details on the derivation of these photon and neutron skeletal DRFs are given in Johnson et al. (2011) and Bahadori et al. (2011), respectively, as well as in Annexes D and E of *Publication 116* (ICRP, 2010).

1.7. Interpretation of bioassay data

(46) The system of dose assessment from bioassay data that is generally applied relies on evaluation of the intake of a radionuclide either from direct measurements (e.g. external monitoring of the whole body or of specific organs and tissues) or indirect measurements (e.g. of urine, faeces, or environmental samples). Predicted values of these measured quantities for intake of a radionuclide are recommended by ICRP, and these values can be used to estimate the intake (ICRP, 1997b). The committed effective dose resulting from any intake is then calculated using the appropriate dose coefficient recommended by ICRP or determined using ICRP's recommended methodology. In some cases, national authorities require assessment of the intake of a radionuclide as well as formal assessment of dose. The data provided also serve for this purpose.

(47) It is possible, as discussed by Berkovski et al. (2003a), to calculate committed effective dose directly from bioassay measurements using functions that relate them to the time of the intake. The main advantage of this approach is that the user does not perform the intermediate step of calculating the intake in order to evaluate the dose. This eliminates the risk of using bioassay functions calculated with a particular biokinetic model and dose coefficients derived from a different (earlier or more recent) version of that model. This has been shown to be a frequent cause of miscalculations in intercomparison exercises (IAEA, 2007).

(48) Whichever approach is adopted, the assessed dose is, in many cases, less sensitive to the choice of parameter values than the assessed intake. Berkovski et al. (2003a) showed that for a number of chemical forms of radionuclides, the 'dose per content function' is largely insensitive to the choice of inhaled particle

size for a wide range of measurement times following an intake. In such circumstances, the need for specific information on the appropriate AMAD of an aerosol may not therefore arise. Similarly, dose per content function may be insensitive to the choice of absorption type for the specific chemical form involved, for specific ranges of measurement times after the intake. Care is still needed in the choice of the most appropriate measurement data and in defining the time of the intake.

(49) Effective dose assessed from bioassay measurements is relatively insensitive to choice of parameter values when the measured quantity is directly related to an organ dose that makes a dominant contribution to the effective dose (e.g. in the case of lung retention measurements after inhalation of an insoluble ^{60}Co compound, where lung dose dominates the effective dose). However, sensitivity to parameter values may be much higher when the measured quantity is less closely related to the effective dose, such as when lung dose makes a dominant contribution to effective dose and urine monitoring is employed. For such a case, the results of urine monitoring can provide a reliable measure of doses to systemic organs, but assessed lung dose is sensitive to choice of absorption parameter values. An example is the assessment of effective dose from urine monitoring data after inhalation of an insoluble uranium compound.

1.8. Structure of the report

(50) This series of reports provides revised dose coefficients for OIR by inhalation and ingestion, replacing the *Publication 30* series (ICRP, 1979, 1980, 1981, 1988b) and *Publication 68* (ICRP, 1994b). It also provides data for the interpretation of bioassay measurements, replacing *Publications 54* and *78* (ICRP, 1988a, 1997b).

(51) Section 2 of this report discusses the application of dose limits and constraints to the control of occupational exposures to radionuclides. It also outlines the objectives and requirements of monitoring programmes designed to ensure compliance with regulatory requirements. Section 3 gives an overview of the biokinetic and dosimetric models used to calculate dose coefficients and bioassay functions. It explains the changes made to the *Publication 66* HRTM (ICRP, 1994a), and describes the main features of the *Publication 100* HATM (ICRP, 2006). Section 3 also provides an introduction to the models used in this series of reports to describe the systemic biokinetics of elements and their radioisotopes. Dosimetric models and the ICRP computational methodology are also explained.

(52) A description of methods for individual monitoring is given in Section 4. The section covers in-vivo measurements and the analysis of excreta and other biological materials, as well as workplace monitoring. The general principles for design of monitoring programmes, types of programmes, and monitoring requirements are summarised in Section 5. Also covered briefly are wound monitoring and the potential effects of medical intervention. General aspects of retrospective dose assessment are considered in Section 6. The section examines the need to understand the exposure situation and radionuclide(s) being handled, as well as their physicochemical form. It discusses the requirements for an

effective monitoring programme, and summarises approaches to data handling for single or multiple measurements. Uncertainties associated with the use of biokinetic models for interpretation of the results of bioassay measurements are considered.

(53) Section 7 provides a brief outline of the types of information included in subsequent parts of this series of reports: biokinetic data; dose coefficients; and data for bioassay interpretation for individual elements and their radioisotopes. Each element section provides: dose coefficients [committed effective dose and committed equivalent doses to organs or tissues per Bq intake (Sv Bq^{-1}) for inhalation and ingestion of all relevant radioisotopes]; dose per content functions [committed effective dose per predicted activity content in the body or in a given organ or per daily excretion (Sv Bq^{-1})]; and reference bioassay functions [values of activity (Bq) retained in the body or specific organs, or excreted in urine or faeces, at various times after unit intake (i.e. 1 Bq) by inhalation or ingestion]. Data are provided in the printed reports of the series and in the electronic annex.

(54) The data provided in the printed reports are restricted to tables of committed effective dose per intake (Sv Bq^{-1}), tables of committed effective dose per content (Sv Bq^{-1}), and graphs for reference bioassay functions. Data are provided for all absorption types of the most common isotope(s), and for an AMAD of 5 μm. In cases for which sufficient information is available (principally for actinide elements), lung absorption is specified for different chemical forms, and dose coefficients and bioassay functions are calculated accordingly.

(55) The electronic annex that accompanies this series of reports contains a comprehensive set of committed effective and equivalent dose coefficients, dose per content functions, and reference bioassay functions for most of the isotopes presented in *Publication 107* (ICRP 2008), and for a range of physicochemical forms and aerosol AMADs. Data for intake by ingestion and for direct input to the blood are also given. The electronic annex provides dose coefficients and other radionuclide-specific data as a set of data files that may be accessed by the user directly or by using the accompanying Data Viewer. The Data Viewer permits rapid navigation of the dataset and visualisation of the data in tabulated and graphical formats, such as graphs of the time series of dose per content function values or predicted activity content per dose (Bq Sv^{-1}) as a function of time after intake.

2. MONITORING AND ASSESSMENT OF INTERNAL OCCUPATIONAL EXPOSURES TO RADIONUCLIDES

2.1. Assessment of worker doses

(56) In an occupational exposure, doses are often received from both external and internal radiation sources. For retrospective assessments of external exposure, individual monitoring is usually performed by measuring the personal dose equivalent using personal dosimeters and taking this measured value as an acceptable estimate of the value of effective dose (ICRP, 2010). For retrospective assessments of internal exposure, committed effective dose values are determined from measurements of radionuclide activities in the body, in bioassay samples, or in the workplace.

(57) As indicated in Section 1.1, the worker's dose of record, E, should be estimated as:

$$E \cong H_{\mathrm{p}}(10) + E(50) \tag{2.1}$$

where $H_{\mathrm{p}}(10)$ is the measured personal dose equivalent (external exposure), and $E(50)$ is the committed effective dose from internal exposure as assessed by:

$$E(50) = \sum_{j} e_{\mathrm{j,inh}}(50) \cdot I_{\mathrm{j,inh}} + \sum_{\mathrm{j}} e_{\mathrm{j,ing}}(50) \cdot I_{\mathrm{j,ing}} \tag{2.2}$$

where $e_{\mathrm{j}}(50)$ is the dose coefficient (committed effective dose per intake, Sv Bq^{-1}) of a radionuclide, integrated over 50 years after intake by inhalation (inh) and/or ingestion (ing). The intakes, I_{j} (Bq), may be for one or a number of radionuclides j.

2.2. Objectives of monitoring

(58) The purpose of monitoring for internal exposure to radionuclides is to verify and document that the worker is protected adequately against radiological risks, and that the protection afforded complies with legal requirements. Two types of monitoring of internal exposures of workers can be identified: individual monitoring and workplace monitoring.

(59) Individual monitoring of internal exposure uses measurements made for individual workers for the assessment of their dose of record, together with other dosimetric quantities if required. The principal objectives of individual monitoring in planned and existing situations are:

- to assess the worker's dose of record and to demonstrate compliance with regulatory requirements; and
- to contribute to the safety management and control of the operation of the facility.

(60) The principal objectives of individual monitoring of workers in emergency situations are:

- to document the worker's exposure in terms of dose of record, and, if appropriate, in terms of absorbed doses in significantly exposed organs or tissues; and
- to provide information for the initiation and support of any appropriate health surveillance and treatment.

(61) Usually, it is only necessary to undertake a simple assessment of dose to demonstrate compliance with regulatory requirements when annual doses are expected to be small fractions of the dose limits. At higher doses, more emphasis will need to be placed upon specific dose assessments and the circumstances of any exposure.

(62) Measurements, together with information about the workplace, should enable each radionuclide to be identified, its activity quantified, and the measurement result interpreted in terms of intake and/or committed effective dose. There may be some circumstances where individual monitoring techniques are not adequate to assess doses, and it may be necessary to combine individual and workplace monitoring techniques.

(63) Workplace monitoring of internal exposures makes use of measurements made in the working environment. An example is the measurement of radionuclide concentration(s) in air using static air samplers. In general, workplace monitoring complements individual monitoring. It may be used for monitoring internal exposures in place of individual monitoring when the latter is not justified, or where the sensitivity of individual monitoring is inadequate. It can be used to provide an assessment of exposure for groups of workers, but this requires assumptions to be made about exposure conditions. It is also of value in demonstrating that working conditions meet safe working criteria and have not changed. It can indicate the release of radionuclides into the working environment, and thus trigger subsequent individual monitoring measurements.

2.3. Categories of individual monitoring programme

(64) Routine monitoring is performed under conditions of essentially continuous risk of contamination of the workplace as a result of normal operations, or where undetected accidental intakes may occur. Measurements in a routine monitoring programme are made at predetermined times not related to known intakes, and therefore it is necessary to make some assumptions about the pattern of intakes. National or local legislation or regulations may also set the requirements for systematic routine monitoring that may be needed if exposures could exceed a specified fraction of the dose limit or a dose constraint.

(65) Other monitoring programmes may be conducted in relation to a particular task, or to determine intakes in actual or suspected abnormal conditions. In these circumstances, the time of intake, or potential intake, is likely to be known, and workplace monitoring programmes may provide some information on the physical

and chemical nature of any contamination. Special monitoring is performed to quantify significant exposures following actual or suspected abnormal events. Confirmatory monitoring is performed where there is a need to check assumptions made about exposure conditions (e.g. in order to confirm the effectiveness of protection measures). Task-related monitoring is undertaken for workers engaged in specific operations.

2.4. Needs for individual monitoring

(66) An important function of an employer and/or licensee is that of maintaining control over sources of exposure and ensuring the protection of workers who are occupationally exposed. In order to achieve this, the Commission continues to recommend the classification of controlled and supervised areas (ICRP, 2007). A controlled area requires consideration of specific protection measures and safety provisions for controlling normal exposures or preventing the spread of contamination during normal operations, and preventing or limiting the extent of accidental exposures. A supervised area is one in which the radiological conditions are kept under review but special procedures are not normally needed.

(67) It is necessary to identify groups of workers for whom individual monitoring is needed. The decision to provide individual monitoring depends on many factors. Routine individual monitoring for intakes of radioactive material should be used for workers in areas that are designated as controlled areas specifically in relation to the control of contamination, and in which significant intakes cannot be excluded.

(68) Workers in controlled areas are the group who are most often monitored for radiation exposures incurred in the workplace, and may also receive special medical surveillance. They should be well informed and specially trained, and form a readily identifiable group.

(69) The use of individual monitoring for workers whose annual effective doses could exceed 1 mSv is common practice in many organisations, although it may not be required by legislation. Regulatory, technical, and managerial considerations may support arguments for the assessment of individual dose at these lower levels, at least for those radionuclides for which assessment is straightforward and practical.

(70) The following examples indicate the type of operations where experience has shown that it is necessary to give consideration to routine individual monitoring for internal exposure of workers:

- the handling of large quantities of gaseous and volatile materials (e.g. tritium and its compounds in large-scale production processes, in heavy water reactors, and in luminising);
- maintenance of reactor facilities;
- handling of radioactive waste (e.g. from nuclear facilities and hospitals);
- the processing of plutonium and other transuranic elements;
- the processing of thorium ores and the use of thorium and its compounds [these activities can lead to internal exposure from both radioactive dusts and thoron (^{220}Rn) and its progeny];

- the mining, milling, and refining of uranium ores;
- natural and enriched uranium processing and fuel fabrication;
- work with large quantities of naturally occurring radioactive materials;
- the production of radiopharmaceuticals; and
- the handling of large quantities of ^{131}I for medical applications.

(71) The results of workplace monitoring may also indicate a need for a temporary programme of special individual monitoring aiming at identifying any need for a routine programme of workplace monitoring.

2.5. Pregnancy and breast feeding

(72) It is the Commission's policy (ICRP, 2007) that the methods of protection at work for women who are pregnant should provide a level of protection for the embryo/fetus broadly similar to that provided for members of the public. The Commission considers that this policy will be adequately applied if any exposures of the mother, prior to her declaration of pregnancy, are controlled under the system of protection recommended by the Commission. Once pregnancy has been declared, and the employer notified, additional protection of the embryo/fetus should be considered. The working conditions of a pregnant worker, after declaration of pregnancy, should be such as to make it unlikely that the additional external dose to the fetus, together with the committed effective dose to the fetus and newborn child from intakes of radionuclides before or during the pregnancy, would exceed approximately 1 mSv.

(73) ICRP has provided information in *Publications 88* and *95* (ICRP, 2001, 2004) on doses to the embryo, fetus, and newborn child following intake of radionuclides by female workers either before or during pregnancy, or during lactation. Comparisons of fetal dose coefficients given in *Publication 88* (ICRP, 2001) with corresponding adult dose coefficients showed that doses received by a woman from intakes before or during pregnancy will, in most cases, be substantially greater than doses to her fetus. However, doses to the offspring can exceed doses to the mother for a number of radionuclides. In particular, the requirements of skeletal development during fetal growth, particularly in late pregnancy, can lead to significant uptake of radioisotopes of phosphorus and calcium and, to a lesser extent, other alkaline earth elements. Thus, offspring to adult dose ratios reached factors of approximately 10–20 for isotopes of P and Ca, and 2–6 for isotopes of Sr (Stather et al., 2003; ICRP, 2004). Uptake of radioisotopes of iodine by the fetal thyroid can also lead to greater doses to the fetus than to the mother following intakes late in pregnancy (dose ratios of up to approximately 3) (Berkovski et al., 2003b). Other radionuclides for which doses to the fetus can exceed doses to the mother include tritium as tritiated water, ^{14}C, and ^{35}S. Offspring to adult dose ratios are greatest following ingestion or inhalation of soluble (Type F) forms. Values of offspring to adult dose ratios may change as a result of future calculations following from *Publication 103* (ICRP, 2007) and associated changes. Offspring protection may also be of concern when the dose ratio is <1, as an effective dose of 1 mSv to the

embryo, fetus, or newborn child might be reached at otherwise acceptable levels of occupational dose (Phipps et al., 2001).

(74) When a worker has declared pregnancy, possible doses to her child will be taken into account in measures taken to limit exposures. Thus, offspring doses resulting from intakes later in pregnancy may, in practice, be of less importance than doses resulting from intakes before the declaration of pregnancy. A number of radionuclides of potential significance in this category have been identified, including ^{63}Ni and ^{55}Fe (Phipps et al., 2001; Noßke and Karcher, 2003).

(75) In general, doses to the infant from radionuclides ingested in breast milk are estimated to be small in comparison with doses to the Reference Adult (ICRP, 2004). On the basis of the models developed in *Publication 95* (ICRP, 2004), it is only in the cases of tritiated water, ^{45}Ca, ^{75}Se, and ^{131}I that infant doses may exceed adult doses, by factors of between one and three. Infant doses are highest when maternal intakes by ingestion occur shortly after birth, because maximum transfer occurs under these conditions. Ratios of infant to adult doses are generally lower for intakes by inhalation than for ingestion. Comparisons with *Publication 88* (ICRP, 2001) doses to the offspring due to in-utero exposures show that, in most cases, these are more important than doses that may result from breast feeding; exceptions include ^{60}Co, ^{131}I, and ^{210}Po. ICRP intends to provide a revision of these dose coefficients in the near future.

3. BIOKINETIC AND DOSIMETRIC MODELS

3.1. Introduction

(76) This section gives an overview of the biokinetic and dosimetric models used to calculate dose coefficients and bioassay functions. It explains the changes made here to the HRTM (ICRP, 1994a), and describes the main features of the HATM (ICRP, 2006). It also provides an introduction to the models used in this series of reports to describe the systemic biokinetics of elements and their radioisotopes. Dosimetric models and methodology are also explained.

(77) Radionuclide exposures in the workplace can lead to intakes by a number of routes: inhalation, ingestion, and entry through intact skin and wounds. Fig. 3.1 summarises the routes of intake, internal transfers, and routes of excretion.

(78) For inhalation, the HRTM (ICRP, 1994a) was applied in *Publication 68* (ICRP, 1994b) and in subsequent publications on dose coefficients (ICRP, 1995c, 1996). For these implementations of the HRTM, chemical forms of radionuclides that had been assigned to Inhalation Classes D, W, and Y in *Publication 30* series (ICRP, 1979, 1980, 1981, 1988b) were assigned to Absorption Types F, M, and S of the HRTM, respectively. In the element sections of this series of reports, information

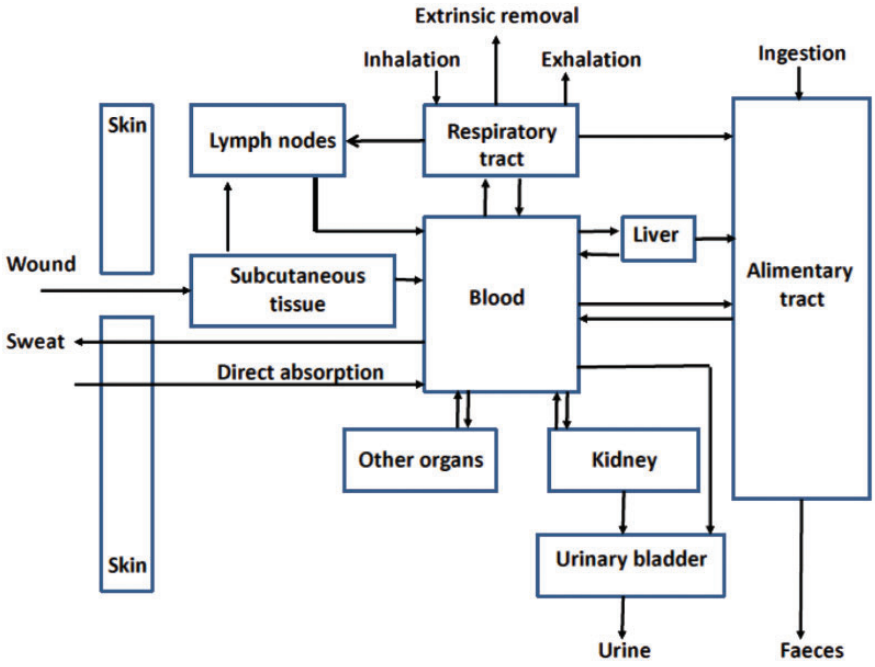

Fig. 3.1. Summary of the main routes of intake, transfer, and excretion of radionuclides in the body.

is reviewed on the lung clearance characteristics of different chemical forms of each element, within the framework of the HRTM. The opportunity has been taken to update some aspects of the HRTM in the light of information that has become available since *Publication 66* (ICRP, 1994a) was issued, as summarised in Section 1.5.2, and described in Section 3.2 and Annex A.

(79) For ingestion of radionuclides, the HATM (ICRP, 2006) is applied. The model is also used for radionuclides in particles cleared to the throat from the respiratory tract after inhalation. In the HATM, fractional absorption of radionuclides is specified by the alimentary tract transfer factor, f_A, instead of the f_1 value as given for the gastrointestinal tract model described in *Publication 30* (ICRP, 1979). The f_A value describes total absorption from all regions of the alimentary tract, although the default assumption is that all absorption takes place in the small intestine.

(80) ICRP has generally not given advice on assessing doses from intakes of radionuclides transferred from wound sites into blood and other organs and tissues. Internal exposure resulting from wounds almost always arises because of accidents in the workplace, rather than as a result of routine operations that are subject to the normal environmental controls. Uptake from wounds can vary greatly depending on the circumstances of a particular incident, and in practice, the assessment of internal contamination is treated on a case-by-case basis. As a result, provision of generic dose coefficients or bioassay functions would be of limited value. Information on the transfer of radionuclides from wound sites has, however, been reviewed by a Scientific Committee of the US National Council on Radiation Protection and Measurements (NCRP), and these data have been used to develop a model to describe the transfer of material from wounds after intakes in different physicochemical forms (NCRP, 2006). Section 3.4 summarises the main features of the NCRP model, as this information may be of use in the interpretation of bioassay data for individual cases of wound contamination.

(81) Time-dependent rates of uptake of a radionuclide from a wound site, computed for an individual case using models such as the NCRP wound model, could be used to compute dose estimates by convoluting these uptake rates with the dose coefficient for direct, acute intake into blood provided in the OIR electronic annex. Similarly, bioassay data for an individual case could be predicted by convoluting the time-dependent uptake rate with the time-dependent reference bioassay function for direct acute intake into blood, also provided in the OIR electronic annex. Similar analyses could be performed where time-dependent uptake rates of radionuclides via intact skin have been computed.

(82) For each route of intake, a portion of the radionuclide entering the body is absorbed into blood and distributed systemically. The systemic distribution of radionuclides in the body can be diffuse and relatively homogeneous, as for the examples of tritiated water and radioisotopes of potassium and caesium, or may be localised in certain organs or tissues, as for the examples of radioisotopes of iodine (thyroid), alkaline earth elements (bone), and plutonium (bone and liver). Systemic biokinetic models are used to describe the distribution and excretion of radionuclides absorbed

into blood. The systemic models for the elements have been reviewed and revised as necessary to take account of more recent information, and provide models that are appropriate for both dosimetry and bioassay interpretation.

(83) Removal of deposited material from the body occurs principally by urinary and faecal excretion, although radionuclides may also be lost by exhalation or through the skin (e.g. tritiated water). Urinary excretion is the removal in urine of radionuclides from blood following filtration by the kidneys. Faecal excretion has two components: systemic (endogenous) faecal excretion, which represents removal of systemic material via the alimentary tract due to biliary secretion from the liver and secretions at other sites along the alimentary tract; and direct (exogenous) faecal excretion of the material passing unabsorbed through the alimentary tract after ingestion or clearance to the throat from the respiratory system after inhalation. The reference models outlined in this section are assigned reference parameter values, and used to calculate body or organ content and daily urinary or faecal excretion at specified times after acute or chronic intake. They are used to calculate reference bioassay functions and, together with dosimetric data, reference dose coefficients. The Reference Worker was assigned the deposition and clearance parameter values of a healthy, non-smoking, normal nose-breathing adult male at light work. Light work is defined on the following basis: 2.5 h sitting, during which the amount inhaled is $0.54\,m^3\ h^{-1}$; and 5.5 h light exercise, during which the amount inhaled is $1.5\,m^3\ h^{-1}$. For both levels of activity, all the inhaled air enters through the nose.

3.2. Human Respiratory Tract Model

(84) The HRTM described in *Publication 66* (ICRP, 1994a) was applied to calculate inhalation dose coefficients for workers and members of the public in *Publications 68*, *71*, and *72* (ICRP, 1994b, 1995c, 1996), and bioassay functions in *Publication 78* (ICRP, 1997b). Further guidance on its use was given in the Guide for the Practical Application of the ICRP HRTM (ICRP, 2002b).

(85) A revised version of the HRTM is used in this series of reports as described below. Simple changes from the original HRTM are noted in this section. The major changes made relate to the clearance of deposited material by both particle transport and absorption into blood. These changes involved review and analysis of relevant recent information, and judgements in implementing the changes in the HRTM; they are described in Annex A.

(86) As in the original version of the HRTM, the respiratory tract is treated as two tissues: the extrathoracic (ET) and the thoracic (TH) airways. The subdivision of these tissues into regions was based mainly on differences in sensitivity to radiation. The TH regions are bronchial (BB: trachea, airway generation 0; bronchi, airway generations 1–8), bronchiolar (bb: airway generations 9–15), AI (gas exchange region, airway generations $\geq$16), and the TH lymph nodes (LN_{TH}). The ET regions are the anterior nasal passage (ET_1); the posterior nasal passage, pharynx, and

larynx (ET_2); and the ET lymph nodes (LN_{ET}) (Fig. 3.2). For consistency with the HATM, the oral passage is no longer included in region ET_2 as it was in *Publication 66* (ICRP, 1994a). This does not affect results obtained with the model, because deposition in the ET from air entering the mouth was taken to occur in the larynx alone.

3.2.1. Deposition

Aerosols of (solid or liquid) particulate materials

(87) The deposition model described in *Publication 66* (ICRP, 1994a) evaluates fractional deposition of an aerosol in each region for all aerosol sizes of practical interest (0.6 nm–100 μm). For the ET regions, measured deposition efficiencies were related to characteristic parameters of particle size and air flow, and were scaled by anatomical dimensions to predict deposition under other conditions (e.g. age, sex). For the TH airways, a theoretical model of gas transport and particle deposition was used to calculate particle deposition in each of the BB, bb, and AI regions, and to quantify the effects of the subject's lung size and breathing rate. To model particle deposition, the regions were treated as a series of filters during both inhalation and exhalation. The efficiency of each was evaluated by considering aerodynamic (gravitational settling, inertial impaction) and thermodynamic (diffusion) processes acting competitively. Regional deposition fractions were calculated for aerosols with log-normal particle size distributions, with geometric standard deviations taken to be a function of the median particle diameter, increasing from a value of 1.0 at 0.6 nm to a value of 2.5 above approximately 1 μm.

(88) No changes are made here to the *Publication 66* (ICRP, 1994a) implementation of the deposition model for aerosols, except for the distribution of the deposit in the ET airways between regions ET_1 and ET_2. As described in Annex A, the total deposit in the ET airways is now partitioned 65% to ET_1 and 35% to ET_2 [instead of approximately 50% to ET_1 and 50% to ET_2 as in *Publication 66* (ICRP, 1994a)].

(89) For occupational exposure, the default value generally recommended for the AMAD is 5 μm (ICRP, 1994b), consistent with the reviews of data by Dorrian and Bailey (1995), Kelso and Wraight (1996), and Ansoborlo et al. (1997), as previously described by ICRP (2002b, Section B9). An AMAD of a few microns is characteristic of aerosols produced by dispersion mechanisms. However, the short-lived progeny of radon are formed as airborne free ions, which react rapidly with trace gases and vapours to form particles with a diameter of approximately 1 nm ('unattached progeny'). These, in turn, may attach to existing atmospheric aerosol particles ('attached progeny'). Appropriate size distributions are recommended in the radon inhalation section [see details in OIR: Part 3 (ICRP, 2016b).

(90) Values of fractional deposition in each region of the respiratory tract of the Reference Worker are given in Table 3.1 for aerosols with an AMAD of 5 μm. Values for aerosols of other sizes are given in Annex A.

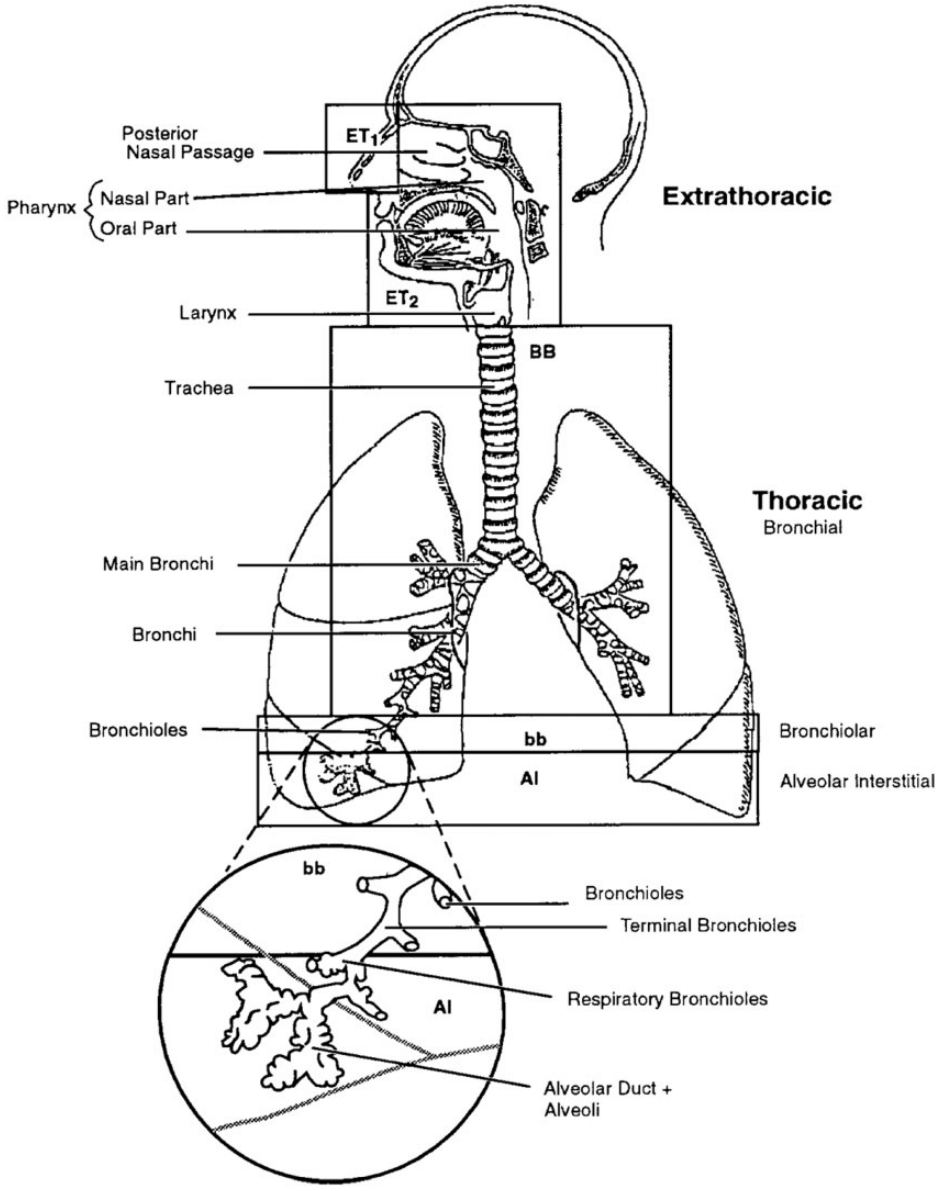

Fig. 3.2. Respiratory tract regions defined in the Human Respiratory Tract Model. Note that the oral part of the pharynx is no longer part of ET_2.
ET_1: extrathoracic region including the anterior nasal passage; ET_2: extrathoracic region including posterior nasal passage, pharynx and larynx; BB: bronchial region; bb: bronchiolar region; AI: alveolar interstitial region.

Table 3.1. Regional deposition of inhaled aerosols with an activity median aerodynamic diameter of 5 μm in the Reference Worker* (% of inhaled activity).

Region	Deposition (%)[†,‡]
ET_1	47.94
ET_2	25.82
BB	1.78
bb	1.10
AI	5.32
Total	81.96

ET_1, anterior nasal passage; ET_2, posterior nasal passage, pharynx, and larynx; BB, bronchial; bb, bronchiolar; AI, alveolar–interstitial.
*The Reference Worker was assigned the deposition and clearance parameter values of a healthy, non-smoking, normal nose-breathing adult male at light work. Light work is defined on the following basis: 2.5 h sitting, during which the amount inhaled is 0.54 m^3 h^{-1}; and 5.5 h light exercise, during which the amount inhaled is 1.5 m^3 h^{-1}. For both levels of activity, all the inhaled air enters through the nose.
[†]Reference values, given to sufficient precision for calculation purposes, which may be greater than would be chosen to reflect the certainty with which the average value of each parameter is known.
[‡]The particles are assumed to have density 3.00 g cm^{-3} and shape factor 1.5. The particle aerodynamic diameters are assumed to be log-normally distributed with geometric standard deviation σ_g of approximately 2.50 [the value of σ_g is not a reference value, but is derived from the corresponding activity median thermodynamic diameter (ICRP, 1994a)].

Gases and vapours

(91) For radionuclides inhaled as aerosols, the HRTM assumes that total and regional deposits in the respiratory tract are determined only by the size distribution of the inhaled particles. The situation is different for gases and vapours, for which deposition in the respiratory tract depends entirely on the chemical form. In this context, deposition refers to how much of the material in the inhaled air remains in the body after exhalation. Almost all inhaled gas molecules contact airway surfaces, but usually return to the air unless they dissolve in, or react with, the surface lining. The fraction of an inhaled gas or vapour that is deposited in each region thus depends on its solubility and reactivity.

(92) As for particulate forms of radionuclides, default parameter values are provided for use in the absence of more specific information. The general defaults for gases and vapours are 100% total deposition in the respiratory tract (regional deposition: 20% ET_2, 10% BB, 20% bb, and 50% AI) with Type F absorption (Section 3.2.3). This classification is somewhat different from that recommended in *Publication 66* (ICRP, 1994a), but simpler to apply. In particular, it is assumed by

default that there is no deposition in ET_1. The SR-0, -1, -2, classification described in *Publication 66* (ICRP, 1994a) was not found to be helpful and is not used here.

(93) In this series of reports, parameter values are adopted for gaseous and vapour forms of compounds of a number of elements, including hydrogen, carbon, sulphur, and iodine. In each case, values are given for total deposition, regional deposition, and absorption.

3.2.2. Clearance: particle transport

(94) The model describes several routes of clearance from the respiratory tract (Fig. 3.3). Some material deposited in ET_1 is removed by extrinsic means such as nose blowing. In other regions, clearance is competitive between the movement of particles towards the alimentary tract and lymph nodes (particle transport), and the absorption into blood of material from the particles in the respiratory tract. Removal rates due to particle transport and absorption into blood are taken to be independent of each other. It is further assumed that all clearance rates are independent of age and sex.

(95) As in the original HRTM, it is assumed that particle transport rates are the same for all materials. A generic compartment model is therefore provided to describe particle transport of all materials. The revised particle transport model adopted here is shown in Fig. 3.4 (the original model is shown in Annex A, with details of the background to the revisions made, and the choice of parameter values in the revised model). Reference values of rate constants were derived, as far as possible, from human studies, as particle transport rates are known to vary greatly among mammalian species.

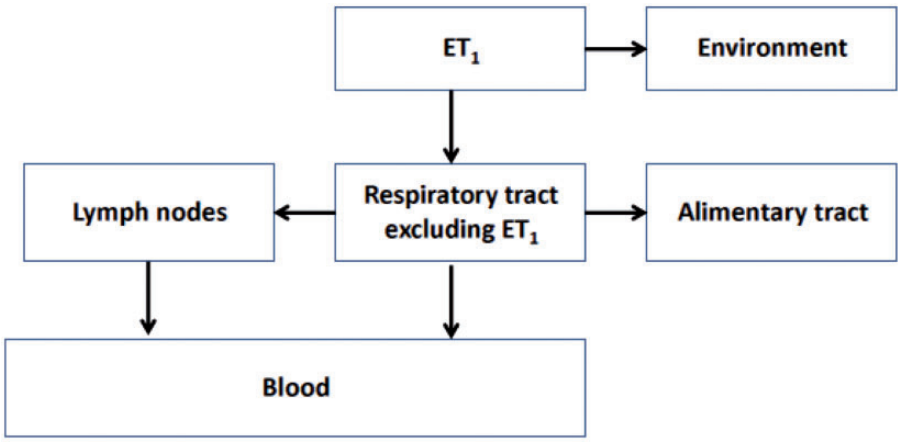

Fig. 3.3. Routes of clearance from the respiratory tract. ET_1, anterior nasal passage.

(96) The clearance rates for most of the material deposited in the conducting airways (regions ET_1, ET_2, BB, and bb) are based on the results of human volunteer experiments. During breathing through the nose, approximately 65% of the deposit in the ET airways is deposited in ET_1, and is cleared with a half-time of approximately 8 h (rate of 2.1 d^{-1}): approximately one-third by nose blowing and two-thirds by transfer to ET_2. This is implemented with particle transport rates of 0.6 d^{-1} from compartment ET_1 to the environment and 1.5 d^{-1} from ET_1 to compartment ET_2' (Fig. 3.4). Most particles deposited in ET_2 or transferred to it from other regions (ET_1 and BB) are cleared rapidly by mucociliary action to the throat, and swallowed with a time scale of approximately 10 min. This is represented by clearance from compartment ET_2' to the oesophagus at a rate of 100 d^{-1}.

(97) Throughout the bronchial tree (regions BB and bb), mucus velocities generally increase towards the trachea, so that residence times range from a few days in the smallest, most distal, bronchioles to less than 1 h in the trachea and main bronchi. This is represented by clearance rates of 0.2 d^{-1} (half-time of approximately 3.5 d) from compartment bb′ to compartment BB′, and 10 d^{-1} (half-time of approximately 2 h) from BB′ to ET_2'.

(98) Experiments in several animal species have shown that a very small fraction of particles deposited in the conducting airways is retained (sequestered) in the airway wall. To take account of this, it is assumed that 0.2% of material deposited in regions ET_2, BB, and bb is retained in the airway wall (compartments ET_{seq}, BB_{seq}, and bb_{seq}, respectively). Material is cleared from these compartments to regional lymph nodes at a rate of 0.001 d^{-1} (half-time of approximately 700 d).

(99) Human lung clearance has been quantified in several experimental studies for up to approximately 1 year after inhalation, by which time approximately 50% of the deposit in the AI region remained. Measurements of activity in the chest after occupational exposure, and of activity in the lungs at autopsy, show that some material can be retained in the lungs for decades (ICRP, 1994a). As described in Annex A, this is represented in the revised model by deposition in the alveolar compartment (ALV), which clears at an overall rate of 0.003 d^{-1} (half-time of approximately 250 d) to the bronchial tree (compartment bb′) at a rate of 0.002 d^{-1} and to the interstitial compartment (INT) at a rate of 0.001 d^{-1}. The INT compartment clears very slowly to the regional lymph nodes (rate of 0.00003 d^{-1}). Thus, approximately 33% of the deposit in the AI region is sequestered in the interstitium.

(100) Fig. 3.4 as it stands would describe the retention and clearance of an insoluble material. However, as noted above, there is, in general, simultaneous absorption into blood.

3.2.3. Clearance: absorption into blood

(101) Absorption into blood depends on the physical and chemical form of the deposited material. In both the original and revised HRTM, it is assumed (by

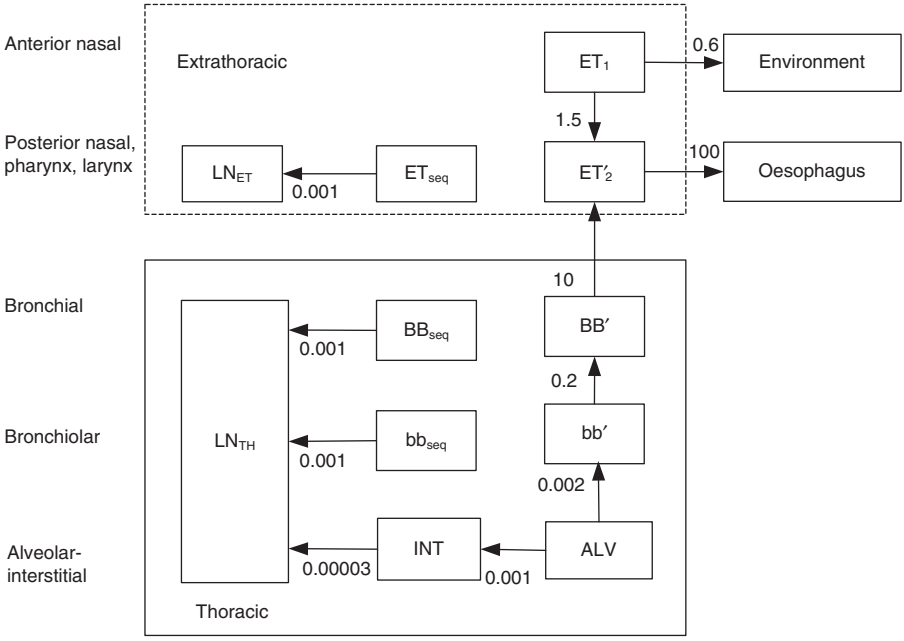

Fig. 3.4. Compartment model representing time-dependent particle transport from each respiratory tract region in the revised Human Respiratory Tract Model. Rates shown alongside arrows are reference values in units of d^{-1}. It is assumed that 0.2% of material deposited in the posterior nasal passage, pharynx, and larynx (ET_2), bronchi (BB), and bronchioles (bb) is retained in the airway wall (ET_{seq}, BB_{seq}, and bb_{seq}, respectively). ET_1: retention of material deposited in the anterior nose (region ET_1, which is not subdivided); ET_{seq}: long-term retention ($t_{½}$ about 700 d) in airway tissue of a small fraction of particles deposited in the nasal passages; LN_{ET}: lymphatics and lymph nodes that drain the ET regions; LN_{TH}: lymphatics and lymph nodes that drain the TH regions; ET'_2: short-term retention ($t_{½}$ about 10 minutes) of the material deposited in the posterior nasal passage, larynx and pharynx (ET_2 region) except for the small fraction (taken to be 0.002) retained in ET_{seq}; BB′: retention ($t_{½}$ about 100 minutes) of particles in the BB, with particle transport to ET'_2; bb′: retention ($t_{½}$ about 3.5 d) of particles in the bb, with particle transport to BB′; BB_{seq}: long-term retention ($t_{½}$ about 700 d) in airway walls of a small fraction of the particles deposited in the bronchial region; bb_{seq}: long-term retention ($t_{½}$ about 700 d) in airway walls of a small fraction of the particles deposited in the bronchiolar region; ALV: retention ($t_{½}$ about 250 d) of particles deposited in the alveoli. A fraction (0.67) of the deposit is removed by particle transport to the ciliated airways (bb′), while the remainder penetrates to the interstitium (INT); INT: very long-term retention ($t_{½}$ about 60 y) of the particles deposited in the alveoli that penetrate to the interstitium: the particles are removed slowly to the lymph nodes.

default) to occur at the same rate in all regions (including the lymph nodes), except ET_1 for which it is assumed that no absorption takes place. It is recognised that absorption is likely to be faster in the AI region where the air–blood barrier is thinner

than in the conducting airways (ET, BB, and bb regions), but insufficient information is available to provide a general systematic basis for taking this into account, such as a scaling factor for different rates in different regions.

(102) In the HRTM, absorption is treated as a two-stage process: dissociation of the particles into material that can be absorbed into blood (dissolution); and absorption into blood of soluble material and of material dissociated from particles (uptake). The clearance rates associated with both stages can be time-dependent.

Dissolution

(103) Both the original and revised HRTM use the same simple compartment model to represent time-dependent dissolution. It is assumed that a fraction (f_r) dissolves relatively rapidly, at a rate s_r, and the remaining fraction ($1 - f_r$) dissolves more slowly, at a rate s_s [Fig. 3.5(a)].

(104) A limitation of this system is that it can only represent an overall dissolution rate that decreases with time. To overcome this, *Publication 66* (ICRP, 1994a) also describes a more flexible system, shown in Fig. 3.5(b). In this, the material deposited in the respiratory tract is assigned to a compartment labelled 'particles in initial state' in which it dissolves at a constant rate s_p. Material is transferred simultaneously (at a constant rate s_{pt}) to a corresponding compartment labelled 'particles in transformed state' in which it has a different dissolution rate, s_t. With this system, the initial dissolution rate is approximately s_p and the final dissolution rate is approximately s_t. Thus, with a suitable choice of parameters, including $s_t > s_p$, an increasing dissolution rate can be represented. The ratio of s_p to s_{pt} approximates to the fraction that dissolves rapidly.

(105) It may be noted that any time-dependent dissolution behaviour that can be represented using the model shown in Fig. 3.5(a) can also be represented by the model shown in Fig. 3.5(b) with a suitable choice of parameter values. Thus, if the dissolution rate decreases with time, as is usually the case, either system could be used, and would give the same results with the following values:

$$\begin{aligned} s_p &= s_s + f_r(s_r - s_s) \\ s_{pt} &= (1 - f_r)(s_r - s_s) \\ s_t &= s_s \end{aligned} \tag{3.1}$$

However, the reverse is not true, as noted above.

(106) The system shown in Fig. 3.5(b) was applied by default in earlier publications (ICRP, 1994b, 1995c, 1997b). The additional flexibility it provides is, however, rarely required in practice, and it is more complex (and less intuitive) to present. The simpler approach, shown in Fig. 3.5(a), is therefore adopted now as the default, with the more flexible approach retained as an alternative. Examples of materials that show dissolution rates that increase with time, which have been represented by

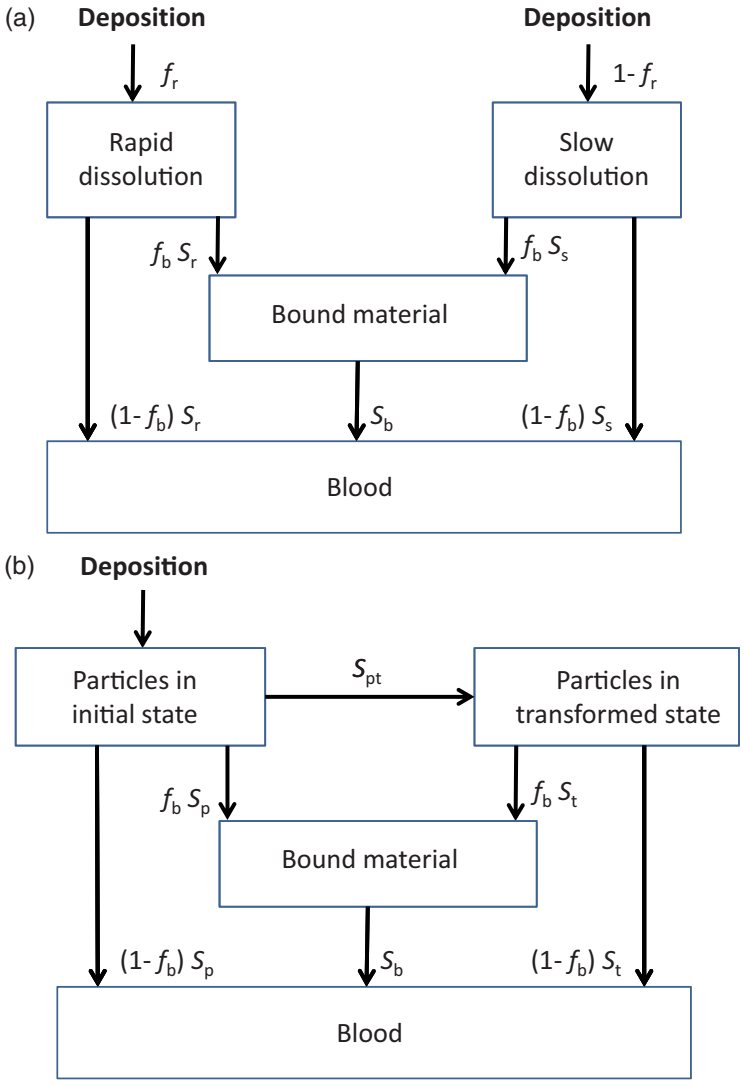

Fig. 3.5. Alternative compartment models representing time-dependent absorption into blood (dissolution and uptake). In the model shown in Fig. 3.5(a), a fraction f_r of the deposit is initially assigned to the compartment labelled 'rapid dissolution', and the rest of the deposit $(1 - f_r)$ is initially assigned to the compartment labelled 'slow dissolution'. In the model shown in Fig. 3.5(b), all the deposit is initially assigned to the compartment labelled 'particles in initial state', and material in the compartment labelled 'particles in transformed state' is subject to particle transport at the same rate as material in the compartment labelled 'particles in initial state'. Material in the compartment labelled 'bound material' is not subject to particle transport and is cleared only by uptake into blood. f_r: fraction of the deposit that dissolves rapidly, at a rate s_r; $(1 - f_r)$: fraction of deposit that dissolves more slowly, at a rate s_s; f_b: fraction of the dissolved material that is retained in the bound state and from which it goes to blood at a rate s_b; s_r: rate of rapid dissolution; s_s: rate of slow dissolution; s_b: transfer rate from the bound state to the blood; s_{pt}:transfer rate of material from the compartment "particles in initial state" to the compartment "particles in transformed state"; s_p: dissolution rate of material from compartment "particles in initial state"; s_t: dissolution rate of material from the compartment "particles in transformed state".

'particles in initial state' and 'particles in transformed state', including uranium aluminide, are given in the element sections in subsequent reports of this series.

Uptake

(107) Uptake into blood of dissolved material is usually assumed to be instantaneous. For some elements, however, part of the dissolved material is absorbed rapidly into blood, but a significant fraction is absorbed more slowly because of binding to respiratory tract components. To represent time-dependent uptake, it is assumed that a fraction (f_b) of the dissolved material is retained in the 'bound' state, from which it goes into blood at a rate s_b, while the remaining fraction ($1 - f_b$) enters blood instantaneously (Fig. 3.5). In the model, material in the 'bound' state is not cleared by particle transport processes, but only by uptake into blood. Thus, only one 'bound' compartment is required for each region, except for ET_1 from which no absorption takes place.

(108) The system shown in Fig. 3.5 applies to each of the compartments in the particle transport model shown in Fig. 3.4. It is assumed that no absorption takes place from ET_1, but if the model in Fig. 3.5(a) is used, the ET_1 deposit still has to be partitioned between fast and slow compartments because material is cleared from ET_1 to ET_2, from which absorption does take place.

(109) For all elements, default values of parameters are recommended, according to whether the absorption is considered to be fast (Type F), moderate (Type M), or slow (Type S). For gases or vapours, instantaneous uptake into blood may be recommended [Type V (very fast)].

(110) The original default reference values for Types F, M, and S [given in *Publication 66* (ICRP, 1994a) and reproduced in Table A.3 of Annex A] were not based on reviews of experimental data but on comparison with particle transport rates. For example, the value of 100 d^{-1} for the rapid dissolution rate, s_r, was chosen to equal the particle clearance rate from the nose (ET_2) to the throat.

(111) In developing the subsequent parts of this report, detailed reviews were conducted of the absorption characteristics of inhaled materials relevant to radiological protection. They are summarised in the inhalation sections of each element.

(112) Where information was available, specific parameter values were derived from experimental data from both in-vivo and in-vitro studies. As described in Annex A, these provided a database to give guidance on selecting values that are representative of materials that are generally considered to clear at 'fast', 'moderate', or 'slow' rates. Values selected on that basis for default Types F, M, and S have been adopted in the revised HRTM used in this series of reports (see below).

(113) Material-specific rates of absorption have been adopted in the element sections (and dose coefficients and bioassay functions provided for them in the accompanying electronic annex) for a limited number of selected materials, i.e. those for which:

- there are in-vivo data from which specific parameter values can be derived;
- results from different studies are consistent;

- it was considered that occupational exposure to the material is likely; and
- the specific parameter values are sufficiently different from default Types F, M, or S parameter values to justify providing additional specific dose coefficients and bioassay functions.

(114) Other materials were assigned to default types using suitable experimental data if available, as reviewed in compiling the element sections. *Publication 66* (ICRP, 1994a) did not give criteria for assigning materials to absorption types on the basis of experimental results. Criteria were developed in *Publication 71* (ICRP, 1995c) and their application was discussed further in Supporting Guidance 3 (ICRP, 2002b). Type M is assumed for all particulate forms of most elements in the absence of information on which assignment to an absorption type could be made. A material is assigned to Type F if the amount absorbed into blood by 30 d after an acute intake is greater than the amount that would be absorbed over the same period from a hypothetical material with a constant rate of absorption of 0.069 d^{-1} (corresponding to a half-time of 10 d) under identical conditions. Similarly, a material is assigned to Type S if the amount absorbed into blood by 180 d after an acute intake is less than the amount that would be absorbed over the same period from a hypothetical material with a constant rate of absorption into blood of 0.001 d^{-1} (corresponding to a half-time of approximately 700 d) under identical conditions.

(115) Particulate forms of each element were assigned to the HRTM default absorption types using these criteria. However, strict application of the criterion for assigning materials to Type S requires experiments of at least 180 d duration, and as this would exclude much useful information, extrapolation has been used in some cases, as indicated in the text. For studies where it was possible to apply the criteria, a statement is made to the effect that results 'are consistent with' (or 'give') assignment to Type F (M or S). For studies where the results point towards a particular type, but there was insufficient information to apply the criteria, a statement is made to the effect that the results 'indicate' or 'suggest' Type F (M or S) behaviour. For some elements for which there are little or no experimental data on absorption from the respiratory tract, materials could be assigned to default types based on chemical analogy.

(116) For soluble (Type F) forms of each element, estimates are made of the overall rate of absorption from the respiratory tract into blood (where information is available). In general, this might result from a combination of processes including: (a) dissolution of the deposited material (if not inhaled as droplets and so already in solution); (b) transfer through the lining fluid to the epithelium, especially in the conducting airways; and (c) transfer across the epithelium. Strictly, in terms of the model structure, the first two of these would be described as 'dissolution' and be represented by the rapid dissolution rate, s_r, because the material is subject to particle transport, whereas transfer across the epithelium, unless extremely rapid, should be represented by a bound fraction. In practice, it would often be difficult to assess how much of the overall rate should be assigned to each process, and for simplicity, s_r is used to represent the overall absorption. However, it is assumed that s_r is a characteristic of the element, and this would be expected for transfers through the lining

fluid and epithelium. Wide variation in values of s_r was found between elements, ranging from approximately 1 d^{-1} (e.g. yttrium) to 100 d^{-1} (e.g. caesium). Some justification for this approach comes from the fact that the value of s_r tends to have more effect on the overall biokinetics of an inhaled material deposited in the conducting airways (where the lining fluid is relatively thick) than on material deposited in the alveolar region, because it competes with particle transport rates of similar magnitude (10 d^{-1} from BB′ to ET_2' and 100 d^{-1} from ET_2' to oesophagus). Due to the wide variation between elements in the estimated value of s_r, element-specific values are adopted in this series of reports for those elements for which an estimate of the value could be made.

(117) For soluble forms of some elements, part of the dissolved material is absorbed rapidly into blood, but a significant fraction is absorbed more slowly. In some cases, this can be represented by formation of particulate material (which is subject to clearance by particle transport). In others, however, some dissolved material appears to be attached to lung structural components, and removed only by absorption into blood. To represent the latter type of time-dependent uptake, it is assumed that a fraction (f_b) of the dissolved material is retained in the 'bound' state, from which it goes into blood at a rate s_b, while the remaining fraction ($1 - f_b$) goes into blood instantaneously (Fig. 3.5). Evidence for retention in the bound state, rather than by transformation into particulate material, may be in one or more forms (e.g. systemic uptake rather than faecal clearance of the retained material; slower clearance than for insoluble particles deposited in the same region of the respiratory tract; or autoradiography showing diffuse rather than focal retention of activity).

(118) Although the bound state was included in the model mainly to take account of slow clearance of soluble materials from the alveolar region, by default it would be assumed that the same bound state parameter values apply in all regions. In some cases (e.g. a long-term bound state for a long-lived alpha emitter), this could lead, unintentionally, to high calculated doses to the BB and bb regions. Due to the high weighting (apportionment factors) that these tissues are given, this could, in turn, lead to high calculated equivalent doses to the lungs. Hence, in this series of reports, it is assumed that for those elements for which a bound state is adopted ($f_b > 0$), it is applied in the conducting airways (ET_2, BB, and bb regions) if there is experimental evidence to support this.

(119) For some elements for which there are little or no experimental data on absorption from the respiratory tract, element-specific absorption parameter values (s_r, f_b, and s_b) could be based on chemical analogy.

(120) As noted above, the specific parameter values derived from experimental data (from both in-vivo and in-vitro studies) provided a database to give guidance on selecting values that are representative of materials that are generally considered to clear at 'fast', 'moderate', or 'slow' rates. It is emphasised that this was not a representative survey from which central values could be derived by some objective statistical means. Rather, it provided a basis for informing judgements as described

Table 3.2. Default absorption parameter values for Type F, M, and S materials*,† in the revised Human Respiratory Tract Model.

Type		F (fast)	M (moderate)	S (slow)
Fraction dissolved rapidly	f_r	1	0.2	0.01
Dissolution rates:				
Rapid (d^{-1})	s_r	30‡	3§	3§
Slow (d^{-1})	s_s	–	0.005	0.0001

*Reference values, given with sufficient precision for calculation purposes, which may be greater than would be chosen to reflect the certainty with which the average value of each parameter is known.
†The bound state is also used for default types of some elements.
‡Element-specific rapid dissolution rates are adopted for Type F forms of many elements.
§The element-specific value for Type F is also used for Types M and S if it is less than 3 d^{-1}.

in Annex A. Updated default values for the revised HRTM and applied in this series of reports are given in Table 3.2.

(121) The default absorption rates, expressed as approximate half-times, and the corresponding amounts of material deposited in each region that reach blood (from the respiratory tract) can be summarised as follows.

- Type V: 100% absorbed instantaneously. Regional deposition does not need to be assessed for such materials, because, in dose calculations, they can be treated as if they were injected directly into blood.
- Type F: For the general default value of 30 d^{-1} for s_r, 100% absorbed with a half-time of approximately 30 min. There is rapid absorption of almost all material deposited in bb and AI, approximately 80% of material deposited in BB, approximately 25% of material deposited in ET_2, and approximately 20% of material deposited in ET_1. The other material deposited in BB and ET_2 is cleared to the alimentary tract by particle transport.
- Type M: For the general default value of 3 d^{-1} for s_r, 20% absorbed with a half-time of approximately 6 h and 80% with a half-time of approximately 140 d. There is rapid absorption of approximately 20%, 5%, 0.5%, and 0.4% of material deposited in bb, BB, ET_2, and ET_1, respectively. Approximately 80% of the deposit in AI eventually reaches blood.
- Type S: For the general default value of 3 d^{-1} for s_r, 1% absorbed with a half-time of approximately 6 h and 99% with a half-time of approximately 7000 d. There is rapid absorption of approximately 1%, 0.25%, 0.03%, and 0.02% of material deposited in bb, BB, ET_2, and ET_1, respectively. Approximately 30% of the deposit in AI eventually reaches blood.

(122) For Types F, M, and S, some of the material deposited in ET_1 is removed by extrinsic means. Most of the material deposited in the respiratory tract that is not absorbed is cleared to the alimentary tract by particle transport. The small amount transferred to lymph nodes continues to be absorbed into blood at the same rate as in the respiratory tract.

(123) For material cleared from the respiratory tract to the alimentary tract, the default assumption made is that fractional absorption in the alimentary tract is the product of f_r and f_A, where f_A is fractional absorption in the alimentary tract for relatively soluble forms of the element (Section 3.3.3). This approach was based on the consideration that f_r represents the soluble fraction of the material which is available for absorption in the alimentary tract, and f_A represents alimentary tract absorption of the soluble fraction. In taking this approach, it was recognised that it is important not to overestimate absorption in the alimentary tract greatly, because this could lead to overestimation of predicted urinary excretion, and hence corresponding underestimation of intakes from urine bioassay measurements.

Progeny radionuclides formed in the respiratory tract

(124) The following applies specifically to progeny formed in the respiratory tract after inhalation of the parent radionuclide. Progeny radionuclides formed before inhalation and inhaled with the parent are generally treated as separate intakes, and so each progeny radionuclide inhaled is assumed to adopt the biokinetics appropriate to the element of which it is an isotope.

(125) *Publication 66* (ICRP, 1994a, Para. 272) noted that it would be expected that:

- the rate at which a particle dissociates is determined by the particle matrix, and therefore the dissolution parameter values of the inhaled material would be applied to progeny formed within particles in the respiratory tract ('shared kinetics');
- progeny radionuclides formed as noble gases, including radon, would be exceptions because they would diffuse from the particles; and
- the behaviour of dissociated material would depend on its elemental form, and so, for example, bound fraction parameter values for a progeny radonuclide would not be those of the parent ('independent kinetics').

(126) Nevertheless, in previous applications of the HRTM [e.g. *Publications 68*, *71*, *72*, and *78* (ICRP, 1994b, 1995c, 1996, 1997b)], with the exception of noble gases, the absorption parameter values of the parent were applied to all members of the decay chain formed in the respiratory tract ('shared kinetics'). After detailed consideration of the issues involved (see Annex A), the same approach is taken in this series of reports.

(127) The recoil of nuclei formed in alpha particle decay could be at least as important as diffusion as a mechanism for emanation of radon from particles. Such recoil also applies to other progeny radionuclides formed by alpha emission. In the case of insoluble particles, this will result in successively lower activities of members of a decay chain compared with the parent. It was considered impractical to implement loss of progeny by alpha recoil in the calculation of dose coefficients in this series of reports. However, the phenomenon should be borne in mind, especially when using progeny to monitor intakes and doses of the parent radionuclide.

(128) Nevertheless, where experimental results are available that allow direct comparisons between the absorption behaviour of a parent radionuclide, and that of its radioactive progeny, they are summarised in the inhalation section of the parent element (e.g. uranium, thorium). Such information may be of use to those undertaking individual monitoring, especially if intakes of a parent are being assessed by means of measurements on one or more of its progeny.

(129) For calculation purposes, the assumption that noble gases, including radon, that are formed as progeny within the respiratory tract escape from the body at a rate of 100 d^{-1} is applied in this series of reports.

(130) For material cleared from the respiratory tract to the alimentary tract, fractional absorption in the alimentary tract is assumed to be $f_{r*} f_A$ (see above). In the case of progeny formed in the respiratory tract, f_r is taken to be that of the parent deposited in the respiratory tract (reflecting the particle matrix), but the value of f_A is taken to be that of the progeny radionuclide entering the alimentary tract.

(131) Following absorption into blood, progeny formed in the respiratory tract are assumed to behave according to the systemic model applied to the element as a daughter of the parent radionuclide.

3.2.4. Respiratory tract dosimetry

(132) The HRTM dosimetric model is described in Section 8 of *Publication 66* (ICRP, 1994a). For dosimetric purposes, the respiratory tract is treated as two tissues: the TH and ET airways. These are subdivided into regions, primarily based on considerations of differences in sensitivity to radiation. The TH regions are BB, bb, AI, and LN_{TH}. The ET regions are ET_1, ET_2, and LN_{ET} (Fig. 3.2).

(133) The dose to each respiratory tract region is calculated as the average dose to the target region that contains the target cells at risk. In the AI region and lymph nodes (LN_{TH} and LN_{ET}), the cells at risk are thought to be distributed throughout the region, and the average dose to the whole lung and the lymph nodes, respectively, is calculated. For the regions making up the conducting airways (ET_1, ET_2, BB, and bb), the target cells are considered to lie in a layer of tissue at a certain range of depths from the airway surface, and the average dose to this layer is calculated. The target cells identified in ET_1, ET_2, BB, and bb, and the masses of tissue containing target cells in each region for dose calculations, are given in Table 3.3.

(134) In each of these regions, there are also several possible source regions. For example, in the bb region, particles retained in the airway wall (bb_{seq}) are taken to be in a macrophage layer at a depth of 20–25 μm (i.e. below the target cells); activity 'bound' to the epithelium is distributed uniformly in it; and account is also taken of irradiation from activity present in the AI region. In the original HRTM, there were two phases of mucociliary clearance: activity in the fast phase of clearance (compartment bb_1, Fig. A.1) was taken to be in a mucus layer above the cilia; and activity in the slow phase of clearance (compartment bb_2) was taken to be in the mucus between the cilia. In the revised HRTM, there is only one phase of clearance.

(135) For each source/target combination, *Publication 66* (ICRP, 1994a) provides absorbed fractions for non-penetrating radiations (alpha, beta, and electrons) as a function of energy. As these absorbed fractions are not represented in the voxel phantoms because of inadequate spatial resolution, the values given in *Publication 66* (ICRP, 1994a) are used here. They were derived using a single cylindrical geometry to represent each region of the conducting airways (ET_1, ET_2, BB, bb): the representative bronchus for BB having a dimater of 5 mm and the representative bronchiole for bb having a diameter of 1 mm. The absorbed fractions for the single phase BB and bb source regions were derived as the thickness-weighted sum of the slow- and fast-clearing source regions, as tabulated in *Publication 66* (ICRP, 1994a).

(136) To take account of differences in sensitivity between tissues, the equivalent dose, H_i, to each region, *i*, is multiplied by an apportionment factor, A_i, representing the region's estimated sensitivity relative to that of the whole organ. The recommended values of A_i are also given in Table 3.3. In *Publication 103* (ICRP, 2007), LN_{ET} and LN_{TH} were included in the tissue 'lymphatic nodes', which is itself included in the list of remainder tissues and organs (Table 1.2), and so are no longer included in the ET and TH airways, respectively, as they were in the original HRTM. The fractions, A_i, of w_T that they were assigned in *Publication 66* (ICRP, 1994a) are re-assigned to other regions in Table 3.3. The weighted sum of the

Table 3.3. Target regions of the respiratory tract.

Tissue	Region	Target cells	Depth of target cell* (μm)	Mass of target region*,† (kg)		Assigned fraction*,‡ A_i of w_T
				Male	Female	
ET	ET_1	Basal	40–50	2.000×10^{-5}	1.729×10^{-5}	0.001
	ET_2	Basal	40–50	4.500×10^{-4}	3.890×10^{-4}	0.999
TH	BB	Secretory (BB_{sec})	10–40	8.648×10^{-4}	7.771×10^{-4}	1/3‡
		Basal (BB_{bas})	35–50	4.324×10^{-4}	3.885×10^{-4}	
	bb	Secretory	4–12	1.949×10^{-3}	1.874×10^{-3}	1/3
	AI		§	1.100	0.904	1/3

ET, extrathoracic; TH, thoracic; ET_1, anterior nasal passage; ET_2, posterior nasal passage, pharynx, and larynx; BB, bronchial; bb, bronchiolar; AI, alveolar–interstitial.

*Reference values, given with sufficient precision for calculation purposes, which may be greater than would be chosen to reflect the certainty with which the average value of each parameter is known. For the BB, bb, and AI regions, each value of A_i is exactly one-third.

†Male values were taken from Table 3 of *Publication 68* (ICRP, 1994b). Female values for ET and AI were taken from Table 5 of *Publication 66* (ICRP, 1994a). Female values for BB were calculated here using information from Tables 2, 4, and B6 of *Publication 66* (ICRP, 1994a). Masses for BB_{sec} and BB_{bas} are the masses of bronchial epithelium through which the secretory cells and basal cells, respectively, are distributed and are based on reference values of airway dimensions. The mass of AI includes blood, but excludes lymph nodes.

‡The dose to BB (H_{BB}) is calculated as the arithmetic mean of the doses to BB_{sec} and BB_{bas}.

§Average dose to region calculated.

equivalent dose, H_i, to each region, is the equivalent dose to the ET or TH airways, respectively:

$$H_{ET} = H_{ET_1} A_{ET_1} + H_{ET_2} A_{ET_2}$$
$$H_{TH} = H_{BB} A_{BB} + H_{bb} A_{bb} + H_{AI} A_{AI} \quad (3.2)$$

(137) The tissue weighting factor, w_T, of 0.12 specified for lung in *Publication 103* (ICRP, 2007) is applied to the equivalent dose to the TH region, H_{TH}. The ET airways are included in the list of remainder tissues and organs (Table 1.2).

3.3. Human Alimentary Tract Model

(138) The *Publication 30* (ICRP, 1979) model of the gastrointestinal tract has been replaced by the HATM described in *Publication 100* (ICRP, 2006). This replacement

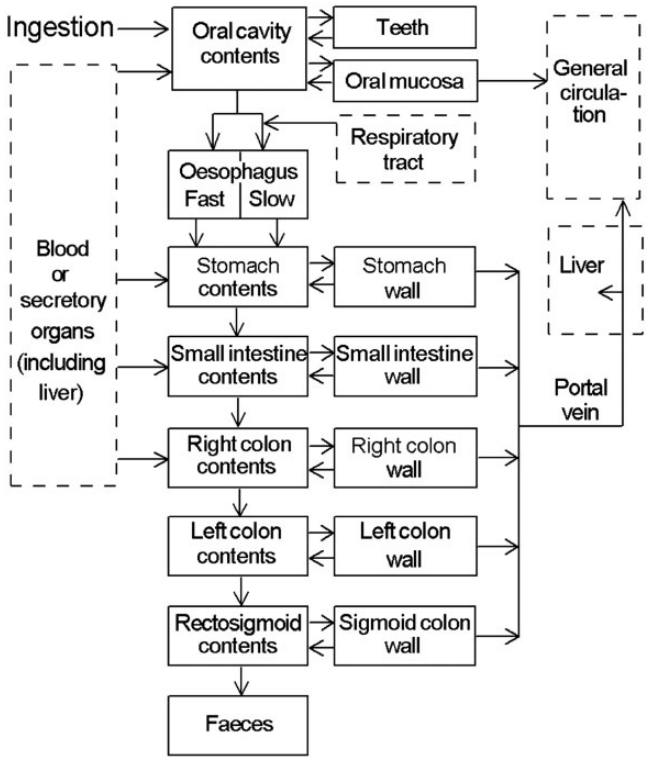

Fig. 3.6. Structure of the Human Alimentary Tract Model (HATM). The dashed boxes are included to show connections between the HATM and the Human Respiratory Tract Model and systemic biokinetic models.

Table 3.4. Default generic Human Alimentary Tract Model transfer coefficients (per d) for total diet for the Reference Worker.*,†

From	To	Transfer coefficient‡ (d^{-1})
Oral cavity contents	Oesophagus fast	6480
Oral cavity contents	Oesophagus slow	720
Oesophagus fast	Stomach contents	12,343
Oesophagus slow	Stomach contents	2160
Stomach contents	Small intestine contents	20.57
Small intestine contents	Right colon contents	6
Right colon contents	Left colon contents	2
Left colon contents	Rectosigmoid contents	2
Rectosigmoid contents	Faeces	2

*The transfer rates of *Publication 100* (ICRP, 2006) for the adult male have been assumed for the Reference Worker.

†Other transfer coefficients not given here are assumed to be zero unless specified in the relevant element section. In most cases, uptake into blood from the alimentary tract is taken to occur from the small intestine (SI) contents, without retention in the SI wall. The corresponding transfer coefficient is: $\frac{f_A \lambda_{SI,RC}}{1-f_A}$, where $\lambda_{SI,RC}$ is the transfer coefficient from SI contents to right colon contents.

‡The degree of precision of the values given is for computational purposes, and does not reflect the certainty with which the central values are known.

was motivated by a number of developments, including the availability of improved information on the gut transit of materials, and developments in our understanding of the location of sensitive cells. The model structure is shown in Fig. 3.6, and parameter values are shown in Table 3.4. As for the HRTM, an important feature of the HATM is the specific calculation of doses to target regions containing sensitive cells for cancer induction, and the consideration of specific absorption and/or retention values, where information is available. The HATM and the HRTM are compatible and interconnected, as shown in Fig. 3.6.

3.3.1. Structure

(139) The HATM depicts the entry of a radionuclide into the oral cavity by ingestion, or into the oesophagus after particle transport from the respiratory tract. It describes the sequential transfer through all alimentary tract regions, including the oral cavity, oesophagus, stomach, small intestine, and segments of the colon, followed by emptying in faeces. Doses are calculated for all these regions. The colon is partitioned, for the purposes of dose calculations, into right colon, left colon, and rectosigmoid (the sigmoid colon and rectum) based on the availability of transit time data. The rectum is included with the sigmoid colon, as the rectosigmoid, because of

difficulties in determining transit times separately and because the rectum does not have a specific w_T value. Total colon doses are combined as a mass-weighted mean to include the right colon, left colon, and rectosigmoid.

3.3.2. Model parameters

(140) The HATM presents different transit times for solid foods, liquids, and total diet in the mouth, oesophagus, and stomach. First-order kinetics are assumed. This is a considerable simplification of the complex processes involved in transfer of material through the lumen of the alimentary tract, but is expected to provide a reasonably accurate representation of the mean residence time of a radionuclide in each segment of the tract.

Modifying factors

(141) The default regional transit times given in the HATM are central estimates based on collected data for a given sex, age group, and type of material (e.g. solids, liquids, caloric liquids, or non-caloric liquids). As illustrated extensively in *Publication 100* (ICRP, 2006), transit of material through each of the major segments of the tract shows considerable inter- and intrasubject variability, even under normal conditions. Extremely large deviations from the norm may result from constipation, diarrhoea, unusual diet, pharmaceuticals, and a variety of diseases that affect the nervous system or increase energy requirements, for example.

Sex-specific values

(142) The HATM provides sex-specific parameter values for adults for dimensions and transit times of contents through the regions. Although the dimensions of the stomach and intestines are generally smaller in females than males, the estimated central transit times through these regions are approximately one-third greater in females than in males. However, taking into account the large variability in transit times through any region of the alimentary tract in both males and females, the Reference Worker is assigned the reference transit times for the adult male.

Material entering from the respiratory tract or in saliva

(143) Mucus and associated materials cleared from the respiratory tract enter the oesophagus via the oropharynx. For ingested food and liquids, the HATM specifies two components of oesophageal transit, representing relatively fast transfer of 90% of the swallowed material (mean transit time of 7 s for total diet) and relatively slow transit of the residual 10% (40 s for total diet). It is assumed that the slower oesophageal transit time applies to all material cleared from the respiratory tract. The same assumption is made for activity entering the alimentary tract in saliva.

3.3.3. Absorption from the alimentary tract

(144) Radionuclides may enter the alimentary tract: directly as a result of ingestion; indirectly after inhalation and mucociliary escalation of particles from the respiratory tract to the oropharynx and oesophagus; or in secretions such as saliva, bile, or gastric juice. Alternatively, they may be produced in the alimentary tract by decay of a parent radionuclide. The absorption of radionuclides into blood is specified in the HATM as a fraction of the amount entering the alimentary tract, with total absorption denoted as f_A (ICRP, 2006). The model structure allows for the use of data on absorption in any region where information is available. In most cases, no information will be available on the regional absorption of radionuclides, and the default assumption is that all absorption takes place in the small intestine (i.e. $f_{SI} = f_A$). As a default, it is also assumed that there is no recycling from the wall to the contents of the alimentary tract.

(145) Some f_A values recommended in this report are the same as the f_1 values given previously for use with the *Publication 30* models (ICRP, 1979, 1980, 1981, 1988b) as there is not sufficient new information to warrant a revision in the value. Specific data of absorption from other regions are considered in the small number of cases for which they were available, although in some cases (e.g. relatively long-lived isotopes of iodine), doses to alimentary tract regions and other tissues are insensitive to assumptions regarding the site of absorption (ICRP, 2006).

(146) The extent of absorption of radionuclides will depend on the element and its chemical forms. Changes in chemical forms are likely to occur during digestive processes, beginning in the mouth, but principally occurring in the stomach and the small intestine. These changes in chemical form or speciation will determine the availability of the radionuclide for absorption, and hence the extent of uptake through the intestinal epithelium into the bloodstream (ICRP, 2006).

(147) The default absorption fraction f_A for a radionuclide X produced in the alimentary tract by decay of an ingested parent radionuclide Y is the reference f_A for X as a parent. If X has multiple reference values corresponding to different chemical or physical forms, the default f_A is the highest reference value provided for X.

(148) For inhaled particles reaching the alimentary tract after clearance from the respiratory tract, it is appropriate to take account of solubility in the lungs in specifying f_A values. For some elements exhibiting a range in solubility according to their physicochemical form, there is evidence that the reduced solubility of Type M or S materials is also associated with reduced intestinal absorption. For a radionuclide that is transferred from the respiratory tract to the alimentary tract, the default f_A value is determined as the product of f_r for the absorption type and the f_A value for soluble forms of the element. The default absorption fraction f_A for a radionuclide X produced in the respiratory or alimentary tract by decay of a parent radionuclide Y inhaled is the product of f_r for the absorption type and the reference f_A for X ingested as a parent radionuclide. If X has multiple reference absorption fractions f_A corresponding to different chemical or physical forms, the default

absorption fraction f_A for X produced in the respiratory or alimentary tract is the product of f_r for the absorption type and the highest reference value provided for X.

(149) Some of the biokinetic models used in this series of reports to predict the systemic behaviour of radionuclides depict secretion from systemic compartments into the contents of the alimentary tract. Activity transferred from systemic compartments into the small intestine or higher segments of the alimentary tract is assumed to be subject to re-absorption into blood. In such cases, the default absorption fraction f_A for the secreted activity is the reference f_A for ingestion of the radionuclide. If multiple reference values of f_A are given for different forms of the ingested radionuclide, the default f_A for the secreted activity is the highest reference value provided for X.

3.3.4. Retention in the alimentary tract regions

(150) The model structure allows, where information is available, for the use of data on retention of radionuclides in different compartments. Human and animal data suggesting or showing retention of ingested radionuclides on teeth or in mucosal tissues of the walls of alimentary tract regions, principally the small intestine, can be used to refine calculation of doses to the alimentary tract. An example given in *Publication 100* (ICRP, 2006) for cadmium shows that retention of ^{115}Cd on teeth increases the estimated dose to the oral mucosa by almost two orders of magnitude compared with that calculated using the *Publication 30* model (ICRP, 1979, 1980). Similarly, retention of ^{59}Fe in the wall of the small intestine may increase the equivalent dose to the wall by approximately a factor of two compared with that calculated with the *Publication 30* model (ICRP, 1979, 1980). However, in both examples, these increases in organ doses do not lead to significant changes in the committed effective doses, which are dominated by contributions from other tissues (ICRP, 2006). Information on retention in alimentary tract tissues is given, where available, in individual element sections of this series of reports.

3.3.5. Alimentary tract dosimetry

(151) The HATM allows explicit calculations of dose to target regions for cancer induction within each alimentary tract region, considering doses from radionuclides in the contents of the regions, and considering mucosal retention of radionuclides when appropriate.

(152) The oesophagus and oral cavity will receive very low doses from ingested radionuclides because of short transit times in these regions (ICRP, 2006). However, they were included because a specific w_T is assigned to the oesophagus (ICRP, 2007), and because retention in the mouth, on teeth for example, can result in a substantial increase in dose to the oral mucosa [which was added to the organs and tissues constituting the remainder in *Publication 103* (ICRP, 2007)].

(153) In general, the alimentary tract regions of greater importance in terms of doses and cancer risk are the stomach and, particularly, the colon. While the small intestine may receive greater doses than the stomach, it is not sensitive to radiation-induced cancer and is not assigned a specific w_T value (ICRP, 2007). Small intestine is therefore included with the organs and tissues constituting the remainder (ICRP, 2007).

(154) An important refinement in the HATM is the methodology used to calculate doses in the various regions from non-penetrating alpha and electron radiations. In *Publication 30* (ICRP, 1979), it is assumed that the dose to the wall of any gastrointestinal region from beta and alpha emitters in the contents is 100% and 1%, respectively, of the dose at the surface of the contents. In contrast, the HATM takes account of the location of the target cells in the mucosal layer of the wall of each gastrointestinal region and the depth of penetration of beta and alpha particles into the wall. The targets relating to cancer induction are taken in each case to be the epithelial stem cells, located in the basal layers of the stratified epithelia of the oral cavity and oesophagus, and within the crypts that replenish the single-cell-layer epithelium of the stomach, and small and large intestines.

(155) This new methodology generally results in substantially lower estimates of doses to the colon from alpha- and beta-emitting radionuclides in the colon contents than obtained using the *Publication 30* model (ICRP, 1979). This is because of the loss of alpha particle and electron energies in the colon contents and in the mucosal tissue overlying the target stem cells (at a depth of 280–300 μm). This reduces energy deposition in the target region for electrons, and results in zero contribution to dose in the target region from alpha particles emitted within the contents. In the absence of retention of radionuclides in the alimentary tract wall, doses from ingested alpha emitters to all regions of the alimentary tract will be solely due to their absorption into blood, and subsequent irradiation from systemic activity in soft tissues.

(156) The consequences of this decrease in local colon dose on the total committed effective dose will vary according to the radionuclide. Examples given in *Publication 100* (ICRP, 2006) for ^{55}Fe, ^{90}Sr, and ^{239}Pu show that this decrease in local dose to the colon has little or no impact on the effective dose as the dominant contributions are from equivalent doses to organs and tissues from activity absorbed into blood. In general, the effect on effective dose is small for radionuclides with large f_A values or long-lived radionuclides with long-term retention in the body. However, for the example of ^{106}Ru, there is a decrease in committed effective dose and colon dose, by approximately a factor of two and five, respectively, due to the major contribution to effective dose from equivalent doses to alimentary tract regions for this radionuclide.

(157) Calculations of doses in *Publication 100* (ICRP, 2006) were based on preliminary values of absorbed fractions of electrons and alpha particles to stem cell layers of each section of the alimentary tract. In this report, new calculations have been performed for particle types, and for content and wall sources. For regions within the small intestine, new models of segment folding have been implemented. Additional details will be given in a forthcoming publication (ICRP, 2016c).

3.4. Intact skin and wounds

3.4.1. Intact skin

(158) Intact skin is an effective barrier to the entry of most substances into the body, and few radionuclides cross it to any significant extent. Exceptions of practical importance are tritiated water in liquid or vapour form, organic carbon compounds, and iodine in vapour form or in solution.

(159) There is no general model for absorption of radionuclides through the skin because of the wide range of possible exposure scenarios. Skin can become contaminated by contact with, for example, aerosols, liquids, contaminated surfaces, or contaminated clothing. The physical and chemical form of the contaminant (including pH) and the physiological condition of the skin are important factors in any dose assessment.

(160) Both the radiation dose to the area of skin contaminated and the dose to the whole body as a result of absorption should be considered. ICRP (1991, 2007) recommends that local skin doses should be calculated to sensitive cells, assumed to be at a depth of 70 μm, or averaged over the layer of tissue 50–100 μm below the skin surface and averaged over the most exposed 1 cm^2 of skin tissue. This applies to activity either distributed over the skin surface or aggregated in particles. No dosimetric models are recommended by ICRP for calculating doses from radionuclides deposited on the skin, and no dose coefficients are given.

3.4.2. Wounds

(161) Radionuclides may be transferred from the site of a contaminated wound into blood and to other organs and tissues. NCRP has developed a model to describe this transfer for materials in different physicochemical forms [NCRP (2006) and Fig. 3.7]. Due to the lack of adequate human data, parameter values for the model were based on experimental animal data. When coupled with an element-specific systemic biokinetic model, the model can be used to calculate committed doses to organs and tissues, and committed effective doses following transfer of the radionuclide to the blood and systemic circulation, as well as to predict urinary and faecal excretion.

(162) This model was designed to be applicable to both soluble and insoluble radioactive materials after injection or penetrating wounds. Five compartments are used to describe physical or chemical states of the radionuclide within the wound site. These comprise: soluble material; colloidal and intermediate-state material; particles, aggregates, and bound state; trapped particles and aggregates; and fragments. In some cases, the compartments contain the radionuclide in its original physicochemical form. In other cases, the originally deposited material changes state and moves from one compartment to another with time. In most cases, the model simplifies to two or three compartments depending on the physical and chemical form of the radionuclide specified.

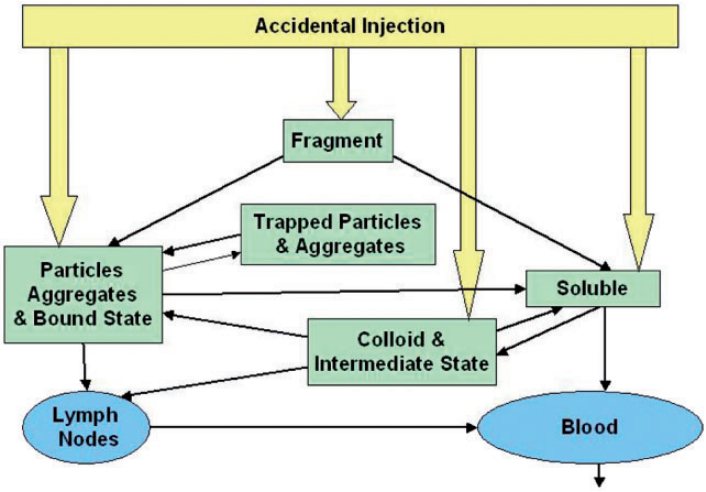

Fig. 3.7. US National Council on Radiation Protection and Measurements model for wounds.

(163) Four retention categories are defined for radionuclides that are present initially in soluble form in a wound: weak, moderate, strong, and avid. These refer generally to the magnitude of persistent retention at the wound site. The criteria for categorisation are based on: (a) the fraction of the intramuscularly injected radioactive material in rats remaining 1 d after deposition; and (b) the rate(s) at which the initially retained fraction was cleared.

(164) Release of the radionuclide from the wound site occurs via the blood for soluble materials and via lymph nodes for particles. Further dissolution of particles in lymph nodes also results in radionuclide transfer to the blood. The blood is the central compartment that links the wound model with the respective radioelement-specific systemic biokinetic model. Once the radionuclide reaches the blood, it behaves as if it had been injected directly into blood in a soluble form. This is the same approach as is taken in the HRTM and HATM.

(165) To illustrate the application of the model for bioassay interpretation, the wound model was coupled to the systemic biokinetic model for ^{137}Cs (ICRP, 1979, 1989, 1997b). The principal default for Cs in the wound model is the weak category. Accordingly, the parameters for this category were applied to the wound model, and urine and faecal excretion patterns were predicted (Fig. 3.8). The patterns show peak excretion of ^{137}Cs in urine at 2–3 d after intake, and in faeces at approximately 5 d. Both patterns reflect the rapid movement of ^{137}Cs from the wound site, and its distribution in and excretion from the systemic organ sites.

(166) For comparison, if the ^{137}Cs in the contaminated wound site is assumed to be present in particles of irradiated power reactor fuel, it can be given parameter values of the particle category. In this case, dissolution and absorption into blood are much slower than for the weak category, and the urine and faecal excretion patterns

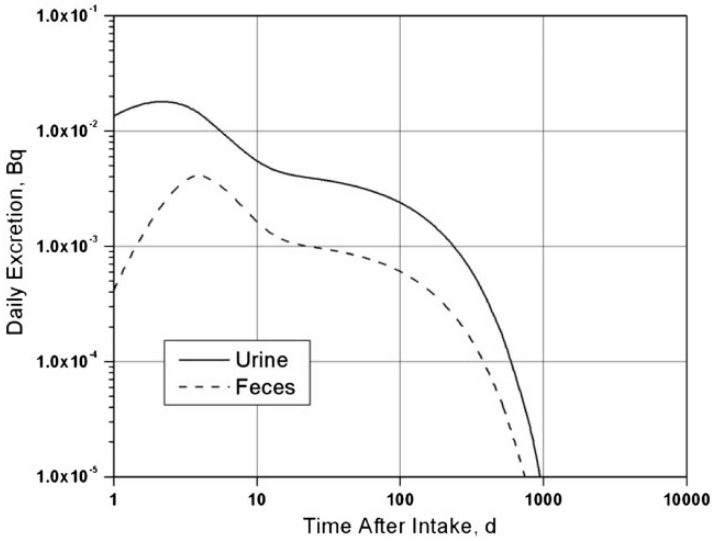

Fig. 3.8. ^{137}Cs wound, weak category; predicted values (Bq per Bq intake) following acute intake.

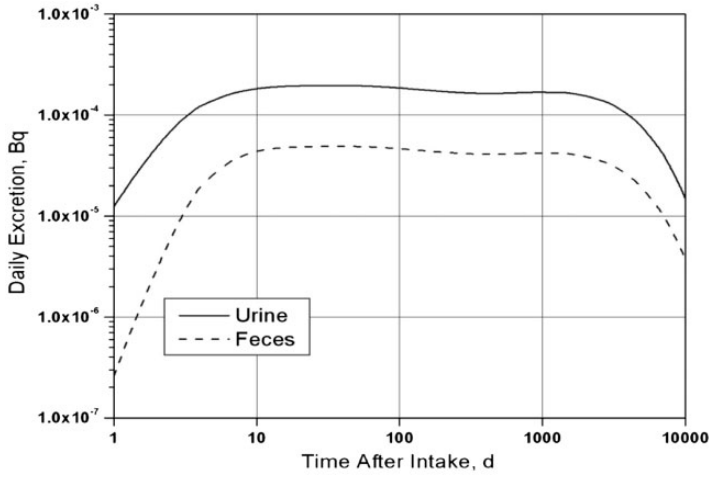

Fig. 3.9. ^{137}Cs wound, particle category; predicted values (Bq per Bq intake) following acute intake.

exhibit a pseudo-equilibrium pattern after approximately 10 d, lasting for several years (Fig. 3.9).

(167) The presence of wounds, abrasions, burns, or other pathological damage to the skin may greatly increase the ability of radioactive materials to reach

subcutaneous tissues and, subsequently, the systemic circulation. Although much of the material deposited at a wound site may be retained at the site, and can be excised surgically, soluble (transportable) material can be transferred to the blood and hence to other parts of the body. As noted in Section 3.1, the assessment of internal contamination resulting from wounds is, in practice, treated on a case-by-case basis using expert judgement. In many cases, the amount of a radionuclide transferred from a wound site into blood may be assessed directly from urine bioassay data. No dosimetric models are recommended by ICRP for calculating doses from radionuclides transferred from wound sites into blood and to other organs and tissues. Such models are, however, published by NCRP (2006), and therefore dose coefficients for injection as the route of intake are given in the electronic annex, which may assist in assessment of doses after wound contamination.

3.5. Biokinetic models for systemic radionuclides

3.5.1. Parent radionuclides

(168) A model that describes the time-dependent distribution and excretion of a radionuclide in the body after it reaches the systemic circulation is referred to here as a systemic biokinetic model. In contrast to ICRP's biokinetic models describing the behaviour of radionuclides in the respiratory and alimentary tracts, ICRP's systemic biokinetic models have usually been element-specific models with regard to model structure as well as parameter values. A generic model structure that depicts all potentially important systemic repositories and paths of transfer of all elements of interest in radiation protection would be too complex to be of much practical use. However, generic model structures have been used occasionally in previous ICRP reports to describe the systemic biokinetics of small groups of elements, typically chemical families, known or expected to have qualitatively similar behaviour in the body. For example, *Publication 20* (ICRP, 1973) introduced a generic model formulation for the alkaline earth elements calcium, strontium, barium, and radium, but provided element-specific values for most model parameters. In Parts 1–3 of *Publication 30* (ICRP, 1979, 1980, 1981), a model developed for plutonium, including parameter values as well as model structure, was applied to most actinide elements. The biokinetic models for several of these actinide elements were modified in Part 4 of *Publication 30* (ICRP, 1988b), where the model structure for plutonium was used as a generic structure; a common set of parameter values was applied to plutonium, americium, and curium; and element-specific values were applied to selected parameters in the models for other elements. The use of generic systemic model structures was increased in ICRP's reports on doses to members of the public from intake of radionuclides (ICRP, 1993, 1995a, 1995b), and is further expanded in the present report because it facilitates the development, description, and application of systemic biokinetic models.

(169) The systemic biokinetic models used in this series of reports generally follow a physiologically descriptive modelling scheme applied on a more limited scale in the series of ICRP reports on doses to members of the public from intake of radionuclides [referred to here as the '*Publication 72* series' (ICRP, 1989, 1993b, 1995b,c, 1996)]. That is, the model structures include one or more compartments representing blood, depict feedback of activity from extravascular repositories into blood (i.e. they are recycling models), and, as far as practical, depict the main physiological processes thought to determine the systemic biokinetics of individual elements.

(170) The systemic biokinetic models for some elements, such as iodine and iron, are developed within model structures specifically designed to describe the unique behaviour of these elements in the body. The models for most elements, however, have been constructed within one of the two generic model structures applied in the *Publication 72* series (ICRP, 1989, 1993b, 1995b,c, 1996) to bone-seeking radionuclides (Figs B.1 and B.2), or variations of those structures. This was done not only for bone-seeking elements but also for a number of elements that show relatively low deposition in bone (e.g. cobalt and ruthenium), because the main repositories and paths of movement of those elements in the body are included in one or the other of these two structures. In some cases, the model structure as applied in the *Publication 72* series (ICRP, 1989, 1993b, 1995b,c, 1996) has been modified slightly to accommodate specific characteristics of an element, or simplified in view of the limited information on certain aspects of the biokinetics of an element.

(171) The systemic biokinetic models used in this report include explicit routes of biological removal of systemic activity in urine and faeces. Additional excretion pathways, such as sweat, are also depicted in the models for some elements.

(172) The biokinetic model adopted for the urinary bladder is described in *Publications 67* and *68* (ICRP, 1993, 1994b). The number of voids per day is taken to be six for workers. To represent the kinetics of the bladder in terms of first-order processes, the rate of elimination from the bladder is taken to be 12 d^{-1}.

(173) In many of the systemic models used in the present series of reports, activity is assumed to be removed in faeces after transfer from systemic compartments into specified segments of the alimentary tract representing element-specific endogenous secretion pathways. The rates of transfer of secreted material through different segments of the alimentary tract are element-independent rates specified in the HATM. Activity transferred from systemic compartments into the contents of the small intestine or higher segments of the tract is assumed to be re-absorbed, in part, into blood. Activity assigned to the contents of the right colon or lower sections of the tract is assumed not to be subject to re-absorption.

3.5.2. Radioactive progeny

(174) In *Publications 30* and *68* (ICRP, 1979, 1994b), the general assumption was made that chain members produced in systemic compartments following intake of a

parent radionuclide adopt the biokinetics of the parent. This is referred to as the assumption of 'shared kinetics'. The alternative assumption of 'independent kinetics' of chain members was made in *Publication 68* (ICRP, 1994b) when the parent was an isotope of lead, radium, thorium, or uranium, and also for iodine progeny of tellurium and for noble gas isotopes arising in various chains. The implementation of independent kinetics of progeny was based on a general pattern of behaviour of systemically produced progeny radionuclides suggested by a review of experimental and occupational studies (Leggett et al., 1984). That is, the data suggested that most radioactive progeny produced in soft tissue or bone surfaces tended to migrate from the parent and begin to follow their characteristic biological behaviour, while radionuclides produced in bone volume tended to remain with the parent radionuclide in bone over the period of observation.

(175) The assumption of independent kinetics is generally applied in this series of reports to progeny radionuclides produced in systemic compartments other than bone volume compartments, or absorbed into blood after production in the respiratory or alimentary tract. The basic assumption is that a progeny radionuclide follows its characteristic behaviour from its time of production in, or absorption into, the systemic pool. The implementation of this assumption is not always straightforward due to structural differences in the systemic models for many parent and progeny combinations. For example, a radionuclide may be born in an explicitly designated tissue in the parent's model that is not an explicitly designated tissue in the progeny radionuclide's characteristic model. When this happens, the rate of removal of the progeny radionuclide and the destination of the removed activity must be defined before the model can be solved.

(176) Even if the progeny radionuclide is produced in a tissue that is an explicitly designated source organ in the progeny radionuclide's characteristic model, implementation of the default treatment of independent kinetics may become somewhat arbitrary if the progeny radionuclide's model divides the tissue into compartments that are not identifiable with compartments in the parent's model. For example, this may occur if the division of the tissue into compartments is based on physiological or anatomical considerations for the parent and on a kinetic basis for the progeny, or vice versa. Such issues of compartment identifiability are addressed on a case-by-case basis.

(177) Each of the element sections in this series of reports describes the implementation of the assumption of independent kinetics for dosimetrically significant progeny of radioisotopes of the element. The method of implementation for a given parent element depends on: the availability of specific information on the behaviour of chain members produced in vivo, the sensitivity of dose estimates to uncertainties in the behaviour of chain members, the lengths of radionuclide chains for that element, and the complexity and consistency of the characteristic systemic models for chain members. In some cases, primarily involving progeny radionuclides with short radiological or biological half-times, the characteristic systemic model for the progeny is replaced by a simpler model judged as adequate for practical purposes in view of the uncertainties in its short-term behaviour following production in vivo. For example, short-lived progeny radionuclides are assumed in some cases to decay at

their site of production. As a second example, relatively detailed mechanistic models applied in this series of reports to noble gases as parent radionuclides are replaced by much simpler models for application to their behaviour following production in vivo. In all cases, the systemic model applied to an element X as a progeny of a parent element Y is the same for all chains headed by Y as the parent. For example, the systemic model applied to ^{224}Ra produced in a systemic pool following intake of ^{228}Th is also applied to ^{223}Ra produced in a systemic pool following intake of ^{227}Th.

3.6. Medical intervention

(178) If medical treatment to prevent uptake or enhance excretion is administered, the data provided in the models summarised in this series of reports cannot be used directly to assess committed effective doses from monitoring information (NCRP, 1980; Gerber and Thomas, 1992; IAEA, 1996). In such circumstances, a programme of special monitoring (Section 5.5) should be undertaken to follow the retention of the particular contaminant in the person, and these data should be used to make a specific assessment of committed dose.

3.7. Methodology for dose calculations: the ICRP dosimetry system

(179) The ICRP dosimetry system is presented below as applied to assessment of organ equivalent dose and effective dose following intakes of radionuclides. The system involves numerical solution of reference biokinetic models, yielding the time-dependent number of nuclear transformations in various source tissues. These solutions are then coupled with reference data on nuclear decay information, target tissue masses, and fractions of emitted energy released from source tissue regions that are deposited in target tissue regions as defined in the reference phantoms in *Publication 110* (ICRP, 2009). Presented below is the computational formalism of these dosimetry calculations consistent with the protection quantities defined in *Publication 103* (ICRP, 2007). Further, more detailed data will be presented in a forthcoming publication (ICRP, 2016c).

3.7.1. Computational solutions to the ICRP reference biokinetic models

(177) The HRTM (ICRP 1994a), the HATM (ICRP 2006), and the systemic biokinetic models of this report describe the dynamic behaviour of radionuclides within the body. Given the routes of intake, the models predict the subsequent uptake to the systemic circulation, the distribution among tissues of the body, and the routes of elimination from the body. Superimposed on these dynamics are in-situ radioactive decay and the ingrowth of radioactive progeny. Consequently, the uptake, distribution, and elimination of all progeny are predicted, in addition to those of the parent radionuclide.

(178) The compartment models of the respiratory and alimentary tract coupled with those of the systemic biokinetics define a system of first-order differential equations. The solution to the set of equations is the time-dependent distribution of the radionuclide and its radioactive progeny, if any, in mathematical compartments (pools) that are associated with anatomical regions in the body. Let $A_{i,j}(t)$ represent the activity of radionuclide i in compartment j at time t. The rate of change in the activity of member i of the decay chain, $i=1, 2,\ldots, N$ with $i=1$ being the parent nuclide, in compartment j, can be written as:

$$\frac{dA_{i,j}(t)}{dt} = \sum_{\substack{k=1 \\ k\neq j}}^{M} A_{i,k}\lambda_{i,k,j} - A_{i,j}\left[\sum_{\substack{k=1 \\ k\neq j}}^{M} \lambda_{i,j,k} + \lambda_i^p\right] \sum_{k=1}^{i-1} A_{k,j}\beta_{k,i}\lambda_i^p \qquad (3.3)$$

where:

M is the number of compartments describing the kinetics;

$\lambda_{i,j,k}$ is the fractional transfer rate of chain member i from compartment j (donor compartment) to compartment k (receiving compartment) in the biokinetic model;

λ_i^p is the physical decay constant of chain member i; and

$\beta_{k,i}$ is the fraction of the decays of chain member k forming member i.

(179) Given the initial conditions specified for the compartments, $A_{i,j}(0)$, Eq. (3.3) defines the dynamic behaviour of the radionuclide and its progeny within the human body. The first term on the right hand side of Eq. (3.3) represents the rate of flow of chain member i into compartment j from all donor compartments. The second term represents the rate of removal of member i from compartment j both by transfer to receiving compartments and by physical decay. The third term addresses the ingrowth of member i within compartment j due to the presence of its precursors k in the compartment. Note that the members of the decay chain are assumed to be of order such that the precursors of member i have indexes less than i. An ordered listing of the chain members can be obtained using the DECDATA software distributed with *Publication 107* (ICRP, 2008).

(180) The system of N x M ordinary first-order differential equations must be solved using suitable numerical methods. The system is generally solved for the initial conditions that $A_{i,j}(0) = 0$ for all compartments with the exception of compartments of intake where non-zero initial conditions are only applied to the parent nuclide (i.e. $j=1$).

(181) To calculate the numerical values of the dose coefficients, it is necessary to associate the biokinetic compartments of Eq. (3.3) with anatomical source regions indexed by r_S. A source region may or may not be living tissue (for example, stomach content may be a source organ but is not a living tissue) and may consist of more than one kinetic compartment. The number of nuclear transformations of chain member i occurring in source region r_S, $\tilde{A}_i(r_S)$ (Bq s), is given by:

$$\tilde{A}_{\mathrm{i}}(r_{\mathrm{S}},\tau)=\sum_{\mathrm{j}}\int_{0}^{\tau}A_{\mathrm{i,j}}(t)\mathrm{d}t \tag{3.4}$$

where τ is the commitment period (taken to be 50 years for workers). The summation in Eq. (3.4) is over all kinetic compartments j associated with source region r_{S}, and the quantity $A_{i,j}(t)$ is obtained by solving Eq. (3.3). The number of nuclear transformations per activity intake in the source region r_{S}, denoted as $\tilde{a}_{\mathrm{i}}(r_{\mathrm{S}},\tau)$ (s), is given by:

$$\tilde{a}_{\mathrm{i}}(r_{\mathrm{S}},\tau)=\frac{\tilde{A}(r_{\mathrm{S}},\tau)}{\sum_{\mathrm{j}}A_{1,\mathrm{j}}(0)} \tag{3.5}$$

where the summation in the denominator is over the compartment contents at $t=0$. In the case of inhalation intakes of particulate and gaseous matter, the denominator excludes the exhaled activity as only a fraction of the activity intake is deposited in the compartments of the HRTM.

3.7.2. Computation of the ICRP reference dose coefficients for organ equivalent dose

(182) The committed equivalent dose coefficient in target region r_{T} of the Reference Adult Male, $h^{\mathrm{M}}(r_{\mathrm{T}},\tau)$, and the Reference Adult Female, $h^{\mathrm{F}}(r_{\mathrm{T}},\tau)$, for integration time τ is given by:

$$h^{\mathrm{M}}(r_{\mathrm{T}},\tau)=\sum_{\mathrm{i}}\sum_{r_{\mathrm{S}}}\tilde{a}_{\mathrm{i}}(r_{\mathrm{S}},\tau)S_{\mathrm{w}}^{\mathrm{M}}(r_{\mathrm{T}}\leftarrow r_{\mathrm{S}})_{\mathrm{i}} \tag{3.6}$$

$$h^{\mathrm{F}}(r_{\mathrm{T}},\tau)=\sum_{\mathrm{i}}\sum_{r_{\mathrm{S}}}\tilde{a}_{\mathrm{i}}(r_{\mathrm{S}},\tau)S_{\mathrm{w}}^{\mathrm{F}}(r_{\mathrm{T}}\leftarrow r_{\mathrm{S}})_{\mathrm{i}} \tag{3.7}$$

where the S coefficients, $S_{\mathrm{w}}^{\mathrm{M}}(r_{\mathrm{T}}\leftarrow r_{\mathrm{S}})_{\mathrm{i}}$ and $S_{\mathrm{w}}^{\mathrm{F}}(r_{\mathrm{T}}\leftarrow r_{\mathrm{S}})_{i}$, are the radiation weighted equivalent doses in target region r_{T} due to the nuclear transformations of chain member i in source region r_{S} [Sv (Bq s)$^{-1}$] for the male and female worker, respectively. Note that the outer summation extends over the parent nuclide and its progeny.

(183) A number of tissues listed in Table 1.2 used to compute the effective dose are considered to be represented by a single target region, r_{T}. In cases where more than one tissue region defines the target tissue, fractional weighting of the equivalent dose must be made. The committed equivalent dose coefficients for tissue T in the Reference Adult Male, $h_{\mathrm{T}}^{\mathrm{M}}(\tau)$, and the Reference Adult Female, $h_{\mathrm{T}}^{\mathrm{F}}(\tau)$, are thus given as:

$$h_{\mathrm{T}}^{\mathrm{M}}(\tau)=\sum_{r_{\mathrm{T}}}f(r_{\mathrm{T}},T)h^{\mathrm{M}}(r_{\mathrm{T}},\tau) \tag{3.8}$$

Table 3.5. Target region fractional weights, $f(r_T, T)$.

Tissue, T	r_T	$f(r_T, T)$
ET	ET_1	0.001
	ET_2	0.999
TH	BB*	1/3
	bb	1/3
	AI	1/3
Colon	Right colon	0.4
	Left colon	0.4
	Rectosigmoid	0.2
Lymphatic nodes	LN_{ET}	0.08
	LN_{TH}	0.08
	Lymph (systemic)	0.84

ET, extrathoracic; TH, thoracic; ET_1, anterior nasal passage; ET_2, posterior nasal passage, pharynx, and larynx; BB, bronchial; bb, bronchiolar; AI, alveolar–interstitial; LN_{ET}, ET lymph nodes; LN_{TH}, TH lymph nodes.
*The basal and secretory cells are the two target regions weighted equally.

$$h_T^F(\tau) = \sum_{r_T} f(r_T, T) h^F(r_T, \tau) \tag{3.9}$$

where the target region fractional weights $f(r_T, T)$ are the proportions of the equivalent dose in tissue T associated with target region r_T. With the exception of the tissues addressed in Table 3.5, the tissues of Table 1.2 are represented by a single target region and thus for these tissues $f(r_T, T) = 1$. In Table 3.5, values of $f(r_T, T)$ for the ET and TH regions are taken to be equivalent to their risk apportionment factors as assigned in the revised HRTM (see Table 3.3). For the colon, values of $f(r_T, T)$ are taken to be the fractional masses of the stem cell layers within the alimentary tract walls [see Table 7.8 of *Publication 100* (ICRP, 2006)]. For the lymphatic nodes, values of $f(r_T, T)$ are taken to be the fractional masses of lymphatic nodes (not lymphatic tissues) within the ET, TH, and non-respiratory regions, consistent with data given previously in *Publication 66* (ICRP, 1994a).

3.7.3. Computation of the ICRP reference dose coefficients for the effective dose

(184) As defined in *Publication 103* (ICRP, 2007), the committed effective dose coefficient, $e(\tau)$, is:

$$e(\tau) = \sum_T w_T \left[\frac{h_T^M(\tau) + h_T^F(\tau)}{2} \right] \tag{3.10}$$

where w_T is the tissue weighting factor for tissue T of Table 1.2, and $h_T^M(\tau)$ and $h_T^F(\tau)$ are the corresponding committed equivalent dose coefficients for these same tissues in the Reference Adult Male and Female, respectively.

3.7.4. Implementation of specific absorbed fractions within the ICRP dosimetry system

(185) The radiation weighted S coefficient [Sv (Bq-s)$^{-1}$] for a radionuclide is calculated as:

$$S_w(r_T \leftarrow r_S) = \sum_R w_R \sum_i E_{R,i} Y_{R,i} \Phi\left(r_T \leftarrow r_S, E_{R,i}\right) \tag{3.11}$$

where:

$E_{R,i}$ is the energy of the i^{th} radiation of type R emitted in nuclear transformations of the radionuclide;
$Y_{R,i}$ is the yield of the i^{th} radiation of type R per nuclear transformation [(Bq s)$^{-1}$];
w_R is the radiation weighting factor for radiation type R (Table 1.1); and
$\Phi\left(r_T \leftarrow r_S, E_{R,i}\right)$ is the specific absorbed fraction, defined as the fraction of energy $E_{R,i}$ of radiation type R emitted within the source tissue r_S that is absorbed per mass in the target tissue r_T (kg^{-1}).

(186) The energies and yields of the emitted radiations, $E_{R,i}$ and $Y_{R,i}$, are taken from *Publication 107* (ICRP, 2008). For beta emissions, the spectral data are used in the calculation of S_w rather than mean values [i.e. the inner summation in Eq. (3.5) is replaced by the integral over the spectrum].

(187) For both sexes, the values of the specific absorbed fractions for all the radiations emitted in nuclear transformations as tabulated in *Publication 107* (ICRP, 2008) will be published in a forthcoming publication (ICRP, 2016c). Specific absorbed fractions at the tabulated energies are found by cubic spline interpolation.

(188) For most combinations of source and target regions, the specific absorbed fractions for photons, electrons, and neutrons are based on Monte Carlo radiation transport calculations performed using the reference phantoms for the Reference Adult Male and Female described in *Publication 110* (ICRP, 2009). These phantoms are constructed from tomographic images of real individuals.

(189) For alpha particles, the specific absorbed fractions are the inverse of the mass of the target region if $r_S = r_T$ and 0 if $r_S \neq r_T$. Exceptions occur for source and target regions within the respiratory and alimentary tracts, skeleton, urinary bladder, and gall bladder. In these cases, only a fraction of the energy emitted within the source region is deposited in the target region, and that fraction may be energy dependent.

(190) In the alimentary and respiratory tracts, absorbed fractions for photons are derived using the reference phantoms (ICRP, 2009). The absorbed fraction data for electrons and alpha particles in the alimentary tract of *Publication 100* (ICRP, 2006) have been updated with supplementary calculations to be included in a forthcoming publication (ICRP, 2016c). The absorbed fractions for electrons and alpha particles in the respiratory tract given in *Publication 66* (ICRP, 1994a) will be presented in a forthcoming publication (ICRP, 2016c).

(191) The biokinetic models consider that uptake occurs in the following skeletal source regions:

- trabecular bone surfaces and volumes;
- cortical bone surfaces and volumes, where surfaces of bone include:
    - Haversian canal within the cortical bone cortex surrounding all regions of trabecular spongiosa;
    - Haversian canal within the cortical bone of the long bone shafts; and
    - surfaces separating medullary marrow cavities and cortical bone shafts of the long bones;
- trabecular bone marrow, corresponding to the marrow within regions of trabecular spongiosa – both active and inactive marrow; and
- cortical bone marrow, corresponding to the marrow within the medullary marrow shafts of the long bones, as well as the fluids within the Haversian canals of cortical bone. In the adult, the marrow of the long bone shafts is inactive marrow.

The skeletal target regions are:

- the 50-μm endosteal region (referred to as bone surface in Table 1.2); and
- active (red) marrow.

The target tissue, bone surface, of Table 1.2 is the soft tissues within 50 μm of the surfaces of mineral bone, and is thought to be the region within which the osteoprogenitor cells associated with bone cancer reside. This target tissue is independent of the marrow cellularity (the fraction of bone marrow volume that is haematopoietically active). The systemic biokinetic models may identify the 'active marrow' or the 'trabecular marrow' as source regions, and specific absorbed fractions will be given for both source regions in a forthcoming publication (ICRP, 2016c).

3.7.5. Contribution of radioactive progeny to dose

(192) As in earlier ICRP publications, the dose coefficients in this series of reports account for ingrowth of radioactive progeny following the intake of the parent radionuclide. The coefficients are for the intake of the parent nuclide (i.e. upon intake, the progeny are absent). Inhalation of radon is an exception where the radioactive progeny are assumed to be present at intake.

(193) Generally, the systemic biokinetic model includes a compartment denoted as 'other' which contains the systemic activity not explicitly assigned to compartments of identified organs and tissues. 'Other' is the complement of the explicitly designated compartments; that is, this compartment consists of all systemic tissues other than those associated with explicitly identified compartments in the systemic biokinetic model. If independent kinetics are assumed for progeny radionuclides, each member of the decay chain may have different sets of compartments, and as a result, the anatomical identity of the 'other' compartment varies among the chain members. Two alternative computational procedures to address this situation were discussed in Annex C.3 of *Publication 71* (ICRP, 1995c).

3.7.6. Bioassay data

(194) A number of issues are noted regarding the use of biokinetic models in retrospective assessment of doses from bioassay data.

- As explained in Section 1.4, equivalent dose coefficients for organs and tissues are calculated for the Reference Male and Female, and averaged in the calculation of effective dose. Some biokinetic models (HATM and HRTM) have sex-specific parameter values. However, as effective dose is a protection quantity developed for the Reference Worker rather than a specific individual, significant advantages arise from adopting a simple approach for routine retrospective dose assessment when tissue/organ absorbed doses are far below the thresholds for tissue reactions. For these reasons, the approach adopted in this series of reports is to determine the intake using male biokinetic models, and thus no female retention or excretion coefficients are provided.
- The dose per content functions presented in this series of reports are for activity within the body (including contents of the urinary bladder and the alimentary tract). For the lungs, the coefficient includes all activity in the TH region of the respiratory tract, including the LN_{TH}. Similarly, for the skeleton, all activity in trabecular and cortical bone (both surface and volume) and in bone marrow (both active and inactive) is included.
- The dose per content functions for bioassay samples are applicable to the content of a 24-h urine or faeces sample. To use these coefficients, measured sample activities should be decay-corrected to the time of the end of the sample collection period.

4. METHODS OF INDIVIDUAL AND WORKPLACE MONITORING

4.1. Introduction

(195) This section briefly describes the main measurement techniques, their advantages, and their limitations for individual monitoring. In most cases, assessment of intakes of radionuclides may be achieved by body activity measurements, excreta monitoring, air sampling with personal air samplers, workplace measurements, or a combination of these techniques. The choice of measurement technique will be determined by a number of factors including the radiation emitted by the radionuclide, the availability of equipment, the biokinetic behaviour of the contaminant, and the likely radiation dose.

4.2. Body activity measurements (in-vivo measurements)

(196) In-vivo measurement of body or organ content provides a quick and convenient estimate of activity in the body. It is performed with one or more photon detectors placed at specific positions in relation to the subject being measured. It is feasible only for those radionuclides emitting radiation that can be detected outside the body. In principle, the technique can be used for radionuclides that emit: x or γ radiation; positrons, as they can be detected by measurement of annihilation radiation; or energetic beta particles that can be detected by measurement of bremsstrahlung radiation (e.g. ^{90}Y, produced by the decay of its ^{90}Sr parent).

(197) The detectors used for in-vivo measurements are usually partially shielded, and the individual to be measured can be placed in a shielded, low-background room to reduce the interference from ambient sources of radiation.

(198) Direct (in-vivo) bioassay is likely to be the monitoring method of choice if the radionuclide is a high-yield, high-energy γ-ray emitter or decays by positron emission (with emission of annihilation radiation), unless the material is excreted rapidly from the body. The γ radiation emitted by such radionuclides is strongly penetrating, and so is readily detected using scintillation or semiconductor detectors positioned close to the body. If the material is absorbed rapidly from the respiratory tract, and is then either distributed uniformly in body tissues (e.g. ^{137}Cs in most common chemical forms), or is distributed preferentially among a number of organs (e.g. ^{59}Fe), whole-body monitoring should be chosen. If the radionuclide deposits preferentially in a single organ such as the thyroid (e.g. ^{125}I, ^{131}I), partial-body monitoring of the relevant organ should be chosen. In the case of materials that are absorbed less rapidly from the respiratory tract (e.g. insoluble forms of ^{60}Co oxide), lung monitoring is preferable to whole-body monitoring soon after the intake, as it gives a more accurate measure of lung deposition and retention than a whole-body measurement.

(199) Direct bioassay is also useful for some radionuclides that emit photons (x or γ rays) at lower energies and/or with lower yields (e.g. ^{241}Am, ^{210}Pb, ^{144}Ce).

However, in the case of radionuclides that mainly emit x rays below 25 keV with low yields (notably, the alpha-emitting isotopes of plutonium and curium), direct bioassay may not achieve the sensitivity required for radiological protection purposes.

(200) If activity is present in a wound, it can be detected with conventional γ detectors if the contaminant emits energetic γ rays. In the case of contamination with alpha-emitting radionuclides, detection is much more difficult, as the low-energy x rays that follow the alpha decay will be strongly attenuated in tissue; this effect is more important for deeper wounds. It is often necessary to localise the active material, and this requires a well-collimated detector. Wound monitors must have an energy discrimination capability if a good estimate is to be made of contamination with mixtures of radionuclides. If whole-body measurements are made, it may be necessary to shield any activity remaining at the wound site.

(201) For activity calibrations of in-vivo monitoring systems, laboratories generally use physical phantoms, either commercially available or handcrafted [e.g. the Bottle-Mannikin-Absorption phantom, the Lawrence Livermore thorax phantom for lung monitoring (Griffith et al., 1986; Snyder and Traub, 2010)]. This approach has some limitations with respect to body size, body shape, and radionuclide distribution. The distribution of the radionuclide in the calibration phantom should match that expected in the human subject as far as possible. Alternatively, numerical calibration techniques may be applied. Mathematical software combines voxel phantoms and Monte Carlo statistical simulations to model photon transport from the phantom and the detection of photons by a simulated detector (Franck et al., 2003; Hunt et al., 2003; Gómez-Ros et al., 2007; Lopez et al., 2011a).

(202) The International Atomic Energy Agency (IAEA) and the International Commission on Radiation Units and Measurements (ICRU) have given guidance on the direct measurement of body content of radionuclides (IAEA, 1996; ICRU, 2002).

4.3. Analysis of excreta and other biological materials

(203) Excreta monitoring programmes usually involve analysis of urine, although faecal analysis may also be required if the material is relatively insoluble. Other samples may be analysed for specific investigations. Examples are the use of nose-blow or nasal smears as routine screening techniques.

(204) The collection of urine samples involves three considerations. Firstly, care must be taken to avoid adventitious contamination of the sample. Secondly, it is usually necessary to assess or estimate the total activity excreted in urine per time from measurements on the sample provided. For most routine analyses, a 24-h collection is preferred but, if this is not feasible, it must be recognised that smaller samples may not be representative. Where a 24-h sample is not easily collected, the first morning voiding is preferable for analysis (IAEA, 2000). Measurement of creatinine concentration in urine has frequently been used to estimate 24-h excretion of radionuclides from urine samples collected over part of a day. Other methods of obtaining an estimate of 24-h excretion include normalisation by volume (with or without a correction for specific gravity) and normalisation by the length of the

sampling interval. The relative merits of the various normalisation methods have been discussed by a number of authors (Jackson, 1966; Graul and Stanley, 1982; Boeniger et al., 1993; Kim, 1995; Duke, 1998; NCRP, 2008). Tritium in the form of tritiated water is an exceptional case for which it is usual to take only a small sample, and to relate the measured activity concentration to the concentration in body water. Thirdly, the volume required for analysis depends upon the sensitivity of the analytical technique. For some radionuclides, adequate sensitivity can be achieved only by analysis of several days' excreta (Duke, 1998).

(205) The interpretation of faecal samples for routine monitoring involves uncertainty due to daily fluctuations in faecal excretion. Ideally, therefore, collection should be over a period of several days. However, in practice, it may be difficult to collect multiple samples, and interpretation may need to be based on a single sample. Faecal monitoring is more often used in special investigations, particularly following a known or suspected intake by inhalation of moderately soluble or insoluble compounds. In these circumstances, measurement of the quantity excreted daily may be useful in the evaluation of clearance from the lungs and in the estimation of intake. As for routine monitoring, collections should be over a period of several days rather than a single day. This is especially important immediately after an incident, because of the large variability in faecal excretion during the first few days. If possible, some samples should be taken soon after the date of the incident, because early results may be useful in identifying exposed individuals.

(206) Radionuclides that emit photons may be determined in biological samples by direct measurement with scintillation or semiconductor detectors. Analysis of alpha- and beta-emitting radionuclides usually requires chemical separation followed by appropriate measurement techniques, including alpha spectrometry and liquid scintillation counting. Measurement of so-called total alpha or beta activity may occasionally be useful as a simple screening technique.

(207) Increasing use is being made of mass spectrometric techniques for the analysis of excreta samples. Examples are inductively coupled plasma mass spectrometry that can achieve much lower detection limits for long-lived radionuclides than is possible with alpha spectrometry, and thermal ionisation mass spectrometry, used to monitor very low activities of ^{239}Pu in urine (Inkret et al., 1998; LaMont et al., 2005; Elliot et al., 2006).

(208) Measurement of activity in exhaled breath may be used as a monitoring technique for some radionuclides such as ^{226}Ra and ^{228}Th, as the decay chains of both these radionuclides include gases that may be exhaled (Youngman et al., 1994; Sathyabama et al., 2005). It can also be used to monitor $^{14}CO_2$ formed in vivo from the metabolism of ^{14}C-labelled compounds (Leide-Svegborn et al., 1999; Gunnarsson et al., 2003).

(209) The measurement of activity on nasal smears and nose-blow samples may be employed as a useful screening technique (Smith et al., 2012). A positive measurement gives an indication that an unexpected situation may have occurred. Excreta measurements or lung monitoring should follow to confirm the intake and to provide a quantitative assessment.

4.4. Exposure monitoring of the workplace

(210) Workplace monitoring is useful for triggering bioassay measurements. In addition, workplace characterisation may be used as a complement to bioassay monitoring as it provides useful information on the physical and chemical composition of the radionuclides present in the working environment [e.g. information on the particle sizes (AMAD)].

(211) Two workplace monitoring methods may be used for monitoring individual exposures: personal air sampling (PAS) and static air sampling (SAS). A personal air sampler is a portable device specifically designed for the estimation of intake by an individual worker from a measurement of concentration of activity in air in the breathing zone of the worker. A sampling head containing a filter is worn on the upper torso within the breathing zone. Air is drawn through the filter by a calibrated air pump carried by the worker. Ideally, sampling rates would be similar to typical breathing rates for a worker (approximately1.2 m^3 h^{-1}). However, sampling rates of current devices are only approximately one-fifth of this value. The activity on the filter may be measured at the end of the sampling period to give an indication of any abnormally high exposures. The difficulties in assessing intakes from PAS measurements were considered by Whicker (2004). Breathing zone measurements can vary significantly as they can be affected by measurement conditions such as orientation of the sampler with respect to source, on which lapel (right or left) the sampler is worn, design of the air sampling head, particle size, local air velocities and directions, and sharp gradients in and around the breathing zone of workers.

(212) Britcher and Strong (1994) reviewed the use of PAS as part of the internal dosimetry monitoring programmes for the Calder Hall reactors and the Sellafield nuclear fuel reprocessing facility in the UK. It was concluded that samplers can be used to obtain satisfactory estimates of intake for groups of workers. However, for individuals, the correlation between assessments using PAS and biological samples was poor, and the authors cast doubt on the adequacy of PAS for estimating annual intakes of individual employees at the levels of exposure encountered in operational environments. The authors also questioned whether, for environmental monitoring, PAS offered any advantages over SAS programmes. The same lack of correlation between PAS and bioassay-sample-based intake estimates was also seen for known acute exposures (Britcher et al., 1998).

(213) A uranium exposure study was conducted by Eckerman and Kerr (1999) to determine the correlation between uranium intakes predicted by PAS and intakes predicted by bioassay at the Y12 uranium enrichment plant in Oak Ridge, TN, USA. This study concluded that there was poor correlation between the two measurements.

(214) Static air samplers are commonly used to monitor workplace conditions, but can underestimate concentrations in air in the breathing zone of a worker. Marshall and Stevens (1980) reported that PAS:SAS air concentration ratios can vary from less than 1 up to 50, depending on the nature of the work. Britcher and Strong (1994) concluded from their review of monitoring data for Magnox plant

workers in the UK that intakes assessed from PAS data were approximately one order of magnitude greater than those implied by SAS data. SAS devices, however, can provide useful information on radionuclide composition, and on particle size, if used with a size analyser such as a cascade impactor.

(215) Overall, the use of PAS and SAS can be an important part of a comprehensive workplace monitoring programme, and provide an early indication of risk of exposure. Experience of the use of PAS and SAS indicates that body activity measurements and/or excreta analysis are preferable for the assessment of individual intakes of airborne radionuclides and effective doses.

(216) However, for some transuranic radionuclides, body activity measurements and urine analysis can only quantify exposures sufficiently reliably above a few mSv unless sensitive mass spectrometric techniques for the analysis of bioassay samples are available. For the detection of lower exposures, a combination of monitoring methods is likely to be needed, which could include air sampling and faecal analysis.

5. MONITORING PROGRAMMES

5.1. Introduction

(217) The design and management of monitoring programmes is considered in this section. It is recommended that the emphasis in any particular monitoring programme should be on the formal assessment of doses to those workers who are considered likely to routinely receive a significant fraction of the relevant dose limit, or who work in areas where exposures could be significant in the event of an accident.

(218) In general, the assignment of an internal exposure monitoring programme to an individual should be based on the likelihood that the individual could receive an intake of radioactive material exceeding a predetermined level as a result of normal operations or in the event of an accident. The use of individual monitoring for workers whose effective doses from annual intakes could exceed 1 mSv is common practice in many organisations, although it may not be required by legislation.

(219) It is important to consider both the monitoring programme design and the dose assessment process as integral parts of the overall radiation protection programme. An appropriately designed monitoring programme should provide the data necessary to enable a dose assessment to meet the specified need; even the most sophisticated dose assessment calculations cannot compensate for inadequate monitoring data.

(220) Where assessed doses could be significant, there is much to be gained from using a combination of different monitoring methods (e.g. lung, urine, faecal monitoring, and exposure monitoring in the workplace), as they provide complementary information. For instance, direct bioassay measurements provide information on deposition and retention in organs, and urine measurements can provide a measure of systemic uptake, but workplace monitoring can provide information on airborne activity, particle size, chemical form, and time of intake.

(221) The assessment of intakes and/or doses using these measured activities (bioassay monitoring results and measurements of the workplace) may be complex and often needs professional judgement on a case-by-case basis. Responsibilities for dose assessment should only be assigned to professionals with adequate expertise and skill, acquired through appropriate education, training, and practical experience.

5.2. General principles for the design of individual monitoring programmes

(222) A specification for an individual monitoring programme includes the monitoring method(s) to be employed (e.g. measurement of activity in the body, in excreta samples, and exposure monitoring in the workplace), the measurement technique used (e.g. photon spectrometry, alpha spectrometry, mass spectrometry), monitoring intervals for routine monitoring, and measurement or sample collection times for special monitoring.

(223) Many factors need to be taken into consideration when designing an individual monitoring programme. These include the purpose of the monitoring (e.g.

whether it is carried out to demonstrate compliance with regulatory requirements, or simply to confirm that doses are very low), local factors such as the number of workers to be monitored and the availability of particular measurement methods, and economic factors. The main factors that determine the dosimetric performance of the monitoring programme relate to the characteristics of the material to which a worker may potentially be exposed (normally by inhalation). These are:

- the radiations emitted by the radionuclide and its progeny;
- the effective half-lives of the radionuclide and its progeny;
- the respiratory tract deposition characteristics of the aerosol;
- the respiratory tract and alimentary tract absorption characteristics of the material;
- the retention in the body or the excretion rate from the body as a function of the time between intake and measurement;
- any preferential deposition in particular body organs and tissues, and subsequent retention in those organs;
- any significant differences between the biokinetic behaviour of a parent radionuclide and its progeny;
- the excretion pathway (e.g. urine, faeces); and
- the technical feasibility of the measurement.

(224) The dosimetric performance of the monitoring programme may be assessed by considering the effect of these factors on the accuracy of assessed doses and on the sensitivity associated with the monitoring programme, which can be quantified in terms of the assessed minimum detectable dose (Carbaugh, 2003; Etherington et al., 2004a,b). One approach to optimising the design of a monitoring programme is to assess how different choices for the type, number, and time period of measurements affect uncertainties in assessed dose.

5.3. Categories of monitoring programmes

(225) Four categories of monitoring programmes can generally be defined.

- Routine monitoring is performed where intakes by workers are probable at any time during normal operations, or where inadvertent intakes could otherwise remain undetected.
- Special monitoring is performed after actual or suspected abnormal events.
- Confirmatory monitoring is performed to demonstrate that working conditions are satisfactory, and that there is no need for routine individual monitoring. It could consist of occasional individual monitoring measurements.
- Task-related monitoring is performed to provide information about a particular operation.

(226) The four categories of monitoring are not mutually exclusive; in fact, there can be considerable overlap. For example, an effective routine monitoring programme not only provides reliable data on individual worker exposures and doses, but can also be used to demonstrate that the work environment and work procedures are under satisfactory control.

5.3.1. Routine monitoring

(227) Routine monitoring programmes may involve a single type of measurement or a combination of techniques, depending on the sensitivity that can be achieved. For some radionuclides, only one measurement technique is practical (e.g. urine monitoring for assessment of intakes of tritium). For radionuclides such as plutonium isotopes that present difficulties for both measurement and interpretation, various techniques may have to be employed. If different methods of adequate sensitivity are available, the general order of preference (highest first) in terms of accuracy of interpretation is: body activity measurements; excreta analysis; and exposure monitoring in the workplace.

(228) These techniques are, in general, complementary and not mutually exclusive. For example, results of monitoring of the working environment (area monitoring) can provide early indication of worker exposure, and can therefore be used to trigger special bioassay monitoring, or they may provide information that assists in interpreting the results of individual monitoring (e.g. information on airborne activity, particle size, chemical form and solubility, and time of intake).

(229) Urine monitoring provides a measure of systemic uptake to organs and tissues after inhalation and ingestion for those elements for which urine excretion rates are sufficiently high. It can also be used to determine the fraction of activity deposited in a wound site that transfers to the systemic circulation.

(230) Caution should be exercised in using urine monitoring for materials that are absorbed relatively slowly from the respiratory tract (i.e. 'insoluble' materials). In these circumstances, it is usually the lung dose that makes the greatest contribution to effective dose, and uncertainties on the knowledge of the absorption characteristics of the material can result in significant errors in assessed dose. For insoluble materials, significant improvements in sensitivity can be achieved by using faecal monitoring in addition to urine monitoring. This is because significant fractions of insoluble material deposited in both the ET airways and the lungs are cleared via the alimentary tract to faeces.

(231) Interpretation of faecal monitoring data needs to take account of a number of factors that are specific to the faecal excretion pathway. Excretion of faeces is a discrete process (although it is usually modelled using first-order kinetics), and so it is advisable to sum the amounts excreted over a 3-d period to obtain a daily excretion rate.

(232) In the workplace, individuals may be exposed to a variety of radionuclides, such as those that occur in fuel reprocessing or manufacturing plants. In such circumstances, it may be feasible to use a radionuclide that is readily detectable to assess the potential for exposure to other radionuclides in the plant. For example, screening for ^{144}Ce could be used to assess the potential for exposure to actinides (Doerfel et al., 2008).

(233) The results of workplace monitoring for air contamination may sometimes be used to estimate individual intakes if individual monitoring is not feasible. However, the interpretation of the results of air sampling measurements in terms of intake is subject to much greater uncertainty and bias.

(234) The probability of exposure and the likely time pattern of intake are often dependent on the tasks being performed. For example, exposures may be chronic for workers in the mining industry. On the other hand, workers in nuclear power plants are not expected to receive significant intakes, except in the rare event of an accident.

(235) The required frequency of measurements in a routine monitoring programme depends upon the retention and excretion of the radionuclide and the sensitivity of the measurement techniques available. Selection of monitoring intervals should also take into account the probability of occurrence of an intake, such that where the risk of intake is high, the frequency of monitoring may need to be increased to reduce the uncertainty in the time of intake. The measurement technique should be selected so that uncertainties in the measured value are small in relation to the major sources of uncertainty.

(236) For situations where an acute exposure situation may be expected, *Publication 78* (ICRP, 1997b) provides a simple rule that limits the possible error on the estimate of intake arising from the unknown time of exposure. Monitoring intervals are selected so that any underestimation introduced by the unknown time of intake is no more than a factor of three. In practice, this is a maximum underestimate because the actual distribution of the exposure in time is unknown. The error in assessed intake can take on both positive and negative values, depending on the probability distribution of the exposure over the monitoring interval, with the result that the mean value of any underestimate is less than a factor of three. However, if a substantial part of the intake occurs just before sampling or measurement, the intake could be overestimated by more than a factor of three. This may be particularly important in the case of excreta monitoring, as the fraction excreted each day may change rapidly with time in the period immediately following the intake.

(237) An alternative, graphical approach has been developed by Stradling et al. (2005), which considers uncertainties in material-specific parameters such as those describing absorption, particle size distribution, and time of intake. Information on the detection limit for a particular measurement technique is used to determine a monitoring interval appropriate for the dose level of interest.

(238) When chronic exposures are expected, the monitoring programme should be chosen taking into consideration the fact that the amount present in the body and in excreta will increase in time until equilibrium is reached. In each monitoring interval, measurements will reflect the activity accumulated in body organs as a result of chronic intakes received in earlier years. The monitoring programme should consider the workers' assignment of duties. For certain radionuclides, there may be a significant difference between measurements taken before and after the weekend, or before and after an absence from work.

5.3.2. Confirmatory monitoring

(239) One method of confirming that working conditions are satisfactory (typically for annual effective doses less than 1 mSv) is to undertake occasional individual monitoring. Unexpected findings would give grounds for further investigation. Confirmatory monitoring of this type is most useful for those radionuclides that are retained in the body for long periods; occasional measurements may be made to confirm the absence of build-up of activity within the body.

5.3.3. Special or task-related monitoring

(240) Monitoring in relation to a particular task or event may often involve a combination of techniques so as to make the best possible evaluation of a novel or unusual situation. As both special and task-related monitoring relate to distinct events, either real or suspected, one of the problems encountered in interpretation of routine monitoring results does not apply as the time of intake is known. Furthermore, there may be more specific information about the physical and chemical form of the contaminant.

(241) In some cases of suspected incidents, screening techniques (such as measuring nose-blow samples or nasal smears) may be employed to give a preliminary estimate of the seriousness of the incident. In these cases, the regional deposition in the nose can be used to confirm that an intake has occurred, and to give an approximate estimate of the intake. Positive nasal swabs should trigger special bioassay measurements (Guilmette et al., 2007).

(242) If therapeutic procedures have been applied to enhance the rate of elimination of a radionuclide from the body, special monitoring may be needed to follow its retention in the body and to provide the basis for a dose assessment. In cases where treatment has been given, care must be taken in selecting the monitoring methods because normal biokinetics of the radionuclides can be altered significantly. For example, Prussian Blue enhances the faecal elimination of radioisotopes of caesium; therefore, faeces bioassay, although not used routinely, should be implemented in addition to in-vivo and urine monitoring.

(243) Following a cut or wound, some radioactive material may penetrate to subcutaneous tissue and hence be taken up by blood and distributed around the body. Depending upon the radionuclide(s) and the amount of activity, it may be necessary to undertake a medical investigation and a programme of special monitoring. In these circumstances, the amount of radioactive material at the site of the wound should be determined, taking into account self-attenuation of the radiation in the foreign material and in tissue, as an aid to decisions on the need for excision. If an attempt is made to remove material from the wound, measurements should be made of the activity recovered and remaining at the wound site in order to maintain an activity balance. The excised material can also provide information on the isotopic ratios and physicochemical composition which can inform the dose assessment. A series of further measurements may also be needed to determine any further

uptake into blood and body tissues from which any additional committed effective dose can be calculated.

5.4. Derived investigation levels

(244) In many situations of potential exposure to radionuclides, it is convenient to set derived investigation levels (DIL) for the quantities that are measured in monitoring programmes (i.e. whole-body content, organ content, daily urinary or faecal excretion, activity concentration in air). The chosen value for the DIL may be directly related to an investigation level (IL) expressed either as a dose quantity or as a predefined intake. For example, an investigation could be required whenever an intake of a radionuclide results in a committed effective dose that exceeds an IL = 1 mSv. Thus, in a routine monitoring programme for a single radionuclide and with a time interval of T days, the corresponding DIL could be based on the body content that would give a committed effective dose of 1 mSv. This would be appropriate where the probability of more than one intake occurring within a year is considered to be low. Where this probability is higher, and the probability of intake through the year is considered to be uniform, the DIL could be derived from a committed effective dose of IL*(T/365) mSv, where IL = 1 mSv in this example.

(245) The value corresponding to the IL can be obtained directly from the relevant graphs or calculated from the tables of dose per content function in the data sets given in this series of reports or the accompanying electronic annex. The use of constraints as described in *Publication 103* (ICRP, 2007) could be used as a basis for setting ILs. In setting such ILs, due attention must be given to other sources of exposure (i.e. other radionuclides and external irradiation). In situations where intakes and doses are known to be low and there is considerable experience of the processes being undertaken, it may be possible to simply set ILs for the measured quantities on the basis of experience. A measurement result in excess of the IL would indicate a departure from normal conditions and the need to investigate further.

5.5. Record keeping and reporting

(246) Dose record keeping is the making and keeping of individual dose records for radiation workers. It is an essential part of the process of monitoring the exposures of individuals to both external radiation and to intakes of radionuclides for demonstrating compliance with dose limits and constraints. It can also provide important information for the purpose of control of exposures. Formal procedures should be established for record keeping, and these have been described in publications by IAEA (1999b, 2004a). The procedures and criteria for reporting individual and workplace monitoring results should be clearly specified by the management and/or regulatory authority. Information reported should be clearly identifiable, understandable, and sufficient for the dose to be recalculated from the measurements at a later time if necessary. Included in the information to be documented must be a specification of the models, assumptions, and computational codes used. In accident

situations, interim information will be needed to judge the need for management actions and the need for follow-up monitoring.

5.6. Quality management system

(247) The need for a quality management system within an overall radiation protection programme has been discussed in two standards published by the International Organization for Standardization (ISO, 2006, 2011). Reference should be made to these standards for a complete account, but some of the more important issues are:

- in deciding on the nature and extent of the quality assurance programme, consideration should be given to the number of workers monitored, and the magnitude and probability of exposures expected;
- assumptions on factors such as radionuclide composition, inhaled particle size, identity of chemical compounds, absorption behaviour, etc., should be verified by appropriate measurements; and
- reviews or audits should be conducted at appropriate times (e.g. when a new monitoring programme is implemented, or when a significant change to a programme is made).

(248) Laboratories should participate in national or international intercomparisons of measurements and dose assessments at appropriate intervals. Such participation enables determination of the accuracy of measurement and dose assessment procedures, improves reliability, and facilitates harmonisation of methods.

6. GENERAL ASPECTS OF RETROSPECTIVE DOSE ASSESSMENT AND RETROSPECTIVE DOSE VERIFICATION

6.1. Introduction

(249) The effective dose calculated for protection purposes is determined from the equivalent doses to organs and tissues of the human body, which are, in turn, calculated from the mean absorbed doses to those organs and tissues (Section 1.2). Effective dose provides a value that takes account of the given exposure conditions, but not of the characteristics of a specific individual. In particular, the tissue weighting factors that are used to determine effective dose are selected, rounded values representing averages over many individuals of different ages and both sexes. The equivalent doses to each organ or tissue of the Reference Male and the Reference Female are averaged, and these averaged doses are each multiplied by the corresponding tissue weighting factor to determine the sex-averaged effective dose for the Reference Person (ICRP, 2007). It follows that effective dose does not provide an individual-specific dose, but rather that for the Reference Person under given exposure conditions (ICRP, 2007).

(250) There are two alternative approaches that may be applied for retrospective dose assessment.

- Calculation of the intake of a radionuclide from direct measurements (e.g. measuring the activity of radionuclides in the whole body or in specific organs and tissues by external counting) and/or from indirect measurements (e.g. measuring the activity of radionuclides in urine or faeces, or exposure monitoring in the workplace). Biokinetic models are used to interpret the measurements in the assessment of radionuclide intake, after which the effective dose is calculated using reference dose coefficients (dose per intake, Sv Bq^{-1}) recommended by ICRP or determined using ICRP's recommended methodology (ICRP, 2007).
- Calculation of the committed effective dose directly from the measurements using functions that relate them to the time of the intake. The measurements could be of whole-body or organ content, activity in 24-h urine or faecal samples, or concentration of radionuclides in air in the workplace. For the interpretation of bioassay data, this approach requires the use of tables of 'dose per content function' as a function of time after the intake (ICRP, 2007).

(251) The two approaches are equivalent and should produce identical results as far as the same biokinetic models, parameter values, and assumptions are used.

(252) 'Dose per intake coefficient' tables for selected radionuclides are given in this series of reports and in the accompanying electronic annex. Committed effective dose corresponding to values of bioassay quantities measured at specified times after an acute intake of the radionuclide is also presented. A more detailed description of the data provided is given in Section 7.3. The tables provide a simple and easy-to-use tool that should promote harmonisation in the interpretation of bioassay data.

(253) There may be some circumstances in which parameter values may be changed from the reference values in the calculation of effective dose. It is therefore

important to distinguish between those reference parameter values that might be changed in the calculation of effective dose under particular circumstances of exposure, and those values that cannot be changed under the definition of effective dose. As effective dose applies to the Reference Person, individual-specific parameter values should not be changed whereas material-specific parameter values may be changed. Examples of individual-specific parameters include those describing the dosimetric phantom, HRTM breathing and particle transport parameters, HATM parameters other than the alimentary tract transfer factor, f_A, and all systemic model parameters. Examples of material-specific parameters include lung-to-blood absorption parameters, aerosol parameters such as the AMAD of the inhaled aerosol, and f_A.

(254) In the majority of cases, assessed doses are low in comparison with dose limits; for such cases, it is likely that dose assessments will make use of the recommended default values for material-specific parameters, the tabulated dose coefficients, and the 'dose per content function' tables that accompany this series of reports. Where assessed doses are likely to be greater, or where more than one monitoring method has been used and a number of monitoring measurements have been made, material-specific parameter values other than the recommended defaults may be used.

(255) In undertaking retrospective assessments of doses from monitoring data, the assessor may need to make assumptions about factors such as the pattern of intake and properties of the material because of lack of specific information on these factors. A European project in the European Commission 5th Framework Programme was established to give general guidelines for the estimation of committed dose from the incorporation of monitoring data (IDEAS project). The IDEAS project developed a structured approach to the interpretation of individual monitoring data (Doerfel et al., 2006, 2007; Castellani et al., 2013), building on the proposals made by the ICRP Working Party on Dose Assessment (Fry et al., 2003). This guidance has been further developed by the European Radiation Dosimetry Group (Marsh et al., 2008; Lopez et al., 2011b).

(256) In addition to this guidance, ISO has published an international standard, ISO 27048:2011 (ISO, 2011), that specifies the minimum requirements for internal dose assessment for the monitoring of workers. The IDEAS guidelines and ISO 27048 both adopt the principle that the effort needed for dose assessment should broadly correspond to the anticipated level of exposure.

(257) In unusual cases where doses to specified individuals may exceed dose limits substantially and radiation risks need to be assessed, specific estimates of organ or tissue doses are necessary to determine organ-specific risks. In such cases, absorbed dose in organs should be calculated and used with the most appropriate biological effectiveness and risk factor data (ICRP, 2007). This retrospective individual dose assessment should only be performed by professionals with recognised expertise, skills, and practical experience. It is beyond the scope of this publication to give advice on how to perform individualised retrospective dose and risk assessments.

(258) The following section discusses the information that should be collected on

the exposure, summarises approaches to data handling for single or multiple measurements, and discusses uncertainties associated with internal dose assessments, including measurement uncertainties. Two types of analysis are discussed: reference evaluation and site-specific evaluation.

6.2. Types of analysis

6.2.1. Basic evaluation with ICRP default biokinetic and dosimetric computational models

(259) For installations and tasks where the annual committed effective doses to workers from intakes of radionuclides assessed prospectively are low, the half-lives of the radionuclides that are handled are short, and the quantity of material present is limited, internal monitoring may be undertaken to demonstrate compliance or may be established for other purposes. For workers in those installations, there is generally no need to evaluate the results of monitoring measurements using site-specific or material-specific parameters. A typical example is a nuclear medicine service. If required by the national authorities, the bioassay monitoring of the technical staff, medical doctors, and nurses will be accomplished, using ICRP standard models, without the need for workplace characterisation (e.g. the determination of the AMAD). Other examples may include university or research laboratories using trace quantities of radioisotopes.

(260) For such routine operations, where a new intake has been confirmed, a reference evaluation may be undertaken with the following default assumptions:

- the intake was an acute event at the mid-point of the monitoring interval;
- the exposure was via inhalation of material with an AMAD of 5 μm; and
- absorption and f_A values: the absorption type or the default specific absorption parameter values for the known material are as described in this report. If the compound is unknown, the absorption type for 'unspecified compounds' should be used.

(261) Alternatively, where site-specific or material-specific default values are available and documented, these may be used provided that they are shown to be appropriate for the process in which the worker was engaged.

(262) If the value of committed effective dose is confirmed to be less than a previously established low value (e.g. 1 mSv), no further evaluation is necessary.

6.2.2. Detailed evaluation of doses

(263) At installations where workers have the potential to be exposed to doses higher than a reference level set at a specified fraction of a dose limit, or higher than a DIL (e.g. in situations such as the loss of control of the source), information should be gathered on the physical and chemical characteristics of the inhaled or ingested radionuclide, as part of a workplace monitoring programme, and on the time and

pattern of intake. This information may be used to refine the assessment and reduce uncertainties in the assessed dose. The types of information that may be used in such an assessment are discussed in Section 6.4.

6.3. Understanding exposure situations

(264) Workplace information should be gathered in order to understand the exposure situations [e.g. radionuclides that may have been incorporated (including equilibrium assumptions for the natural series), chemical form, presumed particle size, likely time, pattern and pathway of any intake].

6.3.1. Time(s) and pattern of intake

(265) A principal source of uncertainty in the interpretation of bioassay data is the assignment of the time(s) and pattern of intake. As the bioassay function that gives the predicted measurement depends on the time since the intake, it follows that the estimate of intake will vary, depending on when it is assumed the intake took place. Consideration should be given to different possible patterns of intake, such as a single contamination event, several individual events during the monitoring period, intakes lasting a short period of time, or chronic intakes.

(266) Where chronic intakes are expected, an assessment should be made as to whether the working schedule should be taken into account when selecting the time of measurement (or sampling), and interpreting the results from bioassay monitoring. For elements where a fraction of the intake is excreted rapidly, the times and duration of periods when no exposure could take place, such as the weekend, days off, or holidays, could strongly influence the assessed intake. With the exception of radionuclides with short half-lives, the selection of a measurement or sampling time immediately following such a period will reduce the uncertainty in assessed intake associated with rapid excretion.

(267) For routine monitoring, when chronic exposures are not expected, it is necessary to estimate an intake from a measurement made at the end of a monitoring interval, often without knowing the time of intake.

(268) When a positive measurement appears from a routine bioassay programme (i.e. a measurement which indicates that an intake may have occurred), a review of workplace monitoring data, such as airborne or surface contamination levels, can indicate a likely time for the intake to have occurred. Similarly, if other workers in the same workplace have exhibited positive routine bioassay samples, a review of the data and monitoring schedules for those individual workers will help determine the time of intake for all. Worker interviews should elucidate whether an incident, an unusual procedure, or equipment failure could have led to the intake. Follow-up bioassay should be scheduled to confirm the positive measurement. When several bioassay results are available, perhaps including different types of measurement, a comparison of these results with the intake retention fraction tables may help in

narrowing the choice of the time the intake occurred.

(269) Another approach has been described by Miller et al. (2002) in which Bayesian-based dosimetry calculations are performed using a Markov chain Monte Carlo algorithm. This method, which analyses all available bioassay data simultaneously, determines probabilistically the number, magnitude, and times for N possible intakes using a previously agreed set of biokinetic models. The weighted likelihood Monte Carlo sampling method is another Bayesian technique (Puncher and Birchall, 2008). In this approach, biokinetic model parameters and times of intake are sampled from probability distributions that express the state of knowledge about the exposure before bioassay data are obtained. Each sample is weighted by the appropriate likelihood function for a given intake to produce a quantity termed the 'weighted likelihood'. The probability of each intake and time of intake, given the observed measurement data, is calculated from the weighted likelihoods using simple numerical integration techniques. These methods, although computationally intensive, obviate the need to assume intake times when other types of circumstantial information are absent.

(270) In *Publications 54* and *78* (ICRP, 1988a, 1997b), it is argued that, in the absence of any information, the time of intake is equally likely to have occurred before the mid-point of the monitoring interval T than after it, and therefore suggests that in these situations, a value of $t = T/2$ should be used (i.e. the intake is assumed to have occurred at the mid-point of the monitoring interval). Alternative approaches have also been suggested (Strom, 2003; Puncher et al., 2006; Birchall et al., 2007; Marsh et al., 2008a; 2008b). However, in most circumstances, the results of these alternative approaches do not differ greatly from the mid-point method, which may overestimate intake and dose by less than a factor of approximately two. The mid-point method is recommended here for reference evaluations (Section 6.2.1).

6.3.2. Route of intake

(271) Although intakes by inhalation alone are the most common in the workplace, intakes by ingestion and uptake through wounds and intact skin cannot be excluded. If the route of intake is not known, and if several bioassay results are available including different types of bioassay measurements, a comparison of these results may help in its determination. In some facilities, simultaneous intakes by several routes can occur.

(272) If the radionuclide activity can be assessed by direct measurements, lung counting can be used to differentiate between inhaled and ingested material. However, if this is not possible and the radionuclide is in an insoluble form, interpretation of activities excreted in faecal and urine samples in terms of intake is quite problematic. Both the ingested material and the inhaled material deposited in the upper respiratory tract will clear through the faeces in the first few days after intake. Consequently, it is important to initiate excreta sampling as soon as possible after an acute intake, continuing for an extended period. Material in the faeces after the

second week will originate mainly from the respiratory tract, so later measurements can be used to correct the earlier faecal sample measurements for this component. In the monitoring of workers chronically exposed to long-lived, insoluble radionuclides, activities in the faeces after a 15-d absence from work will mainly reflect the delayed clearance from inhaled material, which dominates the dose (IAEA, 1999a, 2004b). Intakes of radioactive materials through wounds may occur as a result of accidents. A summary of the wound model developed by NCRP (2006) is presented in Section 3.4.

6.3.3. Particle size

(273) Radionuclides can become airborne through numerous processes, and can be present in various physical forms such as gases, vapours, and particles with a wide range of sizes, shapes, and densities. Most aerosols are composed of particles with complex shapes and varying particle sizes (NCRP, 2010). For modelling purposes in dose calculations, ICRP advises the use of the AMAD (or the AMTD when the AMAD is less than 0.3 μm) which, together with the geometric standard deviation, describes the particle size distribution of the inhaled aerosol (ICRP, 2002b). The AMAD influences deposition in the respiratory tract and, as a consequence, the transfer of unabsorbed particles to the alimentary tract.

(274) The AMAD of the airborne contamination in the workplace may be characterised as part of a workplace monitoring programme. In some working environments, more than one particle size distribution mode may be detected. In cases of accidental releases of material, information on the particle size distribution of the airborne fraction of the release should be obtained whenever possible. When the size distribution of the radioactive aerosol is not known, the default AMAD value for occupational exposures of 5 μm should be used (ICRP, 1994a, 2002b).

6.3.4. Chemical composition

(275) The chemical form of the intake can have a significant effect on the behaviour of the radionuclide that has entered the body. Chemical forms commonly encountered in the working environment are given in subsequent reports in this series for selected radionuclides. Where there are adequate experimental data, chemical forms are assigned to one of the default absorption types (Type F, M, or S), and a value for the alimentary tract transfer factor, f_A, is assigned. In some special cases, material-specific values for the parameters describing absorption into blood are provided (Section 3.2.3).

(276) A compound may have absorption characteristics slightly or considerably different from those of the default. The interpretation of bioassay measurements is sensitive to the choice of absorption parameter values of the inhaled radioactive material. In cases of significant intakes of radionuclides, and in an accident situation, it may be necessary to obtain specific data on the chemical form of the

radionuclide(s) involved to obtain a more realistic assessment of the intake and committed effective dose. However, the gathering of additional source-term information takes time, and often will not be available soon after the incident/accident. The specific/reference ICRP lung absorption parameter and f_A of the chemical form that most closely describes the released material should be used in the first dose calculations following the first monitoring results. Follow-up bioassay monitoring and further investigations of the accident should be used to confirm or modify the results of the first dose calculations.

(277) In many situations, the worker is exposed to several chemical forms of the same radionuclide. Workers exposed in different areas of a uranium enrichment facility, for example, might be exposed to different chemical forms of uranium. Interpretation of bioassay results, excreta results in particular, will rely heavily on the assumptions related to the contributions of the different chemical forms to these results.

6.3.5. Influence of background

(278) Radionuclides from the three natural radioactive decay series occurring in natural and anthropogenic sources are present in all environmental media, and are thus also contained in foodstuffs, drinking water, and the air, leading to intakes by human populations. Their presence should be taken into account when interpreting bioassay measurements. The in-vivo detection capability and minimum detection levels of in-vivo counting are strongly influenced by the presence of ^{40}K in the body.

(279) Excretion data from uranium and thorium series radionuclides may need correction for dietary intakes. A 'blank' bioassay sample should be obtained from the workers prior to the commencement of work. When not possible, bioassay samples from family members or from the population living in the same area should be taken and analysed to allow natural or non-occupational intakes and occupational intakes to be distinguished (Eckerman and Kerr, 1999; Lipsztein et al., 2001, 2003). It may be useful to use this information to define a level above which occupational exposure is indicated. Background values may be subtracted provided that there is clear evidence to support such a procedure, but it should be noted that individual background levels can be highly variable. Little et al. (2007) described a Bayesian method to identify a typical excretion rate of uranium for each individual in the absence of occupational intakes.

(280) In addition, it is important to evaluate the influence of radiopharmaceuticals that may have been administered for diagnostic or therapeutic purposes.

(281) For long-lived radionuclides, bioassay monitoring results may reveal the influence of intakes identified in preceding monitoring intervals. The retained activity in the body from previous intakes should be taken into account.

6.3.6. Special monitoring situations

(282) In many situations, exposure will be to a single radionuclide or a limited number of radionuclides. For some elements, however, exposures may involve a number of isotopes with different decay properties. Uranium and plutonium illustrate the potential for exposure to complex mixtures. Various plutonium isotopes are present in the nuclear industry. Studies have shown a significant difference in isotopic behaviour of plutonium due to differences in specific activity (Guilmette et al., 1992). Workers exposed to uranium are always exposed to a mix of isotopes in different proportions depending on the enrichment level. Knowledge of the enrichment is essential for the correct interpretation of bioassay monitoring results.

(283) Special considerations apply when direct bioassay measurements of radioactive progeny are used to determine the body content of the parent radionuclide (Section 3.2. and Annex A). Significant errors can arise if it is assumed that the progeny are always in secular equilibrium. For example, the activity of ^{232}Th in the lungs can be underestimated when determined from direct measurements of its ^{228}Ac, ^{212}Pb, ^{212}Bi, and ^{208}Tl progeny. Differences in lung retention between the measured element and the radionuclide of concern contribute to the uncertainty of results. For the same reasons, activity of ^{232}Th in the lungs can be underestimated when determined from measurements of ^{220}Rn in breath.

(284) There are also situations when one radionuclide is used as a surrogate for another (e.g. in-vivo bioassay monitoring). One example is the determination of the level of internally deposited Pu in the lung, which is often estimated on the basis of ^{241}Am external monitoring of the chest. ^{241}Am generally accompanies Pu in the workplace or is produced in the body by decay of ^{241}Pu. This procedure is often appropriate. However, depending on the solubility characteristics and isotopic composition of the aerosols, the relative clearance rates from the lung may be different, and ^{241}Am lung results may underestimate Pu activity in the lung (e.g. nitrate aerosols).

6.4. Data collection, processing, and dose assessments

6.4.1. Data collection and processing

(285) Some types of measurement data may need processing before use.

- Generally, the combined activity in lungs and LN_{TH} is referred to as 'lung' activity, and it is this quantity that is calculated by internal dosimetry software. Where estimates of lung and lymph activity are given separately, they should be summed. 'Chest' measurements may also include counts from activity in liver and skeleton for radionuclides that concentrate in these tissues, and their contributions will need to be subtracted.
- Urine and faecal samples collected over periods of less than 24 h should, in general, be normalised to an equivalent 24-h value. This can be achieved by multiplying the ratio of the reference 24-h excretion volume or mass by the

volume or mass of the sample. The reference volumes for males and females, respectively, are 1.6 L and 1.2 L for urine, and 150 g and 120 g for faeces (ICRP, 2002a). For urine sampling, another widely used method is to normalise to the amount of creatinine excreted per day; reference values are 1.7 g d^{-1} and 1.0 g d^{-1} for males and females, respectively (ICRP, 2002a). If the 24-h sample is less than 500 ml for urine or less than 60 g for faeces, it is doubtful that it has been collected over a full 24-h period and normalisation should be considered. For some radionuclides, the collection of spot samples is sufficient for routine sampling (e.g. monitoring of intakes of tritiated water).

6.4.2. Dose assessments: single measurement, acute intake

Special monitoring

(286) For special or task-related monitoring when the time of intake is known, the intake can be estimated from the measured results using the $m(t)$ values given in subsequent reports of this series. An $m(t)$ value is a value of a bioassay quantity calculated at time t after a unit intake of a specified radionuclide, sometimes known as a 'retention or excretion function'. If a single measurement is made, the intake, I, can be determined from the measured quantity, M, if the contribution of previous intakes to the measured quantity, M, is negligible. Care must be taken to ensure that the measurement result, M, and $m(t)$ are comparable: for example, in the case of urinalysis, the bioassay result must be expressed as the total activity in a 24-h urine sample at the end of collection (not at analysis).

$$I = \frac{M}{m(t)} \tag{6.1}$$

(287) The intake should be multiplied by the dose coefficient (e_{ij}, for route of intake i and radionuclide j) to obtain the committed effective dose, E:

$$E(50) = e_{ij} \times I \tag{6.2}$$

(288) Alternatively, the tabulated values of 'dose per content function' for a range of radionuclides and types of materials should be used. Dose per content function, $z(t)$, is given by:

$$z(t) = e(50)/m(t) \tag{6.3}$$

(289) If a single measurement is made, and the contribution of previous intakes to the measured quantity, M, is negligible, the committed effective dose, $E(50)$, associated with the intake, I, can be determined by:

$$E(50) = M \times z(t) \tag{6.4}$$

Routine monitoring

(290) For routine monitoring, an intake during the monitoring interval is assessed from the measurement made at the end of the monitoring interval. When the time of intake is not known (or cannot be determined easily) and a reference evaluation is being performed (Section 6.2.1), it should be assumed that the intake occurred at the mid-point of the monitoring interval of T days. If the contribution of intakes occurring during previous monitoring intervals is negligible, then for a given measured quantity, M, obtained at the end of the monitoring interval, the intake is:

$$I = \frac{M}{m(T/2)} \tag{6.5}$$

where $m(T/2)$ is the predicted value of the measured quantity for a unit intake assumed to have occurred at the mid-point of the monitoring interval. The dose from the intake in the monitoring interval is obtained by multiplying the intake by the dose coefficient. The assessed dose or intake can be compared with the pro-rata fraction of the dose limit or of the intake corresponding to that limit, respectively. Alternatively, the dose or intake can be compared with predetermined ILs.

(291) An intake in a preceding monitoring interval may influence the measurement result obtained. For a series of measurements in a routine monitoring programme, the following procedure may be followed:

- determine the magnitude of the intake in the first monitoring interval;
- predict the contribution to each of the subsequent measurements from this intake;
- subtract the corresponding contributions from all subsequent data if the contributions are judged to be significant (ISO, 2011); and
- repeat above for the next monitoring interval.

(292) Alternatively, using the tables of dose per content function, for a given measured quantity M obtained at the end of the monitoring interval, the mid-point dose $E_{(50)}$ associated with intake I is:

$$E_{(50)} = M \times z(T/2) \tag{6.6}$$

6.4.3. Dose assessments: multiple measurements

Routine monitoring

(293) If the contribution of intakes occurring during previous monitoring intervals is not negligible, the following procedure may be used. For each monitoring

interval n, the associated effective dose $E_{(50)n}$ may be assumed to be either equal to 0 or positive. For a given measured quantity $M(t_k)$ obtained at the end of the last monitoring interval k, the associated effective dose $E_{(50)k}$ is:

$$E_{(50)k} = \left(M(t_k) - \sum_{n=1}^{k-1} \frac{E_{(50)n}}{z(t_k - \tau_n)} \right) z(t_k - \tau_k) \tag{6.7}$$

where t_k is the time of measurement k (end of the last monitoring interval k); and τ_n and τ_k are the times at mid-points of monitoring intervals n and k, respectively. If $M(t_k)$ is below the decision threshold (ISO, 2011) or the result of background subtraction is negative, $E_{(50)k} = 0$.

Special monitoring

(294) The bioassay data to be used for an intake assessment may consist of results for different measurements performed at different times, and even from different monitoring techniques (e.g. direct and indirect measurements).

(295) To determine the best estimate of a single intake when the time of intake is known, it is first necessary to calculate the predicted values, $m(t_i)$, for unit intake of the measured quantities. Next, the best estimate of intake I is determined, such that the product $I\ m(t_i)$ 'best fits' the measurement data (t_i, M_i). In cases where multiple types of bioassay data sets are available, it is recommended that intake and dose should be assessed by fitting predicted values to the different types of measurement data simultaneously. For example, if urine and faecal data sets are available, the intake is assessed by fitting appropriately-weighted predicted values to both data sets simultaneously (Doerfel et al., 2006, 2007; ISO, 2011; Castellani et al., 2013).

(296) Numerous statistical methods for data fitting are available (IAEA, 2004a,b). The two methods that are most widely applicable are the maximum likelihood method (Doerfel et al., 2006; ISO, 2011) and the Bayesian approach (Miller et al., 2002; Puncher and Birchall, 2008). Other methods such as the mean of the point estimates and the least-squares fit can be justified on the basis of the maximum likelihood method for certain assumptions on the error associated with the data. For example, the least-squares method can be derived from the maximum likelihood method if it is assumed that the uncertainty on the data can be characterised by a normal distribution. The assumed distribution (e.g. normal or log-normal) can have a dramatic influence on the assessed intake and dose if the model is a poor fit to the data. However, as the fit of the model to the data improves, the influence of the data uncertainties on the assessed intake and dose reduces.

6.4.4. Chronic exposures

(297) The amount of activity present in the body and the amount excreted daily depend on the period of time over which the individual has been exposed. The bioassay result obtained (e.g. the amount present in the body, in body organs, or in excreta) will reflect the superposition of all the intakes. Retention and excretion functions for chronic intakes are not given in this publication, but can be determined by convoluting the retention and excretion functions given in this series of reports for an acute intake with any specified chronic intake function.

6.4.5. Influence of decorporation therapy

(298) In cases involving internal contamination, chelating agents or other treatment may be used to enhance the body's natural elimination rate of the compound, or possibly to block the uptake of the radionuclide in sites where high uptake may occur (e.g. radioiodine in the thyroid). The aim of both of these is to reduce committed doses.

(299) The use of interventional techniques may partially or completely invalidate the use of standardised model approaches described above to estimate the intake and dose (NCRP, 2009). The use of chelating agents such as diethylenetriaminepentaacetic acid may influence excretion rates for weeks or months after cessation of treatment.

(300) It is not feasible to give specific advice, as the treatment of any bioassay data depends upon the circumstances of the exposure, and the need and timescale required for dose assessment.

6.4.6. Wounds

(301) Due to their nature, intakes of radionuclides resulting from contaminated cuts or wounds typically account for an appreciable proportion of high dose exposures. Radionuclides may be transferred from the wound site into blood and to other organs and tissues, and NCRP has developed a model to describe this transfer for various chemical forms of selected radionuclides (NCRP, 2006). Coupled with an element-specific systemic biokinetic model, the NCRP model can be used to calculate committed doses to organs and tissues, and committed effective doses following transfer of the radionuclide to the blood and systemic circulation, as well as to predict urinary and faecal excretion.

(302) As noted in Section 3.1, the assessment of internal contamination resulting from wounds is, in practice, treated on a case-by-case basis using expert judgement. In many cases, the amount of a radionuclide transferred from a wound site into blood may be assessed directly from urine bioassay data. Section 3.4 summarises the main features of the NCRP model, as this information may be of use in the interpretation of bioassay data for individual cases of wound contamination.

6.5. Uncertainties in internal dose assessment based on bioassay

(303) *Publication 103* (ICRP, 2007) makes the following statement with respect to the assessment of uncertainties:

> *In order to assess radiation doses, models are necessary to simulate the geometry of the external exposure, the biokinetics of incorporated radionuclides, and the human body. The reference models and necessary reference parameter values are established and selected from a range of experimental investigations and human studies through judgements. For regulatory purposes, these models and parameter values are fixed by convention and are not subject to uncertainty.*

(304) It follows that there is no requirement to assess or record the uncertainty associated with an individual dose assessment performed to demonstrate compliance with regulatory requirements. Nevertheless, the assessment of uncertainties associated with a specified monitoring procedure (including the dose assessment procedure) provides important information for optimising the design of a monitoring programme (Etherington et al., 2004a,b; Davesne et al., 2010, 2011; ISO, 2011). Where uncertainties in assessed effective dose are evaluated, uncertainties in material-specific model parameter values should be considered, but individual-specific model parameter values should be taken to be fixed at their reference values (Section 6.1).

(305) This section describes and discusses the important sources of uncertainty in retrospective assessments of dose. The uncertainty in an internal dose assessment based on bioassay data depends on: the uncertainties associated with measurements used to determine the activity of a radionuclide in vivo or in a biological sample; uncertainties in the exposure scenario used to interpret the bioassay results; and uncertainties in the biokinetic and dosimetric models used to interpret the bioassay results. The exposure scenario includes factors such as the route of intake, the time pattern of intake, the specific radionuclide(s) taken into the body, and the chemical and physical form of the deposited radionuclide(s).

6.5.1. Uncertainties in measurements

(306) Uncertainties in measurements of activity in the body or in biological samples have been discussed in IAEA publications (IAEA, 1996, 2000). There are no standard procedures for indirect or direct bioassay measurements, although some examples of bioassay methods are given in this series of reports and elsewhere. The choice of the procedure, detector, or facility will depend on the specific needs such as the nuclides of interest, detection limits, and budget. All procedures used to quantify the activity of a radionuclide are sources of both random and systematic errors. Uncertainties in measurements are typically due mainly to counting statistics, validity of the calibration procedures, possible contamination of the source or the measurement system, and random fluctuations in background. NCRP has developed a

comprehensive report on uncertainties in internal radiation dose assessment that addresses measurement uncertainties in great detail (NCRP, 2010).

(307) The total uncertainty associated with a measurement is generally expressed as an interval within which the value of the measurand is believed to lie with a specified level of confidence (EURACHEM/CITAC, 2000). In estimating the overall uncertainty in a measurement, it may be necessary to take each source of uncertainty and treat it separately to obtain the contribution from that source. Each of the separate contributions to uncertainty is referred to as an 'uncertainty component'.

(308) The components of uncertainty in a quantity may be divided into two main categories referred to as Type A and Type B uncertainties (EURACHEM/CITAC, 2000; Cox and Harris, 2004; BIPM, IEC, IFCC, ISO, IUPAC, IUPAP, OIML, 2010; NCRP, 2010). Essentially, a Type A component is one that is evaluated by a statistical analysis of the variability in a set of observations, and a Type B component is one that is evaluated by other means, generally by scientific judgement using all relevant information available. In the case of measurement of activity in the total body or in a biological sample, Type A uncertainties are generally taken as those that arise only from counting statistics and can be described by the Poisson distribution, while Type B components of uncertainty are taken as those associated with all other sources of uncertainty.

(309) Examples of Type B components for in-vitro measurements include the quantification of the sample volume or weight; errors in dilution and pipetting; evaporation of solution in storage; stability and activity of standards used for calibration; similarity of chemical yield between tracer and radioelement of interest; blank corrections; background radionuclide excretion contributions and fluctuations; electronic stability; spectroscopy resolution and peak overlap; contamination of sample and impurities; source positioning for counting; density and shape variation from calibration model; and assumptions about homogeneity in calibration (Skrable et al., 1994). These uncertainties apply to the measurement of activity in the sample. With excretion measurements, the activity in the sample is used to provide an estimate of the subject's average excretion rate over 24 h for comparison with the model predictions. If the samples are collected over periods of less than 24 h, they should be normalised to an equivalent 24-h value. This introduces additional sources of Type B uncertainty relating to biological (inter- and intrasubject) variability and sampling procedures, which may well be greater than the uncertainty in the measured sample activity. Sampling protocols can be designed to minimise the sampling uncertainty, as shown by Sun et al. (1993) for plutonium urinalysis and Moeller and Sun (2006) for indoor radon exposure.

(310) In-vivo measurements can be performed in different geometries (whole-body measurements, and organ- or site-specific measurements such as measurements over the lung, thyroid, skull, liver, or a wound). Each type of geometry needs specialised detector systems and calibration methods. IAEA (1996) and ICRU (2003) have published reviews of direct bioassay methods that include discussions of sensitivity and accuracy of the measurements.

(311) Examples of Type B components for in-vivo monitoring include: counting geometry errors; positioning of the individual in relation to the detector and movement of the person during counting; determination of chest wall thickness; differences between the phantom and the individual or organ being measured, including geometric characteristics, density, distribution of the radionuclide within the body and organ, and linear attenuation coefficient; interference from radioactive material deposits in adjacent body regions; spectroscopy resolution and peak overlap; electronic stability; interference from other radionuclides; variation in background radiation; activity of the standard radionuclide used for calibration; surface external contamination of the person; interference from natural radioactive elements present in the body; and calibration source uncertainties (Skrable et al., 1994; IAEA, 1996).

(312) For partial-body measurements, it is generally difficult to interpret the result in terms of activity in a specific organ because radiation from other regions of the body may be detected. Interpretation of such measurements requires assumptions concerning the biokinetics of the radionuclide and any radioactive progeny produced in vivo. An illustration using ^{241}Am is given in the IAEA Safety Series Report on Direct Methods for Measuring Radionuclides in the Human Body (IAEA, 1996). A fundamental assumption made in calibrating a lung measurement system is that the deposition of radioactivity in the lung is homogeneous, but depositions rarely follow this pattern. The distribution of the particles in the lung is a function of particle size, breathing rate, and health of the subject (Kramer and Hauck, 1999; Kramer et al., 2000).

(313) Measurement errors associated with counting statistics (Type A uncertainties) decrease with increasing activity or with increasing counting time, whereas the Type B components of measurement uncertainty may largely be independent of the activity or the counting time. When activity levels are low and close to the limit of detection, the total uncertainty is often dominated by the Type A component (i.e. by counting statistics). For radionuclides that are easily detected and present in sufficient quantities, the total uncertainty is often dominated by the Type B components (i.e. by uncertainties other than counting statistics). In general, the contributions to the distribution of a measured bioassay quantity associated with the various components of uncertainty can be described using log-normal distributions, with the uncertainty quantified using the geometric standard deviation. The geometric standard deviation of the distribution of a measured bioassay quantity is often referred to as the 'scattering factor'. Scattering factors for various components of uncertainty in in-vivo and in-vitro measurements have been evaluated in a number of studies (Doerfel et al., 2006; Marsh et al., 2008; ISO, 2011; Lopez et al., 2011b).

6.5.2. Uncertainty in the exposure scenario

Time of intake

(314) The uncertainty in the time pattern of intake can be the dominant source of uncertainty in the estimated dose, or it can make little or no contribution. For

example, if an intake is not recognised for some time after an incident, and total body retention and urinary and faecal excretion rates diminish quickly, the assumed time pattern of intake could be the dominant uncertainty in the dose estimate. On the other hand, if a worker is exposed in the vicinity of an immediately recognised accidental release, or total body retention and excretion rates are fairly constant, the time pattern of intake may be a negligible source of uncertainty in the dose estimate.

(315) When the time of an intake during a routine monitoring interval is unknown, the intake is generally assigned to the mid-point of the monitoring interval. Alternatively, an intake corresponding to each possible intake time can be calculated and averaged, or a constant intake rate throughout the monitoring interval can be assumed. Puncher et al. (2006) and Birchall et al. (2007) argued that a constant intake rate is the only one of these three intake scenarios that provides an unbiased estimate of the true intake under the ideal conditions that the measurement and the excretion/retention function are accurately known or that they are uncertain but unbiased.

Route of intake

(316) In practice, one may encounter situations in which the route of intake is unknown and cannot be easily discerned on the basis of health physics records or available bioassay data. For example, it may not be known if the intake took place by inhalation alone, ingestion alone, or both. Even if it is known that a combination of inhalation and ingestion occurred, there may be little information concerning the relative intakes along the two routes. In the absence of specific information, it should generally be assumed that intake was by inhalation for an occupational exposure as this is typically the most common mode of exposure to radionuclides in occupational settings. The effect of assumed route of intake on assessed doses can be large, and should be investigated when assessed doses are significant.

Radionuclide composition of intake

(317) Assumptions regarding the source term (i.e. the identity of the radionuclides and their relative abundances) may represent major sources of uncertainty when monitoring does not include the measurement of all the radioisotopes present in the working environment. In many situations, a worker is exposed to multiple isotopes of the same element, but monitoring is accomplished through the measurement of one of the isotopes. For example, lung monitoring of uranium through the measurement of ^{235}U relies on assumptions regarding the level of enrichment. In other circumstances, assessments of exposure to certain radionuclides are based on the monitoring results of a progeny radionuclide in the lungs. For example, monitoring of ^{232}Th by measurement of a progeny radionuclide relies on assumptions about the equilibrium of radionuclides in the ^{232}Th decay chain in the material to which the worker is exposed. Also, exposure to some radionuclides may be based on

measurement of a surrogate radionuclide known to be present in the working environment. For example, lung monitoring of ^{239}Pu may be based on the measurement of ^{241}Am, using assumptions about the relative quantities of ^{241}Am, ^{241}Pu (parent of ^{241}Am), and ^{239}Pu in the inhaled material, and the relative rates of clearance of the deposited plutonium isotopes and the deposited and ingrowing ^{241}Am from the lungs.

(318) Information on the chemical form, or mixture of forms, of an inhaled radionuclide is needed to help determine an appropriate dissolution model for activity deposited in the lungs. The dissolution rate in the lungs can represent a major source of uncertainty in a dose assessment, particularly when dose estimates are based on excretion data alone. For example, if dose estimates are based on urinary excretion data, the dose to lungs can sometimes be underestimated by several orders of magnitude if the material is incorrectly assumed to be highly soluble, or overestimated by several orders of magnitude if the material is incorrectly assumed to have low solubility. When no direct information is available on the inhaled form of a radionuclide, a combination of urinary and faecal data and, where feasible, in-vivo lung measurements may greatly reduce the uncertainty in dose estimates associated with the chemical form of the radionuclide.

Particle size

(319) The particle size can be an important source of uncertainty because it influences the assumed deposition in the respiratory tract. The urinary and faecal excretion rates depend on the particle size because the size influences the transfer of unabsorbed particles to the alimentary tract. In some working environments, multimodal aerosols exist within the respirable size range (Dorrian and Bailey, 1995).

6.5.3. Uncertainties in biokinetic models

(320) Biokinetic models are used in radiation protection to predict the time-dependent distribution and retention of a radionuclide in the body, and the rate of excretion of the radionuclide in urine and faeces. These models are used in this series of reports to derive dose coefficients for inhalation or ingestion of radionuclides, and to provide reference rates of urinary and faecal excretion following intake of a radionuclide for use in interpretation of bioassay data.

(321) The following categorisation of the main types of information used to develop biokinetic models and assess model reliability is taken from a paper by Leggett (2001). Investigations of the reliability of many of the biokinetic models that have been used in ICRP reports can be found in the following papers and reports: Apostoaei et al. (1998); Leggett (2001); Leggett et al. (1998, 2007, 2008); Harrison et al. (2001, 2002); Bolch et al. (2001, 2003); Skrable et al. (2002); Likhtarev et al. (2003); Apostoaei and Miller (2004); Sánchez (2007); Pawel et al. (2007); and NCRP (2010).

Uncertainties associated with the formulation (structure) of a biokinetic model

(322) The confidence that can be placed in predictions of a biokinetic model for an element or compound depends not only on uncertainties associated with parameter values of the model, but also on uncertainties associated with the model structure. Such uncertainties may arise because the structure provides an oversimplified representation of the known processes, because unknown processes have been omitted from the model, or because part or all of the model formulation is based on mathematical convenience rather than consideration of processes. Some combination of these limitations in model structure is associated with virtually all biokinetic models for radionuclides. These limitations hamper the assignment of meaningful uncertainty statements to the parameter values of a model because they cast doubt on the interpretation of the parameter values.

Types of information used to construct biokinetic models for elements

(323) Regardless of the model formulation or modelling approach, a biokinetic model for an element or compound, particularly a systemic model, is usually based largely on some combination of the following sources of information:

- H1: direct information on humans (i.e. quantitative measurements of the element in human subjects);
- H2: observations of the behaviour of chemically similar elements in human subjects;
- A1: observations of the behaviour of the element in non-human species; and
- A2: observations of the behaviour of one or more chemically similar elements in non-human species.

H2, A1, and A2 data serve as surrogates for H1 data (direct information on humans), which is the preferred type of information on which to base a biokinetic model.

(324) H1, H2, A1, and A2 data are sometimes supplemented with various other types of information or constraints, such as quantitative physiological information (e.g. rates of bone restructuring); considerations of mass balance; predictions of theoretical models based on fundamental physical, chemical, and mathematical principles (e.g. a theoretical model of deposition of inhaled particles in the different segments of the lung); experimental data derived with anatomically realistic physical models (e.g. hollow casts of portions of the respiratory tract used to measure deposition of inhaled particles); and in-vitro data (e.g. dissolution of compounds in simulated lung fluid). Among these supplemental sources of information, mass balance and quantitative physiological data (P data) have particularly wide use.

Sources of uncertainty in applications of human data

(325) It is desirable to base a biokinetic model for an element or compound on observations of the time-dependent distribution and excretion of that element in

human subjects (H1 data). Some degree of this type of direct information is available for most essential elements, as well as for some important non-essential elements, such as caesium, lead, radium, uranium, americium, and plutonium. Depending on the degree of biological realism in the model formulation, it may be possible to supplement element-specific information for human subjects with quantitative physiological information for humans on the important processes controlling the biokinetics of the element of interest. For example, in *Publications 67*, *69*, and *71* (ICRP, 1993, 1995b,c), long-term removal of certain radionuclides from bone volume is identified with bone turnover.

(326) Although it is the preferred type of information for purposes of model construction, H1 data often have one or more of the following limitations: small study groups, coupled with potentially large intersubject variability in the biokinetics of an element; short observation periods, coupled with potentially large intrasubject variability; use of unhealthy subjects whose diseases may alter the biokinetics of the element; paucity of observations for women and children; collection of small, potentially non-representative samples of tissue; inaccuracies in measurement techniques; uncertainty in the pattern or level of intake of the element; atypical study conditions; and inconsistency in reported values. In some cases, inconsistency in reported values may provide some of the best evidence of the uncertain nature of the data.

(327) An important tool in the development of biokinetic models for radionuclides has been the use of reference organ contents of stable elements, as estimated from autopsy measurements on subjects chronically exposed at environmental levels or at elevated levels encountered in occupational exposures (ICRP, 1975). Such data are commonly used to adjust parameter values of biokinetic models or introduce new model components to achieve balance between reported values of intake, total-body content, and excretion of stable elements. Balance considerations can provide useful constraints on model parameters, provided that the data have been collected under carefully controlled conditions. However, balance considerations have often been based on data from disparate sources of information and unreliable measurement techniques, and, in some cases, may have led to erroneous models or parameter values.

(328) A confidence statement based on H1 data would reflect a variety of factors, such as the reliability of the measurement technique(s), the number and state of health of the subjects, representativeness of the subjects and biological samples, consistency of data from different studies, knowledge concerning the level and pattern of intake, and the relevance of the information to the situation being modelled. For example, confidence in a parameter value based on H1 data would be reduced if the data were determined in a study on any of the following study populations: several seriously ill subjects with known intakes; several healthy subjects with poorly characterised intakes; or one healthy subject with known intake.

Uncertainty in interspecies extrapolation of biokinetic data

(329) Interspecies extrapolation of biokinetic data is based on the concept of a general biological regularity across the different species with regard to cellular structure, organ structure, and biochemistry. Mammalian species with cellular structure, organ structure, biochemistry, and body temperature regulation particularly close to those of man are expected to provide better analogies to man than non-mammalian species with regard to biokinetics of contaminants.

(330) Despite the broad structural, functional, and biochemical similarities among mammalian species, interspecies extrapolation of biokinetic data has proven to be an uncertain process. Similarities across species are often more of a qualitative than quantitative nature, in that two species which handle an internally deposited radionuclide in the same qualitative manner may exhibit dissimilar kinetics with regard to that substance. Moreover, there are important structural, functional, and biochemical differences among the mammalian species, including differences in specialised organs, hepatic bile formation and composition, level of biliary secretion, urine volume and acidity, amount of fat in the body, magnitude of absorption or secretion in various regions of the digestive tract, types of bacteria in the digestive tract, and microstructure and patterns of remodelling of bones.

(331) In general, the choice of an animal model will depend strongly on the processes and subsystems of the body thought to be most important in the biokinetics of the radionuclide in humans, because a given species may resemble humans with regard to certain processes and subsystems but not others. For example, data on monkeys or baboons may be given relatively high weight for purposes of modelling the distribution of a radionuclide in the skeleton, due to the close similarities in the skeletons of non-human primates and humans. Data on dogs may be given relatively high weight for purposes of modelling the rate of loss of a radionuclide from the liver, due to broad quantitative similarities between dogs and humans with regard to hepatic handling of many radionuclides.

(332) A physiologically based model provides the proper setting in which to extrapolate data from laboratory animals to man, in that it helps to focus interspecies comparisons on specific physiological processes and specific subsystems of the body for which extrapolation may be valid, even if whole-body extrapolations are invalid. Depending on the process being modelled, it may be preferable, in some cases, to limit attention to data for a single species or small number of species, and in other cases, to appeal to average or scaled data for a collection of species.

(333) The degree of confidence that can be placed in a model value based on animal data depends on the quality and completeness of the data, and the expected strength of the animal analogy for the given situation. Thus, one must consider potential experimental and statistical problems in the data, as well as the logical basis for extrapolation of those particular data to humans. Relatively high confidence might be placed in a model value based on animal data: if fairly extensive interspecies comparisons have been made and include observations on the species

expected to be most human-like; if these comparisons suggest a strong basis for interspecies extrapolation, either because the data are species-invariant or because the physiological processes governing the biokinetics of the element in different species have been reasonably well established; if the model structure allows meaningful extrapolation to man, usually on the basis of physiological processes; and if such processes have been well quantified in humans (i.e. the central value for humans has been reasonably well established). A fairly wide uncertainty interval is indicated if data are only available for species that frequently exhibit qualitative differences from man (e.g. if data were available only for rats) or if no meaningful basis for extrapolation to man has been established with regard to the quantity of interest. Whatever the quality of the animal data, the uncertainty interval should reflect the fact that some confidence in the predictive strength of the data is lost when the data are extrapolated across species.

Uncertainty in interelement extrapolation of biokinetic data

(334) Biokinetic models for elements are often constructed partly or wholly from data for chemically similar elements on the basis of empirical evidence that chemical analogues often exhibit close physiological similarities. For example, the alkaline earth elements calcium, strontium, barium, and radium exhibit many physiological as well as chemical similarities (ICRP, 1993), and the alkali metals rubidium and caesium closely follow the movement of their chemical analogue, potassium.

(335) There are, however, counterexamples to the premise that chemical analogues are also physiological analogues. For example, the alkali metals potassium and sodium share close physical and chemical similarities, but exhibit diametrically opposite behaviours in the body, with potassium being primarily an intracellular element and sodium being primarily an extracellular element.

(336) Moreover, some of the chemically similar elements that behave in a qualitatively similar fashion in the body may exhibit quite different kinetics. For example, caesium appears to follow the behaviour of potassium in the body in a qualitative sense, but is distributed somewhat differently from potassium at early times after intake, and exhibits a substantially longer whole-body retention time.

(337) The level of confidence that can be placed in a model value based on human data for a chemically similar element depends on the quality and completeness of the data for the analogue, as well as the expected strength of the analogy for the given situation. Whatever the quality of the data for the chemical analogue, the confidence interval should reflect the fact that some confidence in the predictive strength of the data is lost when the data are extrapolated across elements.

(338) The strength of the chemical analogy for a given element depends largely on the extent to which the chemically similar elements have been found to be physiologically similar. That is, the analogy would be considered strong for a pair of elements if a relatively large set of experimental data indicates that these elements have essentially the same qualitative behaviour in the

body, and that their quantitative behaviour is either similar or differs in a predictable fashion. In view of counterexamples to the premise that chemically similar elements are necessarily physiologically similar, the chemical analogy does not provide high confidence if the elements in question have not been compared in animals or man.

(339) If a chemical analogue has been shown to be a good physiological analogue, application of human data on the chemical analogue (H2 data) may be preferable to application of animal data on the element of interest (A1 data). For example, for purposes of constructing or evaluating a biokinetic model for americium in humans, use of quantitative human data on the physiological analogue curium seems preferable to use of the best quantitative animal data on americium. Similar statements can be made for radium and barium, rubidium and potassium, or other pairs of close physiological analogues. On the other hand, if two chemically similar elements show only broad physiological similarities, the animal analogy may be preferred to the chemical analogy, particularly if element-specific data are available for a variety of animal species (as is the case, for example, for uranium and calcium). In general, lower confidence would be placed in animal data for a chemical analogue than in animal data for the element of interest.

Uncertainty in central estimates stemming from variability in the population

(340) 'Uncertainty' refers here to lack of knowledge of a central value for a population, and 'variability' refers to quantitative differences between different members of a population. Although uncertainty and variability are distinct concepts, the variability in biokinetic characteristics within a population is often an important factor contributing to the uncertainty in a central estimate of a biokinetic quantity. This is because such variability complicates the problem of identifying the central tendency of these characteristics in the population due to the small number of observations generally available, and the fact that, usually, subjects of biokinetic studies are not selected at random.

(341) Variability in the biokinetics of radionuclides, pharmaceuticals, or chemicals in human populations appears to result from many different physiological factors or modulating host factors of an environmental nature, including age, sex, pregnancy, lactation, exercise, disease, stress, smoking, and diet. Large interindividual biokinetic variations sometimes persist in the absence of appreciable environmental differences, and suggest that these variations may be controlled genetically. In real-world situations, genetic and environmental factors may interact dynamically, producing sizable variations in the behaviour of substances taken into the human body.

6.5.4. Uncertainties in dosimetric models

(342) Dosimetric models are used to estimate the mean absorbed dose resulting from radiations emitted by nuclear transformations of radionuclides present in the

body. The absorbed dose is computed for target regions (organs, tissues, or regions of tissues) considered to be radiosensitive. Radiation weighting factors and tissue weighting factors are applied to the mean absorbed dose to determine the equivalent and effective dose. The weighting factors are assigned reference values, and, as such, are not regarded as uncertain quantities. Thus, the uncertainties associated with an estimated equivalent dose to an organ, for example, are considered to be those associated with the underlying mean absorbed dose.

(343) The physical and anatomical parameters contributing to uncertainties in the mean absorbed dose for internal emitters are:

- energy and intensity of the nuclear and atomic radiations emitted by the radionuclide and by any radioactive progeny;
- interaction coefficients of the emitted radiations in tissues;
- elemental composition of the tissues of the body;
- volume, shape, and density of the organs of the body; and
- parameters describing the spatial relationship of the source regions (regions containing the radionuclide) and the target regions (radiosensitive organs and tissues for which dose values are desired).

(344) Limitations are present in the computational model representing the anatomy, and in the numerical procedures used to calculate the energy absorbed in the target regions. The magnitudes of these uncertainties vary with radiation type, the energy of the radiation, and the specific source–target pair. The adoption of computational phantoms based upon medical imaging data (often referred to as 'voxel phantoms') has reduced the uncertainties associated with cross-irradiation of tissues by photon and neutron radiations to some extent by providing more realistic spatial relationships of some source and target regions (ICRP, 2009). However, the absorbed dose is frequently dominated by the contributions from non-penetrating radiations. For source and target regions that cannot be resolved in the medical image data (e.g. source and target regions in the respiratory and alimentary tracts and in the skeleton), uncertainties are associated with the computational models used to represent these regions.

(345) The anatomical models are static and thus do not address uncertainties in the spatial position of the organs due to breathing and posture other than reclining.

(346) The parameters of the dosimetric model contributing to uncertainties in the absorbed dose are those physical parameters associated with the nuclear transformation processes that determine the energy and intensity of the emitted radiation, and parameters that govern the transport radiations in the body. Attenuation and absorption coefficients for photons involve relatively small uncertainties, typically less than 10%, but somewhat higher uncertainties are ascribed to soft tissue stopping power values for alpha particles and electrons. Improvements in the basic nuclear data have reduced the uncertainties in the physical half-lives of radionuclides and the branching fractions of decay modes. The simplified procedures used in the dosimetric calculations to address the delayed beta and gamma radiations of spontaneous fission can contribute to substantial uncertainties in the mean absorbed dose in some tissues.

(347) The dosimetric calculations must associate an anatomical region (source region) with each biokinetic compartment. Many biokinetic models partition the systemic activity among a few identified organs/tissues, and include a compartment referred to as 'other tissue' that represents the residual activity (see Section 3.7). The dosimetric procedure distributes the activity in the 'other tissue' compartment uniformly among all tissues not explicitly identified in the model. Substantial uncertainty may be associated with the mean absorbed dose for tissues that are members of 'other tissue'. 'Other tissue' frequently includes tissues assigned an explicit tissue weighting factor. For example, breast tissue is rarely explicitly identified as a source region in biokinetic models, and thus, its mean absorbed dose is often based on its inclusion in 'other tissue'.

(348) A number of numerical methods are capable of solving the set of potentially large numbers (hundreds) of coupled differential 'stiff' equations that describe the kinetics, although the demands of numerical accuracy often have to be balanced with computational time. Compartment-model issues contributing to uncertainties in the mean absorbed dose include the assumed biokinetics of members of a decay chain (independent or shared kinetics), and the representation of 'other tissues' when their anatomical identity varies among the decay chain members [Section 3.7.2 and Annex C of *Publication 71* (ICRP, 1995c)].

7. DATA PROVIDED FOR ELEMENTS AND RADIOISOTOPES

(349) This section describes the information provided in subsequent parts of this series of reports. The data provided are reference values for the purposes of occupational radiation protection and calculation of the worker's dose of record. The biokinetic parameter values of the Reference Worker and data provided here are invariant with sex, age, race, health status, and other individual-specific characteristics.

(350) Each element section of subsequent parts includes: information on chemical forms of various radioactive materials encountered in the workplace; a list of principal radioisotopes and their physical half-lives and decay modes; reviews of data on inhalation, ingestion, and systemic biokinetics; and the structure and parameter values of the reference systemic biokinetic model. Dosimetric data provided include: dose coefficients [committed effective dose and committed equivalent dose to named organs or tissues (Sv Bq^{-1})] for inhalation and ingestion of all relevant radioisotopes; dose per content functions [committed effective dose per predicted activity content in the body or per predicted daily excretion (Sv Bq^{-1})]; and bioassay functions [values of activity (Bq) retained in the body or specific organs, or excreted in urine or faeces, at various times after unit intake (i.e. 1 Bq) by inhalation or ingestion]. Dosimetric data are calculated using the revised HRTM described in Section 3.2, the HATM (ICRP, 2006), and the reference systemic biokinetic models defined in this series of reports for the Reference Worker.

7.1. Dose coefficients and bioassay functions

(351) The following dosimetric data are provided for assessments of the effective dose to the Reference Worker.

- Committed effective dose and committed equivalent dose to named organs and tissues per intake [or 'dose per intake coefficient' $e(50)$ (Sv Bq^{-1})]. These coefficients should be used for the assessments based on the activity of the intake; the activity intake can be assessed prospectively (i.e. at the design or planning stage) or retrospectively (i.e. based on monitoring data).
- Committed effective dose per content function [or 'dose per content function' $z(t)$ (Sv Bq^{-1})] of the radionuclide in selected source regions of the body of the Reference Worker (e.g. lungs, thyroid, whole body) and in 24-h excreta samples tabulated for various times after an acute intake. These time-dependent quantities should be used for retrospective assessments based on the monitoring data, such as whole-body counting or urine analysis data. Dose per content function can also be used prospectively for the design of monitoring programmes, as described in Section 5.

(352) Reference bioassay functions, $m(t)$, are tabulated and plotted in the form of fractional activity related to the intake (i.e. Bq per Bq intake for retention and daily excretion). One exception to this is for intake of tritiated water, where data are given

in Bq l^{-1} per Bq intake as this is directly related to the dose rate.

(353) The use of $z(t)$ simplifies the dose evaluation to a single step, instead of the traditional method of first applying the retention or excretion function $m(t)$ to calculate the intake, and then the dose coefficient $e(50)$ to calculate the resulting effective dose (Section 6.4). Values of dose per content, $z(t)$, are provided to allow a more straightforward assessment of committed dose from bioassay measurements without the need to first determine the intake.

(354) For each radionuclide, the monitoring periods have been selected [as in Para. 91 of *Publication 78* (ICRP, 1997b)] for intake by inhalation for all absorption types so that any underestimation introduced by an unknown time of intake is no more than a factor of three when an acute intake in the middle of the monitoring interval is assumed. The frequency of monitoring, determined using the models that have been applied, is determined both by the behaviour of the radionuclide in the body and its physical half-life.

(355) The bioassay data on the content of radioactive progeny in systemic compartments and compartments of the HRTM are given for selected parent radionuclides alone. Bioassay data on the content of a parent radionuclide are usually sufficient for purposes of individual monitoring.

7.2. Data provided in the printed reports and electronic annex

(356) The data provided in the printed reports are restricted to tables of committed effective dose per intake (Sv Bq^{-1}) for inhalation and ingestion, tables of committed effective dose per content (Sv Bq^{-1}) for inhalation, and graphs of retention and excretion data per Bq intake for inhalation. Data are provided for all absorption types and for the most common isotope(s) of each element section. In cases for which sufficient information is available (principally for actinide elements), lung absorption is specified for different chemical forms, and dose coefficients and bioassay data are calculated accordingly. The sizes of particles inhaled by the Reference Worker are assumed to be log-normally distributed with an AMAD of 5 μm and geometric standard deviation σ_g of approximately 2.5 (ICRP, 1994a, Para. 170). They are assumed to have a density of 3.00 g cm^{-3} and a shape factor of 1.5 (ICRP, 1994a, Para. 181). An exception is made for the short-lived progeny of radon, described in the inhalation section in OIR: Part 3 (ICRP, 2016b).

(357) The electronic annex that accompanies this series of reports contains a comprehensive set of committed effective and equivalent dose coefficients per intake, committed effective dose per content functions, and reference bioassay functions. Data are presented for almost all radionuclides included in *Publication 107* (ICRP, 2008) that have half-lives equal to or greater than 10 min, and for other selected radionuclides. Data are provided for a range of physicochemical forms and for aerosols with median sizes ranging from an AMTD of 0.001 μm to an AMAD of 20 μm. Data for intake by ingestion (for specified values of f_A) and for direct input to the blood are also provided.

7.3. Quality assurance of data presented

(358) The Commission attaches particular importance to quality assurance. The Task Group of Committee 2 on Internal Dose Coefficients arranged for the quantities given in this series of reports to be calculated independently at different laboratories using different computer codes. Any discrepancies in these calculations were investigated and resolved before publication.

REFERENCES

Anderson, M., Philipson, K., Svartengren, M., et al., 1995. Human deposition and clearance of 6 μm particles inhaled with an extremely low flow rate. Exp. Lung Res. 21, 187–195.

Ansoborlo, E., Boulard, D., LeGuen, B., 1997. Particle size distribution of uranium aerosols in the French nuclear fuel cycle. Radioprotection 32, 319–330.

Apostoaei, A.I., Lewis, C.J., Hammonds, J.H., et al., 1998. Uncertainties in doses from ingestion of Cs-137, Sr-90, Co-60, Ru-106, and I-131. Health Phys. 74, S14–S15.

Apostoaei, A.I., Miller, L.F., 2004. Uncertainties in dose coefficients from ingestion of ^{131}I, ^{137}Cs, and ^{90}Sr. Health Phys. 86, 460–482.

Bahadori, A.A., Johnson, P.B., Jokisch, D.W., et al., 2011. Response functions for computing absorbed dose to skeletal tissues from neutron irradiation. Phys. Med. Biol. 56, 6873–6897.

Baron, P.A., Willeke, K. (Eds.), 2001. Aerosol fundamentals. in Aerosol Measurement – Principles, Techniques and Applications, second ed. Wiley intersciences, Inc, New York USA.

Bailey, M.R., Dorrian, M-D., Birchall, A., 1995. Implications of airway retention for radiation doses from inhaled radionuclides. J. Aerosol Med. 8, 373–390.

Berkovski, V., Bonchuk, Y., Ratia, G., 2003a. Dose per unit content functions: a robust tool for the interpretation of bioassay data. Radiat. Prot. Dosim. 105, 399–402.

Berkovski, V., Eckerman, K.F., Phipps, A.W., et al., 2003b. Dosimetry of radioiodine for embryo and fetus. Radiat. Prot. Dosim. 105, 265–268.

Bihl, D.E., Lynch, T.P., Carbaugh, E.H., et al., 1988a. Problems with Detection of Intakes of Very Insoluble Plutonium. Presented at the Thirty Fourth Annual Conference on Bioassay, Analytical, and Environmental Radiochemistry, 17–21 October 1988, Las Vegas, NV, USA. PNL-SA-15981. National Technical Information Service, Springfield, VA.

Bihl, D.E., Carbaugh, E.H., Sula, M.J., et al., 1988b. Human data supporting a super class Y form of plutonium (abstract). Health Phys. 54, S4.

Bihl, D.E., Lynch, T.P., Carbaugh, E.H., et al., 1988c. Methods to Improve Routine Bioassay Monitoring for Freshly Separated, Poorly Transported Plutonium. PNL-6695. Pacific Northwest Laboratory, Richland, WA.

BIPM, IEC, IFCC, ISO, IUPAC, IUPAP, OIML, 2010. Guide to the Expression of Uncertainty in Measurement. JGCM 100:2008. First edition 2008, corrected version 2010.

Birchall, A., Puncher, M., Marsh, J.W., 2007. Avoiding biased estimates of dose when nothing is known about the time of intake. Radiat. Prot. Dosim. 127, 343–346.

Boeniger, M.F., Lowry, L.K., Rosenberg, J., 1993. Interpretation of urine results used to assess chemical exposure with emphasis on creatinine adjustments: a review. J. Am. Ind. Hyg. Assoc. 54, 615–627.

Bolch, W.E., Farfan, E.B., Huh, C.H., et al., 2001. Influences of parameter uncertainties within the ICRP-66 respiratory tract model: particle deposition. Health Phys. 81, 378–394.

Bolch, W.E., Huston, T.E., Farfan, E.B., et al., 2003. Influences of parameter uncertainties within the ICRP-66 respiratory tract model: particle clearance. Health Phys. 84, 421–435.

Borle, A.B., 1981. Control, modulation and regulation of cell calcium. Rev. Physiol. Biochem. Pharmacol. 90, 13–153.

Britcher, A.R., Strong, R., 1994. Personal air sampling – a technique for the assessment of chronic low level exposure? Radiat. Prot. Dosim. 53, 59–62.

Britcher, A.R., Battersby, W.P., Peace, M.S., 1998. The practical application of models for assessing intakes of radionuclides by workers. Radiat. Prot. Dosim. 79, 71–74.

Camner, P., Anderson, M., Philipson, K., et al., 1997. Human bronchiolar deposition and retention of 6-, 8- and 10-μm particles. Exp. Lung Res. 23, 517–535.

Carbaugh, E.H., 2003. Minimum detectable dose as a measure of bioassay programme capability. Radiat. Prot. Dosim. 105, 391–394.

Carbaugh, E.H., La Bone, T.R., 2003. Two case studies of highly insoluble plutonium inhalation with implications for bioassay. Radiat. Prot. Dosim. 105, 133–138.

Castellani, C.M., Marsh, J.W., Hurtgen, C., et al., 2013. IDEAS Guidelines (Version 2) for the Estimation of Committed Doses from Incorporation Monitoring Data. EURADOS Report 2013-01. Braunschweig.

Coombs, M.A., Cuddihy, R.G., 1983. Emanation of ^{232}U daughter products from submicrometer particles of uranium oxide and thorium dioxide by nuclear recoil and inert gas diffusion. J. Aerosol Sci. 14, 75–86.

Cox, M.G., Harris, P.M., 2004. Best Practice Guide No. 6. Uncertainty Evaluation. Technical Report. National Physical Laboratory, Teddington.

Crawford-Brown, D.J., Wilson, J., 1984. Observations on very long term removal of uranium compounds. Health Phys. 47, 443–446.

Cristy, M., 1980. Mathematical Phantoms Representing Children of Various Ages for Use in Estimates of Internal Dose. Oak Ridge National Laboratory Report ORNL/NUREG/TM-367.

Cristy, M., Eckerman, K.F., 1987. Specific Absorbed Fractions of Energy at Various Ages for Internal Photon Sources. Oak Ridge National Laboratory Report ORNL/NUREG/TM-8381, Vol. 1–7.

Davesne, E., Casanova, P., Chojnacki, E., et al., 2010. Integration of uncertainties into internal contamination monitoring. Health Phys. 99, 517–522.

Davesne, E., Casanova, P., Chojnacki, E., et al., 2011. Optimisation of internal contamination monitoring programme by integration of uncertainties. Radiat. Prot. Dosim. 144, 361–366.

Davis, K., Marsh, J.W., Gerondal, M., et al., 2007. Assessment of intakes and doses to workers followed for 15 years after accidental inhalation of ^{60}Co. Health Phys. 92, 332–344.

Doerfel, H., Andrasi, A., Bailey, M.R., et al., 2006. General Guidelines for the Estimation of Committed Effective Dose from Incorporation Monitoring Data (Project IDEAS – EU Contract No. FIKR-CT2001-00160). Research Report FZKA 7243. Research Centre Karlsruhe, Karlsruhe.

Doerfel, H., Andrasi, A., Bailey, M.R., et al., 2007. General guidelines for the assessment of internal dose from monitoring data: progress of the IDEAS Project. European Workshop on Individual Monitoring of Ionising Radiation. 11–15 April 2005, Vienna, Austria. Radiat. Prot. Dosim. 125, 19–22.

Doerfel, H., Andrasi, A., Bailey, M.R., et al., 2008. Internal Dosimetry: the Science and Art of Internal Dose Assessment. Proceedings of the 12th International Congress of the International Radiation Protection Association, 19–24 October 2008, Buenos Aires, Argentina. IRPA12 RC-6. pp. 1–63.

Dorrian, M.D., Bailey, M.R., 1995. Particle size distribution of radioactive aerosols measured in the workplace. Radiat. Prot. Dosim. 60, 119–133.

Duke, K., 1998. Use of the urinary excretion of creatinine in plutonium in urine bioassay. Radiat. Prot. Dosim. 79, 125–128.

Eckerman, K.F., Westfal, R.J., Ryman, J.C., et al., 1994. Availability of nuclear decay data in electronic form, including beta spectra not previously published. Health Phys. 67, 338–345.

Eckerman, K.F., Kerr, G.D., 1999. Y12 Uranium Exposure Study. ORNL/TM-1999-114. Oak Ridge National Laboratory, Oak Ridge, TN.

Elliot, N.L., Bickel, G.A., Linauskas, S.H., et al., 2006. Determination of femtogram quantities of ^{239}Pu and ^{240}Pu in bioassay samples by thermal ionization mass spectrometry. J. Radioanal. Nucl. Chem. 267, 637–650.

Endo, A., Yamaguchi, Y., Eckerman, K.F., 2003. Development and assessment of a new radioactive decay database use for dosimetry calculation. Radiat. Prot. Dosim. 105, 565–569.

Endo, A., Yamaguchi, Y., Eckerman, K.F., 2005. Nuclear Decay for Dosimetry Calculations: Revised Data of ICRP Publication 38. JAERI 1347. Japan Atomic Energy Research Institute. Available at: http://jolissrch-inter.tokai-sc.jaea.go.jp/pdfdata/JAERI-1347.pdf (last accessed 5 May 2015).

Epker, B.N., Frost, H.M., 1965a. Correlation of bone resorption and formation with the physical behaviour of loaded bone. J. Dent. Res. 44, 33–41.

Epker, B.N., Frost, H.M., 1965b. The direction of transverse drift of actively forming osteons in human rib cortex. J. Bone Joint Surg. 47, 1211–1215.

Etherington, G., Cossonnet, C., Franck, D., et al., 2004a. Optimisation of Monitoring for Internal Exposure (OMINEX). NRPB-W60. National Radiological Protection Board, Chilton.

Etherington, G., Ansoborlo, E., Bérard, P., et al., 2004b. OMINEX: Development of Guidance on Monitoring for Internal Exposure. Proceedings of the 11th IRPA International Congress, 23–28 May 2004, Madrid, Spain.

EURACHEM/CITAC, 2000. EURACHEM/CITAC Guide, Quantifying Uncertainty in Analytical Measurement, second ed. EURACHEM, Berlin.

Falk, R., Philipson, K., Svartengren, M., et al., 1997. Clearance of particles from small ciliated airways. Exp. Lung Res. 23, 495–515.

Falk, R., Philipson, K., Svartengren, M., 1999. Assessment of long-term bronchiolar clearance of particles from measurements of lung retention and theoretical estimates of regional deposition. Exp. Lung Res. 25, 495–516.

Ferin, J., Oberdörster, G., Penney, D.P., et al., 1990. Increased pulmonary toxicity of ultrafine particles. I. Particle clearance, translocation, morphology. J. Aerosol Sci. 21, 381–384.

Ferin, J., Oberdörster, G., Soderholm, S.C., et al., 1991. Pulmonary tissue access of ultrafine particles. J. Aerosol Med. 4, 57–68.

Foster, P.P., 1991. Study of a plutonium oxide fuel inhalation case. Radiat. Prot. Dosim. 38, 141–146.

Franck, D., Borissov, N., de Carlan, L., et al., 2003. Application of Monte Carlo calculations to calibration of anthropomorphic phantoms used for activity assessment of actinides in lungs. Radiat. Prot. Dosim. 105, 403–408.

Frost, H.M., 1986. Intermediary Organization of the Skeleton. Volume I & II, CRC Press, Boca Raton, FL.

Fry, F.A., 1976. Long term retention of americium-241 following accidental inhalation. Health Phys. 31, 13–20.

Fry, F.A., Lipsztein, J.L., Birchall, A., 2003. The ICRP working party on bioassay interpretation. Radiat. Prot. Dosim. 105, 297–302.

Gerber, G.B. Thomas, R.G., Eds. 1992. Guidebook for the treatment of accidental internal radionuclide contamination of workers. Radiat. Prot. Dos. 41(1), 1–49.

Gómez-Ros, J.M., Moraleda, M., López, M.A., et al., 2007. Monte Carlo based voxel phantoms for in vivo internal dosimetry. Radiat. Prot. Dosim. 125, 161–165.

Graul, R.J., Stanley, R.L., 1982. Specific gravity adjustment of urine analysis results. Am. Ind. Hyg. Assoc. J. 43, 863.

Gregoratto, D., Bailey, M.R., Marsh, J.W., 2010. Modelling particle retention in the alveolar–interstitial region of the lungs. J. Radiol. Prot. 30, 491–512.

Griffith, R.V., Anderson, S.L., Dean, P.N., et al., 1986. Tissue-equivalent Torso Phantom for Calibration of Transuranic Nuclide Counting Facilities. UCRL-93776. Lawrence Livermore National Laboratory, Livermore, CA. Available at: http://www.osti.gov/bridge/servlets/purl/5796207-idwX6y/5796207.pdf (last accessed 5 May 2015).

Griffith, W.C., Cuddihy, R.G., Hoover, M.D., et al., 1980. Simulation of the retention and dosimetry of ^{232}U and its daughters after inhalation of ThO_2 and UO_2 particles. In: Pulmonary Toxicology of Respirable Particles, Proceedings of the 19th Annual Hanford Life Sciences Symposium, October 1979, Richland, WA, USA. National Technical Information Service, Springfield, VA, pp. 193–208.

Guilmette, R.A., Hickman, A.W., Griffith, W.C., 1992. The effect of isotope on the dosimetry of inhaled plutonium oxide. In: Proceedings of the 8th International Congress of the International Radiation Protection Association, 17–22 May 1992, Montreal, Canada, pp. 900–903. Available at: http://www.irpa.net/irpa8/cdrom/VOL.1/M1_221A.pdf (last accessed 5 May 2015).

Guilmette, R.A., Bertelli, L., Miller, G., et al., 2007. Technical basis for using nose swab bioassay data for early internal dose assessment. Radiat. Prot. Dosim. 127, 356–360.

Gunnarsson, M., Stenström, K., Leide-Svegborn, S., et al., 2003. Biokinetics and radiation dosimetry for patients undergoing a glycerol tri-[14C]oleate fat malabsorption test. Appl. Radiat. Isot. 58, 517–526.

Gupton, E.D., Brown, P.E., 1972. Chest clearance of inhaled cobalt-60 oxide. Health Phys. 23, 767–769.

Harrison, G.E., Carr, T.E., Sutton, A., 1967. Distribution of radioactive calcium, strontium, barium and radium following intravenous injection into a healthy man. Int. J. Radiat. Biol. Relat. Stud. Phys. Chem. Med. 13, 235–247.

Harrison, J.D., Leggett, R.W., Nosske, D., et al., 2001. Reliability of the ICRP's dose coefficients for members of the public II. Uncertainties in the absorption of ingested radionuclides and the effect on dose estimates. Radiat. Prot. Dosim. 95, 295–308.

Harrison, J.D., Khursheed, A., Lambert, B., 2002. Uncertainties in dose coefficients for intakes of tritiated water and organically bound forms of tritium by members of the public. Radiat. Prot. Dosim. 98, 299–311.

Hart, H.E., Spencer, H., 1976. Vascular and extravascular calcium interchange in man determined with radioactive calcium. Radiat. Res. 67, 149–161.

Heaney, R.P., 1964. Interpretation of calcium kinetic data. In: Pearson, O.H., Joplin, G.F. (Eds.), Dynamic Studies of Metabolic Bone Disease. Blackwell, Oxford, pp. 11–23.

Hoover, M. D., Myers, D. S., Cash, L. J., Guilmette, R. A., Kreyling, W.G., Oberdörster, G., Smith, R., Cassata, J. R., Boecker, B. B., Grissom, M. P., 2015. Application of an informatics-based decision-making framework and process to the assessment of radiation safety in nanotechnology. Health. Phys. 108, 179–194.

Hough, M., Johnson, P.B., Rajon, D., et al., 2011. An image-based skeletal dosimetry model for the ICRP reference adult male – internal electron sources. Phys. Med. Biol. 56, 2309–2346.

Hunt, J.G., Dantas, B.M., Lourenco, M.C., et al., 2003. Voxel phantoms and Monte Carlo methods applied to in vivo measurements for simultaneous ^{241}Am contamination in four body regions. Radiat. Prot. Dosim. 105, 549–552.

IAEA, 1996. Basic Safety Standards for Direct Methods for Measuring Radionuclides in the Human Body. Safety Series 114. International Atomic Energy Agency, Vienna.

IAEA, 1999a. Occupational Radiation Protection. Safety Guide RS-G-1.1. International Atomic Energy Agency, Vienna.
IAEA, 1999b. Occupational Exposure Due to Intakes of Radionuclides. Safety Guide RS-G-1.2. International Atomic Energy Agency, Vienna.
IAEA, 2000. Basic Safety Standards for Indirect Methods for Assessing Intakes of Radionuclides Causing Occupational Exposure. Safety Series 18. International Atomic Energy Agency, Vienna.
IAEA, 2004a. Basic Safety Standards for Methods for Assessing Occupational Radiation Doses Due to Intakes of Radionuclides. Safety Series 37. International Atomic Energy Agency, Vienna.
IAEA, 2004b. Assessment and Treatment of External and Internal Radionuclide Contamination. TECDOC-869. International Atomic Energy Agency, Vienna.
IAEA, 2007. Intercomparison Exercise on Internal Dose Assessment. Final report of a Joint IAEA-IDEAS Project. TECDOC-1568. International Atomic Energy Agency, Vienna.
ICRP, 1973. Alkaline Earth Metabolism in Adult Man. ICRP Publication 20. Pergamon Press, Oxford.
ICRP, 1975. Report on the Task Group on Reference Man. ICRP Publication 23. Pergamon Press, Oxford.
ICRP, 1977. Recommendations of the International Commission on Radiological Protection. ICRP Publication 26. Ann. ICRP 1(3).
ICRP, 1979. Limits for intake of radionuclides by workers. ICRP Publication 30, Part 1. Ann. ICRP 2(3/4).
ICRP, 1980. Limits for intakes of radionuclides by workers. ICRP Publication 30, Part 2. Ann. ICRP 4(3/4).
ICRP, 1981. Limits for intakes of radionuclides by workers. ICRP Publication 30, Part 3. Ann. ICRP 6(2/3).
ICRP, 1983. Radionuclide transformations: energy and intensity of emissions. ICRP Publication 38. Ann. ICRP 11–13.
ICRP, 1988a. Individual monitoring for intakes of radionuclides by workers: design and interpretation. ICRP Publication 54. Ann. ICRP 19(1–3).
ICRP, 1988b. Limits for intakes of radionuclides by workers: an addendum. ICRP Publication 30, Part 4. Ann. ICRP 19(4).
ICRP, 1989. Age-dependent doses to members of the public from intake of radionuclides. ICRP Publication 56, Part 1. Ann. ICRP 20(2).
ICRP, 1991. 1990 Recommendations of the ICRP. ICRP Publication 60. Ann. ICRP 21(1–3).
ICRP, 1993. Age-dependent doses to members of the public from intake of radionuclides: Part 2. Ingestion dose coefficients. ICRP Publication 67. Ann. ICRP 23(3/4).
ICRP, 1994a. Human respiratory tract model for radiological protection. ICRP Publication 66. Ann. ICRP 24(1–3).
ICRP, 1994b. Dose coefficients for intake of radionuclides by workers. ICRP Publication 68. Ann. ICRP 24(4).
ICRP, 1995a. Basic anatomical and physiological data for use in radiological protection: the skeleton. ICRP Publication 70. Ann ICRP 25(2).
ICRP, 1995b. Age-dependent doses to members of the public from intake of radionuclides: Part 3. Ingestion dose coefficients. ICRP Publication 69. Ann. ICRP 25(1).
ICRP, 1995c. Age-dependent doses to members of the public from intake of radionuclides: Part 4. Inhalation dose coefficients. ICRP Publication 71. Ann. ICRP 25(3/4).

ICRP, 1996. Age-dependent doses to members of the public from intake of radionuclides: Part 5. Compilation of ingestion and inhalation dose coefficients. ICRP Publication 72. Ann. ICRP 26(1).
ICRP, 1997a. General principles for the radiation protection of workers. ICRP Publication 75. Ann. ICRP 27(1).
ICRP, 1997b. Individual monitoring for internal exposure of workers – replacement of ICRP Publication 54. ICRP Publication 78. Ann. ICRP 27(3/4).
ICRP, 2001. Dose to the embryo and fetus from intakes of radionuclides by the mother. ICRP Publication 88. Ann. ICRP 31(1–3).
ICRP, 2002a. Basic anatomical and physiological data for use in radiological protection: reference values. ICRP Publication 89. Ann. ICRP 32(3/4).
ICRP, 2002b. Guide for the practical applications of the ICRP Human Respiratory Tract Model. Supporting Guidance 3. Ann. ICRP 32(1/2).
ICRP, 2004. Doses to the infant from radionuclides ingested in mothers' milk. ICRP Publication 95. Ann. ICRP 34(3/4).
ICRP, 2006. Human alimentary tract model for radiological protection. ICRP Publication 100. Ann. ICRP 36(1/2).
ICRP, 2007. The 2007 Recommendations of the International Commission on Radiological Protection. ICRP Publication 103. Ann. ICRP 37(2–4).
ICRP, 2008. Nuclear decay data for dosimetric calculations. ICRP Publication 107. Ann. ICRP 38(3).
ICRP, 2009. Adult reference computational phantoms. ICRP Publication 110. Ann. ICRP 39(2).
ICRP, 2010. Conversion coefficients for radiological protection quantities for external radiation exposures. ICRP Publication 116. Ann. ICRP 40(1).
ICRP, 2016a. Occupational intakes of radionuclide: Part 2. ICRP Publication 13Y. Ann. ICRP 4Y(Y) (In preparation).
ICRP, 2016b. Occupational intakes of radionuclides: Part 3. ICRP Publication 13Z. Ann. ICRP 4Z(Z) (In preparation).
ICRP, 2016c. Specific absorbed fractions for internal emitters in the adult reference computational phantoms. ICRP Publication (In preparation).
ICRU, 2002. Retrospective assessment of exposure to ionising radiation. ICRU Report 67. J. ICRU 2(2).
ICRU, 2003. Direct determination of the body content of radionuclides. ICRU Report 69. J. ICRU 3(1).
Inkret, W.C., Efurd, D.W., Miller, G., et al., 1998. Applications of thermal ionization mass spectrometry to the detection of ^{239}Pu and ^{240}Pu intakes. Int. J. Mass Spectrom. 178, 113–120.
ISO, 2006. Radiation Protection – Monitoring of Workers Occupationally Exposed to a Risk of Internal Contamination with Radioactive Material. ISO 205553:2006. International Organization for Standardization, Geneva.
ISO, 2010a. Determination of the Characteristic Limits (Decision Threshold, Detection Limit and Limits of the Confidence Interval) for Measurements of Ionizing Radiation – Fundamentals and Application. ISO 11929:2010. International Organization for Standardization, Geneva.
ISO, 2010b. Radiation Protection – Performance Criteria for Radiobioassay. ISO 28218:2010. International Organization for Standardization, Geneva.

ISO, 2011. Radiation Protection – Dose Assessment for the Monitoring of Workers for Internal Radiation Exposure. ISO 27048:2011. International Organization for Standardization, Geneva.

Jackson, S., 1966. Creatinine in urine as an index of urinary excretion rate. Health Phys. 12, 843.

Johnson, J.R., Peterman, B.F., 1984. A model to describe thoron exhalation following an inhalation exposure to thoria powders. In: Lung Modelling for Inhalation of Radioactive Materials. EUR Report 9384. Commission of the European Communities, Luxembourg, pp. 193–196.

Johnson, P.B., Bahadori, A.A., Eckerman, K.F., et al., 2011. Response functions for computing absorbed dose to skeletal tissues from photon irradiation – an update. Phys. Med. Biol. 56, 2347–2366.

Jokisch, D.W., Rajon, D.A., Patton, P.W., et al., 2011a. Methods for inclusion of shallow marrow and adipose tissue in pathlength-based skeletal dosimetry. Phys. Med. Biol. 56, 2699–2713.

Jokisch, D.W., Rajon, D.A., Bolch, W.E., 2011b. An image-based skeletal dosimetry model for the ICRP reference adult male – specific absorbed fractions for neutron-generated recoil protons. Phys. Med. Biol. 56, 6857–6872.

Kanapilly, G.M., Diel, J.H., 1980. Ultrafine $^{239}PuO_2$ aerosol generation, characterization and short-term inhalation study in the rat. Health Phys. 39, 505–519.

Kathren, R.L., Strom, D.J., Sanders, C.L., et al., 1993. Distribution of plutonium and americium in human lungs and lymph nodes and relationship to smoking status. Radiat. Prot. Dosim. 48, 307–315.

Kawrakow, I., Mainegra-Hing, E., Rogers, D.W.O., et al., 2009. The EGSnrc code system: Monte Carlo simulation of electron and photon transport. PIRS Report 701. National Research Council of Canada, Ottawa.

Kelso, S.M., Wraight, J.C., 1996. The measurement of aerosol size distributions (AMAD) in buildings on BNFL's Sellafield site. Radiat. Prot. Dosim. 63, 127–131.

Kim, E.M., 1995. Determination of Time Interval of Urine Sample by Measuring Creatinine in Urine. ESH-HPT-95007. Westinghouse Savannah River Company, Aiken, SC.

Kramer, G.H., Hauck, B.M., 1999. The effect of lung deposition patterns on the activity estimate obtained from a large area germanium detector lung counter. Health Phys. 77, 24–32.

Kramer, G.H., Lopez, M.A., Webb, J., 2000. A joint HML-CIEMAT-CEMRC project: testing a function to the counting efficiency of a lung counting germanium detector array to muscle-equivalent chest wall thickness and photon energy using a realistic torso phantom over an extended energy range. Radiat. Prot. Dosim. 92, 324–327.

Kramer, R., Zankl, M., Williams, G., et al., 1982. The Calculation of Dose from External Photon Exposures Using Reference Human Phantoms and Monte Carlo Methods. Part I: the Male (ADAM) and Female (EVA) Adult Mathematical Phantoms. GSF-Report S-885. Gesellschaft für Strahlen und Umweltforschung mbH, München.

Kuempel, E.D., O'Flaherty, E.J., Stayner, L.T., 2001. A biomathematical model of particle clearance and retention in the lungs of coal miners. Regul. Toxicol. Pharmacol. 34, 69–87.

Kvasnicka, J., 1987. Assessing dose equivalent from intensive short term U product inhalation. Health Phys. 53, 673–678.

LaMont, S.P., Schick, C.R., Cable-Dunlap, P., 2005. Plutonium determination in bioassay sample using radiochemical thermal ionization mass spectrometry. J. Radioanal. Nucl. Chem. 263, 477–481.

Lauweryns, J.M., Baert, J.H., 1977. Alveolar clearance and the role of the pulmonary lymphatics. Am. Rev. Respir. Dis. 115, 625–683.

Leggett, R.W., 1985. A model of the retention, translocation and excretion of systemic plutonium. Health Phys. 49, 1115–1137.

Leggett, R.W., 1992. A retention–excretion model for americium in humans. Health Phys. 62, 288–310.

Leggett, R.W., 2001. Reliability of ICRP's dose coefficients for members of the public I. Sources of uncertainty in the biokinetic models. Radiat. Prot. Dosim. 95, 199–213.

Leggett, R.W., Dunning, D.E., Jr, Eckerman, K.F., 1984. Modelling the behaviour of chains of radionuclides inside the body. Radiat. Prot. Dosim. 9, 778–791.

Leggett, R.W., Bouville, A., Eckerman, K.F., 1998. Reliability of the ICRP's systemic biokinetic models. Radiat. Prot. Dosim. 79, 335–342.

Leggett, R.W., Harrison, J.D., Phipps, A., 2007. Reliability of the ICRP's dose coefficients for members of the public: IV. Basis of the human alimentary tract model and uncertainties in model predictions. Radiat. Prot. Dosim. 123, 156–170.

Leggett, R.W., Eckerman, K.F., Meck, R.A., 2008. Reliability of Current Biokinetic and Dosimetric Models for Radionuclides: a Pilot Study. ORNL/TM-2008/131. Oak Ridge National Laboratory, Oak Ridge, TN.

Leide-Svegborn, S., Stenström, K., Olofsson, M., 1999. Biokinetics and radiation doses for 14C-urea in adults and children undergoing the *Helicobacter pylori* breath test. Eur. J. Nucl. Med. 26, 573–580.

Likhtarev, I., Minenko, V., Khrouch, V., et al., 2003. Uncertainties in thyroid dose reconstruction after Chernobyl. Radiat. Prot. Dosim. 105, 601–608.

Lipsztein, J.L., Dias da Cunha, K.M., Azeredo, A.M.G., et al., 2001. Exposure of workers in mineral processing industries in Brazil. J. Environ. Radioact. 54, 189–199.

Lipsztein, J.L., Melo, D.R., Sousa, W., et al., 2003. NORM workers: a challenge for internal dosimetry programmes. Radiat. Prot. Dosim. 105, 317–320.

Little, T.T., Miller, G., Guilmette, R., et al., 2007. Uranium dose assessment: a Bayesian approach to the problem of dietary background. Radiat. Prot. Dosim. 127, 333–338.

Lopez, M.A., Balásházy, I., Bérard, P., et al., 2011b. EURADOS coordinated action on research, quality assurance and training of internal dose assessments. Radiat. Prot. Dosim. 144, 349–352.

Lopez, M.A., Broggio, D., Capello, K., et al., 2011a. EURADOS intercomparison on measurements and Monte Carlo modelling for the assessment of americium in a USTUR leg phantom. Radiat. Prot. Dosim. 144, 295–299.

Mann, J.R., Kirchner, R.A., 1967. Evaluation of lung burden following acute inhalation exposure to highly insoluble PuO_2. Health Phys. 13, 877–882.

Marsh, J.W., Castellani, C.M., Hurtgen, C., 2008a. Internal dose assessments: uncertainty studies and update of IDEAS guidelines and databases within CONRAD project. Radiat. Prot. Dosim. 131, 34–39.

Marsh, J.W., Blanchardon, E., Castellani, C.M., et al., 2008b. Evaluation of scattering factor values for internal dose assessment following the IDEAS guidelines: preliminary results. Radiat. Prot. Dosim. 127, 339–342.

Marshall, M., Stevens, D.C., 1980. The purposes, methods and accuracy of sampling for airborne particulate radioactive materials. Health Phys. 39, 409–423.

Miller, G., Martz, H.F., Little, T., et al., 2002a. Using exact Poisson likelihood functions in Bayesian interpretation of counting measurements. Health Phys. 83, 512–518.

Miller, G., Martz, H.F., Little, T.T., et al., 2002b. Bayesian internal dosimetry calculations using Markov chain Monte Carlo. Radiat. Prot. Dosim. 98, 191–198.

Moeller, D.W., Sun, L.S., 2006. Comparison of natural background dose rates for residents of the Amargosa Valley, NV, to those in Leadville, CO, and the states of Colorado and Nevada. Health Phys. 91, 338–353.

NCRP, 1980. Management of Persons Accidentally Contaminated with Radionuclides. Report No. 65. National Council on Radiation Protection and Measurements, Bethesda, MD.

NCRP, 2006. Development of a Biokinetic Model for Radionuclide-contaminated Wounds and Procedures for their Assessment, Dosimetry and Treatment. Report No. 156. National Council on Radiation Protection and Measurements, Bethesda, MD.

NCRP, 2008. Management of Persons Contaminated with Radionuclides. Report No. 161. National Council on Radiation Protection and Measurements, Bethesda, MD.

NCRP, 2009. Radiation Dose Reconstruction: Principles and Practices. Report No. 163. National Council on Radiation Protection and Measurements, Bethesda, MD.

NCRP, 2010. Uncertainties in Internal Radiation Dose Assessment. Report No. 164. National Council on Radiation Protection and Measurements, Bethesda, MD.

Newton, D., 1977. Clearance of radioactive tantalum from the human lung after accidental inhalation. Am. J. Roentgenol. Rad. Ther. Nucl. Med. 129, 327–328.

Newton, D., Rundo, J., 1971. The long term retention of inhaled cobalt-60. Health Phys. 21, 377–384.

Newton, D., Taylor, B.T., Eakins, J.D., 1983. Differential clearance of plutonium and americium oxides from the human lung. Health Phys. 44(Suppl. 1), 431–439.

Niita, K., Matsuda, N., Iwamoto, Y., et al., 2010. PHITS - Particle and Heavy Ion Transport Code System, Version 2.23. JAEA-Data/Code 2010-022. Japan Atomic Energy Research Institute. Available at: http://jolissrch-inter.tokai-sc.jaea.go.jp/pdfdata/JAEA-Data-Code-2010-022.pdf (last accessed 5 May 2015).

Noßke, D., Karcher, K., 2003. Is radiation protection for the unborn child guaranteed by radiation protection for female workers? Radiat. Prot. Dosim. 105, 269–272.

ORAUT, 2007. Estimating Doses for Plutonium Strongly Retained in the Lung. ORAUT–OTIB–0049. Oak Ridge Associated Universities Team, Oak Ridge, TN.

Parfitt, A.M., Kleerekoper, M., 1980. The divalent ion homeostatic system: physiology and metabolism of calcium, phosphorus, magnesium and bone. In: Maxwell, M., Kleeman, C.R. (Eds.), Clinical Disorders of Fluid and Electrolyte Metabolism, third ed. McGraw Hill, New York, NY, pp. 269–398.

Pawel, D.J., Leggett, R.W., Eckerman, K.F., et al., 2007. Uncertainties in Cancer Risk Coefficients for Environmental Exposure to Radionuclides. An Uncertainty Analysis for Risk Coefficients Reported in Federal Guidance Report No. 13. ORNL/TM-2006/583. Oak Ridge National Laboratory, Oak Ridge, TN.

Pelowitz, D.B., 2008. MCNPX User's Manual, Version 2.6.0. LA-CP-07-1473. Los Alamos National Laboratory, Los Alamos, NM.

Philipson, K., Falk, R., Gustafsson, J., et al., 1996. Long-term lung clearance of ^{195}Au-labelled teflon particles in humans. Env. Lung Res. 22, 65–83.

Philipson, K., Falk, R., Svartengren, M., 2000. Does lung retention of inhaled particles depend on their geometric diameter? Exp. Lung Res. 26, 437–455.

Phipps, A.W., Smith, T.J., Fell, T.P., et al., 2001. Doses to the Embryo/Fetus and Neonate from Intakes of Radionuclides by the Mother. Contract Research Report to the Health and Safety Executive. CRR 397. HSE Information Services, Caerphilly.

Price, A., 1989. Review of methods for the assessment of intake of uranium by workers at BNFL Springfields. Radiat. Prot. Dosim. 26, 35–42.

Priest, N.D., Haines, J.W., Humphreys, J.A.M., et al., 1992. The bone volume effect on the dosimetry of plutonium-239 and americium-241 in the skeleton of man and baboon. J. Radioanal. Nucl. Chem. 156, 33–53.

Puncher, M., Marsh, J.W., Birchall, A., 2006. Obtaining an unbiased estimate of intake in routine monitoring when the time of intake is unknown. Radiat. Prot. Dosim. 118, 280–289.

Puncher, M., Birchall, A., 2008. A Monte Carlo method for calculating Bayesian uncertainties in internal dosimetry. Radiat. Prot. Dosim. 132, 1–12.

Raghavendran, K.V., Satbhai, P.D., Abhyankar, B., et al., 1978. Long term retention studies of ^{131}I, ^{137}Cs and ^{60}Co in Indian workers. Health Phys. 34, 185–188.

Ramsden, D., 1976. Assessment of plutonium in lung for both chronic and acute exposure conditions. In: Diagnosis and Treatment of Incorporated Radionuclides. International Atomic Energy Agency, Vienna, pp. 139–161.

Ramsden, D., 1984. A modified lung model to match observed lung and urinary data following the inhalation of plutonium oxide: the problems of long term retention in the pulmonary lymph nodes. In: Smith, H., Gerber, G. (Eds.), Lung Modelling for Inhalation of Radioactive Materials. EUR 9384. CEC, Brussels, pp. 281–286.

Ramsden, D., Bains, M.E.D., Frazer, D.C., 1978. A case study of multiple low level exposure to plutonium oxide. Health Phys. 34, 649–659.

Ronen, M., 1969. A case of insoluble natural uranium exposure (a two year follow up study). In: Handling of Radiation Accidents. Proceedings of a Symposium on the Handling of Radiation Accidents Organized with IAEA in Collaboration with WHO, 19–23 May 1969, IAEA, Vienna, Austria, pp. 451–457.

Rundo, J., 1965. A case of accidental inhalation of irradiated uranium. Br. J. Radiol. 38, 39–50.

Sánchez, G., 2007. Fitting bioassay data and performing uncertainty analysis with BIOKMOD. Health Phys. 92, 64–72.

Sathyabama, N., Eappen, K.P., Mayya, Y.S., 2005. Calibration of an electrostatic chamber for thoron measurements in exhaled breath. Radiat. Prot. Dosim. 118, 61–69.

Saxby, W.N., Taylor, N.A., Garland, J., et al., 1964. A case of inhalation of enriched uranium dust. In: Assessment of Radioactivity in Man, Volume II. International Atomic Energy Agency, Vienna, pp. 535–547.

Schultz, N.B., 1966. Inhalation cases of enriched insoluble uranium oxides. In: Proceedings of First International Congress of Radiation Protection, 5–10 September 1966, Rome, Italy. Pergamon Press, Oxford, pp. 1205–1213.

Scott, L.M., West, C.M., 1967. An evaluation of U_3O_8 exposure with an estimate of systemic body burden. Health Phys. 13, 21–26.

Shah, A.P., Bolch, W.E., Rajon, D.A., et al., 2005. A paired-image radiation transport (PIRT) model for skeletal dosimetry. J. Nucl. Med. 46, 344–353.

Skrable, K., Chabot, G., French, C.M., 1994. Estimation of intakes from repetitive bioassay measurements. In: Raabe, O.G. (Ed.) Internal Radiation Dosimetry. Medical Physics Publishing, Madison, WI.

Skrable, K., French, C.M., Chabot, G., et al., 2002. Variance models for estimating intakes from repetitive bioassay measurements. In: Bolch, W.E. (Ed.) Practical Applications of Internal Dosimetry. Medical Physics Publishing, Madison, WI.

Smith, H., Stradling, G.N., Loveless, B.W., et al., 1977. The in vivo solubility of plutonium 239 dioxide in the rat lung. Health Phys. 33, 539–551.

Smith, J.R.H., Etherington, G., Shutt, A.L., et al., 2002. A study of aerosol deposition and clearance from the human nasal passage. Ann. Occup. Hyg. 46(Suppl. 1), 309–313.

Smith, J.R.H., Bailey, M.R., Etherington, G., et al., 2007. Further study of the effect of particle size on slow particle clearance from the bronchial tree. Radiat. Prot. Dosim. 127, 35–39.

Smith, J.R.H., Bailey, M.R., Etherington, G., et al., 2008. Effect of particle size on slow particle clearance from the bronchial tree. Exp. Lung Res. 34, 287–312.

Smith, J.R.H., Bailey, M.R., Etherington, G., et al., 2011. An experimental study of clearance of inhaled particles from the human nose. Exp. Lung Res. 37, 109–129.

Smith, J.R.H., Etherington, G., Youngman, M.J., 2012. An Investigation of Monitoring by Nose Blow Sampling. HPA-CRCE-030. Centre for Radiation, Chemical and Environmental Hazards, Public Health England, Chilton.

Smith, J.R.H., Birchall, A., Etherington, G., et al., 2014. A revised model for the deposition and clearance of inhaled particles in human extra-thoracic airways. Radiat. Protect. Dos. 158, 135–147.

Snyder, W.S., Ford, M.R., Warner, G.G., et al., 1969. Estimates of absorbed fractions for monoenergetic photon sources uniformly distributed in various organs of a heterogeneous phantom. MIRD Pamphlet No. 5. J. Nucl. Med. 10(Suppl. 3), 46–51.

Snyder, S.F., Traub, R.J., 2010. The Livermore phantom history and supplementation. Health Phys. 98, 459–465.

Stradling, G.N., Ham, G.J., Smith, H., et al., 1978a. Factors affecting the mobility of plutonium 238 dioxide in the rat. Int. J. Radiat. Biol. 34, 37–47.

Stradling, G.N., Loveless, B.W., Ham, G.J., et al., 1978b. The biological solubility in the rat of plutonium present in mixed plutonium sodium aerosols. Health Phys. 35, 229–235.

Stradling, N., Hodgson, A., Phipps, A.W., et al., 2005. Can low doses from inhaled thorium be confirmed by personal monitoring? In: Proceedings of the 9th International Conference on Health Effects of Incorporated Radionuclides (HEIR), 29 November–1 December 2004. GSF-Report 06/05. GSF, Neuherberg, pp. 261–268.

Stather, J.W., Phipps, A.W., Harrison, J.D., et al., 2003. Dose coefficients for the embryo and fetus following intakes of radionuclides by the mother. Radiat. Prot. Dosim. 105, 257–264.

Strom, D.J., 2003. Eliminating bias in routine bioassay when there is an unknown time of intake. Radiat. Prot. Dosim. 105, 339–340.

Sun, L.C., Clinton, J.H., McDonald, J., et al., 1993. Urine collection protocol in the Republic of the Marshall Islands. Radiat. Prot. Manag. 10, 64–72.

Svartengren, M., Sommerer, K., Scheuch, G., 2001. Comparison of clearance of particles inhaled with bolus and extremely slow inhalation techniques. Exp. Lung Res. 27, 367–386.

Takahashi, S., Patrick, G., 1987. Long-term retention of ^{133}Ba in the rat trachea following local administration as barium sulfate particles. Radiat. Res. 110, 321–328.

Takahashi, S., Kubota, Y., Sato, H., et al., 1993. Retention of ^{133}Ba in the trachea of rabbits, dogs and monkeys following local administration of $^{133}BaSO_4$ particles. Inhal. Tox. 5, 265–273.

Toohey, R.E., Essling, M.A., 1980. Measurements of ^{241}Am in vivo at long times after inhalation. Health Phys. 38, 139–145.

Tyler, G.R., Lister, B.A.J., 1973. The biological half life of ^{144}Ce in the human chest as determined from in vivo measurements following an accidental inhalation. In: Proceedings of the 2nd IRPA European Congress on Radiation Protection, pp. 249–253.

Wernli, C., Eikenberg, J., 2007. Twenty-year follow-up of a Pu/Am inhalation case. Radiat. Prot. Dosim. 125, 506–512.

West, C.M., Scott, L.M., 1966. A comparison of uranium cases showing long chest burden retentions. Health Phys. 12, 1545–1555.

West, C.M., Scott, L.M., 1969. Uranium cases showing long chest burden retention – an updating. Health Phys. 17, 781–791.

West, C.M., Scott, L.M., Schultz, N.B., 1979. Sixteen years of uranium personnel monitoring experience – in retrospect. Health Phys. 36, 665–669.

Whicker, J.L., 2004. Relationship of air sampling measurements to internal dose: a review. In: Proceedings of 37th Midyear Health Physics Society Meeting on Air Monitoring and Internal Dosimetry, 8–11 February 2004, Augusta, GA, USA. pp. 73–77. Available at: http://hps.org/meetings/midyear/abstract508.html (last accessed 5 May 2015).

Youngman, M.J., Smith, J.R.H., Kovari, M., 1994. The determination of thorium lung burden by measurements of thoron in exhaled air. Radiat. Prot. Dosim. 53, 99–102.

Zankl, M., Fill, U., Petoussi-Henss, N., et al., 2002. Organ dose conversion coefficients for external photon irradiation of male and female voxel models. Phys. Med. Biol. 47, 2367–2385.

Zankl, M., Petoussi-Henss, N., Fill, U., et al., 2003. The application of voxel phantoms to the internal dosimetry of radionuclides. Radiat. Prot. Dosim. 105, 539–548.

Zankl, M., Eckerman, K., Bolch, W.E., 2007. Voxel-based models representing the male and female ICRP reference adult – the skeleton. Radiat. Prot. Dosim. 127, 174–186.

ANNEX A. REVISION OF THE HUMAN RESPIRATORY TRACT MODEL

A.1. Introduction

(A1) The publication of the OIR series provides an opportunity for updating the HRTM described in *Publication 66* (ICRP, 1994a) in the light of experience and new information. The revised version of the HRTM used in the OIR series is summarised in Section 3.2, and simple changes from the original HRTM are described. The major changes made relate to the clearance of deposited material by both particle transport and absorption into blood. These involved reviews and analyses of relevant recent information, and judgements in implementing the changes in the HRTM. These developments are described below. Changes to the model describing particle transport from the ET airways involved changes to the distribution between ET_1 and ET_2 of material deposited in the ET airways, which are described below. Detailed consideration given to the treatment of progeny formed in the respiratory tract is also described in this annex.

A.2. Clearance: particle transport

(A2) As in the original HRTM, it is assumed that particle transport rates are independent of age and sex, and the same for all materials. A generic compartment model is therefore provided to describe particle transport of all materials. It is recognised [see Annex E of *Publication 66* (ICRP, 1994a)] that there are exceptions to this assumption. In particular, the clearance of some nanoparticles from the AI region may be different from the behaviour assumed in the model (see Section A.3.4). However, it was considered that the additional complexity involved in taking account of this was not justified for radiation protection purposes.

(A3) The original model is shown in Fig. A.1. Reference values of each parameter are shown in Fig. A.1 and listed in Table A.1. Reference values of rate constants were derived, as far as possible, from human studies, as particle transport rates are known to vary greatly among mammalian species.

(A4) New studies enable more reliable particle transport parameter values to be chosen for the ET, BB, bb, and AI regions than was possible when *Publication 66* was issued (ICRP, 1994a).

(A5) The revised particle transport model adopted here is shown in Fig. A.2 (also Fig. 3.4). Reference values of each parameter are shown in Fig. A.2 and listed in Table A.1. Differences between the two models are summarised here, and the background to the changes is given in detail below.

(A6) Region ET_2 is described in the model by two compartments: ET_{seq} and ET'_2. As the oral passage is no longer included in ET_2, compartment ET'_2 is redefined as consisting of the posterior nasal passage, pharynx, and larynx.

(A7) In each of the BB and bb regions, there is now one phase of clearance towards the throat, instead of two. Hence, compartments BB_1 and BB_2 in Fig. A.1 are replaced by compartment BB′ in Fig. A.2, and compartments bb_1 and bb_2 in Fig. A.1 are replaced by compartment bb′ in Fig. A.2.

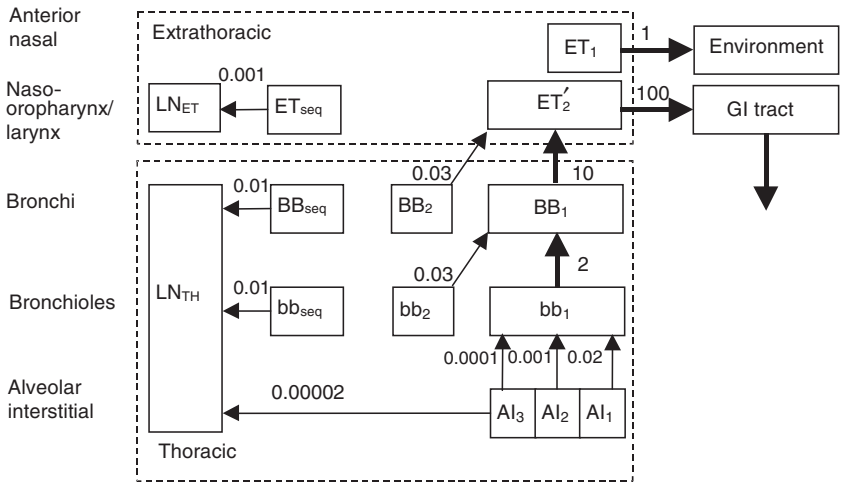

Fig. A.1. Compartment model representing time-dependent particle transport from each respiratory tract region in the original Human Respiratory Tract Model. Rates shown alongside arrows are reference values in units of d^{-1}. It was assumed that: (1) the alveolar–interstitial (AI) deposit is divided into AI_1, AI_2, and AI_3 in the ratio 0.3:0.6:0.1; (2) the fraction of the deposit in the bronchi (BB) and bronchioles (bb) that is cleared slowly (BB_2 and bb_2) is 50% for particles of physical size <2.5 μm and decreases with diameter >2.5 μm, and the fraction retained in the airway wall (BB_{seq} and bb_{seq}) is 0.7% at all sizes; and (3) 0.05% of material deposited in the ET_2 region is retained in its wall (ET_{seq}) and the rest in compartment ET'_2 which clears rapidly to the gastrointestinal (GI) tract.
AI_1: relatively short-term retention (half-time, $t_{½}$ about 35 d) of a fraction, taken to be 0.3, of the deposit in the alveolar-interstitial region; AI_2: long-term retention ($t_{½}$ about 700 d) of a fraction, taken to be 0.6, of the deposit in the alveolar-interstitial region; AI_3: very long-term retention ($t_{½}$ about 6000 d) of a fraction, taken to be 0.1, of the deposit in the alveolar-interstitial region; BB_1: short-term retention ($t_{½}$ about 100 minutes) of particles in the bronchial region: the particles are removed by rapid mucociliary clearance; bb_1: short-term retention ($t_{½}$ about 8 hours) of particles in the bronchiolar region: the particles are removed by rapid mucociliary clearance; BB_2: intermediate retention ($t_{½}$ about 20 d) of particles in the bronchial region; bb_2: intermediate retention ($t_{½}$ about 20 d) of particles in the bronchiolar region; BB_{seq}: long-term retention ($t_{½}$ about 70 d) in airway walls of a small fraction of the particles deposited in the bronchial region; bb_{seq}: long-term retention ($t_{½}$ about 70 d) in airway walls of a small fraction of the particles deposited in the bronchiolar region; ET_1: retention of material deposited in the anterior nose (region ET_1, which is not subdivided); ET'_2: short-term retention ($t_{½}$ about 10 minutes) of the material deposited in the posterior nasal passage, larynx, pharynx and mouth (region ET_2), except for the small fraction, taken to be 0.0005, retained in ET_{seq}. (In Publication 66 this compartment was labelled ET_2. It is here, as in Publication 71, labelled ET'_2 to distinguish it from the region ET_2 which also includes compartment ET_{seq}.); ET_{seq}: long-term retention ($t_{½}$ about 700 d) in airway tissue of a small fraction of particles deposited in the nasal passages; LN_{ET}: lymphatics and lymph nodes that drain the extrathoracic region; LN_{TH}: lymphatics and lymph nodes that drain the thoracic regions.

Table A.1. Reference values of parameters for the compartment model to represent time-dependent particle transport from the human respiratory tract.

(a) Clearance rates

Original HRTM (from ICRP, 1994a, Table 17A)				Revised HRTM			
From	To	Rate (d^{-1})	Half-time*	From	To	Rate (d^{-1})	Half-time*
AI_1	bb_1	0.02	35 d	ALV	bb′	0.002	–
AI_2	bb_1	0.001	700 d	ALV	INT	0.001	–
AI_3	bb_1	0.0001	–	INT	LN_{TH}	0.00003	–
AI_3	LN_{TH}	0.00002	–				
bb_1	BB_1	2	8 h	bb′	BB′	0.2	4 d
bb_2	BB_1	0.03	23 d	bb_{seq}	LN_{TH}	0.001	700 d
bb_{seq}	LN_{TH}	0.01	70 d				
BB_1	ET'_2	10	100 min	BB′	ET'_2	10	100 min
BB_2	ET'_2	0.03	23 d	BB_{seq}	LN_{TH}	0.001	700 d
BB_{seq}	LN_{TH}	0.01	70 d				
ET'_2	Gastrointestinal tract	100	10 min	ET'_2	Oesophagus	100	10 min
ET_{seq}	LN_{ET}	0.001	700 d	ET_{seq}	LN_{ET}	0.001	700 d
ET_1	Environment	1	17 h	ET_1	Environment	0.6	–
				ET_1	ET'_2	1.5	–

(b) Partition of deposit in each region between compartments

Original HRTM (from ICRP, 1994a, Table 17B)			Revised HRTM		
Region or deposition site	Compartment	Fraction of deposit in region assigned to compartment†	Region or deposition site	Compartment	Fraction of deposit in region assigned to compartment
ET_1	ET_1	1	ET_1	ET_1	1
ET_2	ET'_2	0.9995	ET_2	ET'_2	0.998
	ET_{seq}	0.0005		ET_{seq}	0.002
BB	BB_1	$0.993–f_s$	BB	BB′	0.998
	BB_2	f_s		BB_{seq}	0.002
	BB_{seq}	0.007			
bb	bb_1	$0.993–f_s$	bb	bb′	0.998
	bb_2	f_s		bb_{seq}	0.002

(continued on next page)

Table A.1. *(continued)*

Original HRTM (from ICRP, 1994a, Table 17B)			Revised HRTM		
Region or deposition site	Compartment	Fraction of deposit in region assigned to compartment[†]	Region or deposition site	Compartment	Fraction of deposit in region assigned to compartment
	bb_{seq}	0.007			
AI	AI_1	0.3	AI	ALV	1
	AI_2	0.6			
	AI_3	0.1			

HRTM, Human Respiratory Tract Model; Regions or depositions sites: ET_1, anterior nasal passage; ET_2, posterior nasal passage, pharynx, and larynx; BB, bronchial; bb, bronchiolar; AI, alveolar–interstitial; INT, interstitial; ALV, alveolar; LN_{ET}, extrathoracic lymph nodes; LN_{TH}, thoracic lymph nodes.

Compartments: ET_1: retention of material deposited in the anterior nose (region ET1, which is not subdivided); ET_{seq} long-term retention ($t_{½}$ about 700 d) in airway tissue of a small fraction of particles deposited in the nasal passages; ET'$_2$ short-term retention ($t_{½}$ about 10 minutes) of the material deposited in the posterior nasal passage, larynx and pharynx (ET_2 region) except for the small fraction (taken to be 0.002) retained in ET_{seq}; BB′: retention ($t_{½}$ about 100 minutes) of particles in the BB, with particle transport to ET'$_2$; bb′: retention ($t_{½}$ about 3.5 d) of particles in the bb, with particle transport to BB′; BB_{seq} long-term retention ($t_{½}$ about 700 d) in airway walls of a small fraction of the particles deposited in the bronchial region; bb_{seq}: long-term retention ($t_{½}$ about 700 d) in airway walls of a small fraction of the particles deposited in the bronchiolar region; ALV retention ($t_{½}$ about 250 d) of particles deposited in the alveoli. A fraction (0.67) of the deposit is removed by particle transport to the ciliated airways (bb′), while the remainder penetrates to the interstitium (INT); INT very long-term retention ($t_{½}$ about 60 y) of the particles deposited in the alveoli that penetrate to the interstitium: the particles are removed slowly to the lymph nodes.

*The half-times are approximate because the reference values are specified for the particle transport rates and are rounded in units of d^{-1}. A half-time is not given for the transport rate from AI_3 to LN_{TH}, or from INT to LN_{TH}, because these rates were chosen to direct the required amount of material to the lymph nodes. The clearance half-times of compartment AI_3 in the original HRTM, and compartments ALV and ET_1 in the revised HRTM are determined by the sum of the clearance rates from them.

[†]As noted in the caption to Fig. A.1, it is assumed in the original HRTM that the slow-cleared fraction f_s is particle-size-dependent. For details, see Table 17 and Section E.5.6 in *Publication 66* (ICRP 1994a).

(A8) In the AI region, three AI compartments of the original HRTM have been replaced by the ALV and INT compartments. Particles are cleared from the ALV compartment either to the ciliated airways (bb′) or to the INT compartment. Particles clear very slowly from the INT compartment to the lymph nodes.

(A9) Thus, the following compartments have been defined in the revised HRTM.

- ET_1: retention of material deposited in the anterior nasal passage (region ET_1, which is not subdivided).
- ET_{seq}: long-term retention (half-time of approximately 700 d) in airway tissue of a small fraction of particles deposited in the nasal passages.
- LN_{ET}: lymphatics and lymph nodes that drain the ET regions.

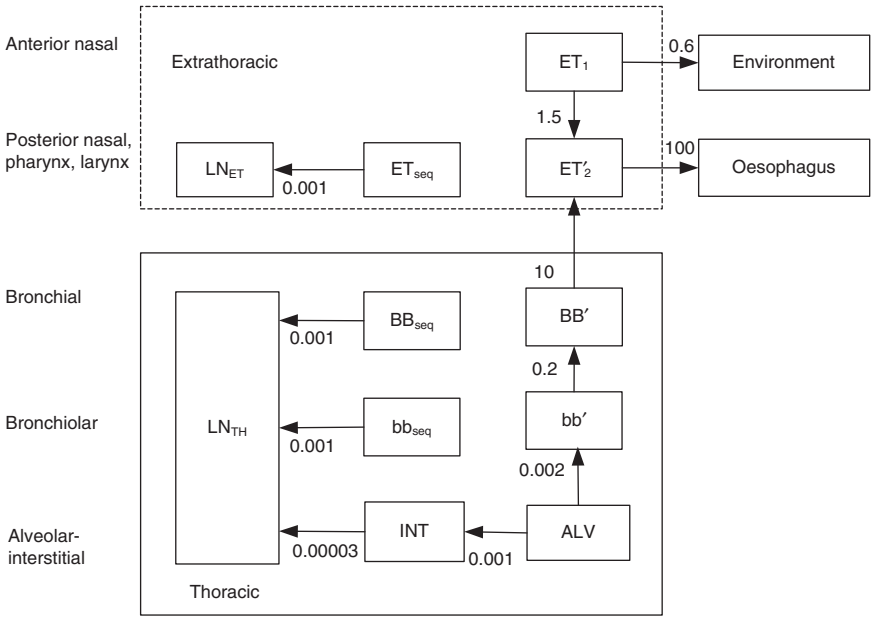

Fig. A.2. Revised compartment model representing time-dependent particle transport from each respiratory tract region. Rates shown alongside arrows are reference values in units of d^{-1}. It is assumed that 0.2% of material deposited in the posterior nasal passage, pharynx, and larynx (ET_2), bronchial (BB), and bronchiolar (bb) regions is retained in the airway wall (ET_{seq}, BB_{seq}, and bb_{seq}, respectively).

ET_1: retention of material deposited in the anterior nose (region ET_1, which is not subdivided); ET_{seq}: long-term retention (t½ about 700 d) in airway tissue of a small fraction of particles deposited in the nasal passages; LN_{ET}: lymphatics and lymph nodes that drain the ET regions; LN_{TH}: lymphatics and lymph nodes that drain the TH regions; ET'_2: short-term retention (t½ about 10 minutes) of the material deposited in the posterior nasal passage, larynx and pharynx (ET_2 region) except for the small fraction (taken to be 0.002) retained in ET_{seq}; BB′: retention (t½ about 100 minutes) of particles in the BB, with particle transport to ET'_2; bb′: retention (t½ about 3.5 d) of particles in the bb, with particle transport to BB′; BB_{seq}: long-term retention (t½ about 700 d) in airway walls of a small fraction of the particles deposited in the bronchial region; bb_{seq}: long-term retention (t½ about 700 d) in airway walls of a small fraction of the particles deposited in the bronchiolar region; ALV: retention (t½ about 250 d) of particles deposited in the alveoli. A fraction (0.67) of the deposit is removed by particle transport to the ciliated airways (bb′), while the remainder penetrates to the interstitium (INT); INT: very long-term retention (t½ about 60 y) of the particles deposited in the alveoli that penetrate to the interstitium: the particles are removed slowly to the lymph nodes.

- LN_{TH}: lymphatics and lymph nodes that drain the TH regions.
- ET'_2: short-term retention (half-time of approximately 10 min) of the material deposited in the posterior nasal passage, pharynx and larynx (ET_2 region) except for the small fraction (taken to be 0.002) retained in ET_{seq}.

- BB′: retention (half-time of approximately 100 min) of particles in the BB, with particle transport to ET'_2.
- bb′: retention (half-time of approximately 3.5 d) of particles in the bb, with particle transport to BB′.
- BB_{seq}: long-term retention (half-time of approximately 700 d) in airway walls of a small fraction of the particles deposited in the BB.
- bb_{seq}: long-term retention (half-time of approximately 700 d) in airway walls of a small fraction of the particles deposited in the bb.
- ALV: retention (half-time of approximately 250 d) of particles deposited in the alveoli. A fraction (0.67) of the deposit is removed by particle transport to the ciliated airways (bb′), while the remainder penetrates to the interstitium (INT).
- INT: very long-term retention (half-time of approximately 60 years) of the particles deposited in the alveoli that penetrate to the interstitium. The particles are removed slowly to the lymph nodes.

A.2.1. Particle transport: extrathoracic airways

(A10) In *Publication 66* (ICRP, 1994a), it was assessed, on the basis of the available information, that deposition in ET_1 is somewhat higher than deposition in ET_2 during inhalation through the nose, and that most of the particles deposited in ET_1 are cleared by nose blowing, but some clear to ET_2 and hence to the alimentary tract in a time scale of hours. There was also a considerable amount of experimental data showing that particles cleared from ET_2 to the throat, and were swallowed in a time scale of the order of 10 min.

(A11) Due to the lack of quantitative information on clearance from ET_1, these judgements were applied in a simplified form in the original HRTM. It was assumed (Fig. A.1) that of material deposited in the ET airways, approximately 50% deposits in ET_1, which is cleared by nose blowing at a rate of 1 d^{-1}, and the rest deposits in ET_2, which clears to the gastrointestinal tract at a rate of 100 d^{-1}.

(A12) In experiments intended to address this deficiency, subjects inhaled 1.5-, 3- or 6-μm aerodynamic diameter (d_{ae}) radiolabelled insoluble particles through the nose while sitting at rest or performing light exercise (Smith et al., 2002, 2011). Retention in the nasal airways and clearance by voluntary nose blowing were followed until at least 95% of the initial ET deposit had cleared (typically approximately 2 d). On average, 19% of the initial ET deposit was cleared by nose blowing (geometric mean time for 50% clearance was 8 h), and the rest was cleared to the alimentary tract: 15% within a few minutes, 21% between a few minutes and 1 h, and 45% in a similar time scale to the fraction cleared by nose blowing. Measurements in this study, and the previous studies on which the original model was based, indicate that most particles that have not cleared within 1 h are retained in the anterior nasal passage.

(A13) On the basis of these data, it is assumed in the revised model that material deposited in ET_1 (now taken to be 65% of the deposit in ET) is cleared at a rate of 2.1 d^{-1} (half-time of approximately 8 h): approximately one-third by nose blowing, and two-thirds by transfer to ET_2 (Smith et al., 2014). This is implemented with particle transport rates of 0.6 d^{-1} from compartment ET_1 to the environment, and 1.5 d^{-1} from compartment ET_1 to compartment ET'_2. Clearance from ET'_2 is unchanged, with a rate to the alimentary tract of 100 d^{-1} (half-time of approximately 10 min).

(A14) As in the original HRTM, the revised model assumes that a small fraction of particles deposited in ET_2 (but not cleared to it from ET_1) is sequestered in the airway wall (ET_{seq}) and transferred to lymph nodes. However, the fraction sequestered is increased from 0.05% of the deposit in ET_2 in the original HRTM to 0.2% in the revised model, partly because of the smaller fractional deposition in ET_2, but also from reconsideration of the experimental data relating to long-term retention of inhaled particles in the nasal passages, which were reviewed in *Publication 66* (ICRP, 1994a; Smith et al., 2014).

(A15) In the original HRTM, it was assumed that particles deposited in the nasal passages during inhalation are partitioned equally between ET_1 and the posterior nasal passage, which is part of ET_2 [however, because of the way the deposition efficiencies were calculated for polydispersed aerosols during inhalation and exhalation, for most aerosol sizes of interest in radiation protection, the deposition fractions given in *Publication 66* (ICRP, 1994a) are somewhat higher for ET_2 than for ET_1]. In the revised HRTM, based on the recent experiments (Smith et al., 2011), it is assumed that for nose breathing, the deposit in the ET airways is distributed 65% to ET_1 and 35% to ET_2. To calculate the fractions of inhaled material deposited in ET_1 and ET_2 in the revised HRTM, the fractions deposited in ET_1 and ET_2 (calculated using the original HRTM) were summed to give the total deposit in the ET airways, and then repartitioned 65% to ET_1 and 35% to ET_2 (for mouth breathing, there is no deposition in ET_1 and the fraction deposited in ET_2 remains as calculated using the original HRTM).

(A16) Table A.2 gives values of fractional deposition in each region of the respiratory tract as a function of aerosol size for (a) an adult male sitting at rest, (b) an adult male undertaking light exercise, and (c) the Reference Worker. Values for the Reference Worker for aerosols with an AMAD of 5 μm are given in Table 3.1.

(A17) For aerosols with an AMAD below approximately 0.3 μm, deposition in the respiratory tract is dominated by thermodynamic mechanisms (i.e. diffusion); as a result, deposition fractions are mainly dependent on the AMTD. Table A.2 therefore tabulates deposition fractions against the AMTD in this size range. For aerosols with an AMAD above approximately 0.3 μm, deposition in the respiratory tract is dominated by impaction and sedimentation, and so deposition fractions are mainly dependent on the AMAD. Therefore, in this size range, Table A.2 tabulates deposition fractions against AMAD.

(A18) The changes from the original HRTM treatment of ET will, in many cases, increase dose coefficients because of the transfer from ET_1 to ET_2 and hence greater

Table A.2. Fractional deposition in regions of the respiratory tract as a function of aerosol size*,† (adult male, normal nose breather).

μm	ET_1	ET_2	BB	bb	AI	Total
(a) Adult male resting (sitting) (breathing rate = 0.54 m^3 h^{-1})						
AMTD						
0.0006	5.953×10^{-1}	3.205×10^{-1}	6.144×10^{-2}	1.568×10^{-2}	3.762×10^{-6}	9.930×10^{-1}
0.001	5.424×10^{-1}	2.921×10^{-1}	9.541×10^{-2}	5.381×10^{-2}	2.054×10^{-4}	9.839×10^{-1}
0.002	4.268×10^{-1}	2.298×10^{-1}	1.194×10^{-1}	1.735×10^{-1}	9.412×10^{-3}	9.590×10^{-1}
0.003	3.390×10^{-1}	1.826×10^{-1}	1.104×10^{-1}	2.591×10^{-1}	4.395×10^{-2}	9.351×10^{-1}
0.005	2.347×10^{-1}	1.264×10^{-1}	8.279×10^{-2}	3.038×10^{-1}	1.509×10^{-1}	8.985×10^{-1}
0.01	1.317×10^{-1}	7.093×10^{-2}	4.638×10^{-2}	2.454×10^{-1}	3.541×10^{-1}	8.485×10^{-1}
0.02	7.707×10^{-2}	4.150×10^{-2}	2.656×10^{-2}	1.678×10^{-1}	4.375×10^{-1}	7.505×10^{-1}
0.03	5.963×10^{-2}	3.210×10^{-2}	2.060×10^{-2}	1.338×10^{-1}	3.953×10^{-1}	6.414×10^{-1}
0.05	4.441×10^{-2}	2.391×10^{-2}	1.554×10^{-2}	9.960×10^{-2}	3.111×10^{-1}	4.946×10^{-1}
0.1	3.411×10^{-2}	1.837×10^{-2}	1.077×10^{-2}	6.594×10^{-2}	2.170×10^{-1}	3.462×10^{-1}
0.2	4.384×10^{-2}	2.361×10^{-2}	7.815×10^{-3}	4.351×10^{-2}	1.632×10^{-1}	2.820×10^{-1}
AMAD						
0.3	4.231×10^{-2}	2.279×10^{-2}	7.949×10^{-3}	4.469×10^{-2}	1.656×10^{-1}	2.833×10^{-1}
0.5	7.109×10^{-2}	3.828×10^{-2}	7.070×10^{-3}	3.354×10^{-2}	1.478×10^{-1}	2.978×10^{-1}
0.7	1.036×10^{-1}	5.580×10^{-2}	7.445×10^{-3}	2.968×10^{-2}	1.470×10^{-1}	3.435×10^{-1}
1	1.502×10^{-1}	8.088×10^{-2}	8.673×10^{-3}	2.800×10^{-2}	1.509×10^{-1}	4.187×10^{-1}
2	2.657×10^{-1}	1.431×10^{-1}	1.270×10^{-2}	2.803×10^{-2}	1.511×10^{-1}	6.006×10^{-1}
3	3.343×10^{-1}	1.801×10^{-1}	1.497×10^{-2}	2.734×10^{-2}	1.369×10^{-1}	6.936×10^{-1}
5	4.011×10^{-1}	2.159×10^{-1}	1.626×10^{-2}	2.373×10^{-2}	1.040×10^{-1}	7.610×10^{-1}
7	4.257×10^{-1}	2.293×10^{-1}	1.574×10^{-2}	1.977×10^{-2}	7.815×10^{-2}	7.686×10^{-1}
10	4.336×10^{-1}	2.335×10^{-1}	1.402×10^{-2}	1.493×10^{-2}	5.244×10^{-2}	7.485×10^{-1}
15	4.235×10^{-1}	2.281×10^{-1}	1.109×10^{-2}	9.647×10^{-3}	2.939×10^{-2}	7.017×10^{-1}
20	4.087×10^{-1}	2.200×10^{-1}	8.780×10^{-3}	6.540×10^{-3}	1.793×10^{-2}	6.620×10^{-1}
(b) Adult male at light exercise (breathing rate = 1.5 m^3 h^{-1})						
AMTD						
0.0006	5.788×10^{-1}	3.116×10^{-1}	5.918×10^{-2}	4.311×10^{-2}	3.406×10^{-4}	9.930×10^{-1}
0.001	5.192×10^{-1}	2.796×10^{-1}	7.855×10^{-2}	1.037×10^{-1}	4.225×10^{-3}	9.852×10^{-1}
0.002	3.979×10^{-1}	2.142×10^{-1}	8.325×10^{-2}	2.217×10^{-1}	4.829×10^{-2}	9.654×10^{-1}
0.003	3.110×10^{-1}	1.674×10^{-1}	7.156×10^{-2}	2.670×10^{-1}	1.302×10^{-1}	9.472×10^{-1}
0.005	2.118×10^{-1}	1.140×10^{-1}	5.045×10^{-2}	2.560×10^{-1}	2.897×10^{-1}	9.220×10^{-1}
0.01	1.187×10^{-1}	6.393×10^{-2}	2.745×10^{-2}	1.799×10^{-1}	4.909×10^{-1}	8.808×10^{-1}
0.02	7.224×10^{-2}	3.890×10^{-2}	1.616×10^{-2}	1.194×10^{-1}	4.950×10^{-1}	7.417×10^{-1}

(continued on next page)

Table A.2. *(continued)*

μm	ET_1	ET_2	BB	bb	AI	Total
0.03	5.638×10^{-2}	3.036×10^{-2}	1.258×10^{-2}	9.370×10^{-2}	4.167×10^{-1}	6.097×10^{-1}
0.05	4.268×10^{-2}	2.299×10^{-2}	9.405×10^{-3}	6.829×10^{-2}	3.109×10^{-1}	4.543×10^{-1}
0.1	4.302×10^{-2}	2.317×10^{-2}	6.758×10^{-3}	4.399×10^{-2}	2.057×10^{-1}	3.226×10^{-1}
0.2	8.048×10^{-2}	4.334×10^{-2}	6.445×10^{-3}	2.777×10^{-2}	1.427×10^{-1}	3.007×10^{-1}
AMAD						
0.3	7.657×10^{-2}	4.123×10^{-2}	6.378×10^{-3}	2.864×10^{-2}	1.458×10^{-1}	2.986×10^{-1}
0.5	1.374×10^{-1}	7.399×10^{-2}	8.097×10^{-3}	2.016×10^{-2}	1.172×10^{-1}	3.568×10^{-1}
0.7	1.926×10^{-1}	1.037×10^{-1}	1.022×10^{-2}	1.677×10^{-2}	1.068×10^{-1}	4.301×10^{-1}
1	2.601×10^{-1}	1.401×10^{-1}	1.304×10^{-2}	1.465×10^{-2}	9.938×10^{-2}	5.272×10^{-1}
2	3.927×10^{-1}	2.114×10^{-1}	1.809×10^{-2}	1.263×10^{-2}	8.253×10^{-2}	7.174×10^{-1}
3	4.523×10^{-1}	2.435×10^{-1}	1.930×10^{-2}	1.138×10^{-2}	6.733×10^{-2}	7.938×10^{-1}
5	4.923×10^{-1}	2.650×10^{-1}	1.801×10^{-2}	8.949×10^{-3}	4.488×10^{-2}	8.292×10^{-1}
7	4.955×10^{-1}	2.668×10^{-1}	1.565×10^{-2}	6.961×10^{-3}	3.098×10^{-2}	8.159×10^{-1}
10	4.819×10^{-1}	2.595×10^{-1}	1.241×10^{-2}	4.858×10^{-3}	1.897×10^{-2}	7.777×10^{-1}
15	4.523×10^{-1}	2.436×10^{-1}	8.593×10^{-3}	2.846×10^{-3}	9.571×10^{-3}	7.169×10^{-1}
20	4.273×10^{-1}	2.301×10^{-1}	6.185×10^{-3}	1.789×10^{-3}	5.411×10^{-3}	6.707×10^{-1}
(c) Reference Worker[‡] (breathing rate = 1.2 m^3 h^{-1})						
AMTD						
0.0006	5.811×10^{-1}	3.129×10^{-1}	5.950×10^{-2}	3.925×10^{-2}	2.932×10^{-4}	9.931×10^{-1}
0.001	5.225×10^{-1}	2.814×10^{-1}	8.092×10^{-2}	9.672×10^{-2}	3.660×10^{-3}	9.852×10^{-1}
0.002	4.019×10^{-1}	2.164×10^{-1}	8.834×10^{-2}	2.149×10^{-1}	4.282×10^{-2}	9.644×10^{-1}
0.003	3.149×10^{-1}	1.695×10^{-1}	7.702×10^{-2}	2.659×10^{-1}	1.181×10^{-1}	9.455×10^{-1}
0.005	2.150×10^{-1}	1.157×10^{-1}	5.500×10^{-2}	2.627×10^{-1}	2.702×10^{-1}	9.187×10^{-1}
0.01	1.206×10^{-1}	6.492×10^{-2}	3.011×10^{-2}	1.891×10^{-1}	4.717×10^{-1}	8.764×10^{-1}
0.02	7.292×10^{-2}	3.927×10^{-2}	1.763×10^{-2}	1.263×10^{-1}	4.869×10^{-1}	7.430×10^{-1}
0.03	5.684×10^{-2}	3.060×10^{-2}	1.371×10^{-2}	9.934×10^{-2}	4.137×10^{-1}	6.142×10^{-1}
0.05	4.292×10^{-2}	2.312×10^{-2}	1.027×10^{-2}	7.269×10^{-2}	3.109×10^{-1}	4.599×10^{-1}
0.1	4.177×10^{-2}	2.249×10^{-2}	7.323×10^{-3}	4.707×10^{-2}	2.073×10^{-1}	3.260×10^{-1}
0.2	7.532×10^{-2}	4.056×10^{-2}	6.638×10^{-3}	2.998×10^{-2}	1.456×10^{-1}	2.981×10^{-1}
AMAD						
0.3	7.176×10^{-2}	3.864×10^{-2}	6.599×10^{-3}	3.089×10^{-2}	1.486×10^{-1}	2.965×10^{-1}
0.5	1.281×10^{-1}	6.897×10^{-2}	7.953×10^{-3}	2.203×10^{-2}	1.215×10^{-1}	3.486×10^{-1}
0.7	1.801×10^{-1}	9.695×10^{-2}	9.833×10^{-3}	1.859×10^{-2}	1.125×10^{-1}	4.180×10^{-1}
1	2.447×10^{-1}	1.318×10^{-1}	1.242×10^{-2}	1.652×10^{-2}	1.066×10^{-1}	5.120×10^{-1}
2	3.749×10^{-1}	2.018×10^{-1}	1.732×10^{-2}	1.479×10^{-2}	9.218×10^{-2}	7.010×10^{-1}

(continued on next page)

Table A.2. *(continued)*

μm	ET_1	ET_2	BB	bb	AI	Total
3	4.357×10^{-1}	2.346×10^{-1}	1.869×10^{-2}	1.363×10^{-2}	7.712×10^{-2}	7.797×10^{-1}
5	4.795×10^{-1}	2.582×10^{-1}	1.777×10^{-2}	1.103×10^{-2}	5.319×10^{-2}	8.197×10^{-1}
7	4.857×10^{-1}	2.615×10^{-1}	1.567×10^{-2}	8.763×10^{-3}	3.761×10^{-2}	8.093×10^{-1}
10	4.751×10^{-1}	2.558×10^{-1}	1.265×10^{-2}	6.275×10^{-3}	2.368×10^{-2}	7.735×10^{-1}
15	4.482×10^{-1}	2.414×10^{-1}	8.944×10^{-3}	3.803×10^{-3}	1.236×10^{-2}	7.147×10^{-1}
20	4.247×10^{-1}	2.287×10^{-1}	6.550×10^{-3}	2.457×10^{-3}	7.171×10^{-3}	6.695×10^{-1}

ET_1, anterior nasal passage; ET_2, posterior nasal passage, pharynx, and larynx; BB, bronchial; bb, bronchiolar; AI, alveolar–interstitial; AMTD, activity median thermodynamic diameter; AMAD, activity median aerodynamic diameter.

*Reference values are given to a greater degree of precision than would be chosen to reflect the certainty with which the average value of each parameter is known.

†The particles are assumed to have density of 3.00 g cm^{-3} and shape factor of 1.5 [typical of compact, irregular (i.e. non-spherical) particles]. The particle diameters are assumed to be log-normally distributed with geometric standard deviation σ_g increasing from a value of 1.0 at 0.6 nm to a value of 2.5 above approximately 1 μm [*Publication 66* (ICRP, 1994a, Para. 170)]. The value of σ_g is not a reference value, but is derived from the corresponding AMTD (ICRP, 1994a).

‡Light work is defined on the following basis: 2.5 h sitting, at which the amount inhaled is 0.54 m^3 h^{-1}; and 5.5 h light exercise, at which the amount inhaled is 1.5 m^3 h^{-1}. For both levels of activity, all the inhaled air enters through the nose. The deposition fractions are therefore volume-weighted average values for the two levels of activity given for normal nose-breathing adult males sitting and at light exercise in Table A.2(a,b). As described in the text, the fractions deposited in ET_1 and ET_2 were summed to give the total deposit in the extrathoracic airways, and partitioned 65% to ET_1 and 35% to ET_2.

systemic uptake in ET_2 and the alimentary tract. The changes will also affect interpretation of measurements of radionuclides in faecal samples; a larger fraction of the material deposited in the nose (which is typically approximately 50% of the material inhaled) is cleared through the alimentary tract.

A.2.2. Particle transport: bronchial and bronchiolar airways

Slow clearance

(A19) The original HRTM includes a slow phase of clearance of particles deposited in the BB and bb regions (compartments BB_2 and bb_2 in Fig. A.1), with a half-time of 23 d. It was based mainly on the results of experiments in which volunteers inhaled a 'shallow bolus' of radiolabelled particles (i.e. a small volume of aerosol at the end of each breath, designed to deposit particles in the major airways). A 'slow-cleared' fraction was observed, which was considered to show better correlation with particle geometric diameter d_p than with d_{ae} (ICRP, 1994a). The original HRTM assumes that the slow-cleared fraction of particles deposited in BB and in bb (f_s) is 0.5 for $d_p \leq 2.5$ μm, and decreases exponentially for larger particles.

(A20) In the revised HRTM, a different approach has been taken to slow clearance from the bronchial tree based on more recent human volunteer experiments. In particular, in a series of studies, large particles (6-μm d_{ae}) were inhaled extremely slowly, which theoretically should result in most deposition occurring in the bronchioles (e.g. Anderson et al., 1995; Camner et al., 1997; Falk et al., 1997, 1999; Philipson et al., 2000; Svartengren et al., 2001). Retention at 24 h was much greater than the predicted AI deposition, supporting the concept of slow clearance in the bronchial tree.

(A21) Falk et al. (1997, 1999) compared lung retention of 6-μm d_{ae} Teflon particles inhaled slowly (approximately 45 cm^3 s^{-1}) with retention of similar particles inhaled at a normal flow rate (approximately 450 cm^3 s^{-1}) for up to 6 months. Approximately 50% of the initial lung deposit (ILD) cleared in the first 24 h following both modes of inhalation. Retention after 24 h was well described by a two-component exponential function, the clearance rates having half-times of approximately 3.7 d ('intermediate' phase) and 200 d (attributed to clearance from the AI region). The fractions associated with the intermediate phase were approximately 18% ILD after slow inhalation and 6% ILD after normal inhalation. Deposition in the BB, bb, and AI regions calculated using three different models showed good agreement with, on average, 17%, 63%, and 18% ILD after slow inhalation, and 30%, 26%, and 43% after normal inhalation, respectively. Thus, there was strong correlation between predicted bronchiolar deposition and the amount cleared in the intermediate phase, suggesting that the intermediate phase was associated with approximately 25% of particles deposited in the bronchioles.

(A22) Svartengren et al. (2001) found very similar retention in each subject when 6-μm d_{ae} particles were inhaled as a shallow bolus and by slow inhalation on separate occasions. One interpretation was that slow clearance is a characteristic of the bronchioles, and the pattern of deposition was very similar, despite the fact that the techniques were different, a view supported by complementary deposition modelling. However, the possibility could not be excluded that the deposition patterns were different, with more bronchial deposition following bolus inhalation than following slow inhalation, and as assumed in the HRTM, slow clearance occurring to a similar extent in both large and small airways.

(A23) Philipson et al. (2000) investigated the effect of d_p directly by administering particles with the same d_{ae}, and hence the same lung deposition pattern, but different densities and so different values of d_p ($d_{ae} \approx d_p\sqrt{\rho}$ where ρ is the particle density). Volunteers inhaled 6-μm d_{ae} particles of polystyrene (PSL, density 1.05 g cm^{-3}) and Teflon (density 2.13 g cm^{-3}). The geometric diameter d_p of the Teflon was smaller (4.5 μm) than that of the PSL (6.1 μm), and the HRTM predicts f_s to be greater (14% vs 5%). However, retention of the two particles was similar in each subject.

(A24) Smith et al. (2007, 2008) tested these alternative hypotheses more critically, also administering two particles of the same d_{ae}, but with a greater difference in densities and as shallow boluses to minimise alveolar deposition. In one study, volunteers inhaled 5-μm d_{ae} PSL and gold ($\rho = 19.3$ g cm^{-3}) particles; corresponding d_p values were 5 and 1.2 μm, and values of f_s were approximately 10% and 50%,

respectively. Hence, according to the HRTM, lung retention of the gold should have been much greater than that of the PSL. However, no significant difference was observed between them in any subject. In another study, 8-μm d_{ae} PSL and gold particles were used, and broadly similar results were obtained.

(A25) These results are thus inconsistent with the dependence of f_s on d_p assumed in the HRTM. However, the apparent discrepancy with the results of the bolus experiments on which the *Publication 66* (ICRP, 1994a) assumptions were based has not been resolved. A possible explanation may be that the inferred dependence on d_p was fortuitous. It was based mainly on measurements made with relatively large particles (d_p or d_{ae} >4 μm), and relatively few measurements were available at the time.

(A26) Another recent study showed inconsistencies with the original HRTM's assumptions on slow particle clearance from the bronchial tree. Gregoratto et al. (2010), in analysing alveolar retention in the study by Philipson et al. (1996) (see below), observed that there was far less lung clearance between 7 and 50 d after inhalation than predicted by the HRTM as a result of slow clearance from the BB and bb regions, even assuming no clearance from the AI region over that period.

(A27) Most of the relevant recent human studies thus suggest that slow clearance in the conducting airways is associated with particles deposited in the bronchioles; a simpler explanation than the particle-size-dependent clearance mechanism assumed in *Publication 66* (ICRP, 1994a). In the revised HRTM, it is assumed that slow clearance in the conducting airways only occurs in the bb region, and following Falk et al. (1997, 1999), as described above, particles are taken to be cleared from the bb region to the BB region at a rate of 0.2 d^{-1} (half-time of approximately 3.5 d) (except for the small sequestered fraction, see below). The rate of rapid clearance from the BB region to the ET region is unchanged at 10 d^{-1}.

(A28) The results of Falk et al. (1997, 1999) suggest that only a fraction of particles deposited in the bb region is cleared slowly, perhaps 25% for the conditions of their experiments. If so, it is reasonable to suppose that it occurs mainly in the smaller bronchioles, as proposed by Camner et al. (1997). However, given the remaining uncertainties (and the lack of deposition fractions available for subdivisions of the bb region), it is assumed here for simplicity that it applies to all particles deposited in the bb region. It is also assumed that it applies to all particles cleared from the AI region to the bb region, unlike the original HRTM which assumed that slow clearance only applied to particles deposited directly in the BB and bb regions. These changes result in a simplification of the model: a single compartment BB′ replaces BB_1 and BB_2, and a single compartment bb′ replaces bb_1 and bb_2 (Fig. A.2). Associated changes to the dosimetric model are described in Section 3.2.4.

Sequestration in the airway walls

(A29) The original HRTM assumed that the fraction of particles deposited in the BB and bb regions and retained in the airway wall (BB_{seq} and bb_{seq}) is 0.7% for all

sizes, and that this material clears to lymph nodes at a rate of 0.01 d^{-1}. When the original HRTM was finalised, the phenomenon had only been well quantified by Patrick and colleagues (e.g. Takahashi and Patrick, 1987), who followed retention of activity after deposition of radiolabelled particles on to the distal trachea of rats. Subsequently, Takahashi et al. (1993) conducted similar experiments, instilling ^{133}Ba-labelled $BaSO_4$ on to the distal trachea of rabbits, dogs, and monkeys. The amounts retained 1 week after injection were 0.145%, 0.044%, and 0.043% of the injected amount, respectively. These values are far lower than found in rats, suggesting interspecies differences. The value chosen above for retention of particles in the wall of the nasal epithelium, ET_{seq}, of 0.2%, which was based on results for several different materials in several species, is within the range observed for the trachea. On that basis, it is assumed here that values for both the fractions retained in BB_{seq} and bb_{seq}, and clearance rates from them to regional lymph nodes are the same as those for ET_{seq} (i.e. 0.2% and 0.001 d^{-1}). As a result, the revised model assumes less transfer to LN_{TH} from BB and bb. To maintain consistency with the ratio of lung to LN_{TH} contents observed in autopsy studies, it assumes correspondingly more transfer from the AI region to LN_{TH} (see below).

(A30) The changes from the treatment of slow clearance from the bronchial tree in the original HRTM will, in many cases, decrease dose coefficients. The decreases will be considerable for Type M alpha-emitting radionuclides with half-lives of weeks or more, for which slow clearance gave the largest component of the effective dose coefficient (Bailey et al., 1995). Changes to parameter values relating to sequestration have little impact on effective dose coefficients because it only ever makes a small contribution to them.

A.2.3. Particle transport: AI region

(A31) In the original HRTM, the AI region was represented by three compartments: AI_1, AI_2, and AI_3, which mainly clear to the gastrointestinal tract via the bronchial tree at rates of 0.02, 0.001, and 0.0001 d^{-1}, respectively (approximate half-times of 35, 700, and 7000 d) (Fig. A.1). Human lung clearance had been quantified in experimental studies up to approximately 1 year after inhalation (ICRP, 1994a). It was considered that lung retention of insoluble particles over this time typically follows a two-component exponential function: approximately 30% with a half-time of approximately 30 d, and the rest with a half-time of several hundred d, giving approximately 50% retention of the initial alveolar deposit at 300 d. This information was used to define the parameter values for AI_1.

(A32) Measurements of activity in the chest after occupational exposure, and of activity in the lungs at autopsy, indicate that some material can be retained in the lungs for decades. Information on TH retention in humans following accidental inhalation, based on in-vivo measurements of radionuclides, was reviewed in *Publication 66* (ICRP, 1994a). As retention up to 300 d after intake had been characterised in controlled experiments, only studies of accidental intakes in which

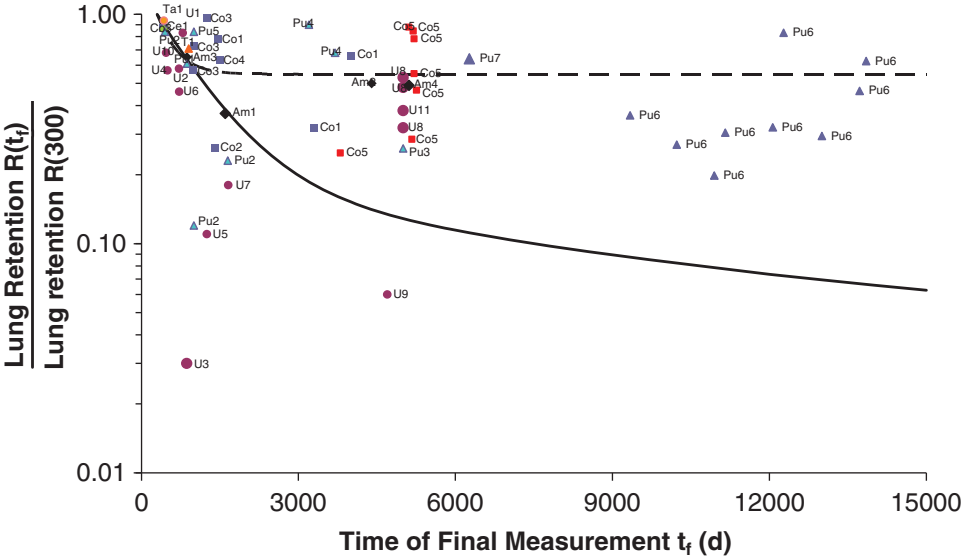

Fig. A.3. Long-term retention in the thoracic airways following accidental inhalation. References for data included in the figure are listed in Table A.3. Separate symbols are used for each element. The solid and dashed curves show retention of insoluble particles as predicted by the original Human Respiratory Tract Model (HRTM) and the revised HRTM, respectively. Thoracic retention $R(t_f)$ at t_f, the time of the final measurement, is expressed as a fraction of $R(300)$, retention at 300 d.

retention was followed for at least 400 d were included. As the aim was to obtain guidance on the likely fate of the approximately 50% of the initial alveolar deposit that remains at 300 d after intake, TH retention $R(t_f)$ at t_f, the time of the final measurement, was expressed as a fraction of $R(300)$, retention at 300 d. This also facilitated the inclusion of information in cases where the first measurement was made some time after intake, and avoided the effects of differences in early clearance due to factors such as aerosol size, breathing patterns, and soluble components. In Fig. E.10 of *Publication 66* (ICRP, 1994a), TH retention $R(t_f)$, as a fraction of $R(300)$, was plotted against t_f. The information is shown here in Fig. A.3. Evidence for very long-term retention of a significant fraction (>10%) of the material remaining in the thorax at 300 d was seen for each of the elements (cobalt, uranium, plutonium, and americium) for which measurements extended to 10 years after acute intake of the oxide.

(A33) The results were not used to set parameter values for AI_2 and AI_3 quantitatively because it was considered possible that the published in-vivo studies were not typical, but represented unusually slow lung clearance. It was noted (ICRP, 1994a) that: 'The fraction of the AI deposit that goes to AI_3 (a_3) is not easily quantified. As only 50% of the initial alveolar deposit is retained at 300 d, a_3 is less than 0.5. As there is measurable TH retention at 5000 d after intake in some subjects (Fig. A.3), a_3

is likely to be at least a few percent of the initial alveolar deposit. As a rounded value it is assumed that $a_3 = 0.1$, and, hence, by difference, that $a_2 = 0.6$'. Fig. A.3 also shows retention of insoluble particles as predicted by the original HRTM; it fits quite well to results where the final measurement was made less than 2000 d after intake, but underestimates those with later measurements.

(A34) In the revised model, account has been taken of additional human studies published since the original HRTM was adopted, which all show greater long-term retention in the AI region than was assumed.

(A35) A recent study by Davis et al. (2007) provides better in-vivo information on long-term lung retention than any available when *Publication 66* (ICRP, 1994a) was adopted. A group of workers had a simultaneous brief inhalation exposure to particles containing cobalt-60, and most (seven) had been followed for approximately 15 years. It is reasonable to assume that they are representative of nuclear industry workers. They all showed much slower clearance than the HRTM predicts, consistent with the few data on retention beyond 2000 d available at the time when the HRTM was published (Fig. A.3).

(A36) A review of long-term lung retention data has therefore been conducted (Gregoratto et al., 2010). Three other major relevant studies were identified that have been published since the HRTM was finalised. Their results, together with those on which the HRTM was based, were used to develop a new compartment model of particle transport from the AI region.

(A37) Philipson et al. (1996) followed lung retention in 10 volunteers for approximately 3 years after inhalation of ^{195}Au-labelled Teflon particles. The duration of this study was approximately three times longer than for the experiments available when the HRTM was developed, and it seems likely that there was less leakage of the radioactive label from the test particles. Lung retention has been followed for over 30 years in workers who inhaled plutonium oxide during a fire at the Rocky Flats Plant in October 1965 (Mann and Kirchner, 1967; ORAUT, 2007); another group who should be representative of nuclear industry workers (Gregoratto et al., 2010). Kuempel et al. (2001) developed a model of particle retention in the AI region that is both physiologically more realistic and simpler than that in the original HRTM. Instead of the three AI compartments in the HRTM, it has an ALV compartment that clears both to the bronchial tree and the INT compartment, which clears to lymph nodes. This model was applied to a group of US coal miners with exposure histories from which particle mass deposition rates could be assessed, and autopsy measurements of dust concentration in lung (and also for lymph nodes in approximately 50% of cases). The model was considered to be the simplest consistent with the data, and no evidence was found for impaired clearance at high lung loadings over the range observed. The optimised parameter values derived by Kuempel et al. (2001) were a rate $m_T = 0.001$ d^{-1} for clearance from the ALV to the bb, a rate $m_I = 0.00047$ d^{-1} for clearance from the ALV to the INT, and a rate $m_{LN} = 10^{-5}$ d^{-1} for clearance from the INT to lymph nodes. The main difference from the original HRTM AI model is that a significant fraction of the AI deposit is sequestered in the

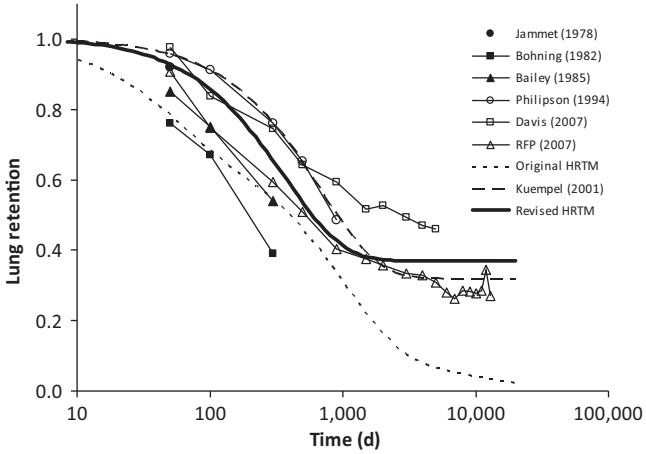

Fig. A.4. Measured lung retention data [Philipson et al., 1996; Davis et al., 2007; Rocky Flats Plant (RFP) (ORAUT, 2007)] and studies reported in Annex E of *Publication 66* (ICRP, 1994a) are shown together with the model predictions by assuming initial deposition in the alveolar–interstitial (AI) region alone. Predictions of both the original Human Respiratory Tract Model (HRTM) and the Kuempel et al. (2001) model with default parameter values are shown. The 'revised HRTM' curve was obtained with optimised AI particle transport parameters $AI_{seq} = 0.37$ and $m = 0.0027$ d^{-1} (from Gregoratto et al., 2010; reproduced with the permission of the publishers, © IOP Publishing. All rights reserved.)

INT [$m_I/(m_I + m_T) = 0.32$]. Kuempel et al. (2001) noted that the HRTM underestimated lung retention in the miners by approximately a factor of four.

(A38) Gregoratto et al. (2010) showed that the Kuempel et al. (2001) model provides an adequate representation of AI retention for the data in the other three studies outlined above. They developed a new model using the Kuempel et al. model structure but fitted to both the experimental datasets on which the HRTM parameter values were based, and the more recent long-term studies (Fig. A.4). They obtained particle transport rates from the ALV of $m_T = 0.0017$ d^{-1} and $m_I = 0.0010$ d^{-1}. These values are adopted here, but the value of m_T is rounded to 0.002 d^{-1}, reflecting the underlying uncertainty in the model (Fig. A.2). These rates give a clearance half-time from the ALV of approximately 250 d ($m_I + m_T = 0.003$ d^{-1}), and approximately 33% of the ALV deposit of insoluble particles is sequestered in the INT. The greater AI retention than in the original HRTM is likely to result in lung doses per intake that are 50–100% higher for Type S long-lived alpha emitters, but will have little, if any, effect on more soluble forms.

(A39) No clear difference was observed by Gregoratto et al. (2010) between smokers and non-smokers in the long-term studies they analysed. This contrasts with the greater retention in smokers than in non-smokers observed in those studies reviewed in *Publication 66* (ICRP, 1994a) in which the comparison could be made, although it is noted that the earlier studies were of relatively short duration. It also contrasts

with the much greater retention in smokers than in non-smokers observed in studies of alveolar retention of iron oxide followed using magnetopneumography [see the iron inhalation section in OIR: Part 2 (ICRP, 2016a)], but for which absorption into blood rather than particle transport is considered to be the dominant clearance mechanism. The modifying functions proposed in Table 19 of *Publication 66* (ICRP, 1994a) relating to the effect of cigarette smoking on particle transport from the AI region are therefore not considered applicable to the revised model. Furthermore, it is not recommended that the other modifying factors in that table are applied in individual dose assessments.

(A40) In the original HRTM, the transport rate from the AI region to LN_{TH} was set at 2×10^{-5} d^{-1} to give the ratio of material concentration in lymph nodes and lungs equal to that estimated from autopsy data; for non-smokers, [LN]/[L] $\approx$ 20 after 10,000 d after inhalation of Pu (Kathren et al., 1993). Due to the smaller fraction of the deposit in the BB and bb regions cleared to LN_{TH} via the airway walls (BB_{seq} and bb_{seq}), and the longer AI retention in the model adopted here than in the *Publication 66* (ICRP, 1994a) model, the amount cleared to LN_{TH} from the BB and bb regions is now negligible compared with that from the AI region. The ratio [LN]/[L] $\approx$ 20 is obtained with a transport rate from the INT to LN_{TH} of 3×10^{-5} d^{-1} (Gregoratto et al., 2010).

A.3. Clearance: absorption into blood

(A40) As summarised in Section 3.2.3, absorption into blood depends on the physical and chemical form of the deposited material. In both the original and revised HRTM, it is assumed (by default) to occur at the same rate in all regions (including the lymph nodes), except ET_1 for which it is assumed that no absorption takes place. It is recognised that absorption is likely to be faster in the AI region where the air–blood barrier is thinner than in the conducting airways (ET, BB, and bb regions), but there is insufficient information available to provide a general systematic basis for taking this into account, such as a scaling factor for different rates in different regions.

(A41) In the HRTM, absorption is treated as a two-stage process: dissociation of the particles into material that can be absorbed into blood (dissolution); and absorption into blood of soluble material and of material dissociated from particles (uptake). The clearance rates associated with both stages can be time-dependent.

Dissolution

(A42) Both the original and revised HRTM use the same simple compartment model to represent time-dependent dissolution. It is assumed that a fraction f_r dissolves relatively rapidly at a rate s_r, and the remaining fraction $(1 - f_r)$ dissolves more slowly at a rate s_s [Fig. A.5(a)]. A limitation of this system is that it can only represent an overall dissolution rate that decreases with time. To overcome this, *Publication 66* (ICRP, 1994a) also describes a more flexible system, shown in

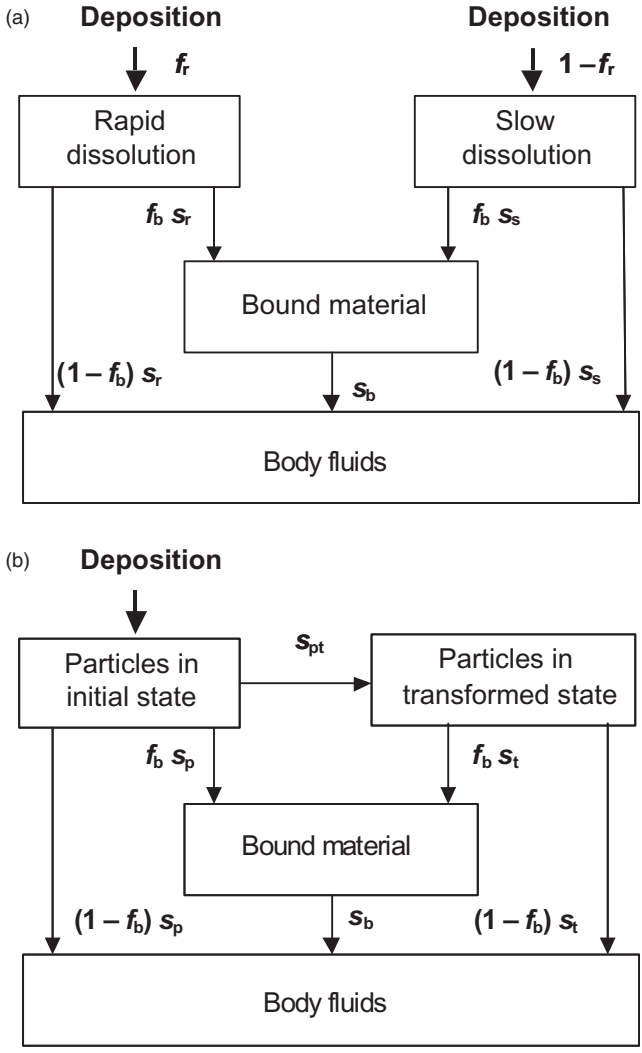

Fig. A.5. Alternative compartment models representing time-dependent absorption into blood (dissolution and uptake). In the model shown in Fig. A.5(a), a fraction f_r of the deposit is initially assigned to the compartment labelled 'Rapid dissolution', and the rest of the deposit $(1 - f_r)$ is initially assigned to the compartment labelled 'Slow dissolution'. In the model shown in Fig. A.5(b), all the deposit is initially assigned to the compartment labelled 'Particles in initial state', and material in the compartment labelled 'Particles in transformed state' is subject to particle transport at the same rate as material in the compartment labelled 'Particles in initial state'. Material in the compartment labelled 'Bound material' is not subject to particle transport and is cleared only by uptake into blood.

fr: fraction of the deposit that dissolves rapidly, at a rate sr; (1-fr): fraction of deposit that dissolves more slowly, at a rate ss; fb: fraction of the dissolved material that is retained in the bound stqte and from which it goes to blood at a rate sb; sr: rate of rapid dissolution; ss: rate of slow dissolution; sb: transfer rate from the bound state to the blood; spt:transfer rate of material from the compartment ''particles in inital state'' to the compartment ''particles in transformed state''; sp: dissolution rate of material from compartment ''particles in inital state''; st: dissolution rate of material from the compartment ''particles in transformed state''.

Table A.3. Sources of data on retention in the thoracic airways used in Fig. A.3.

Cobalt	**Uranium**	**Plutonium**
Co1 Newton and Rundo (1971)	U1 Ronen (1969)	Pu1 Newton et al. (1983)
Co2 Gupton and Brown (1972)	U2 Saxby et al. (1964)	Pu2 Ramsden (1976)
Co3 Raghavendran et al. (1978)	U3 Rundo (1965)	Pu3 Ramsden et al. (1978); Ramsden (1984)
Co4 Ramsden (1984)	U4 Schultz (1966)	Pu4 Bihl et al. (1988a,b,c)
Co5 Davis et al. (2007)	U5 Scott and West (1967)	Pu5 Foster (1991)
	U6 West and Scott (1966)	Pu6 ORAUT (2007)
	U7 West and Scott (1969)	Pu7 Carbaugh and La Bone (2003)
Cerium		
Ce1 Tyler and Lister (1973)	U8 West et al. (1979)	
	U9 Crawford-Brown and Wilson (1984)	**Americium**
Tantalum	U10 Kvasnicka (1987)	Am1 Fry (1976)
Ta1 Newton (1977) ^{195}Au-labelled teflon	U11 Price (1989)	Am2 Toohey and Essling (1980)
T1 Philipson et al. (1996)		Am3 Newton et al. (1983)
		Am4 Wernli and Eikenberg (2007)

Fig. A.5(b). In this system, the material deposited in the respiratory tract is assigned to the compartment labelled 'Particles in initial state' in which it dissolves at a constant rate s_p. Material is transferred simultaneously (at a constant rate s_{pt}) to a corresponding compartment labelled 'Particles in transformed state' in which it has a different dissolution rate s_t. With this system, the initial dissolution rate is approximately s_p, and the final dissolution rate is approximately s_t. Thus, with a suitable choice of parameters, including $s_t > s_p$, an increasing dissolution rate can be represented. The ratio of s_p to s_{pt} approximates to the fraction that dissolves rapidly. It may be noted that any time-dependent dissolution behaviour that can be represented using the model shown in Fig. A.5(a) can also be represented by the model shown in Fig. A.5(b) with a suitable choice of parameter values. However, the reverse is not true, as noted above.

(A43) If the dissolution rate decreases with time, as is usually the case, either system could be used and would give the same results, with the following values:

$$s_p = s_s + f_r(s_r - s_s)$$
$$s_{pt} = (1 - f_r)(s_r - s_s)$$
$$s_t = s_s$$

(A44) The system shown in Fig. A.5(b) was applied by default in earlier publications (ICRP, 1994b, 1995a, 1997a). The additional flexibility it provides is, however, rarely required in practice, and it is more complex (and less intuitive) to present. The simpler approach is therefore adopted now as the default, with the more flexible approach retained as an alternative. Examples of materials that show dissolution rates that increase with time, which have been represented by 'particles in initial state' and 'particles in transformed state', including uranium aluminide, are given in the element sections in subsequent reports of this series.

Uptake

(A45) Uptake of dissolved material into blood is usually assumed to be instantaneous. For some elements, however, part of the dissolved material is absorbed rapidly into blood, but a significant fraction is absorbed more slowly because of binding to respiratory tract components. To represent time-dependent uptake, it is assumed that a fraction (f_b) of the dissolved material is retained in the 'bound' state, from which it goes into blood at a rate s_b, while the remaining fraction ($1 - f_b$) goes into blood instantaneously (Fig. A.5). In the model, material in the 'bound' state is not cleared by particle transport processes, but only by uptake into blood. Thus, only one 'bound' compartment is required for each region, except for ET_1, from which no absorption takes place.

(A46) The system shown in Fig. A.5 applies to each of the compartments in the particle transport model shown in Fig. A.2 except ET_1. It is assumed that no absorption takes place from ET_1, but if the model in Fig. A.5(a) is used, the ET_1 deposit still has to be partitioned between fast and slow compartments because material is cleared from ET_1 to ET_2, from which absorption does take place.

(A47) For all elements, default values of parameters are recommended, according to whether the absorption is considered to be fast (Type F), moderate (Type M), or slow (Type S). The original reference values, given in *Publication 66* (ICRP, 1994a) and reproduced in Table A.4, were specified in terms of the parameter's initial dissolution rate s_p, transformation rate s_{pt}, and final dissolution rate s_t [Fig. A.5(b)], rather than f_r, s_r, and s_s [Fig. A.5(a)], for which approximate values were given. For gases or vapours, instantaneous uptake into blood has also been recommended, as in *Publication 68* (ICRP, 1994b), and defined as Type V (very fast) in *Publication 71* (ICRP, 1995b).

(A48) The original default values for Types F, M, and S (ICRP, 1994a,b, Table A.4) were not based on reviews of experimental data but on comparison with particle transport rates. The value of 100 d^{-1} for the rapid dissolution rate, s_r, was chosen to equal the particle clearance rate from the nose (ET_2) to the throat. Hence, for Type F, approximately half the material deposited in ET_2 is absorbed into blood and the rest is swallowed. The slow dissolution rate for Type S of 10^{-4} d^{-1} was chosen to equal the slowest particle transport rate from the AI region to the gastrointestinal tract (Fig. A.2) to ensure that there was some long-term lung retention.

Table A.4. Original Human Respiratory Tract Model (HRTM) default absorption parameter values for Type F, M, and S materials [based on *Publication 66* (ICRP 1994a, Table 18)].*

Type		F (fast)	M (moderate)	S (slow)
Model parameters				
Initial dissolution rate (d^{-1})	s_p	100	10	0.1
Transformation rate (d^{-1})	s_{pt}	0	90	100
Final dissolution rate (d^{-1})	s_t	–	0.005	0.0001
Fraction dissolved rapidly	f_r	1	0.1	0.001
Approximate dissolution rates				
Rapid (d^{-1})	s_r	100	100	100
Slow (d^{-1})	s_s	–	0.005	0.0001
Fraction to bound state	f_b	0	0	0
Uptake rate from bound state (d^{-1})	s_b	–	–	–

*The model values s_p, s_{pt}, and s_t in this table are the original HRTM reference values (i.e. the recommended default values for use in the model). No 'bound' state was assumed for default types.

Type M values were chosen to be intermediate between the two. It has, however, been recognised that the parameter values for default Type F and Type S represent extremes of 'fast' and 'slow' dissolution rather than being representative of these classes of materials.

A.3.1. Review of absorption characteristics of inhaled materials

(A49) In developing the subsequent parts of this series of reports, detailed reviews were conducted of the absorption characteristics of inhaled materials relevant to radiological protection. They are summarised in the inhalation sections of each element.

(A50) Where information was available, specific parameter values were derived from experimental data from both in-vivo and in-vitro studies. As described below, these provided a database to give guidance on selecting values that are representative of materials that are generally considered to clear at 'fast', 'moderate', or 'slow' rates. Values selected on that basis for default Types F, M, and S have been adopted in the revised HRTM used in this series of reports.

(A51) Material-specific rates of absorption have been adopted in the element sections (and dose coefficients and reference bioassay functions provided for them in the accompanying electronic annex) for a limited number of selected materials, i.e. those for which:

- there are in-vivo data from which specific parameter values can be derived;
- results from different studies are consistent;
- it was considered that occupational exposure to the material is likely; and

- the specific parameter values are sufficiently different from default Type F, M, or S parameter values to justify providing additional specific dose coefficients and bioassay functions.

(A52) Other materials were assigned to default types using suitable experimental data if available, as reviewed in compiling the element sections. *Publication 66* (ICRP, 1994a) did not give criteria for assigning materials to absorption types on the basis of experimental results. Criteria were developed in *Publication 71* (ICRP, 1995c), and their application was discussed further in Supporting Guidance 3 (ICRP, 2002b). Type M is assumed for all particulate forms of most elements in the absence of information on which assignment to an absorption type could be made. A material is assigned to Type F if the amount absorbed into blood by 30 d after an acute intake is greater than the amount that would be absorbed over the same period from a hypothetical material with a constant rate of absorption of 0.069 d^{-1} (corresponding to a half-time of 10 d) under identical conditions. Similarly, a material is assigned to Type S if the amount absorbed into blood by 180 d after an acute intake is less than the amount that would be absorbed over the same period from a hypothetical material with a constant rate of absorption into blood of 0.001 d^{-1} (corresponding to a half-time of approximately 700 d) under identical conditions.

(A53) Particulate forms of each element were assigned to the HRTM default absorption types using these criteria. However, strict application of the criterion for assigning materials to Type S requires experiments of at least 180 d duration, and as this would exclude much useful information, extrapolation has been used in some cases, as indicated in the text. For studies where it was possible to apply the criteria, a statement is made to the effect that results 'are consistent with' (or 'give') assignment to Type F (M or S). For studies where the results point towards a particular type, but there was insufficient information to apply the criteria, a statement is made to the effect that the results 'indicate' or 'suggest' Type F (M or S) behaviour. For some elements for which there are little or no experimental data on absorption from the respiratory tract, materials could be assigned to default types based on chemical analogy.

(A54) For soluble (Type F) forms of each element, estimates are made of the overall rate of absorption from the respiratory tract into blood (where information is available). In general, this might result from a combination of processes including: (a) dissolution of the deposited material (if not inhaled as droplets and so already in solution); (b) transfer through the lining fluid to the epithelium, especially in the conducting airways; and (c) transfer across the epithelium. Strictly, in terms of the model structure, the first two of these would be described as 'dissolution' and be represented by the rapid dissolution rate, s_r, because the material is subject to particle transport, whereas transfer across the epithelium, unless extremely rapid, should be represented by a bound fraction. In practice, it would often be difficult to assess how much of the overall rate should be assigned to each process, and for simplicity, s_r is used to represent the overall absorption. However, it is assumed that s_r is a characteristic of the element, and this would be expected for transfers through the lining fluid and epithelium. Wide variation in values of s_r was found between elements,

ranging from approximately 1 d^{-1} (e.g. yttrium) to 100 d^{-1} (e.g. caesium). Some justification for this approach comes from the fact that the value of s_r tends to have more effect on the overall biokinetics of an inhaled material deposited in the conducting airways (where the lining fluid is relatively thick) than on material deposited in the alveolar region, because it competes with particle transport rates of similar magnitude (10 d^{-1} from BB′ to ET_2', and 100 d^{-1} from ET_2' to oesophagus). Due to the wide variation between elements in the estimated value of s_r, element-specific values are adopted in this series of reports for those elements for which an estimate of the value could be made.

(A55) For soluble forms of some elements, however, part of the dissolved material is absorbed rapidly into blood, but a significant fraction is absorbed more slowly. In some cases, this can be represented by formation of particulate material (which is subject to clearance by particle transport). In other cases, however, it appears to be attached to lung structural components, and removed only by absorption into blood. To represent the latter type of time-dependent uptake, it is assumed that a fraction (f_b) of the dissolved material is retained in the 'bound' state, from which it goes into blood at a rate s_b, while the remaining fraction ($1 - f_b$) goes into blood instantaneously (Fig. A.5). Evidence for retention in the bound state, rather than by transformation into particulate material, may be in one or more forms (e.g. systemic uptake rather than faecal clearance of the retained material; slower clearance than for insoluble particles deposited in the same region of the respiratory tract; or autoradiography showing diffuse rather than focal retention of activity).

(A56) Although the bound state was included in the model mainly to take account of slow clearance of soluble materials from the alveolar region, by default, it is assumed that the same bound state parameter values apply in all regions. In some cases (e.g. a long-term bound state for a long-lived alpha emitter), this could lead, unintentionally, to high doses to the BB and bb regions. Due to the high weighting (apportionment factors) that these tissues are given, this could, in turn, lead to high calculated equivalent doses to the lungs. Hence, in this series of reports, it is assumed that for those elements for which a bound state is adopted ($f_b > 0$), it is only applied in the conducting airways (ET_2, BB, and bb regions) if there is experimental evidence to support it.

(A57) For some elements for which there are little or no experimental data on absorption from the respiratory tract, element-specific absorption parameter values (s_r, f_b, and s_b) could be based on chemical analogy.

A.3.2. Revision to default absorption parameter values

(A58) As noted above, the specific parameter values derived from experimental data (from both in-vivo and in-vitro studies) provided a database to give guidance on selecting values that are representative of materials that are generally considered to clear at 'fast', 'moderate', or 'slow' rates.

(A59) When approximately 100 sets of parameter values were available (i.e. when most of the reviews for Part 2 and 3 elements were completed), the results were

Table A.5. Central values of dissolution parameters for Type F, M, and S materials from a review of experimental data.*

Type		F (fast)	M (moderate)	S (slow)
Fraction dissolved rapidly	f_r	0.95 (0.84) [1.4]	0.20 (0.18) [4]	0.007 (0.003) [9]
Dissolution rates:				
Rapid (d^{-1})	s_r	12 (9) [8]	1.7 (1.5) [9]	2.0 (3.8) [14]
Slow (d^{-1})	s_s	0.02 (0.02) [8]	0.003 (0.003) [4]	0.00018 (0.00008) [9]

*Median value, with geometric mean in parentheses, and geometric standard deviation in square brackets.

Table A.6. Updated default absorption parameter values for Type F, M, and S materials.*,†

Type		F (fast)	M (moderate)	S (slow)
Fraction dissolved rapidly	f_r	1	0.2	0.01
Dissolution rates:				
Rapid (d^{-1})	s_r	30‡	3§	3§
Slow (d^{-1})	s_s	–	0.005	0.0001

*Reference values (see footnote to Table 3.1).
†The bound state is also used for default types of some elements.
‡Element-specific rapid dissolution rates are adopted for Type F forms of many elements.
§The element-specific value for Type F is also used for Types M and S if it is less than 3 d^{-1}.

collated and analysed. It is emphasised that this was not a representative survey from which central values could be derived by some objective statistical means. Rather, it provided a basis for informing judgements as described below.

(A60) Parameter values given in the text of the current draft element sections were sorted into Types F, M, and S according to the *Publication 71* (ICRP, 1995c) criteria given above, and tabulated. Some selection was made. A few values noted to be particularly uncertain were excluded. Where there was more than one set of results for a material (or very similar materials), they were merged and central values were taken to avoid giving too much weight to a few compounds. Note that for some sets of parameter values, because of limitations in data fitting, the value of s_r was fixed and only the values of f_r and s_s were assessed. In such cases, the assumed value of s_r was not included in the derivation of central values.

(A61) Medians, geometric means, and geometric standard deviations (σ_g) of the assessed values of f_r, s_r, and s_s are given in Table A.5. Except for the value of f_r for Type F materials, σ_g are very large (4–14) reflecting the wide ranges of estimated values, and hence indicating large uncertainties in the central values.

(A62) Updated default values, given in Table A.6, were based mainly on the following considerations, but also take account of the large uncertainties in the central values and the need for simple rounded numbers.

Rapid fraction, f_r

(A63) For Type F, the median value (0.95) is close to the current default value of 1.0. For simplicity in implementation, it is preferable not to change to two-phase dissolution. The default value remains 1.0.

(A64) For Type M, the median value is higher (0.20) than the current default (0.1). The updated default value is taken to be 0.2.

(A65) For Type S, the median value is higher (0.007) than the current default (0.001). The updated default value is rounded to 0.01.

Rapid dissolution rate, s_r

(A66) For Type F, the median value of s_r estimated from experimental data for materials that would be assigned is 12 d^{-1} (Table A.5), which is much lower than the original HRTM default value of 100 d^{-1}. However, this outcome is heavily influenced by results for a few elements; approximately half of the results are from only four elements. To include information from a wider range of elements in choosing the default value, consideration was also given to the element-specific values of s_r for soluble (Type F) forms of the element, which were assessed where suitable experimental information was available (see above). There are element-specific values for several elements for which no material-specific values were assessed. Hence, the distribution of element-specific values covers a wider range of elements, in which each element makes the same contribution (one entry); its median value is 50 d^{-1}. Taking both medians into account, the updated default value of s_r for Type F is taken to be 30 d^{-1}.

(A67) For Types M and S, the medians of estimated values of s_r for materials that would be assigned are 1.7 d^{-1} and 2 d^{-1}, respectively (Table A.5), which are very much lower than the original HRTM default of 100 d^{-1}. As for Type F, the distributions are heavily influenced by results for a few elements. For Type F, consideration of element-specific values of s_r involved a wider range of elements, and led to the choice of a somewhat higher value than the material-specific values. However, whereas the rapid dissolution rate s_r represents overall absorption, and is assumed to be element-specific for Type F materials, s_r is more likely to be determined by dissolution of the particle matrix, and so less characteristic of the element for Type M and S materials. Thus, element-specific values of s_r were not assessed for Type M and S materials. Taking account of these factors and the overall large variation in estimated values of s_r, the updated default values for Types M and S were taken to be the same and rounded up to 3 d^{-1}. It is assumed here that the default s_r value of 3 d^{-1} for Type M and S materials applies to all elements, unless the Type F element-specific value is itself less than 3 d^{-1}, in which case the Type F element-specific value is also applied to Types M and S. For example, for sulphur, default values are used for all three types, as in Table A.6; for barium, the element-specific value of s_r is 20 d^{-1} for Type F, but the default value of 3 d^{-1} is used for Types M and S; for yttrium, the element-specific value of s_r is 1 d^{-1} for Type F, and so 1 d^{-1} is also used for Types M and S.

Slow dissolution rate, s_s

(A68) For Types M and S, median values are 0.003 d^{-1} and 0.00018 d^{-1} (Table A.5), similar to the current default values of 0.005 d^{-1} and 0.0001 d^{-1}. The default values remain 0.005 d^{-1} and 0.0001 d^{-1}, respectively.

(A69) Thus, the currently available data suggest larger typical rapid fractions for Type M and S materials, but with lower rapid dissolution rates than original default values for all three types. This has the effect of reducing rapid absorption in the ET airways and increasing it in the lungs.

A.3.3. Progeny radionuclides formed in the respiratory tract

(A70) Note that the following applies specifically to progeny formed in the respiratory tract after inhalation of the parent radionuclide. Progeny radionuclides formed before inhalation and inhaled with the parent are generally treated as separate intakes, and so each progeny radionuclide is assumed to adopt the biokinetics appropriate to the element of which it is an isotope. Many issues relating to the behaviour of progeny in the respiratory tract arise in connection with the natural decay series, which are therefore shown in Figs A.6 (uranium-238 series), A.7 (uranium-235 series), and A.8 (thorium-232 series).

(A71) *Publication 66* (ICRP, 1994a, Para. 272) noted that it would be expected that:

- the rate at which a particle dissociates is determined by the particle matrix, and therefore the dissolution parameter values of the inhaled material would be applied to progeny radionuclides formed within particles in the respiratory tract ('shared kinetics');
- progeny formed as noble gases, including radon, would be exceptions because they would diffuse from the particles; and
- the behaviour of dissociated material would depend on its elemental form, and so, for example, bound fraction parameter values for a progeny radionuclide would not be those of the parent ('independent kinetics').

(A72) These points are considered in turn below. However, it should be noted that in previous applications of the HRTM [e.g. *Publications 68*, *71*, *72*, and *78* (ICRP, 1994b, 1995c, 1996, 1997b)], with the exception of noble gases, the absorption parameters of the parent were applied to all members of the decay chain formed in the respiratory tract (shared kinetics). After consideration (see below), the same approach is taken in this series of reports.

Retention in the particle matrix

(A73) Generally, the assumption applied to the slowly-dissolving fractions of Type M and S materials is that the dissolution of a progeny radionuclide is determined by

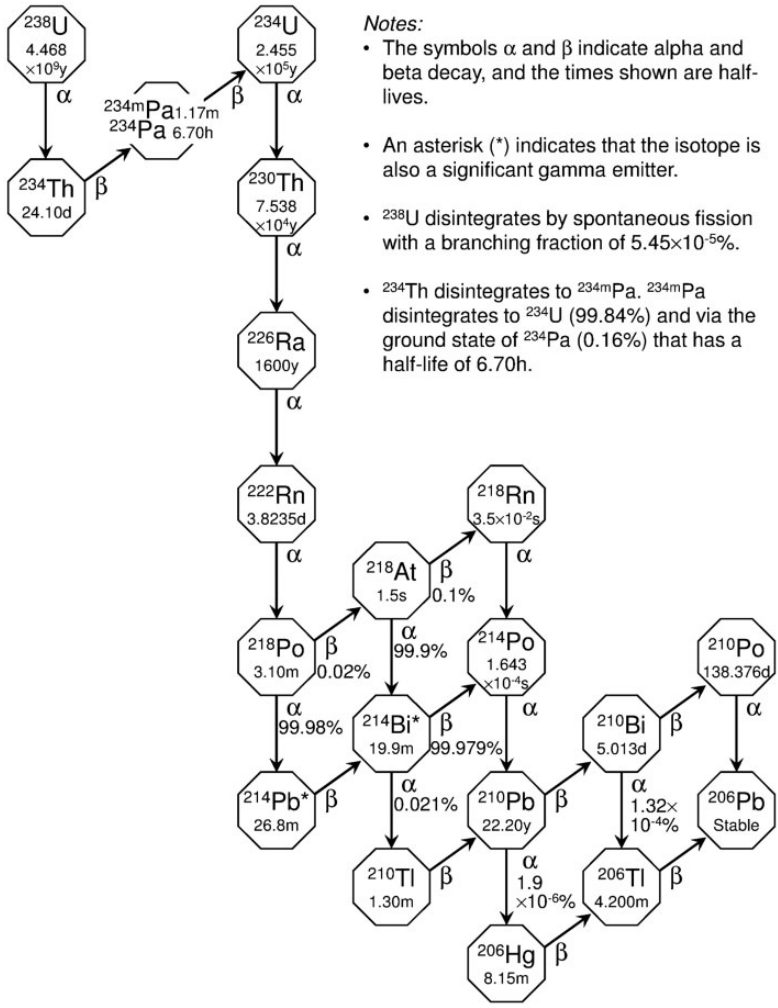

Fig. A.6. Natural decay series: uranium-238 (ICRP, 2008).

that of the particle matrix in which it is formed. Thus, its dissolution parameter values should be those of the inhaled material.

Emanation of radon and alpha recoil

(A74) In applying the HRTM, general exceptions have been made for noble gases formed as progeny (ICRP, 1994b). Radioisotopes of xenon formed from the decay of iodine were assumed to escape from the body without decay, as assumed in *Publication 30* Part 1 (ICRP, 1979). This included xenon formed in the respiratory

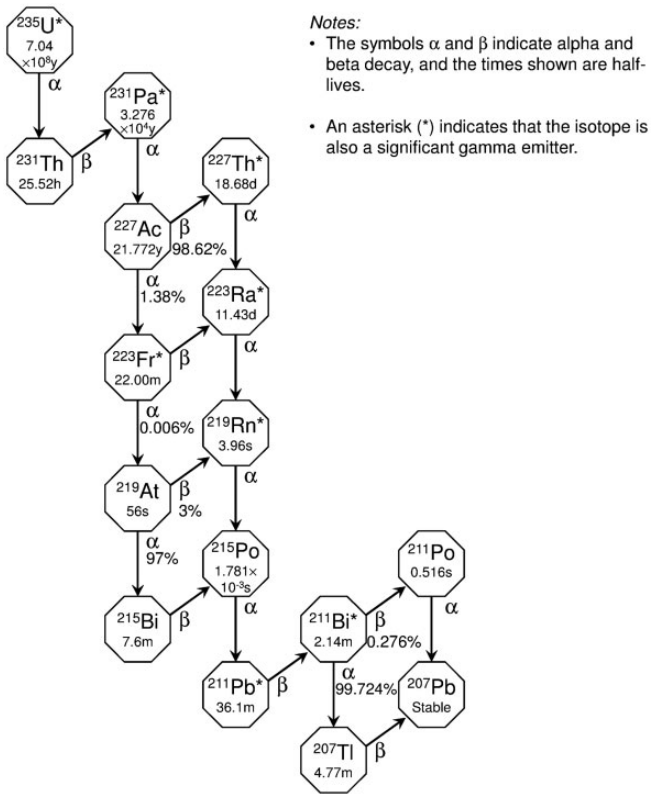

Fig. A.7. Natural decay series: uranium-235 (ICRP, 2008).

tract. For calculation purposes, it has been assumed that radon formed as a progeny radionuclide within the respiratory tract escapes from the body at a constant rate of 100 d^{-1} (ICRP, 1994b). This rate was set as a convenient, arbitrary, rapid rate. The underlying assumption is that loss of radon (for example) is a continuous process such as diffusion. The three radon isotopes in the natural decay series – ^{222}Rn (radon), ^{220}Rn (thoron), and ^{219}Rn (actinon) – have half-lives of approximately 3.8 d, 56 s, and 4 s, and therefore decay rates of approximately 0.18, 1100, and 15,000 d^{-1}, respectively. Hence, the assumption of a rate of loss of 100 d^{-1} implies that nearly all ^{222}Rn escapes from the particles before it decays, approximately 10% of ^{220}Rn escapes, and nearly all ^{219}Rn decays within the particles. As described in the thorium inhalation section [OIR: Part 3 (ICRP, 2016b)], studies that have compared thorium lung contents with exhaled thoron seem broadly consistent with the assumption that approximately 10% of thoron formed within particles in the lungs escapes, but measurements of emanation of radon (^{222}Rn) from uranium ore dust give values much lower than 100%.

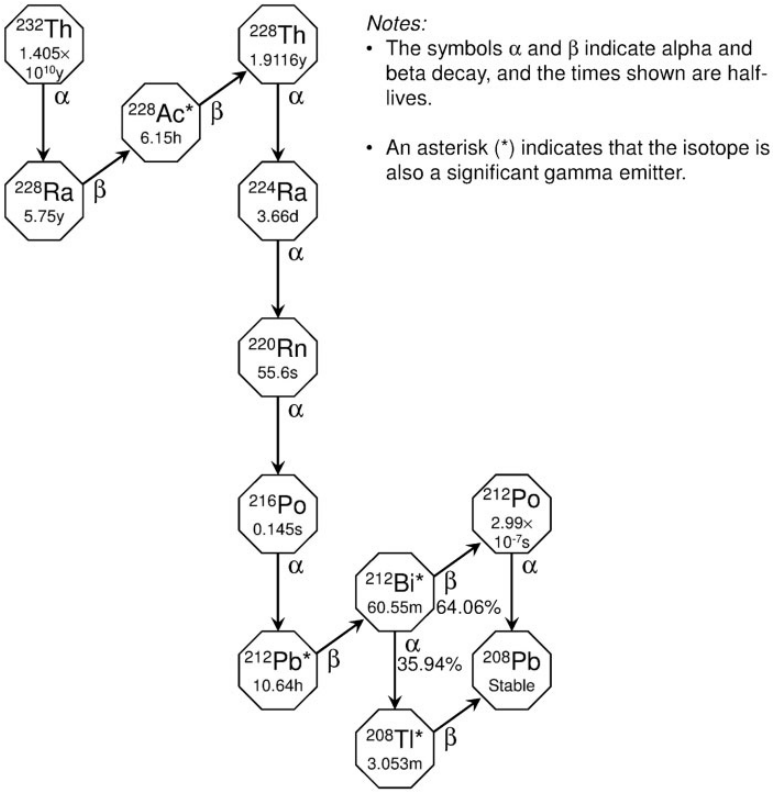

Fig. A.8. Natural decay series: thorium-232 (ICRP, 2008).

(A75) Griffith et al. (1980) developed a model to describe the retention of ^{232}U and its progeny (which include ^{228}Th) in the lungs following inhalation of ThO_2 or UO_2 particles. In addition to chemical dissolution, they considered emanation of ^{220}Rn from particles by diffusion, and emanation of progeny, including ^{220}Rn, as a result of the recoil of nuclei formed in alpha-particle decay. They presented equations to calculate fractional losses by diffusion and recoil as functions of particle size (but only for spherical particles). They calculated recoil ranges of approximately 0.05 μm for the progeny (assuming a particle density of 10 g cm^{-3}), and fractional losses by recoil emanation in the range of 0.3–0.1 for aerosols with an AMAD in the range of 1–10 μm. The calculated loss of ^{220}Rn from particles by diffusion emanation was difficult to predict, ranging from 0.03 to 0.7 depending on the assumed diffusion coefficient (10^{-15}–10^{-11} cm^2 s^{-1}).

(A76) Coombs and Cuddihy (1983) measured the fraction of ^{228}Th escaping by recoil, and the fraction of ^{220}Rn escaping by diffusion, from size-fractionated samples of ThO_2 and uranium oxide (mixture of $UO_{2.2}$ and U_3O_8) containing 1% ^{232}U. The fraction of ^{228}Th escaping increased from approximately 0.07 for particles with

an AMAD of 2.5 μm (CMD[1] of approximately 1 μm) to approximately 0.3 for particles with an AMAD of 0.65 μm (CMD of approximately 0.1 μm). This was in reasonable agreement with the model of Griffith et al. (1980). Calculated recoil range was expressed in terms of recoil range multiplied by density, with values of approximately 20 μg cm^{-2}. The fraction of ^{220}Rn escaping by diffusion increased from approximately 0.07 for particles with an AMAD of 2.5 μm to approximately 0.35 for particles with an AMAD of 0.65 μm (and gave a diffusion coefficient of approximately 3×10^{-14} cm^2 s^{-1}). This was similar to the fraction of ^{228}Th escaping by recoil, and therefore presumably similar to the fraction of ^{220}Rn escaping by recoil, as the recoil ranges of ^{220}Rn and ^{228}Th are similar (Griffith et al., 1980).

(A77) Johnson and Peterman (1984) developed a model to describe the emanation of ^{220}Rn from ThO_2 particles by alpha-particle recoil, and its exhalation from the lungs. They calculated that the fraction of ^{220}Rn atoms produced that escaped from particles (density 10 g cm^{-3}) by recoil decreased from approximately 1.0 at 1 nm to approximately 0.5 at 10 nm and approximately 0.1 at 0.5 μm diameter. The average fraction for an aerosol with an AMAD of 1 μm was calculated to be 0.2, which seems to be broadly consistent with the results derived by Griffith et al. (1980).

(A78) Thus, it seems that recoil is a mechanism that is at least as important as diffusion for emanation of radon from particles. It seems possible that it is the dominant mechanism, in which case for aerosols with an AMAD of approximately 1 μm, there would be a release to lung air of approximately10% of ^{222}Rn, ^{220}Rn, or ^{219}Rn formed in particles in the lungs. Furthermore, alpha-particle recoil applies not only to radon formed as a progeny radionuclide, but also to other progeny formed by alpha emission. In the case of decay chains, this will result in successively lower activities of members of the chain compared with the parent retained in relatively insoluble particles. There is some experimental evidence confirming this [see thorium inhalation section in OIR: Part 3 (ICRP, 2016b)]. However, it was considered impractical to implement loss of progeny by alpha recoil in the calculation of dose coefficients and bioassay functions in this series of reports. Assessment of the fractional loss for representative workplace aerosols would be complex, because it depends on the alpha decay energy, the size distribution of deposited particles, and their shape and density; simplifying assumptions would be needed for practical implementation. Investigations conducted here (by the task groups) into the effect of

[1]Fifty percent (by number) of the particles in the sample measured (e.g. by microscopy) have diameters greater than the CMD. For a log-normal distribution with geometric standard deviation σ_g, the mass median diameter (MMD) can be calculated from the CMD [see, e.g., Baron and Willeke (2001)]:

$$MMD = CMD + 3\exp((\ln \sigma_g)^2)$$

Fifty percent of the mass of material in the aerosol is associated with particles of diameter greater than the MMD. If the material is of uniform specific activity, the MMD will be equal to the activity median diameter (AMD). Fifty percent of the activity in the aerosol is associated with particles of diameter greater than the AMD. The relationship of particle diameter (d_p) to particle aerodynamic diameter (d_{ae}), and hence of AMD and CMD to AMAD of an aerosol formed from the particles, depends on the density and shape of the particles, and on how the diameters were measured. See, for example, *Publication 66* (ICRP, 1994a, Section D.4.1) or Supporting Guidance 3 (ICRP, 2002b, Section B.1.2). However, for particles of compact shape larger than approximately 0.1 μm, $d_{ae} \approx d_p\sqrt{\rho}$, where ρ is the particle density.

recoil on doses for inhaled ^{232}U and its progeny following inhalation in relatively insoluble particles found, as expected, that doses to the respiratory tract decreased and doses to tissues resulting from systemic uptake increased. However, there was little impact on effective dose in this example. The computational effort involved in identifying radionuclides formed by alpha decay, and partitioning the progeny atoms between a fraction remaining in the particle and a fraction escaping to lung fluids would be considerable, and was considered disproportionate to the benefit gained on a routine basis in these reports. Nevertheless, this phenomenon should be borne in mind, especially when using progeny to monitor intakes and doses of the parent radionuclide.

(A79) For calculation purposes, the assumption that radon formed as a progeny radionuclide within the respiratory tract escapes from the body at a rate of 100 d^{-1} is retained in this series of reports, and applied to all noble gases. However, in the previous implementation of the HRTM (ICRP, 1994b), it was assumed that radon formed as a progeny radionuclide within the respiratory tract escapes from the body at a rate of 100 d^{-1}, in addition to other routes of removal (ICRP, 1994b). In this series of reports, it is assumed that noble gases produced in compartments of the respiratory tract (and in the alimentary tract) by radioactive decay escape from these compartments directly to the environment at a rate of 100 d^{-1} without transfer to the blood compartment and without transfer between compartments of respiratory tract and alimentary tract. Thus, this rate of 100 d^{-1} is not superimposed on other routes of removal.

Soluble (dissociated) material

(A80) The behaviour of soluble or dissolved material (specifically the rate of uptake into blood) of progeny formed in the respiratory tract can be expected to depend on the element of which the progeny formed is an isotope. As discussed above, for soluble (Type F) materials, the rapid dissolution rate, s_r, represents the overall absorption from the respiratory tract into blood and is element-specific for many elements. Hence, when a Type F material is deposited in the respiratory tract, the value of s_r for a progeny formed would be expected to be that of the element formed ('independent kinetics'), rather than following that of the parent ('shared kinetics'). Similarly, element-specific bound state parameter values would be expected to apply to progeny radionuclides formed in the respiratory tract. However, analysis carried out by the task groups showed that application of independent kinetics rather than shared kinetics within the respiratory tract to progeny of Type F radionuclides would make little difference to respiratory tract tissue dose coefficients (up to a factor of two, but in most cases much less), and less difference to effective dose coefficients. For Type F materials, absorption into blood is rapid, and doses from deposition in systemic tissues will often make greater contributions to effective dose than doses to respiratory tract tissues. The additional complexity involved in application of independent kinetics was therefore considered to be unjustified. Furthermore, in many practical exposure situations, an intake of a parent nuclide will often be accompanied

by simultaneous intakes of its progeny. Their activities (which being treated as separate intakes will be given absorption kinetics appropriate to the element) will often be considerably greater than the activities of progeny formed within the respiratory tract, because (unless its half-life is short) very little decay of the parent takes place before a Type F material is absorbed into blood.

(A81) Thus, in this series of reports, radioactive progeny formed within the respiratory tract (with the exception of noble gases) are assumed by default to follow the absorption behaviour of the parent nuclide, and are given the same dissolution and uptake parameter values as the parent (shared kinetics). Following absorption into blood, they are assumed to behave according to the systemic model applied to the element as a daughter of the parent radionuclide.

(A82) Nevertheless, where experimental results are available which allow direct comparison between the absorption behaviour of a parent radionuclide, and that of its radioactive progeny, they are summarised in the inhalation section of the parent element (e.g. uranium, thorium). Such information may be of use to those carrying out individual monitoring, especially if intakes of a parent are being assessed by means of measurements on one or more of its progeny. The behaviour of thorium and its progeny can be of particular importance in this context, because there is generally significant long-term retention of thorium in the lungs following its deposition in soluble form, whereas soluble forms of important progeny, notably radium and lead, are absorbed relatively readily.

A.3.4. Radioactive nanoparticles

(A83) In recent years, there has been enormous growth in interest in nanoparticles (particles with physical diameters less than 100 nm, also known as 'ultrafine particles'), their applications, and their toxicology. The National Council on Radiation Protection and Measurements (NCRP) recently established NCRP Scientific Committee 2–6 to develop a report on the current state of knowledge and guidance for radiation safety programs involved with nanotechnology (Hoover et al, 2015). The radiation dosimetry of radioactive particles in this size range has, however, been considered for many years.

(A84) Deposition of nanoparticles in the respiratory tract has been of specific interest because of its importance in the dosimetry of inhaled radon progeny. After decay of radon gas, the newly formed radionuclides react rapidly (<1 s) with trace gases and vapours forming particles around 1 nm in size, described as the 'unattached' fraction. They may also attach to existing aerosol particles in the air (within 1–100 s) forming the 'attached' fraction, part of which is <100 nm [for details, see the radon inhalation section in OIR: Part 3 (ICRP, 2016b)]. Hence, the deposition model in the HRTM [see Section 3 and ICRP (1994a)] covers the size range from 0.6 nm upwards.

(A85) With regard to nanoparticle clearance from the respiratory tract, it is assumed for general radiation protection purposes that particle transport

mechanisms (e.g. mucociliary action, macrophage migration) are independent of material or particle size; the particles act as tracers of these mechanisms. However, it is recognised in Annex E of *Publication 66* (ICRP, 1994a) that some nanoparticles may behave differently from the default model.

(A86) Section E.3.3.2 in Annex E of *Publication 66* (ICRP, 1994a), which addresses the assumption of 'independence of particle transport on material', includes consideration of particle size. It reports evidence that particles in the approximate size range 20–30 nm are cleared more slowly than the larger particles on which the clearance model is based: 'Ferin et al. (1990, 1991) found with both titanium and aluminium oxides greater lung retention in rats for particles with diameters of 0.02 μm to 0.03 μm, than for particles of 0.2 μm to 0.5 μm, and suggested that this might be due to greater penetration of the ultrafine particles to the interstitium.' Slower alveolar clearance of particles in the range of tens of nanometres is not specifically included in the HRTM clearance model for various reasons, but mainly to avoid undue complexity. Relatively insoluble particles in this size range are not generally very important in radiation protection; in most situations, most of the activity is associated with larger particles. Furthermore, these findings were in rats, which have much faster alveolar clearance than man. It appears that in man, a much larger fraction of particles deposited in alveoli goes to the interstitium than in rats, and so it would be difficult to predict the effect in man.

(A87) Annex E (Section E.2.2) reports evidence that particles smaller than a few nanometres are readily transported into the blood (studies of the biokinetics of inhaled plutonium-sodium aerosols had shown remarkably high transfer of plutonium into the blood, which was attributed to the formation of plutonium oxide nanoparticles). ICRP (1994a) stated that 'The term absorption as used here also includes any transport of particulate material to the blood, although this appears to be important only for particles smaller than a few nanometres. Smith et al. (1977) and Stradling et al. (1978a,b) found that 1 nm particles of $^{239}PuO_2$ or $^{238}PuO_2$ were readily translocated from the lungs to the blood in rats, but there was negligible translocation of particles larger than 25 nm. This is consistent with observations that the intercellular clefts in pulmonary blood capillaries do not exceed 4 nm (Lauweryns and Baert, 1977)'. Kanapilly and Diel (1980) did not observe similar high rapid uptake with 9-nm diameter particles of $^{239}PuO_2$ inhaled by rats. This phenomenon can be treated in the framework of the HRTM using material-specific absorption parameter values. However, the plutonium transferred into blood may not follow the normal plutonium systemic model.

ANNEX B. EVOLUTION OF ICRP'S SYSTEMIC BIOKINETIC MODELS

B.1. Formulation of systemic models in modern ICRP reports

(B1) *Publication 30* (ICRP, 1979, 1980, 1981, 1988b) provided a comprehensive set of systemic biokinetic models for radionuclides commonly encountered in occupational settings. The models were generally in the form of retention functions (e.g. sums of exponential terms) that may be interpreted as first-order compartmental models with one-directional flow. These models were designed mainly to estimate the cumulative activities of each radionuclide in its main repositories in the body. They do not depict realistic paths of movement of radionuclides in the body, but describe only the initial distribution of elements after uptake into blood and the net biological half-times of elements in source organs. Activity absorbed from the gastrointestinal or respiratory tract or through wounds is assumed to enter a transfer compartment, from which it transfers to source organs with a specified half-time, typically 0.25 d or longer. Retention in a source organ is usually described in terms of one to three first-order retention components, with multiple biological half-times representing retention in multiple hypothetical compartments within a source organ. Feedback of activity from tissues into blood is not treated explicitly in *Publication 30* with the exception of the model for iodine (ICRP, 1979). It is generally assumed that activity leaving an organ moves directly to a collective excretion compartment (i.e. radioactive decay along actual routes of excretion is not assessed). Relatively short-lived radionuclides (half-lives of up to 15 d) depositing in bone are generally assigned to bone surface, and longer-lived radionuclides are assigned either to bone surface or bone volume, depending on their main sites of retention in bone as indicated by available data.

(B2) The systemic biokinetic models of *Publication 30* series (ICRP, 1979, 1980, 1981, 1988b) were intended primarily for calculation of dose per intake coefficients for planning purposes rather than for retrospective evaluation of doses. For some elements, these systemic biokinetic models were developed separately from ICRP's concurrent bioassay models. For example, urinary and faecal excretion models for plutonium, americium, and curium recommended in *Publication 54* (ICRP, 1988a) were derived independently of the concurrent systemic biokinetic model for these elements, shown in Fig. B.1.

(B3) A series of ICRP reports on doses to members of the public from intake of radionuclides (ICRP, 1989, 1993b, 1995b,c, 1996) provide age-specific systemic biokinetic models for selected radioisotopes of 31 elements: hydrogen, carbon, sulphur, calcium, iron, cobalt, nickel, zinc, selenium, strontium, zirconium, niobium, molybdenum, technetium, ruthenium, silver, antimony, tellurium, iodine, caesium, barium, cerium, lead, polonium, radium, thorium, uranium, neptunium, plutonium, americium, and curium. These reports are referred to here as the '*Publication 72* series', after the summary report that concluded the series (ICRP, 1996). Most of the systemic biokinetic models in the *Publication 72* series (ICRP, 1989, 1993b, 1995b,c, 1996) follow the same modelling scheme as applied in *Publication 30* series (ICRP, 1979, 1980, 1981, 1988b) and illustrated in Fig. B.1, except that explicit excretion

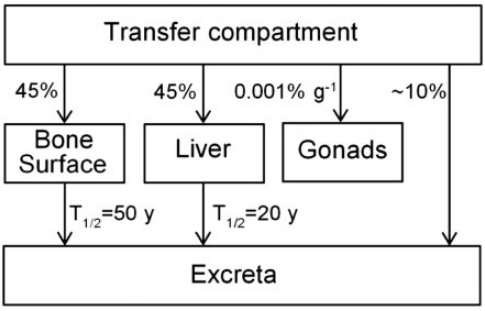

Fig. B.1. Systemic biokinetic model for plutonium, americium, and curium recommended in *Publication 30*, Part 4 (ICRP, 1988b). This illustrates the one-directional flow of systemic activity depicted in models of *Publication 30* series (ICRP, 1979, 1980, 1981, 1988b) and, for many radionuclides, in later ICRP reports on occupational or environmental exposure to radionuclides.

pathways are included in reports completed after the issue of *Publication 60* (ICRP, 1991). These pathways are included to allow the assessment of doses to the urinary bladder and colon, both of which are assigned tissue weighting factors in *Publication 60* (ICRP, 1991). A different modelling scheme involving more realistic paths of movement of systemic radionuclides is applied in the *Publication 72* series (ICRP, 1989, 1993b, 1995b,c, 1996) to iron and the following 'bone-seeking' elements: calcium, strontium, barium, lead, radium, thorium, uranium, neptunium, plutonium, americium, and curium. The model structures for these elements and the structure for iodine, carried over from *Publication 30*, depict feedback of material from organs into blood and, where feasible, physiological processes that determine the biokinetics of radionuclides. Examples of such physiological processes are bone remodelling, which results in removal of plutonium or americium from bone surface, and phagocytosis of aging erythrocytes by reticuloendothelial cells, which results in transfer of iron from blood to iron storage sites.

(B4) The physiologically based modelling scheme applied in the *Publication 72* series (ICRP, 1989, 1993b, 1995b,c, 1996) is illustrated in Fig. B.2, which shows the generic model structure used for the actinide elements thorium, neptunium, plutonium, americium, and curium. The systemic tissues and fluids are divided into five main components: blood, skeleton, liver, kidneys, and other soft tissues. Blood is treated as a uniformly mixed pool. Each of the other main components is further divided into a minimal number of compartments needed to model the available biokinetic data on these five elements or, more generally, 'bone-surface-seeking' elements. The liver is divided into compartments representing short- and long-term retention. Activity entering the liver is assigned to the short-term compartment (Liver 1), from which it may transfer back into blood, to the intestines via biliary secretion, or to the long-term compartment from which activity slowly returns to blood. The kidneys are divided into two compartments: one that loses activity to urine over a period of hours or days (urinary path) and another that slowly returns

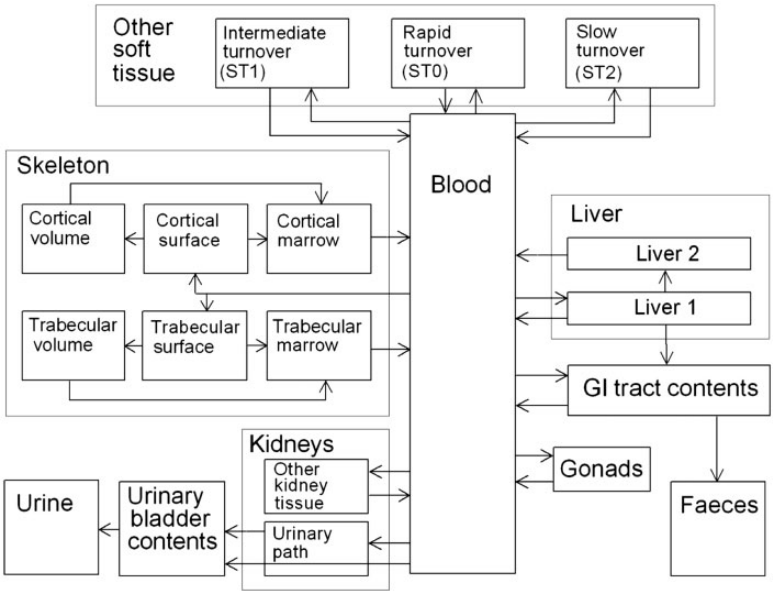

Fig. B.2. Model structure applied in the *Publication 72* series (ICRP, 1989, 1993b, 1995b,c, 1996) to the bone-surface seekers thorium, neptunium, plutonium, americium, and curium. This structure (or its modest variations) is applied to a number of elements in this series of reports, including elements not regarded as bone seekers. GI, gastrointestinal.

activity into blood (other kidney tissue). The remaining soft tissue other than bone marrow is divided into compartments ST0, ST1, and ST2 representing rapid, intermediate, and slow return of activity into blood, respectively. ST0 is used to account for a rapid build-up of activity in soft tissues and rapid feedback into blood after acute input of activity into blood, and is regarded as part of the activity circulating in blood. The skeleton is divided into cortical and trabecular fractions, and each of these fractions is subdivided into bone surface, bone volume, and bone marrow. Activity entering the skeleton is assigned to bone surface, from which it is transferred gradually to bone marrow and bone volume by bone remodelling processes. Activity in bone volume is transferred gradually to bone marrow by bone remodelling. Activity is lost from bone marrow into blood over a period of months, and is subsequently redistributed in the same pattern as the original input into blood. The rates of transfer from cortical and trabecular bone compartments to all destinations are functions of the turnover rate of cortical and trabecular bone, assumed to be 3% and 18% per year, respectively. Other parameter values in the model are element-specific.

(B5) A variation of the model structure shown in Fig. B.2 was applied in the *Publication 72* series (ICRP, 1989, 1993b, 1995b,c, 1996) to calcium, strontium, barium, radium, lead, and uranium (Fig. B.3). These elements behave differently

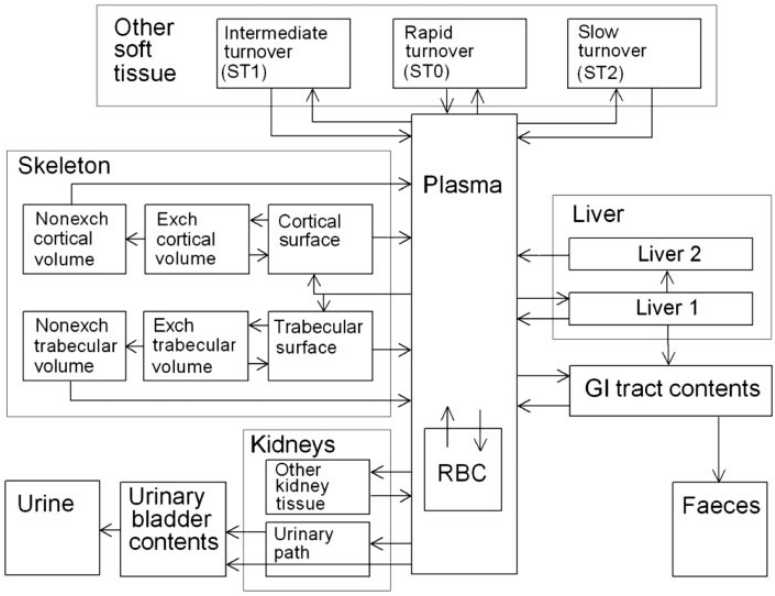

Fig. B.3. Model structure applied in the *Publication 72* series (ICRP, 1989, 1993b, 1995b,c, 1996) to calcium, strontium, barium, lead, radium, and uranium. This structure (or modest variations of it) is applied to a number of elements in this series of reports, including elements not regarded as bone seekers. Exch, exchangeable; Nonexch, non-exchangeable; RBC, red blood cells; GI, gastrointestinal.

from the bone-surface seekers addressed above in that they diffuse throughout bone volume within hours or days after depositing in bone. After reaching bone volume, these elements may migrate back to plasma (via bone surface in the model) or they may become fixed in bone volume and then gradually transfer to blood at the rate of bone remodelling. The compartments in Fig. B.2 representing bone marrow and gonads are omitted from the model for bone-volume seekers because these are not generally sites of elevated accumulation of these elements. Some of the compartments shown in Fig. B.3 are not applicable to all bone-volume seekers. For example, the liver, kidneys, and red blood cells are not important sites of accumulation of calcium and strontium, but are important repositories for lead. If a particular compartment or pathway shown in Fig. B.3 is not important for a given element, it is not considered separately in the model for that element. For example, in the model for calcium, blood is treated as a single well-mixed pool, and the liver and kidneys are assumed to be part of 'other soft tissue'.

(B6) The systemic models used in Parts 2–4 of the *Publication 72* series (ICRP, 1993, 1995b,c) were applied in *Publication 68* (ICRP, 1994b), along with ICRP's HRTM (ICRP, 1994a), to update dose coefficients for occupational intake of radionuclides based on recommendations in *Publication 60* (ICRP, 1991). For elements not addressed in Parts 2–4 of the *Publication 72* series (ICRP, 1993, 1995b,c), the

systemic biokinetic models applied in *Publication 68* (ICRP, 1994b) were taken from *Publication 30* series (ICRP, 1979, 1980, 1981, 1988b) and modified to include specific excretion pathways to address doses to the urinary bladder and colon.

(B7) The biokinetic models applied in *Publication 68* (ICRP, 1994b) were used in *Publication 78* (ICRP, 1997b) to update recommendations concerning interpretation of bioassay data for workers for selected radioisotopes of 15 elements. The systemic models for nine of the 15 elements addressed in *Publication 78* (ICRP, 1997b) were physiologically based models adopted in the *Publication 72* series (ICRP, 1989, 1993b, 1995b,c, 1996).

B.2. Systemic model structures used in this series of reports

(B8) It is now generally recognised that the physiologically descriptive model structures introduced for selected elements in the *Publication 72* series (ICRP, 1989, 1993b, 1995b,c, 1996) have a number of potential advantages over the retention–function models traditionally used in radiation protection. For example, a physiological descriptive model structure:

- facilitates the use of physiological information and physiologically reasonable assumptions as a supplement to radiobiological data in the development of model parameter values;
- provides a basis for extrapolating beyond the radiobiological database to different subgroups of the population and to times outside the period of observation (e.g. a parameter value found to depend on the rate of bone remodelling can be varied with age on the basis of age-specific data on bone remodelling rates);
- facilitates the extrapolation of biokinetic data from laboratory animals to man, in that it helps to focus interspecies comparisons on specific physiological processes and specific subsystems of the body for which extrapolation may be valid, even if whole-body extrapolations are not;
- facilitates the extrapolation of biokinetic data from an element to its chemical analogues, in that the degree of physiological similarity of chemical analogues may vary from one physiological process to another (e.g. the alkaline earth elements show similar rates of transfer from blood to bone but very different rates of transfer to non-exchangeable sites in bone);
- links excretion with exchanges of activity among body tissues and fluids, so that the same model can be used for dose calculation and bioassay interpretation;
- allows modelling of the differential biokinetics of parent radionuclides and their radioactive progeny produced in the body; and
- allows the addition of compartments and pathways to the model for purposes of extending the model to new applications, as was demonstrated in the ICRP publication on doses to the embryo and fetus (ICRP, 2001) and to the nursing infant (ICRP, 2004) from intakes of radionuclides by the mother.

(B9) On the other hand, the level of physiological realism in the systemic biokinetic models currently used in radiation protection, including those recommended in

the present report, should not be overstated. Even the most sophisticated models represent a compromise between biological realism and practical considerations regarding the quantity and quality of information available to determine parameter values. For example, all of the recycling models applied to bone-seeking radionuclides in the *Publication 72* series (ICRP, 1989, 1993b, 1995b,c, 1996) include soft tissue compartments representing fast, intermediate, and slow exchange with blood for all soft tissues not explicitly identified in the models. These soft tissue compartments are typically defined on a kinetic basis rather than a physiological basis (i.e. the compartment sizes and turnover rates are set for reasonable consistency with data on accumulation and loss of elements by soft tissues). For some elements, these soft tissue compartments appear to be associated with specific sites or processes, but the associations are not generally confirmed by available information. For example, biokinetic studies of calcium suggest, but do not establish, that: the rapid-turnover pool in soft tissues may correspond approximately to interstitial fluids plus some rapidly exchangeable cellular calcium (Heaney, 1964; Harrison et al., 1967; Hart and Spencer, 1976); the intermediate turnover rate may stem from a composite of several pools with slower exchange rates, including mitochondrial calcium, cartilage calcium, and exchangeable dystrophic calcium (e.g. arterial plaque and calcified nodes) (Heaney, 1964; Borle, 1981); and long-term retention in soft tissues may be associated with relatively non-exchangeable dystrophic calcium that accumulates gradually in the human body (Heaney, 1964).

(B10) For many elements, it is not feasible to develop genuine physiological system models due to inadequate information on the processes that determine the systemic behaviour of these elements. Even for relatively well-understood elements, the model components are often intended only to represent the net result of multiple processes. For example, in the model for bone-surface-seeking radionuclides shown in Fig. B.2 and its precursors (Leggett, 1985, 1992), the depiction of burial of activity in bone volume is intended to approximate the net result over time of a number of known or suspected burial processes occurring at different rates. Activity depositing in bone remodelling units, either in the formation period or in the transitional period between resorption and formation, may be buried relatively quickly. Delayed burial of surface activity may result from 'local recycling' during bone restructuring processes (i.e. some of the surface activity removed by osteoclasts during bone remodelling may be redeposited almost immediately at closely adjacent sites of new bone formation that are supplied by the same blood vessels). Such local redeposition of mineral ions is thought to occur, particularly in cortical bone (Parfitt and Kleerekoper, 1980). Burial of surface deposits may also occur as a result of 'bone drift', a phenomenon in which new bone is deposited on previously formed bone without any prior resorption process. Bone drift occurs on a larger scale in immature bone than in mature bone, but drift within bones and expansion of bone volume via periosteal–endosteal drift continues throughout life in humans (Epker and Frost, 1965a,b; Frost, 1986; Priest et al., 1992). 'Drifting osteons' are observed at all ages within human cortical bone, and their count is used in forensics for age-at-death estimation.